University of Udine
Dept. of Agricultural, Food, Animal and Environmental Sciences
Doctoral course in Agricultural Science and Biotechnology (ASB)
Cycle XXIX, Coordinator: prof. Giuseppe Firrao

FLAVONOID ROLE IN PLANT STRESS RESPONSES

Supervisor
prof. Enrico Braidot

PhD student
Antonio Filippi

Co-supervisor
dott. Elisa Petrussa

This thesis was presented
by
Antonio Filippi

with the permission of the Dept. of Agricultural, Food, Animal and Environmental Sciences,
University of Udine,
for public examination

and approved by the supervisor:
prof. Enrico Braidot

Alla mia mamma

ABSTRACT

FLAVONOID ROLE IN PLANT STRESS RESPONSES

Flavonoids are the most powerful bioactive plants metabolites, able to interact with both plant and animal metabolism. They have occurred in terrestrial plants since their land colonization and are part of mammalian diet since millions of years. Flavonoids exert many different biological activities both in plants (UV-protection, ROS scavenging, enzymatic activity modulation, flower and fruit coloration, signalling and cellular communication) and in mammals (antioxidant activity, cancer cell proliferation inhibition, enzymatic activity modulation). Flavonoid biological activities are strongly connected to plant cellular ability to transport, store, excrete and sequester them into specific cellular compartments. The scientific community has debated upon flavonoid metabolism many times in the last 30 years, trying to obtain a complete overview of the synthesis, the transport systems and the role in plants, but up to date a full understanding of such a complicated mechanism is far from being elucidated.

This PhD thesis aims to provide a contribution to the comprehension of flavonoid function in plants, particularly considering the role of quercetin (QC), the most abundant flavonoid in plant kingdom, in different physiological contests. The role of flavonoids has been explored starting from pathogen attack, up to the senescence, and from cellular transport, up to the role in heavy metal detoxification.

TABLE OF CONTENTS

SUMMARY

Plant flavonoids are one of the most studied members of natural polyphenolic family due to their biochemical, physiological and pharmacological effects both in plants and humans. The observation that the flavonoid metabolic pathway has remained unaffected for millions of years is consistent with the view that natural selection favoured the conservation of these phenolic metabolites thanks to their numerous functional roles in plants. Flavonoids encompass more than 10,000 molecules present in plant tissues at different molar concentrations and differentially produced during all the developmental stages. The enormous variability of biological effects ascribed to flavonoids lies mainly on their specific and, at the same time, variable chemical structure. For all these reasons, nowadays a complete and clear vision of the role of flavonoids in plants is really far to be elucidated and new discoveries are constantly made upon these important metabolites. For these reasons, in my PhD thesis I focused the attention on flavonoids and their role in plant stress response. Initially the work focused mainly on the identification of proteins involved in flavonoid binding that are expressed in mature tissues, such as seed and berry skin of *Vitis vinifera.* Their detection was initially performed on microsomes through Western Blot (WB) assays using a monoclonal antibody targeting a flavonoid-binding site of a mammalian organic anion carrier. The immuno-purification and sequencing were performed on the proteins that cross-reacted with that antibody. Chitinase was one of the proteins identified by amino acid sequencing. I then investigated the modulation of its activity by two different classes of flavonoids (quercetin as a flavonol and catechin as a flavan-3-ol). The second line of research focused on the development of a new methodology for the analysis of *in vivo* transport of quercetin. To this purpose, I used first the cellular model of *V. Vinifera* liquid suspension cultures and then on microsomal vesicles obtained from *Pisum sativum* stems. This work has allowed us to propose a new easy-to-use and fast flavonoid transport assay. In the third line of research, biochemical investigations were carried out on barley plants to evaluate the contents of ATP and reactive oxygen species (ROS), and assessing the impact of nanoparticles of cerium and titanium on cellular energy processes. Finally, I was involved in the study of quercetin role as a reducing agent, in order to obtain silver nanoparticles (NPs) from salt solutions. The purpose was to finely control the process of "green biosynthesis" and produce nature-friendly NPs, nanomaterial that has huge interest in medical and agricultural fields.

INTRODUCTION

Flavonoids

Plant adaptation to land and evolution of flavonoid pathway

The multicellular algae that moved from their marine environment to invade the harsh terrestrial land had to face lots of negative factors, including higher oxygen concentration, desiccation, increasing gravity, damaging heat and UV light, greater daily and seasonal fluctuations of temperatures, chances to be infected and eaten by new pathogens and grazers, and need to establish communications with organisms of the same and even other kingdoms. Also the co-evolution with other living organisms (the insects, in particular) forced plants to develop new strategies for the recruitment of pollinators, leading the appearance of the first colorful flowers and the synthesis of a large amount of volatile chemicals.

Today, more than 500 million years later, we observe modern plants representing the most evolutionarily successful and longevous eukaryotic species, colonizing all parts of our planet, spanning from North to South poles. This evolutionary success has been possible thanks to the biosynthesis of numerous new bioactive metabolites.

Secondary metabolites synthesis, including flavonoids, represents an important step in the colonization process of Earth's terrestrial environment by vascular plants. Physiological functions of flavonoids and the reasons for their ubiquitous existence have been widely discussed. A short list of these functions includes:

(i) protection against insect predation and defence against microbes;

(ii) action as sunscreens to absorb UV radiation and strong light, thus replacing mycosporine-like amino acids usually present in algae;

(iii) attraction of insect pollinators through production of colourful anthocyanins, absorbing different spectra of visible light;

(iv) action as antioxidants, inhibiting the generation of reactive oxygen species (ROS), by maintaining their concentration within a sub-lethal range;

(v) involvement in pollen germination;

(vi) involvement in biological communication in the rhizosphere;

(vii) action as developmental regulators, involved in auxin transport and catabolism;

(viii) modulation of enzymatic activities.

Under an evolutionary point of view, small quantities of flavonoids may have existed also in the primordial algae. Several studies have actually demonstrated that algae are capable of forming *p*-coumaric acid, the precursor of the flavonoid synthesis, having many essential flavonoid enzymes such as chalcone synthase or chalcone isomerase, although genes for other important enzymes such as flavanone-3- hydroxylase or flavonol synthase have not yet been detected in their genomes (Goiris et al. 2014).

It is most probable that genes involved in primary metabolism pathways could later evolve into codifying sequences for enzymes of phenylpropanoid pathway via gene duplication. Alternatively, they could be acquired via horizontal gene transfer during plant symbioses with bacteria and fungi that are known to be established very early during the first steps of land colonization (Mouradov and Spangenberg 2014).

Three main hypotheses regarding the primary roles of flavonoids proposed that these metabolites evolved (i) as an effective sunscreen protecting against UV radiation as plants began colonizing land, (ii) as developmental regulators of auxin transport/catabolism and (iii) as useful moieties for radicals scavenging. Protection from damaging UV light as a presumable primary function of ancestral flavonoids does not match well with the observation that representatives of flavonols (as quercetin), produced in early land plants do not absorb UV-B wavelengths as efficiently as other flavonoids and phenolics. Moreover, these flavonols have much lesser ability to absorb UV-B light than the molecule used by ancestral algae, mycosporine like amino acid (Mouradov and Spangenberg 2014).

So probably, at the beginning of plant adaptation, flavonoids acted as hormonal regulators. Many papers have already explained the role of flavonoids as modulators of auxin transport, by affecting expression and localization of secondary transporters acting in the efflux of this hormone from cells (PIN proteins), the cycling of PIN proteins to endosomal vesicles, as well as modifying the activity of ABCB-type auxin transporters (Ng et al. 2015).

The mechanism of their protective action against reactive oxygen species (ROS) is another role for long time subjected to considerable debates. As polyphenolic compounds, flavonoids have the ability to act as antioxidants, by a free radical scavenging mechanism leading to the formation of less reactive flavonoid phenoxyl radicals. It is widely believed that the antioxidant property of flavonoids resides mainly in their ability to donate hydrogen atoms and thereby scavenge the free radicals generated during lipid peroxidation. On the other hand, thanks to their known capacity to chelate transition metals, these compounds may inactivate ions through complexation: metal chelation has generally been regarded to play a minor role in the antioxidant activity of these compounds and, hence, has not been studied much by researchers involved in this topic.

Classification

Flavonoids are a group of plant secondary metabolites that share a common C6-C3-C6 carbon framework. More than 6000 different flavonoids have been identified and surely this number will increase (Falcone Ferreyra, Rius, and Casati 2012).

This group of molecules may be divided into three main classes, depending on the position of the linkage of the phenyl aromatic ring (B ring) to the benzopyrano moiety (A, C rings), located in position 2, 3 or 4 respectively: **1** flavonoids (2-phenylbenzopyrans), such as flavones, flavanols (flavan-3-ols), flavonols and anthocyanins; **2** isoflavonoids (3-benzopyrans); **3** neoflavonoids (4-benzopyrans) (Figure 1). These groups usually share a common chalcone precursor, and therefore are biogenetically and structurally related (Marais et al. 2006).

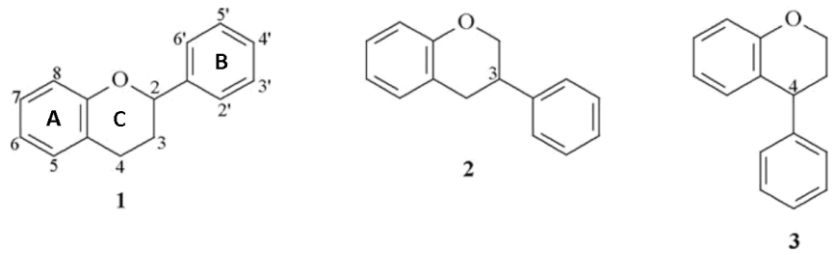

Figure 1. Chemical structure of flavonoids **1**, isoflavonoids **2**, and neoflavonoids **3** (Marais et al. 2006).

Particularly the flavonoids belonging to the first class can be better described according to whether the central heterocyclic ring is unsaturated or not. When unsaturation is present, as in the anthocyanins, flavones and flavonols, the molecule is planar and present unique spectral properties. Saturated flavonoids (flavanones, flavans) have one or more chiral centres, and can thus exist in more than one optically active form (de Pascual-Teresa, Moreno, and García-Viguera 2010).

Based on the degree of oxidation and saturation present in the heterocyclic C-ring, the over 6000 flavonoids discovered until now may be further divided into several different sub-classes of molecules (Falcone Ferreyra, Rius, and Casati 2012), as shown in Figure 2.

In plants, flavonoids are often glycosylated. The glycoside residues can be attached to O and C atoms of the flavonoids, giving rise to O-glycosides, C-glycosides and O-C-glycosides. Flavonoid glycosides usually contain one or two glycoside residues, but molecules with more residues have been identified in nature. In theory, flavonoids could be glycosylated in any position, but O-glycosylation occurs mainly at position 7, as in flavones, isoflavones, flavanones and flavonols; C-glycosyl flavonoids are usually

flavones, and the glycosyl moieties are attached at positions 6 or 8 (Pinheiro and Justino 2012). Over this huge diversity of molecules, the three highly most represented classes in nature are: flavanols, flavones, and anthocyanidins.

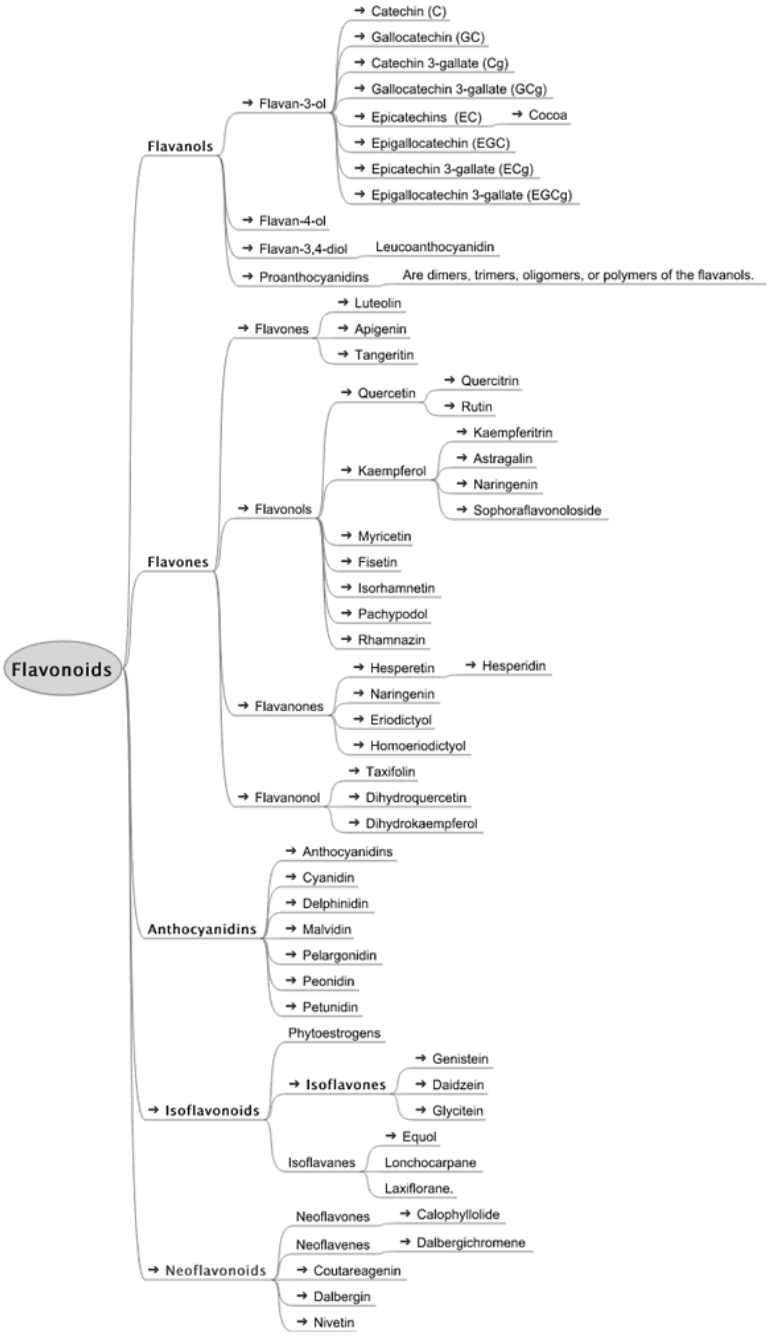

Figure 2. Diagram of the different classes and sub-classes of flavonoids (Cashin-Garbutt 2012).

Flavanols

Monomeric flavanols or catechins, biosynthetic precursors of proanthocyanidins, are characterized for having a C6-C3-C6 skeleton with a hydroxyl group in position 3 of the C-ring (Figure 3).

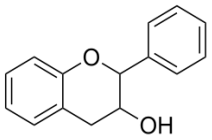

Figure 3. General chemical structure of flavanols.

Catechin and epicatechin represent the most common flavanols so far known, sharing a distribution almost as widespread as the related flavonol, quercetin. Catechins are rarely found in nature in their glycosylated form, unlike anthocyanidins which are commonly bound to a sugar (anthocyanins). On the other hand, flavanols are commonly found in plant-derived food products in their polymerized forms as oligomers (dimers to pentamers) or polymers (six or more units), also called proanthocyanidins or tannins (Figure 4).

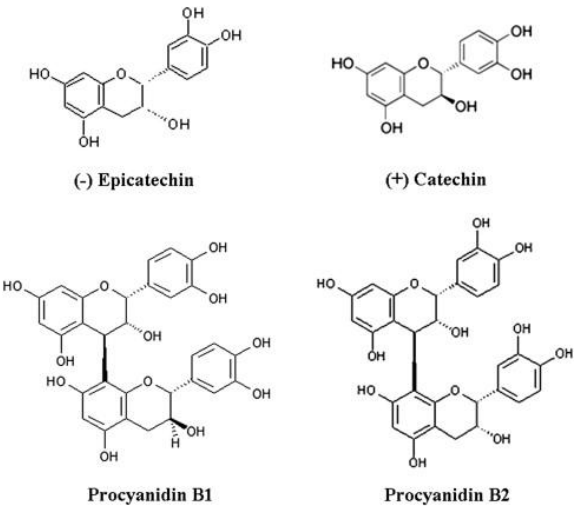

Figure 4. Catechin and epicatechin and their dimmers (Ramos, Goya, and Martín 2014).

The food sources of catechins (tea, chocolate, apples, pears, grapes and red wine) are very popular and highly consumed. In many cases flavanols are present in the peels or

seeds of fruits and vegetables, being discarded when eaten or during processing, and therefore their dietary intake is limited (Table 1).

Source	Flavanol Content, mg/kg or mg/L
Chocolate	460–610
Legume-type beans	350–550
Apricots	100–250
Grapes	30–175
Blackberries	130
Apples	20–120
Green tea	100–800
Black tea	60–500
Red wine	80–300

Table 1. Flavanols content into plant-derived foods and fruits (http://www.morethanjustdessert.com/2014/05/02/did-you-know-fridayis-dark-chocolate-good-for-me).

Flavones/ flavonols

Flavones, including flavonols, have three functional groups, such as hydroxy, carbonyl, and conjugated double bond; consequently they are characterized for the typical reactions of all three functional groups. Flavones are colourless-to-yellow crystalline substances, more soluble in ethanol than in water. They present a planar structure. In the literature many reports are present that underline the ability of flavones to scavenge free radicals or to competitively inhibit xanthine oxidases. Three structural features are essential for antioxidant activity: (i) the catechol group (3- OH) in the B-ring, (ii) the C2=C3 double bond in the C-ring that enables the conjugation of the B-ring to the 4-oxo group, and (iii) the 3- and 5-OH groups together with the 4-oxo group. Flavones also have the ability to form chelates with oxidizing metal ions and prevent various redox reactions, thus imparting antioxidant effects. The 5-hydroxyl group in association with the 4-keto group on the A and C rings chelates catalytically active metal ions involved in redox reactions, which may prevent the formation of oxidizing species (Figure 5) (Singh, Kaur, and Silakari 2014).

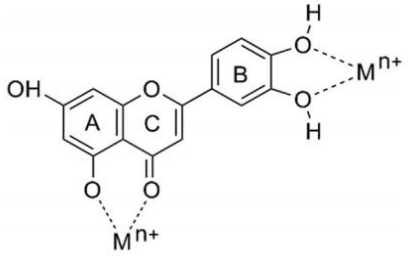

Figure 5. Flavone chelates with oxidizing metal ions (Singh, Kaur, and Silakari 2014).

Quercetin is one of the most represented member of this class. Dietary quercetin has been associated with the protection against different diseases including cardiovascular pathologies, cancer and neurodegenerative disorders. The precise mechanisms through which quercetin and other flavonoids exert their biological action are still under discussion, although they have been attributed, at least partially, to their antioxidant and free-radical scavenging properties and to their ability of modulating the activity of various endogenous enzymes. Quercetin occurs in foods predominantly in the form of glycosides, especially 3-O-glycosides namely, quercetin-3-O-glucoside (QC-3-Glc) and quercetin-3-O-rutinoside (rutin). However, the most evidence for the biological activity of quercetin has been obtained using the aglycone, despite glycosylation is known to deeply affect the bioavailability and biological activity of the flavonoids (Dueñas et al. 2013).

Anthocyanins

Anthocyanins are natural pigments responsible for the blue, purple, red and orange colors of many fruits and vegetables (Figure 6). More than 600 different anthocyanins have been shown to be synthesized in plant kingdom as protective compounds in response to UV, cold, and drought stresses. Anthocyanins are one of the most important classes of food bioactive compounds, due to their impact on the sensorial characteristics of food products and for their strong beneficial properties for human health. The health-promoting effects mostly depend on the consumption of high levels of dietary anthocyanins (Dueñas et al. 2013). Structurally, anthocyanins are glycosides/acylglycosides of anthocyanidins, and the aglycones basic structures differ in the different hydroxyl or methoxyl substitutions. The core of the anthocyanidin, the flavylium, has the typical C6-C3-C6 flavonoid skeleton. In the cation form, anthocyanidins have two double bonds in the C ring and hence carry a positive charge (He et al. 2010).

Plants can differentially regulate anthocyanins synthesis in various tissues, organs and even different cell-types. Therefore, species with typical anthocyanin-pigmented flowers may or may not accumulate anthocyanins into the other vegetative tissues (Valle et al. 2015).

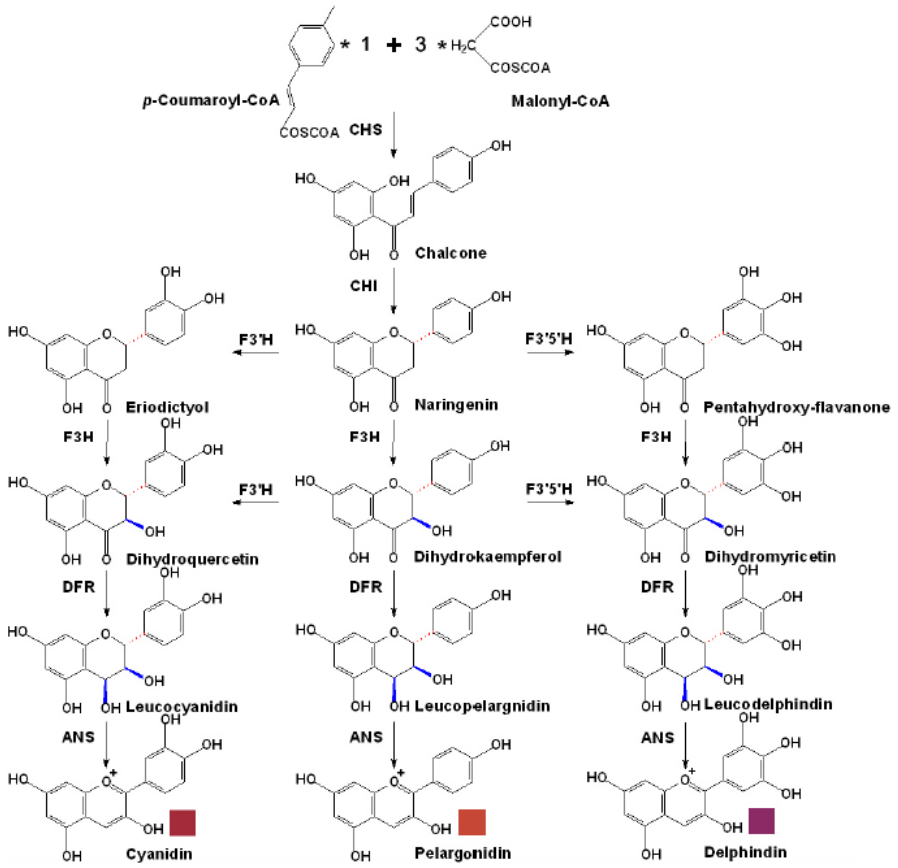

Figure 6. The basis upstream flavonoid pathway leading to the biosynthesis of coloured anthocyanidins. CHS, chalcone synthase; CHI, chalcone isomerise; F3H, flavanone 3β-hydroxylase; F3'H, flavonoid 3'-hydroxylase; F3'5'H, flavonoid 3',5'-hydroxylase; DFR, dihydroflavonol 4-reductase; ANS, anthocyanidin synthase (He et al. 2010).

Depending on the number and position of the hydroxyl and methoxyl groups as substituents, different anthocyanidins have been described, and six of them are commonly found in fruits and vegetables: pelargonidin, cyanidin, delphinidin, petunidin, peonidin and malvidin (Figure 7).

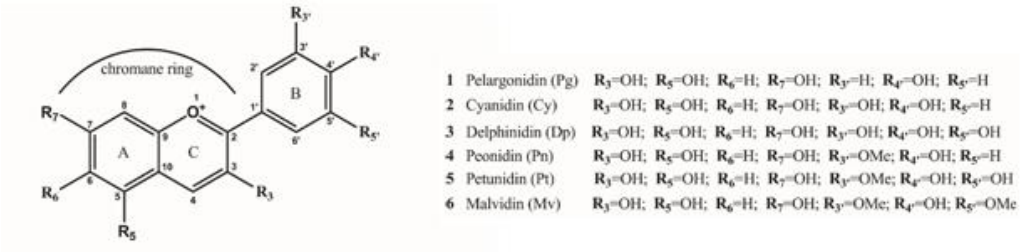

Figure 7. Basic chemical structure of anthocyanidins and their functional substituted groups in the most represented anthocyanins (Ananga et al. 2013).

Anthocyanidins are unstable to light and are water-insoluble, so that they do not usually occur in their free state. Instead, they are present in the cell vacuole linked to sugars, which provide stability, lower reactivity and water solubility. These glycosides are called anthocyanins (Figure 8) (de Pascual-Teresa, Moreno, and García-Viguera 2010).

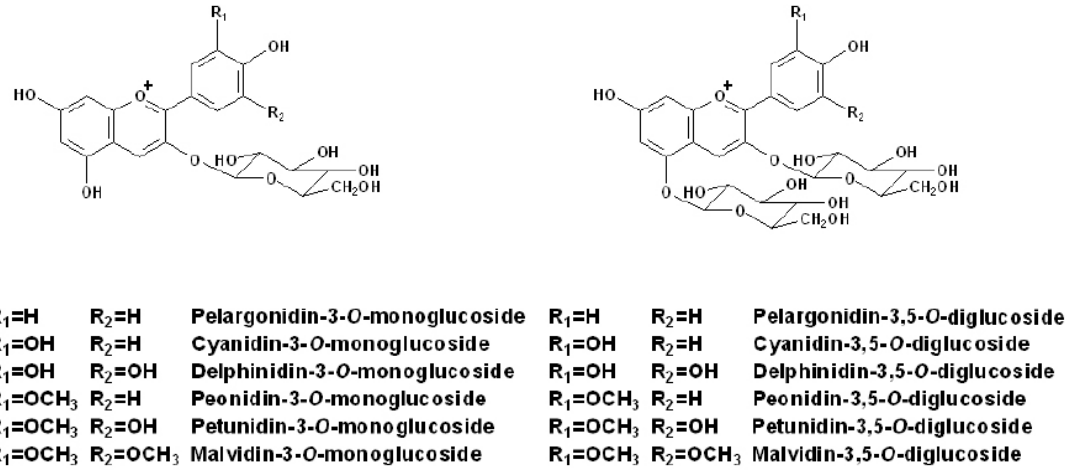

Figure 8. Chemical structure of the six common plant anthocianins and the site of linkage with single or multiple sugars (He et al. 2010).

Bio-synthesis

Over the years, a huge number of enzymes involved in metabolites biosynthesis has been identified, making it very difficult to have a complete view of their synthesis. The scenario gets even more articulated if one considers that various degrees of cellular differentiation and more than one cell type present into a single plant might be necessary for biosynthesis, accumulation, transformation, storage and secretion of the end-product secondary metabolites. In addition to this, many plant metabolites require 20–30 enzymes for their synthesis, and each synthetic pathway is branched into a network that leads to a multiplicity of related chemical structures (Kutchan 2005). Plant phenolics are products of the shikimate, phenylpropanoid, flavonoid, anthocyanin, and lignin pathways. The shikimate pathway produces the aromatic aminoacids, including phenylalanine, which can be further modified through the sequential of elongation and cyclization steps to form the flavonoids (Mouradov and Spangenberg 2014; Mellway et al. 2009) (Figure 9).

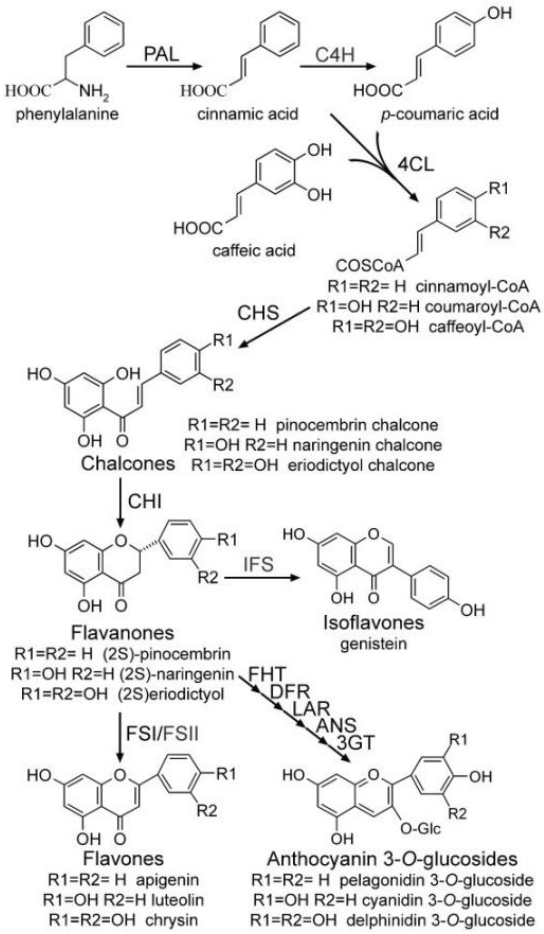

Figure 9. Scheme leading the biosynthesis pathway of phenolic compounds (Chemler, Yan, and Koffas 2006).

Although the central pathway for flavonoid biosynthesis is conserved in plants, depending on the species, a group of enzymes, such as isomerases, reductases, hydroxylases and several $Fe^{2+/2-}$ oxoglutarate-dependent dioxygenases modify the basic flavonoid skeleton, leading to the different flavonoid subclasses. At last, tranferases modify the flavonoid backbone with sugars, methyl groups and/or acyl moieties, modulating the physiological activity of the resulting flavonoids by altering their solubility, reactivity and interaction with cellular targets. Most of the sequential enzymes of the phenylpropanoid and flavonoid biosynthesis pathways are recovered in soluble cell fractions; immunolocalization experiments suggest that they are loosely bound to the endoplasmic reticulum (ER), possibly in a multi-enzyme complex (Falcone Ferreyra, Rius, and Casati 2012).

Some of these enzymes belong to the cytochrome-P450 family and possess in fact the ability of binding the membranes. On the other hand, some of the enzymes involved in

the biosynthetic pathway are loosely associated with membranes of other organelles, such as vacuole, plastids and nucleus. In particular, plastids from grapevine show the presence of the chalcone synthase (CHS) and leucoanthocyanidin oxidase (LDOX), the latter being described also in the nucleus. Such findings may suggest that a multi-branching distribution of the enzymes involved in flavonoid biosynthesis might correspond to a distinctive function during berry maturation (Petrussa et al. 2013).

So, as explained above, flavonoids are likely synthesized by a cytoplasmic multimeric complex, lightly or strongly bound to many different light-exposed cellular membranes (Buer, Muday, and Djordjevic 2007).

Cell-specific and intracellular localization of flavonoids has indeed been extensively investigated. Flavonoids were found in epidermal cells, including trichomes as well as within palisade and spongy mesophyll cells. Intracellular flavonoids also occur in various cell compartments such as chloroplasts, vacuole and nucleus where probably they exert their different biological activities (Mouradov and Spangenberg 2014).

Flavonoid transport

Flavonoids have evolved in vascular plants since the latter colonized the land and their transport through plant tissues and organs has a double pattern:

1. long-distance movement, where flavonoids move within the entire plant, from the source to the target organ;
2. short-distance movement, where flavonoids move within the cell or at least into the extracellular compartment.

1. Long-distance movement

The current and most accepted view is that flavonoids are synthesized in cells exposed to light (flavonoids are scarcely produced in plants or organs grown in the dark, because the expression of genes encoding for *chalcone synthase* –CHS is strictly light-dependent), where they accumulate and serve local functions. Nevertheless, they are also present in roots, contributing to lateral development and gravitropic response. Furthermore, there is evidence on the role of flavonoids during legume nodulation, the induction of the hyphal branching of arbuscular mycorrhizal fungi, as well as the response to phosphate starvation and the inhibition of polar auxin transport at the level of roots. All these pieces of evidence suggested that flavonoids may be transported from the light-exposed tissue all around the plant and to the roots too.

Aiming to show that endogenous flavonoids are capable of long distance movement, Buer et al. (2008) used a fluorescent probe (diphenyl boric acid 2-amino ethyl ester - DPBA) to detect flavonoid movement into flavonoid deficient *transparent testa4* (*tt4*) tissues: they demonstrate how flavonoids accumulated in tissues far away from the application site.

Other experiments using confocal microscopy analysis showed that, in flavonoid-pathway mutants of *Arabidopsis*, flavonoids accumulated inside cells and were not present in regions among cells, suggesting that the long distance movement of these molecules occurs and could be symplastic (Petrussa et al. 2013).

2. Short-distance movement

Short-distance movement is the most investigated flavonoid transport system at the cellular level and although wide information is easily available, the scenario is really articulated. Although some enzymes involved in flavonoid biosynthesis are present in many organelles, they are mainly synthesized in the cytoplasmic side of ER and then transported into the vacuole for storage or to other cellular compartments, as well as nucleus, plastid or extracellular space, where they can function as bioactive molecules.

The existence of multiple biological functions of flavonoids and the necessity to be transported from their biosynthetic site towards their final storage organelle, require efficient transport mechanisms.

In addition, the complexity of the flavonoid biosynthetic pathway and the large number of modified flavonoids that can be formed through the complex series of glycosylation/conjugations reactions suggest that distinct flavonoid molecules may exert many unique functions into fixed biological plant processes (Buer, Muday, and Djordjevic 2008).

The compartmentation of their synthesis, degradation and storage is achieved by a series of integrated processes controlled mainly by the permeability properties of the membranes and by the different physico-chemical conditions of membrane's compartments. As for humans, most secondary metabolites are toxic to the plant itself, which need an effective mechanism of sequestration from the cytoplasm immediately after synthesis. Once secondary metabolites have been transported to their target sites, they may interact with chemicals and/or proteins to form long-lasting structures, or be degraded by catabolic enzymes and/or chemical reactions for recycling in other metabolic pathways. The most common storage compartment in the cell for secondary metabolites is the vacuole. The central vacuole is the largest compartment of a mature plant cell and may occupy more than 90% of the total cell volume. Thanks to its acidic internal environment, this compartment may change the physical/chemical properties of secondary metabolites, avoiding harmful effects in the cells.

Many transport systems for secondary metabolites such as carotenoids, anthocyanins and alkaloids have been investigated in the vacuole membrane (tonoplast). Three principal mechanisms for vacuolar accumulation have been proposed: primary transport, catalyzed by ATP-Binding Cassette (ABC) transporters, secondary transport with H^+-antiport/uniport, and diffusion transport. The latter consists in a facilitated/passive diffusion where metabolites may passively equilibrate across the vacuolar membrane and be trapped into the vacuole by protonation, altered configuration due to the acidic environment, isomerization, complexation with ions, binding to phenolics or other vacuolar constituents and even crystallization (Roytrakul and Verpoorte 2007).

Unfortunately, nowadays it is still unclear what step connects flavonoid biosynthesis with their entering into the vesicular system involving or not ER and Golgi apparatus.

Considering the characterization on flavonoid transport systems in plant cells, four distinct non-exclusive, collaborative and well integrated mechanisms have been proposed: (i) autophagy-like pathway, (ii) membrane transporters, (iii) vesicle trafficking, (iiii) GST-mediated complex (Zhao 2015).

Autophagy-like pathway

Autophagy is the process by which materials are transported from the cytoplasm/extracellular compartment into the vacuole for degradation by membrane invagination. In autophagy-related pathways, double membrane vesicles called autophagosomes, are formed around the cytoplasmic cargo.

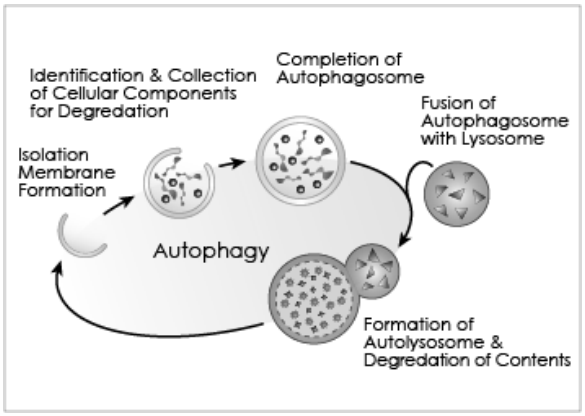

Figure 10. Scheme of the autophagy-related pathways (http://roguehealthandfitness.com/how-to-increase-autophagy-for-lifespan-extension/).

The autophagosomes move within the cell following the cytoskeleton structures and fuse with the vacuolar membrane, depositing the inner membrane cargo into the vacuolar compartment. A recent hypothesis connected this pathway to the anthocyanin vacuolar inclusions (AVIs). Vacuolar localization prevents anthocyanin from oxidation and the low pH environment confers the typical intense coloration, helping them to condensate into a compact, crystal form. This hypothesis contemplates the scenario that anthocyanins could be engulfed by autophagosomes and delivered to the vacuole. If anthocyanins are transported by vesicle trafficking, anthocyanins would not be surrounded by any membrane after fusion with the tonoplast,: the ER membrane would be melted with tonoplast membrane, releasing anthocyanins into the vacuolar lumen (Chanoca et al. 2015).

Recently, some authors found, surprisingly, that some AVIs were surrounded by a single membrane, compelling them to rethink current models. They proposed a mechanism that involves the tonoplast directly into the autophagy process (Figure 11) (Bassham 2015).

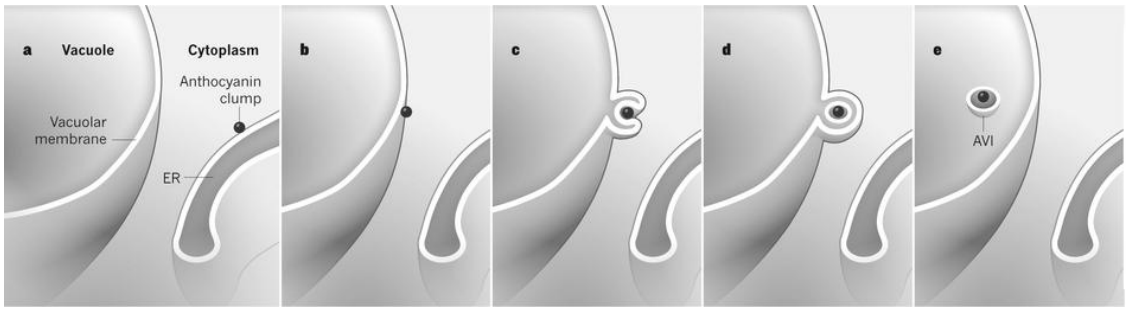

Figure 11. Schematic representation of the possible passive process of flavonoid internalization into vacuole (Bassham 2015).

Membrane transporters

Cells are separated from their external environment by a double phospholipid barrier, which ensures that certain ions, metabolic intermediates and macromolecules, such as proteins, remain within the cell. However, life is not possible without the exchange of material and information with the external environment. Therefore, during evolution, efficient transport systems have been developed to allow interaction with the environment, ensuring that essential ions and metabolites enter the cell and other compounds leave it. Many molecules are transported against a concentration gradient, requiring the use of energy. For several transport systems, this energy is directly provided by ATP hydrolysis. Well known examples of ATP-powered transport systems are ion pumps, such as the Ca^{2+}-, H^+-, Na^+/K^+-, and H^+/K^+- ATPases. This is the so-called *primary active transport*. On the other hand, a *secondary active transport* (also known as coupled transport or co-transport) exists. In this case, there is no direct coupling of ATP and the energy used to transport molecules across a membrane relies upon the electrochemical potential difference, created by ATPase proton pumping through the membrane (Figure 12) (Jasinski et al. 2003).

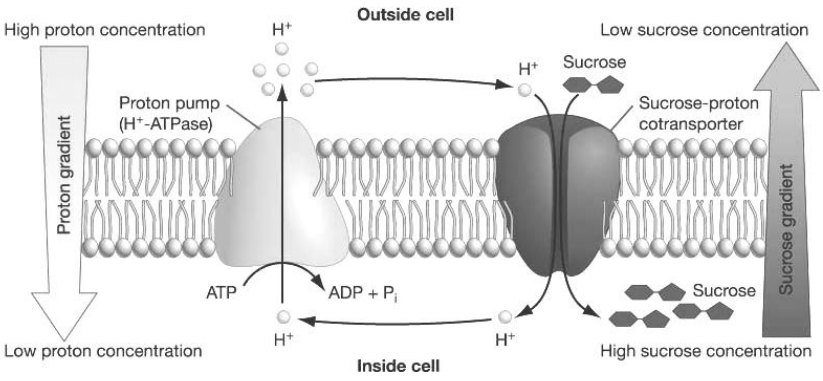

Figure 12. General scheme of secondary active transport (Jasinski et al. 2003).

A third system of transport doesn't require ATP hydrolysis to drive molecules across membrane, but only their concentration gradient. Within this group we find both *facilitated and passive diffusion*: in the first case the movement of molecules takes place using proteins (carrier or channels) that are embedded within the cellular membrane, in the second case molecules simply permeate membrane without the involvement of any kind of membrane proteins (Figure 13).

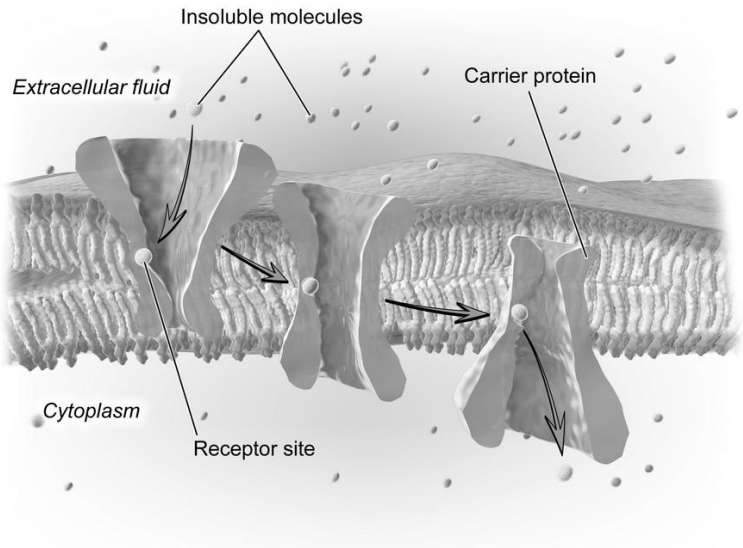

Figure 13. Scheme of facilitated transport, involving membrane protein (carriers) to drive molecules across membrane (https://en.wikipedia.org/wiki/Facilitated_diffusion).

Within the enormous class of protein-mediated transporters, the most important families of transporters ubiquitously found in "higher" eukaryotes are ATP-Binding Cassette (ABC), Major Facilitator Superfamily (MFS), and Multidrug And Toxic compound Extrusion (MATE). These transporter are involved in the acquisition of resistance to multiple structurally and functionally unrelated cytotoxic compounds. As with many other conserved gene families, those of the ABC and MATE appear significantly more expanded in plants than in bacteria, yeast or animals: the *Arabidopsis thaliana* genome encodes around 131 and 58 ABC- and MATE-type transporters, respectively (Remy and Duque 2014).

Primary active transport – ATP-binding cassette

Besides the well-known role in secondary metabolism and xenobiotic detoxification, ATP-binding cassette (ABC) transporters have also been claimed to play a role in sequestration of flavonoids into organelles like vacuole. The ABC transporter family is very large (79 members in *Escherichia coli*, 29 in *Saccharomyces cerevisiae*, and 131 in

Arabidopsis thaliana) and its members are found in all organisms. These proteins couple the hydrolysis of ATP to a direct translocation, through the membranes, of many substrates (lipids, heavy metal ions, inorganic acids, glutathione conjugates, sugars, amino acids, peptides, secondary metabolites, and xenobiotics, used as drugs), mainly after their conjugation with reduced glutathione (GSH), by a reaction catalysed by glutathione-*S*-transferases (GST). ABC proteins are able to transport a wide range of structurally and functionally unrelated compounds, thanks to their particular structure (Figure 14): they consist of two transmembrane domains (TMD) hydrophobic domains, which constitute the membrane- spanning pore and two cytosolic domains, which are referred to as the nucleotide-binding domains (NBD) or nucleotidebinding folds (NBF), as they contain the ATP-binding Walker A and B motifs (Kang et al. 2011).

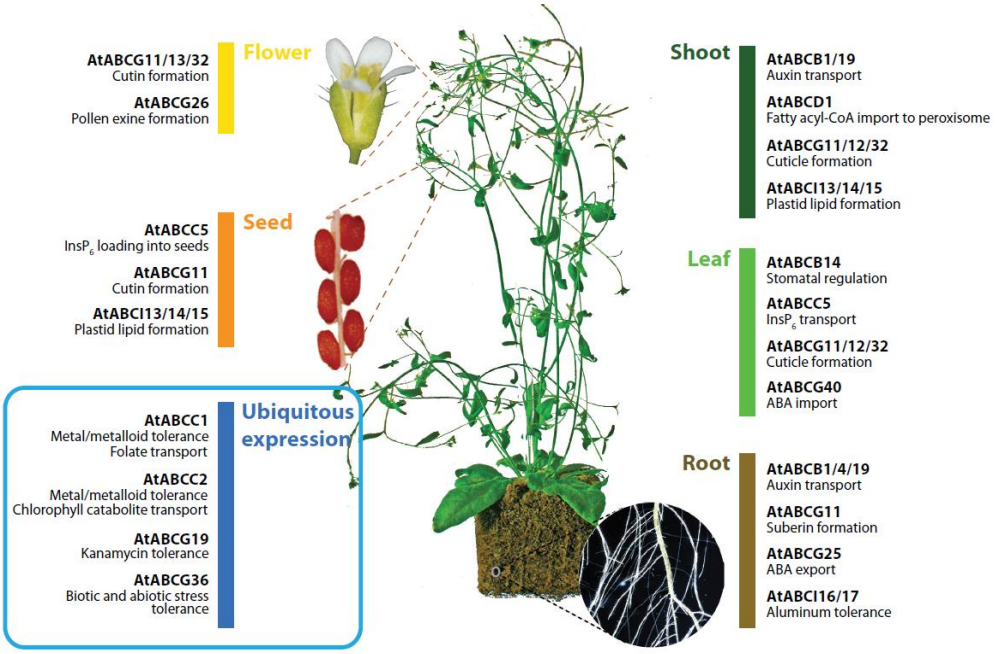

Figure 14. Scheme of the different iso-forms of ATP-binding cassettes expressed in different tissues of *A. Thaliana* (Kang et al. 2011).

Recently, it has been proposed that the above-mentioned large membrane units might contain multi-substrate binding sites, able to establish a variable number of Van der Waal's interactions with surrounding hydrophobic residues.

Plants genome contain many different open reading frame (ORFs) of ABC proteins, nearly twice in respect to ORFs of the genomes of the fly (*Drosophila melanogaster*) and worm (*Caenorhabditis elegans*) (Andolfo et al. 2015). However, although *Arabidopsis* is a plant with a particularly wide range of ABC transporters, new 121 ABC protein ORFs

have been identified in the next-best genomically characterized plant, rice (*Oryza sativa)*.

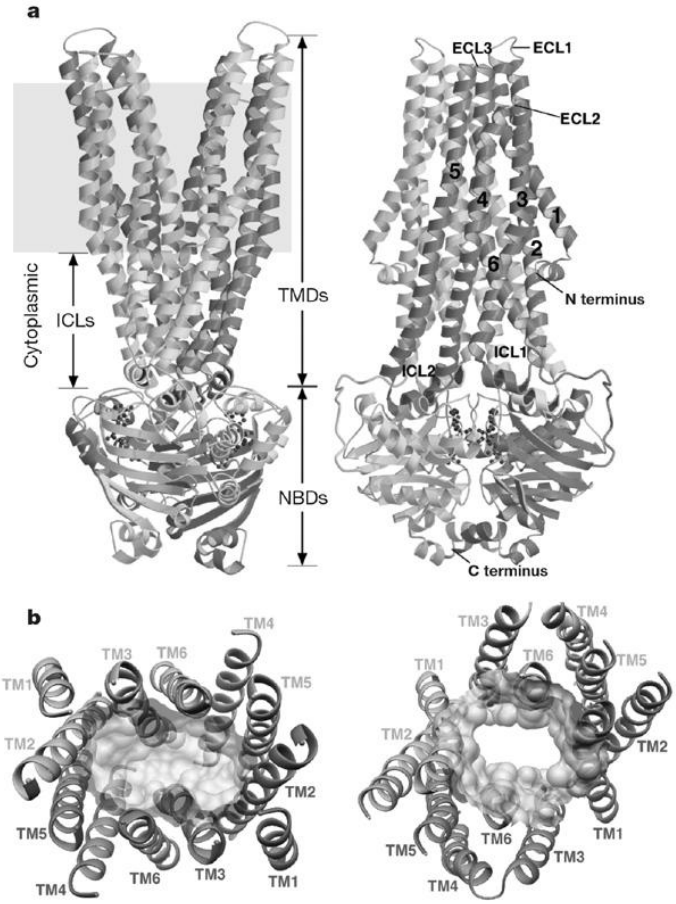

Figure 15. Structure of ABC multidrug transporters. a, View perpendicular to the cell membrane, in two orientations at right angles to each other. b, View in the plane of the membrane showing the substrate translocation pathway, from the intracellular (left panel) and extracellular (right panel) faces of the membrane. ICLs, intracellular loops (Higgins 2007).

The three best-characterized ABC subfamilies are multidrug resistance (MDR), multidrug resistance-associated protein (MRP) and the pleiotropic drug resistance (PDR) subfamilies (Figure 16) (Jasinski et al. 2003; Kang et al. 2011):

- multidrug resistance homologs (MDRs), representing the largest ABC transporter subfamily in plants (22 members in *Arabidopsis* and 24 in rice). Firstly identified in mammalian cells, they are mainly plasma membrane efflux pumps competent in the transport of large amphipathic neutral or weakly cationic species and/or in the translocation of cationic phospholipids. The two most studied plant MDRs are the member of the *Arabidopsis* subfamily, *AtPGP1* and *AtMDR1*. Both are clearly implicated in auxin transport. The properties of another *AtMDR*, i.e. *AtPGP4*

further substantiate the concept that plant MDRs, or at least a subset thereof, participate in auxin transport. *AtPGP4* is a root-specific auxin influx pump, because *Atpgp4* mutants are impaired in the basipetal redistribution of auxin in the root tip, and exhibit diminished linear and gravitropic root growth.

- multidrug resistance-associated protein homologs (MRPs), recently named ABCC subfamily, are the second largest ABC transporter subfamily in plants (16 members in *Arabidopsis* and 17 in rice). MRPs are forward-orientated and larger then MDR, consisting of at least 1500 amino acid residues, and contain three additional structures containing 5 putative transmembrane spans, a linker (L) domain contiguous with NBF1, rich in charged amino acid residues and a hydrophilic C-terminal extension. Many plant MRPs, like their yeast counterparts, are crucial for the vacuolar sequestration of both endogenous compounds and xenobiotics that are susceptible to conjugation with GSH and/or other adducts. (Francisco et al. 2013; Zhao 2015; Çakır and Kılıçkaya 2013)

  To date, five unique MRPs, *AtMRPs 1–5*, have been cloned from *Arabidopsis* and all five are capable of transporting GS-conjugates to different degrees *in vitro* and several are also competent in transporting other amphipathic anions, including glucuronate conjugates, linearized tetrapyrrole catabolites, and the essential vitamin cofactor folate and its derivatives.
- pleiotropic drug resistance homologs (PDRs) are encoded by over 15 ORFs in *Arabidopsis* and 23 in rice. Yeast PDR5, a reverse-orientation 1511-amino acid protein, is the prototype of this family. With a reverse orientation in respect to MDRs, yeast PDR5 is a plasma membrane-localized protein competent in the extrusion of a broad range of anticancer drugs, cyclic peptides and steroids. The first plant PDR genes to be identified were SpTUR2 in the aquaphyte *Spirodela polyrrhiza* and NpPDR1 (NpABC1) in tobacco (*Nicotiana plumbaginifolia*). The transcription of SpTUR2 is enhanced by a broad range of stress factors, including cold and salinity, but diminished by kinetins and antifungal diterpene.

Subfamily/Domains	Gene name	Localization	Function/Activity
MDR multidrug resistance 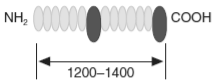	*AtPGP1*	Plasma membrane	Auxin export
	AtMDR1	Plasma membrane	Auxin export
	AtPGP4	Plasma membrane	Auxin import
	BR2	Plasma membrane	Auxin export
	DWF3	Plasma membrane	Auxin export
	CjMDR1	Plasma membrane	Berberine import
MRP multidrug resistance-associated protein 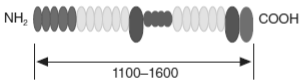	*AtMRP1*	Vacuolar membrane	GS-conjugate, glucuronide and folate transport
	AtMRP2	Vacuolar membrane	GS-conjugate, glucuronide and chlorophyll catabolite transport
	AtMRP3	Vacuolar membrane	GS-conjugate and chlorophyll catabolite transport
	AtMRP4	Plasma membrane	GS-conjugate and folate transport; stomatal regulation
	AtMRP5	Plasma membrane	Stomatal regulation
	ZmMRP3	Vacuolar membrane	Anthocyanin transport
	ZmMRP4	Vacuolar membrane	Anthocyanin transport
PDR pleiotropic drug resistance 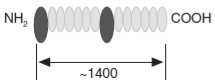	*AtPDR12*	Unknown	Lead tolerance
	NpPDR1	Plasma membrane	Sclareolide export and resistance to *Botrytis cinerea*
	SpTUR2	Plasma membrane	Sclareol export

Figure 16. Putative domain organization of the three largest ABC transporter subfamilies (Rea 2007).

There are three salient features of ABC protein-mediated transport in plants:
(i) it is directly energized by Mg-ATP, but not by free ATP or non-hydrolyzable ATP analogues, although other nucleoside triphosphates such as GTP or UTP can, depending on the transporter, partially replace ATP;
(ii) transport is insensitive to the transmembrane H^+ electrochemical potential difference. The dissipation of the transmembrane pH gradient and electrical potential, established across plant membranes by primary H^+ pumps, by the addition of protonophores or ionophores does not usually inhibit transport;
(iii) transport is specifically sensitive to vanadate, while is insensitive to bafilomycin, a specific inhibitor of vacuolar (V-)ATPases. In the presence of vanadate, a metastable analogue of Mg-ATP, ABC proteins establish a tight complex with nucleoside diphosphates. Vanadate thereby arrests the catalytic cycle by substituting for the released phosphate and trapping the other product of hydrolysis, ADP, in the nucleotide-binding site (Rea 2007; Martinez and Falson 2014).
Multidrug transporters, whether from *Escherichia coli* or an elephant, have similar (but not identical) multispecificity for many relatively lipophilic, planar molecules of molecular weight less than around 800 Da that are often, but not exclusively, weakly cationic (Fig.17) (Higgins 2007).

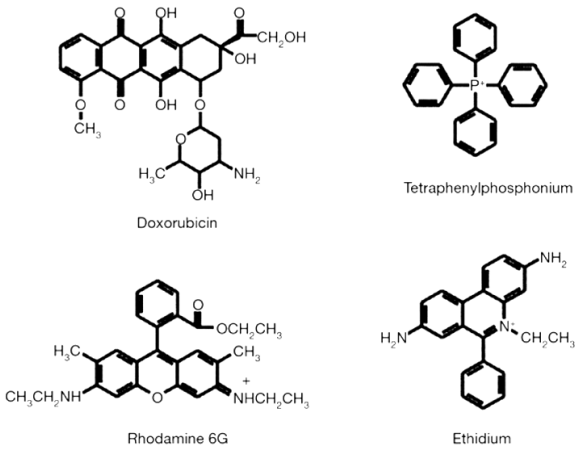

Figure 17. Chemical structures of lipophilic, planar molecules, substrates of multidrug transporters (Higgins 2007).

Among the huge number of substrates involved, ABC transporters are also able to transport flavonoid glycosides, glucuronides and glutathione conjugates to the vacuole. The involvement of a subfamily of the ABC transporters, the multidrug resistance-associated protein (MRP/ABCC)-type (also named glutathione *S*-conjugate pump), in the transport of glutathionated anthocyanins has been previously suggested by mutant analysis in maize and petunia and also in *Vitis* (Higgins 2007).

Secondary active transport - MATE

Multidrug and toxic compound extrusion proteins (MATE) make up the most important and representative family of secondary active transporters, which exploit the membrane electrochemical gradient, maintained by ATPase and/or PPiase pumps, for their transport activity. Members of this transporter family are ubiquitous in all the organisms, including human and plants. Most of the earlier studies suggested that MATE proteins generally act as efflux pumps that export drugs and xenobiotic compounds outside the cell and largely contribute to drug resistance in bacteria (Tiwari et al. 2014).

The establishment of a proton gradient between the cytosol and the vacuole (or the apoplast) by H^+-ATPases (and H^+-PPiases in the tonoplast) has been proposed as the main driving force for transport of some flavonoids (anthocyanins in particular) into vacuole. Once these compounds are in the vacuole, the acidic pH inside the vacuolar compartment and the acylation of flavonoids are both necessary for the induction of a conformational modification, responsible for the appropriate trapping and retention of the metabolites (Petrussa et al. 2013).

Recently the chemical properties of flavonoids under pH influence have been investigated and the hypothesis that flavonoid permeability characteristics depends on it has been supported by a large consensus (Jurasekova et al. 2014; Tarahovsky et al. 2014). Flavonoids are usually formed by at least seven functional groups, each of them characterized by different pK values, thus conferring to the moieties many chemical pH-dependent structures (Figure 18).

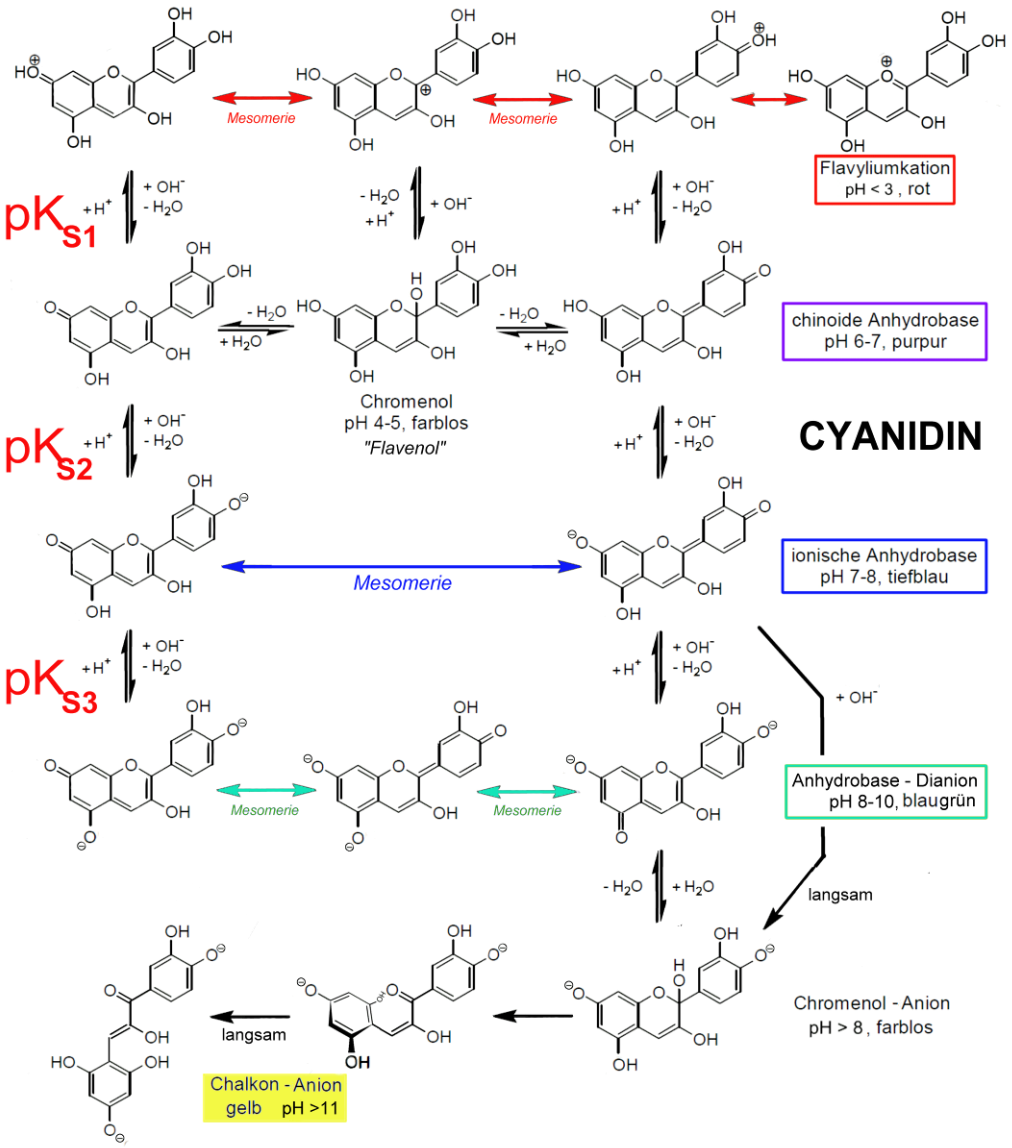

Figure 18. Chemical modifications on carbon structure of flavonoids under different pH conditions (Jurasekova et al. 2014).

The first member of MATE family was originally characterized in *Vibrio parahaemolyticus*; however, orthologues in higher organisms have been characterized only

in recent years, and some plant MATE members showed particular physiological functions, with strict transport substrate specificity. *Arabidopsis* contains 58 MATE transporter genes in its genome. This family is remarkably numerous if compared to the human counterpart (only 2 members), although only recently the functions of some members have been elucidated (Yazaki et al. 2008).

Depending on the established functions of this gene family in plants, MATEs have been classified into three major classes. The first group has been demonstrated to be associated with disease resistance in *Arabidopsis*. Several *enhanced disease susceptibility* mutant (*eds5*) of *Arabidopsis* have been identified and examined for understanding the molecular mechanism of pathogen resistance. A second group of MATE proteins is known for exporting outside the cell small organic molecules such as citrate, which acts as a ligand molecule to bind aluminium (Al) in the rhizosphere. Unlike other metals, Al toxicity is much pronounced in acidic soil and several genetic studies were performed to map the *locus* responsible for Al tolerance in plants. The third group of MATE transporters are mainly involved in trafficking of secondary metabolites in vacuoles. Usually, vacuoles are the major repository site of most of the conjugated form of flavonoids, mainly comprising flavonols, anthocyanins and flavone glycoside. The transport and storage of these flavonoids into the vacuole are mediated by the different classes of transporters localized on tonoplast. A member of MATE gene family (*TT12*) was elucidated for sequestration of proanthocyanidins in vacuoles of seed that leads to pigmentation of seed coat. The kinetic study of vesicles isolated from *TT12* expressing yeast revealed that it can specifically transport glycosylated form, like epicatechin 3′-O-glucoside and cyanidin 3-O glucoside or mediates the antiport of H^+/acylated anthocyanins. Consistent with *TT12*, MATEs from *Medicago* and *Vitis* have been characterized for mobilization of flavonoids in cell organelles. Similar to the role in vacuolar flavonoids sequestration, MATE proteins are also recognized for alkaloids trafficking into vacuoles in tobacco (Tiwari et al. 2014; Gomez et al. 2009).

Facilitated/passive transport

The hydrophobic region in the middle of membrane phospholipid bilayer is a barrier to any large, charged, or hydrophilic molecule. Therefore, simple diffusion is the slow unassisted passage of small, hydrophobic, non-polar molecules from higher concentration to a lower concentration that does not depend on genes expressing of specific membrane transport proteins. Diffusion of gasses, for instance, is very important in plants, since it is the only modality for their movement within the plant body.

So, although small substances soluble in lipids could easily diffuse through the membrane, substances that have an hydrophilic moiety are prevented to pass freely through the membrane; their movement has to be facilitated by proteins.

Facilitated diffusion is a passive transport mechanism based on integral membrane proteins that enable larger, charged, hydrophilic and polar molecules to be transported across membranes exploiting a concentration gradient. These integral membrane proteins span the phospholipid bilayer, connecting the inside to the outside of the cell and/or the subcellular compartment.

There are two types of integral membrane proteins that help the transport of molecules. The first are carrier proteins, which are proteins able to bind a molecule and facilitate its transport through a cell membrane, using a sort of "flip flop" mechanism. The second are channel proteins, which are proteins that create a passageway through the membrane to transport molecules and ions to the other side of the membrane. This channel protein creates a pore through the hydrophobic region that allows polar molecules to just pass right through (Klein and Roos 2009).

Transport rate reaches a maximum when all of the transporters are occupied by their substrates (saturation). Facilitated diffusion is very specific: it allows cell to select substances for uptake. It is sensitive to protein modifiers, which react with protein side chains. Few are the examples of facilitated passive transport of secondary metabolites, such as oleanolic monoglucuronide in Calendula (Szakiel and Janiszowska 2002) and sucrose in sugar beet (Jung et al. 2015; Willenbrink and Doll 1979).

Recently a new interest raised upon the role of this transport mechanism on flavonoid movement across the membranes, particularly taking in consideration their strong importance in mammalians.

Flavonoid affinity to animal cell membranes seems to be influenced by degree of hydroxylation, molecular conformation, length of the side chain of flavonoids and eventually chemical modifications. Using a model of permeation (passive) assay based on intestinal Caco-2 membrane, Tian et al. (2009) discovered that some flavonoid glycosides (like myricitrin and isoquercitrin) exhibited very low rate (<5%) of cell accumulation, while isoflavonoids and flavonoids aglycone exhibited an accumulation rate of <20%. For flavonol aglycon and methylated flavonol aglycon, the cell accumulation was relative high (>25%). Quercetin exhibited a cell accumulation capacity close to 30% while galangin and kaempferide exhibited the highest cell accumulation value of ~60%.

Brand et al. (2008) demonstrated that the use of specific inhibitors of ABC transporters did not affect the permeation of a common juice flavonoid (hesperetin aglycone) across an artificial intestinal membrane based on Caco-2 monolayers. This evidence indicates

that the small and relatively lipophilic hesperetin molecule moves through the Caco-2 monolayer by passive transcellular diffusion (i.e., not transporter-mediated).
Considering a large spectrum of different cell types and flavonoids, Gonzales et al. (2015) showed that flavonoids are differently taken up in different cell types. The "classical" absorption pathway of flavonoids is passive diffusion through the cell membrane, although membrane transport proteins also play a crucial role in cellular flavonoid absorption. In addition to the well known flavonoid transporters described in the previous paragraph, particular importance has been given to solute carriers (SLCs): this class of transporters include organic anion transporting polypeptide (OATP), intestinal apical cells proteins that play a relevant role in the uptake of quercetin in Caco-2 cells at low pH, whereas passive diffusion is responsible for transport at higher pH. In other cellular models (HEK 293, HepG2 and RBE 4), quercetin seems to passively cross the membrane too (Gonzales et al. 2015).

Vesicle trafficking

Cell biology studies have shown that anthocyanins or proanthocyanidins (PAs) can be transported into the central vacuole via vesicle trafficking in a Golgi-dependent or independent mechanism (Zhao and Dixon 2010). Recent observations in grapevine hairy roots and *Arabidopsis* seed endothelium cells further demonstrate that small vesicles filled with anthocyanins or PAs are moved toward the central vacuole (Gomez et al. 2011). The process of vesicle trafficking from the ER to the vacuole usually includes several parallel pathways. ER-derived small vesicles filled with flavonoids move forwards and fuse with destination membranes. The first committed step required for vesicle trafficking is loading flavonoids into the ER lumen. Unfortunately, little is known about this process.
Three flavonoid-loading hypotheses have been proposed:
i) flavonoid transporters of ER–Golgi secretory vesicles system, may transport flavonoids into secretory vesicles, as they localize to the small vesicle or the Golgi pool;
ii) the GST–flavonoid complex is membrane associated, which may facilitate flavonoid loading into ER vesicles, vesicle fission, and fusion dynamics. Several pieces of evidence support the involvement of GSTs in loading flavonoids into small vesicles and thereafter trafficking towards their destinations;
iii) flavonoids may also be loaded into the ER as soon as they are synthesized on the ER via other unknown mechanisms (Zhao 2015).

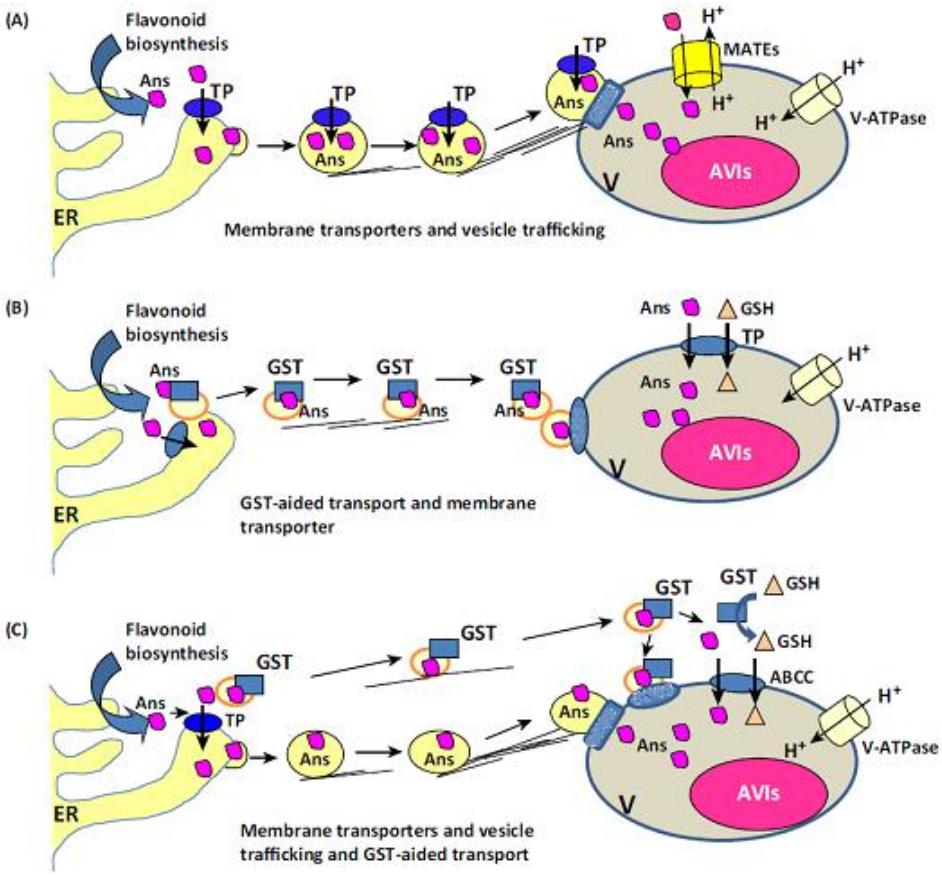

Figure 19. Trafficking models of vesicles filled with anthocyanins (Ans) from the cytosolic side of the endoplasmic reticulum (ER) to the vacuole (V). Membrane transporter (TP), glutathione S-transferase (GST), multidrug and toxin extrusion (MATE), g lutathione S-transferases (GST), ATP-binding cassette (ABCC), glutathione (GSH), anthocyanin vacuolar inclusions (AVIs) (Zhao 2015).

Glutathione S-transferases (GST) mediated complex

Glutathione (GSH) is an essential antioxidant system present in plants, animals, fungi, some bacteria and archaea. GSH is a tripeptide capable of preventing damages caused by reactive oxygen species such as free radicals, peroxides, lipid peroxides and heavy metals (Figure 20).

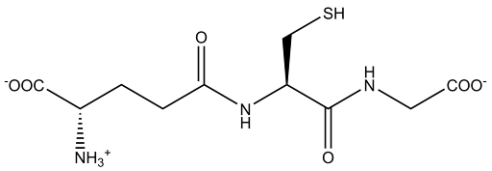

Figure 20. Chemical structure of glutathione

Together with ascorbate, GSH represents one of the most common antioxidants of plant cells. Glutathione reduces accessible disulfides cytoplasmic proteins, by serving

as an electron donor. A GSH-deficient mutant of *Arabidopsis thaliana*, *gsh2*, displayed defective secretory trafficking with the appearance of small vacuole-like vesicles and disappearance of the large vacuole (Au et al. 2012). GSTs that are involved in vacuolar flavonoid accumulation may not catalyze flavonoid glutathionation, but rather physically bind to flavonoids and act as shuttle proteins for flavonoid. Probably they facilitate flavonoid transport from the cytoplasm into the vacuole by an indirect activity, since they enable flavonoid binding to membrane transporters. GSTs were also associated with membranes, likely ER and vacuole, in plant cells that produce high levels of anthocyanins.

Genetic studies have shown that multidrug resistance-associated protein (MRP)/C-type of ABC (ABCC) transporters, such as maize MRP1, are involved in anthocyanin accumulation, with the assumption that they transport flavonoid conjugates with glutathione (GSH). Only recently it was shown that free GSH is strictly required for transport of an anthocyanin, malvidin 3-O-glucoside (M3G), into yeast vacuoles over-expressing grapevine ABCC1 (Francisco et al. 2013). *In vitro* assays demonstrated that, although ABCC1 mediated simultaneous vacuolar sequestration of both M3G and GSH, neither structural alterations of M3G nor formation of a GSH–M3G conjugate were detected during the transport process. Therefore, grapevine ABCC1 is a GSH-dependent anthocyanin transporter, rather than an anthocyanin–GSH transporter (Zhao 2015).

Flavonoid role in plants

Biological functions of flavonoids in plants

Flavonoids constitute a variegated array of plant secondary metabolites that perform a wide range of physiological and ecological functions. Although the role of flavonoids as visible pigments in angiosperms is well known, this function was acquired late in evolution (Rausher 2006). The probably more ancient functions of flavonoids include internal regulation of hormone transport and signalling, roles in plant structural integrity, UV photoprotection, and plant communication with insects and microbes, either as attractants or repellents, and defence against pathogens and herbivores. They provide protection against stress, by acting as scavengers of free radicals such as reactive oxygen species (ROS) and they exert chelating activity when metals are present into the rhizosphere. At least their biological functions are linked to their potential direct cytotoxicity and their interaction with enzymes through protein complexation and activity modulation (Falcone Ferreyra, Rius, and Casati 2012) (Figure 21).

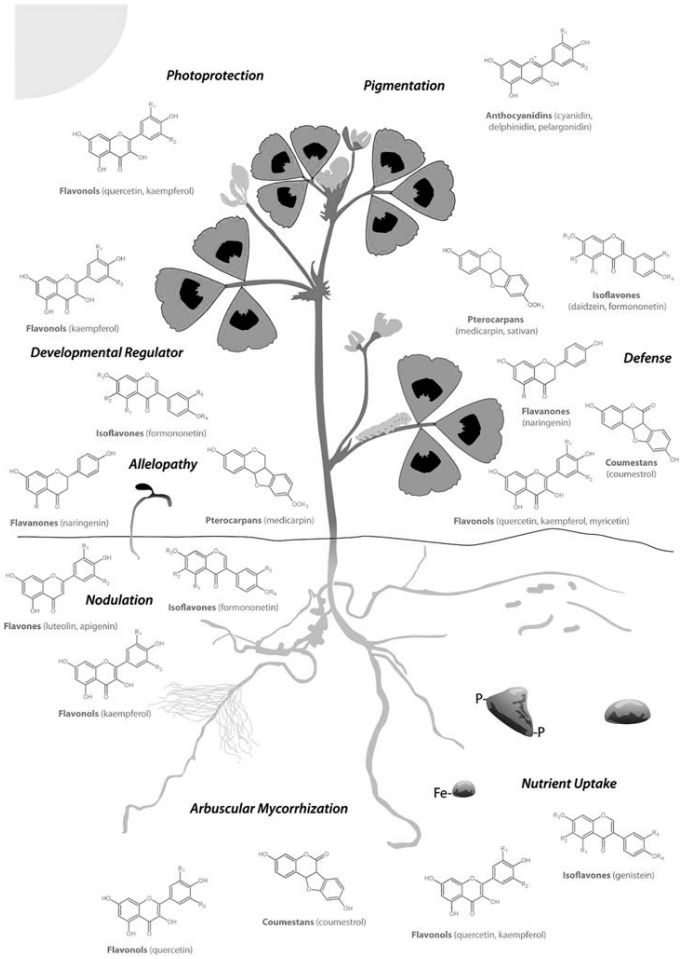

Figure 21. Scheme of different flavonoids used by plants in different environmental conditions (Gholami et al. 2014).

Hormonal regulation and signal control

During their physiological growth and development, plants synthesize a wide variety of flavonoids in organs like shoots, where usually cells are under strict hormonal control (Samanta, Das, and Das 2011).

Recent studies confirm the presence of an indirect link between flavonoids and plant architecture that for sure involves auxin transport. Flavonoid-defective mutants (like Arabidopsis *tt4* mutant, which is defective in flavonoid biosynthesis) display a wide range of alterations, including alterations of root growth, gravity sensibility, lateral root density, root hair development and length, shoot/flower organ number, overall architecture and stature, and seed organ density.

Moreover, normal root architecture and gravity response can be restored in some mutants by direct flavonoid supplementation. For example, adding naringenin to the media restores the looping *tt4* root phenotype (Figure 22, panel A) to that of the wild type (panel B) (Peer et al. 2001).

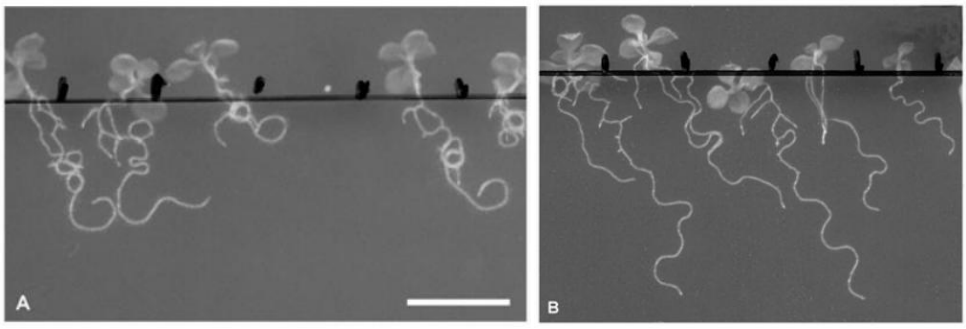

Figure 22. Effect of external neringenin administer (panel B) in roots conformation of looping *tt4* root phenotype (panel A) (Peer et al. 2001).

Even the morphology and cell membrane structure of prokaryotic organisms capable to photosynthetize like cyanobacteria, are strongly affected by flavonoid like 5,4'-dihydroxyflavone and apigenin and this interaction can influence the photosynthetic apparatus too (Huang et al. 2015). Other experiments with Arabidopsis *tt* mutants show an accumulation of quercetin in the distal elongation zone compared with the wild-type plants. As quercetin is a potent inhibitor of auxin transport, these mutants have different gravity responses and so a possibly greater alteration of auxin transport. Considering the action of flavonoid as spanning beyond the plant kingdom, recently it has been shown that these secondary metabolites are able to bind mammalian actin and affect its rate of polymerization. In this case, a direct interaction of flavonoid with molecules involved in cytoskeleton organization of the cell was observed. Similar

experiments conducted in plants, showed an auxin/actin interaction, that can have effects on gravitropism in rice (Buer, Imin, and Djordjevic 2010).
A recent study took in consideration the interaction between flavonoid and two important growth regulators: the hormone ABA (abscisic acid) and the molecule ALA (5-aminoevulinic acid). It was already known that flavonols accumulate in guard cells of *Arabidopsis thaliana*, but not in surrounding pavement cells, and in these cells they control the ABA-induced ROS content, a key messenger of stoma movement (Watkins, Hechler, and Muday 2014).
But An et al. (2016) went further, demonstrating how quercetin and kaempferol production could be improved by a treatment with ALA, and how these flavonols are accumulated into the guardian cells of the stoma where they might play an important role in the inhibition of ABA-induced stomatal closure.

Enzyme regulation and membrane interaction

Flavonoids have several bioactivities in plants and animals. Surprisingly, a better understanding of the interacting partners for flavonoids exists in animals, in respect to the complicate scenario that is present in plants. Flavonoids interact with plasma membrane and cytosolic targets, and some similarities exist between plant and mammalian molecular targets, like proteins and enzymes. For example, a potential pharmacological effect of flavonoids is their ability to inhibit the P-glycoprotein MDR1, an integral membrane protein in mammals with similarity to the plant auxin efflux protein, PIN. Similarly, the activity of plant peroxidases that destroy auxin is also affected by flavonoids (Buer, Imin, and Djordjevic 2010).
It is already known that flavonoids, and in particular quercetine, affect membrane ion transport, by inhibition of Ca^{2+}, Mg^{2+} ATPase, Na^{+}, K^{+} ATPase, mitochondrial ATPase, cAMP- and cGMP-phosphodiesterase (Graziani and Chayoth 1979). Quercetin in fact is also known to inhibit the enzymatic activities of alkaline phosphatase, phospholipase A2 and protein kinases. Ca^{2+} influx and/or Ca^{2+}metabolism are also influenced by quercetin. By acting as an antioxidant, quercetin seems to interact with phospholipid bilayers too, suggesting that membranes would be one of its main targets, in a chemical system that strongly depends on pH (Pawlikowska-Pawlęga et al. 2007).

Pollen fertility, pollination and seed dispersal

Flavonoids like anthocyanins are intensely coloured and provide a wide range of red to blue colours in flowers, fruits and leaves. Others, like the flavones, are essentially colourless and provide the whiteness of white flowers and also act as co-pigments for the widespread anthocyanins. One of the best established function of flavonoid

pigments is shown to be the provision of flower colours for pollinators. Plants that are insect-pollinated generally have flowers with large, brightly coloured petals, in contrast to most wind-pollinated plants whose flowers are small, dull, and often apetalous. Pigmentation presumably acts as a signal to attract pollinating insects or birds. Thanks to a co-evolution between plants and insects/birds eye' system, flavonoids can determine which vector is attracted to effect pollination. It is clear that bees generally prefer blue and yellow, butterflies pink or white, birds red, and moths white flowers (Figure 23).

Flavonoids in fruits probably serve to attract frugivores, useful in seed dispersal. This is especially important for larger plants such as trees, whose seeds need to be transported to some critical distance away from the parent to ensure germination.

Besides attracting pollinators, flavonoid pigments also play important roles in pollen germination and pollen tube growth, though mechanisms still unclear.

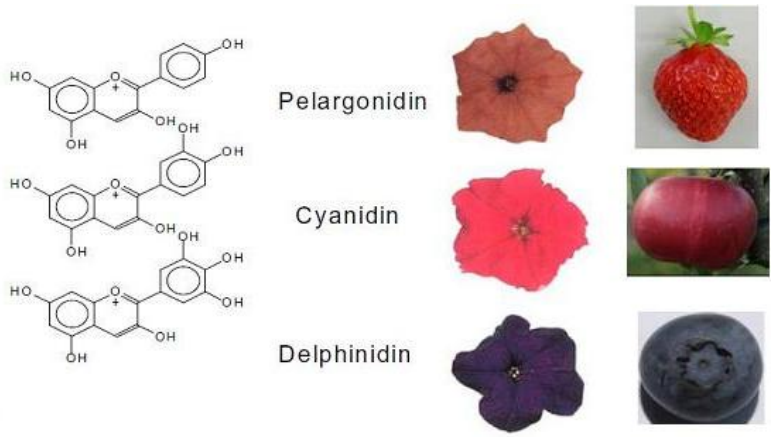

Figure 23. Chemical structure of three common anthocyanins and their presence in three edible fruits (Halbwirth 2010).

The unique structure and combination of different flavonoids in each species produce yellow pollen with a range of visible and UV reflection spectra that can be detected by the targeted insects and larger animals, so facilitating successful pollination. Flavonoids impart a distinctive yellow colour to pollen and they can represent 2–4% of the dry weight. The correlation between pollen fertility and flavonoids was first established in wind pollinated maize, with its numerous and well-characterized anthocyanin mutants. These mutants were not only deficient in flavonoids, but were also male sterile due to their failure to produce a functional pollen tube. This deficiency could be reversed by adding the flavonol kaempferol at pollination. The silencing of gene involved in flavonoid biosynthesis results in parthenocarpy, causes

production of less-seeded fruits in tomato plants and the pollen of these silenced lines are unable to produce functional pollen tubes. This capacity can be reversed with quercetin (*in vivo* and *in vitro*). All these evidences imply that flavonols (quercetin in particular) have essential roles in pollen germination and consequently in plant fertility (Mahajan, Ahuja, and Yadav 2011). Similar analyses performed on *Arabidopsis* mutant plants, showed however fertile plants with no pollen tube growth aberrations, indicating that flavonols are not universally essential for pollen fertility (Falcone Ferreyra, Rius, and Casati 2012).

Responses against biotic stress

When microorganisms infect plants, the latter produce an extremely high number of organic compounds with enormous chemical diversity. Many of these secondary plant products have antimicrobial activities and are considered to be part of the cellular defence system of the plant against microbial phytopathogen attack. These chemicals, known as phytoalexins, include phenolics, stilbenoids, alkaloids, terpenoids, coumarins, polyacetylenes, and flavonoids (Figure 24) (Yamane 2013).

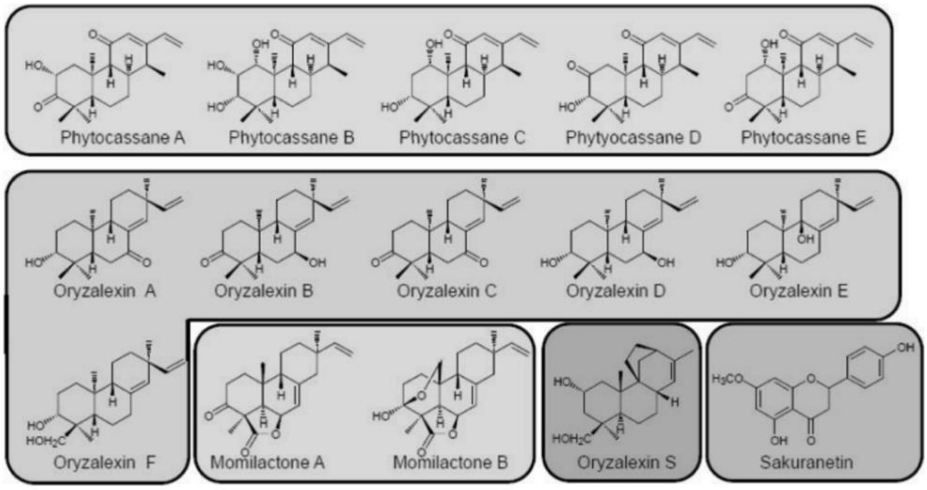

Figure 24. Scheme and chemical structures of the most common phytoalexins present in rice (Yamane 2013).

About the latter group, many different papers reported their biological actions: isoflavonoids are characterized by a migration of the phenyl ring and are principally involved in the defence response of legumes against pathogens. In lotus species, the main phytoalexin synthesized is vestitol, which belongs to the class of isoflavans; rhamnetin, a flavonol aglycone (3,5,3',4'-tetrahydroxy-7-O-methoxyflavone), was reported as the first phytoalexin in cucumber; finally the synthesis of C-glycosyl flavonoid phytoalexins was reported as a site-specific response to fungal penetration

in cucumber. Phytochemical analyses and fluorescence microscopy observations revealed the production of autofluorescent C-glycosyl flavonoid phytoalexins within the epidermal tissues of disease-resistant plants undergoing fungal entry (Samanta, Das, and Das 2011).

According to the phytochemical co-evolution theory, the secondary metabolites are likely to be the most important mediators of plant-insect interactions too. Thus, both plants and insect herbivores have co-evolved proper systems leading to a balnce between the plant defence and herbivore offense. The mechanisms of stress response seem to be so connected in an evolutionary stable system that the response to herbivore or pathogen attack is shared with other plant stress responses, such as high UV radiation. It seems in facts that some genes associated with the response of *Nicotiana longiflora* plants to insect herbivory were also induced by UV-B radiation (Izaguirre et al. 2003). Furthermore, genes regulating the phenyl-propanoid pathway that leads to the synthesis of phenolic compounds like flavonoids are regulated by both UV light levels and herbivores interactions. Thus, plants present a strong connection between the pathways of reaction to biotic (microorganisms) and abiotic (UV-B radiation) stresses. In the first case they act through the synthesis of defence-related compounds, such as phytoalexins and lignin as structural barriers to restrict pathogen spread, while in the second case they modify the expression of genes involved in the production of protective metabolites, such as flavonols.

During microbial interaction, there is a sharp and rapid up-regulation of genes encoding enzymes involved in the phenylpropanoid pathway, in particular for the synthesis of isoflavones and isoflavanones. The responses of soybean to avirulent and virulent strains of the bacterial pathogen *Pseudomonas syringae* pv. glycinea show a down regulation of genes involved in anthocyanin branch of the flavonoid pathway, while the largest group of up-regulated genes are those involved in the flavone and isoflavone biosynthesis. Thus, it is suggested that the opposite regulation of these branches enhances production of isoflavones that act as antioxidants and antimicrobial compounds *vs.* those responsible for flower and fruit colour.

One type of natural maize resistance towards corn earworm pest (*Helicoverpa zea*) is associated with the presence in silks of a C-glycosyl flavone (maysin), as well as related compounds like apimaysin and methoxymaysin. These compounds are insecticidal to *H. zea* larvae and are thought to interfere with the amino acid metabolism in the insect gut, through their subsequent conversion to more toxic quinines (Falcone Ferreyra, Rius, and Casati 2012).

Photoprotection

The spectrum of UV radiation reaching the earth's surface has been divided into lower energy UV-A (320-400 nm), higher energy UV-B (280-320 nm) and UV-C (254-280 nm) regions. The most severe damages are caused by UV-B radiation since it affects photosynthesis and transpiration, pollination and DNA. It also induces changes in plant foliar chemistry, including decreases in carbohydrate concentration (Samanta, Das, and Das 2011).

Flavonoids have long been suggested to play multiple functions in photoprotection. This function, largely depends on their cellular localisation and transport mechanisms. Early views suggest that flavonoids were mostly located in the wall and the vacuole of epidermal cells and in external side of the organs (such as trichomes). But, depending on sunlight irradiance, flavonoids are also found in the leaf interior (palisade and spongy mesophyll cells), and in particular into the nucleus, the chloroplast and the vacuole (Agati and Tattini 2010).

Flavonoids generally absorb UV-B band and thus act as UV filters, reducing epidermal penetration of UV-B radiation without interfering with photosynthesis. Old and recent evidences suggest that flavonoids served important roles during the establishment of plants on the land that may go beyond their UV-B screening capacities. When plants moved from water, carbon-based flavonoids replaced mycosporyne-like aminoacids (nitrogen-rich MAAs, usually detected in algae) as UV-B screening pigments, although flavonoids, particularly flavonols, have much lesser ability than MAAs to absorb wavelengths over the 290/320 nm range (Figure 25).

Therefore, flavonoids have been hypothesized to play a primary role by scavenging ROS rather than avoiding light-induced ROS-generation by UV-B protection. It may be not a mere coincidence that flavonols display the greatest antioxidant potential, but the less effective UV-B screening potential among the thousands of flavonoid structures encountered in plants. This is consistent with the previous hypothesis that UV-absorbing flavonoids may have evolved from other ancestral roles to later fulfil UV-B screening functions, as a consequence of the evolution of different branches of the general phenylpropanoid and flavonoid biosynthetic pathways when early plants colonized the land. UV-B radiation is not a pre-requisite for the biosynthesis of flavonoids, and the very same 'antioxidant' flavonoids accumulate because of sunlight in the absence or in the presence of UV-radiation (Agati and Tattini 2010).

Metabolite	Molecular structure	λmax (± 2nm) over UV-B/UV-A	$\int_{290}^{320} \varepsilon$	$\int_{321}^{390} \varepsilon$
p-Coumaric acid	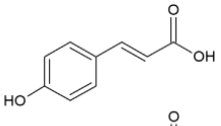	312	4.5E+05	0.048E+06
Caffeic acid	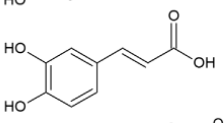	327	4.6E+05	0.66E+06
Apigenin-7-O-Glc	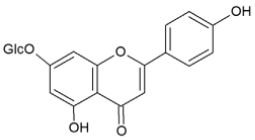	337	3.9E+05	0.92E+06
Luteolin-7-O-Glc	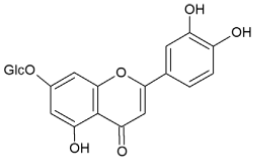	348	2.5E+05	0.81E+06
Quercetin-3-O-Glc	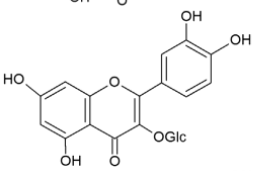	355	3.5E+05	1.0E+06
Kaempferol-3-O-Glc	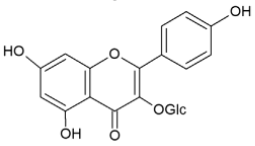	351	3.9E+05	1.3E+06
Mycosporine-glycine	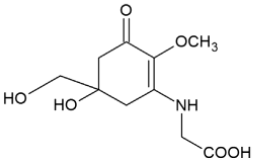	310	7.2E+05	0.97E+06

Figure 25. Chemical structures of flavonoid glycosides and mycosporine together with their UV-spectral properties. Molar extinction coefficients have been integrated over 290–320 (UV-B) and 321–390 nm (UV-A) spectral regions (Agati and Tattini 2010).

A different prospective must be taken when we consider the role of anthocyanins in the photoprotection system. Anthocyanin biosynthesis is just one component of a suite of metabolic adjustments made in response to high sunlight irradiance. Since the constitutive morpho-anatomical traits of a leaf can, to some degree, control the extent to which sunlight affects its biochemistry, the significance of possible photo-protective functions of anthocyanins may vary substantially. When the incident radiant flux exceeds the plant's ability to utilize or dissipate that energy, the exceeding excitation energy within the photosynthetic apparatus can lead to impairment of chloroplast performance, as revealed by a rapid decline in quantum efficiency of photosystem II (PSII), and a decrease in carbon fixation. Plants have developed various mechanisms (both morphological and physiological) to avoid or accommodate excessive irradiance,

such as leaf or chloroplast movement, ROS scavenging systems, dissipation of absorbed light energy as heat, activation of cyclic electron flow and photo-respiratory pathways. The biosynthesis of UV- and visible light-absorbing compounds (e.g., phenylpropanoids) may further contribute to attenuate the burden of irradiance excess. There is substantial empirical evidence that foliar anthocyanins can protect chloroplasts from the adverse effects of excess light, since they have the potential to reduce both the light incidence and the severity of photo-oxidative damage by intercepting a portion of supernumerary photons that would otherwise strike the chloroplasts, thus increasing the ROS production and ROS-triggered damage. Anthocyanins, by absorbing a fraction of the yellow/green and ultraviolet wavelengths, may significantly reduce the damage to PSII (Figure 26).

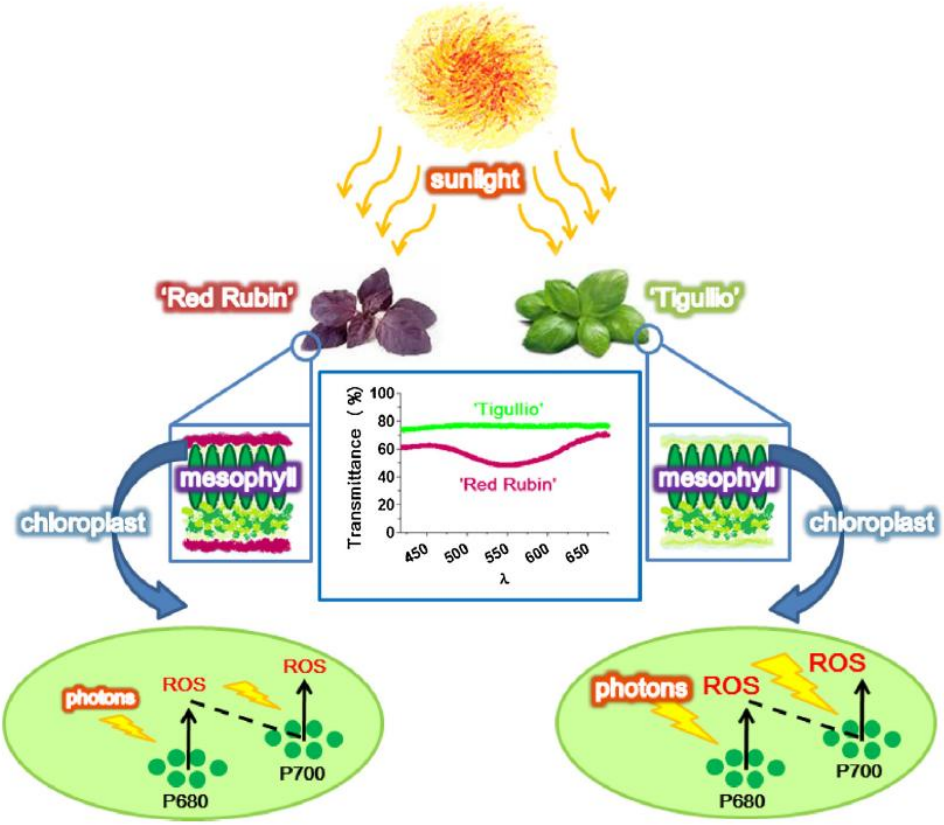

Figure 26. Sunlight attenuation mechanism proposed for anthocyanins in leaves of red (cv 'Red Rubin') and green basil (cv 'Tigullio') (Landi, Tattini, and Gould 2015).

Some anthocyanins have the capacity to absorb parts of the UV-A (315–400 nm) and UV-B (280–315 nm) spectra in addition to visible wavebands. The common anthocyanin glycosides have negligible molar absorption coefficients in the UV region, but after acylation with phenolic acids, anthocyanins may contribute substantially to

UV protection. Since acylated anthocyanins are not as common as the non-acylated forms, their UV-absorbing functions are unlikely to play a universal primary role for anthocyanins in plants (Figure 27) (Landi, Tattini, and Gould 2015).

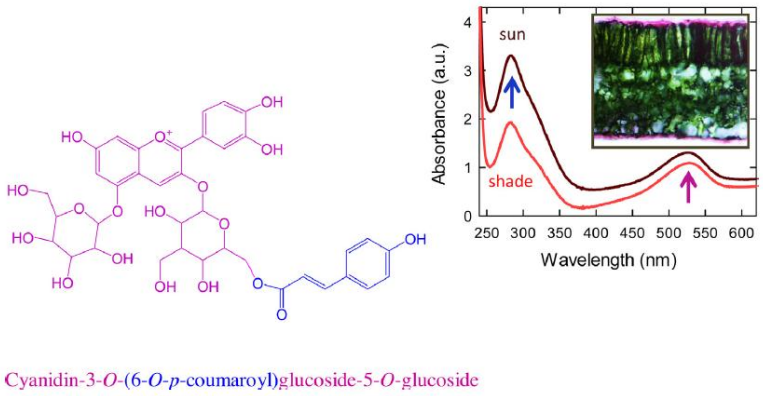

Figure 27. Cyanidin-3-O-(6-O-p-coumaroyl)glucoside-5-O-glucoside, one of the most abundant acylated anthocyanins in leaves of red basil cv 'Red Rubin'. Spectral features of leaf extracts of 'Red Rubin' leaves reveal that major anthocyanins are acylated. The presence of p-coumaric acid (280–320 nm; blue arrow) increase the UV-B absorbance during sun exposure (Landi, Tattini, and Gould 2015).

Another study reported that orthodihydroxy B-ring substituted flavonoids, like quercetin and luteolin, are accumulated in the mesophyll and epidermal tissue of leaves of *Ligustrum vulgare*, in response to high intensity of sunlight, and protect the tissue from the oxidative damage induced by sunlight (Samanta, Das, and Das 2011).
An increased ratio of the 'effective antioxidant' quercetin/ luteolin glycosides versus the 'poor antioxidant' kaempferol/ apigenin glycosides has been reported for plants exposed to high levels of UV-B or sunlight irradiance. Flavonoids occur not only in the vacuoles and cell walls of epidermal cells, but also in the vacuoles of mesophyll cells and in chloroplasts. As a consequence, they are optimally located to reduce light-induced oxidative damage near or within the sites of ROS production. Recently, a nuclear distribution of orthodihydroxylated B-ring flavonoids has been suggested to protect DNA from oxidative damage. In this case orthodihydroxy B-ring substitution is crucial for conferring effective antioxidant properties, however altering UV protection features: orthodihydroxy B-ring substituted flavonoids may in fact inhibit the generation of free radicals by both chelating metal ions and decreasing the enzymatic activity of xanthine oxidase (which generates the superoxide anion), in addition to effectively quenching ROS once they are formed (Agati and Tattini 2010).

Nodulation

During their life, plants continuously produce and secrete compounds into the rhizosphere through their roots. Root exudates include ions, free oxygen and water, enzymes, mucilage, and a diverse array of carbon-containing primary and secondary metabolites. These molecules are often divided into two classes of compounds: low-molecular weight compounds (amino acids, organic acids, sugars, phenolics, and other secondary metabolites) that account for much of the diversity of root exudates, whereas high molecular weight exudates, such as mucilage (polysaccharides) and proteins, are less diverse, but often compose a larger fraction of the root exudates mass (Bais et al. 2006). All these compounds play a crucial role in plant communication with organisms living around their roots.

Plant–microorganism interactions can be described as either compatible or incompatible interaction: in the first case a mutual cooperation is set, in the second a resistant host plant establishes a set of different defence mechanisms directed against the pathogen, such as cell wall fortification, generation and accumulation of reactive oxygen species (ROS) and phenylpropanoids (including phytoalexins), as well as the expression of pathogenrelated (PR) proteins. On the other side, symbiotic interactions are beneficial to both partners. An ecologically and agronomically important symbiosis occurs between leguminous plants and rhizobia, involving the de novo development of a specialized plant organ, the root nodule (Figure 28) (Mithöfer 2002).

Figure 28. Picture of nodules present in plant roots (https://www.realagriculture.com/2014/06/pulse-school-nodulation-show-tips-rescue-n-app/).

Indeterminate nitrogen-fixing nodules are formed on the roots of the model legume, *Medicago truncatula*, due to the symbiosis established with the bacterium, *Sinorhizobium*

meliloti. In the nodules, rhizobia fix N_2 into ammonia, which is then assimilated by the host plant, and, in turn, rhizobia are supplied with carbon compounds. Flavonoids play several roles in establishing this symbiosis through a precise molecular dialogue. The nodulation process in rhizobia–legume symbiosis requires a sequence of highly regulated and coordinated events, initiated by an exchange of specific signalling compounds between both partners. First, Nod factors (chito-lipo-oligosaccharides) are produced by *S. meliloti* in response to specific flavonoids released by the plant roots into the rhizosphere. Recent studies showed that different flavonoid classes also play distinct roles in establishing root nodules. In particular, specific flavones such as 7,4-dihydroxyflavone, are required to stimulate the production of Nod factor synthesis in *Sinorhizobia* and in plants. Also flavonols such as kaempferol play direct roles in orchestrating plant organogenesis. This most likely occurs via the ability of kaempferol to induce localized inhibition of auxin transport, thus establishing more favorable hormonal gradients to enable root nodule formation from differentiated root cells. A third finding was that isoflavones appear to act as anti-inducers in plants to presumably modulate flavone-dependent Nod factor synthesis (Buer, Imin, and Djordjevic 2010).

Stress condition and detoxification

The antioxidant activity of a flavonoid is closely related to its chemical structure. Three structural requirements are important for high antioxidant activity of a flavonoid: (i) the catechol structure in the B-ring (Figure 29 panel A and B); (ii) the 2,3-double bond, in conjugation with the 4-oxo function in the C-ring (Figure 29 panel C); and (iii) the 3- and 5-OH groups in the A-ring (Figure 29 panel D). The catechol group induces a greater stability of aryloxy radicals produced as a result of flavonoid oxidation, possibly through H-bonding and electron-delocalization. Another function of the catechol moiety in the B-ring is the chelation of transition metal ions that may otherwise cause radical oxygen species formation via Fenton-type reaction. The unsaturated bonds localized in the C-ring enhance the electron-transfer and radical scavenging actions through electron delocalization. Finally, the presence of OH groups in the A-ring enables the formation of stable quinonic structures upon flavonoid oxidation. Furthermore, the substitution of the 3-OH group results in an increase in the torsion angle and a loss of co-planarity, and subsequently, a reduced antioxidant activity. On the other hand, the antioxidant activity of flavonoids is related to their high tendency to undergo deep chemical changes. Quercetin possesses all the reactive sites that confer instability to flavonoids, thus displaying the highest antioxidant capacity (Jurasekova et al. 2014).

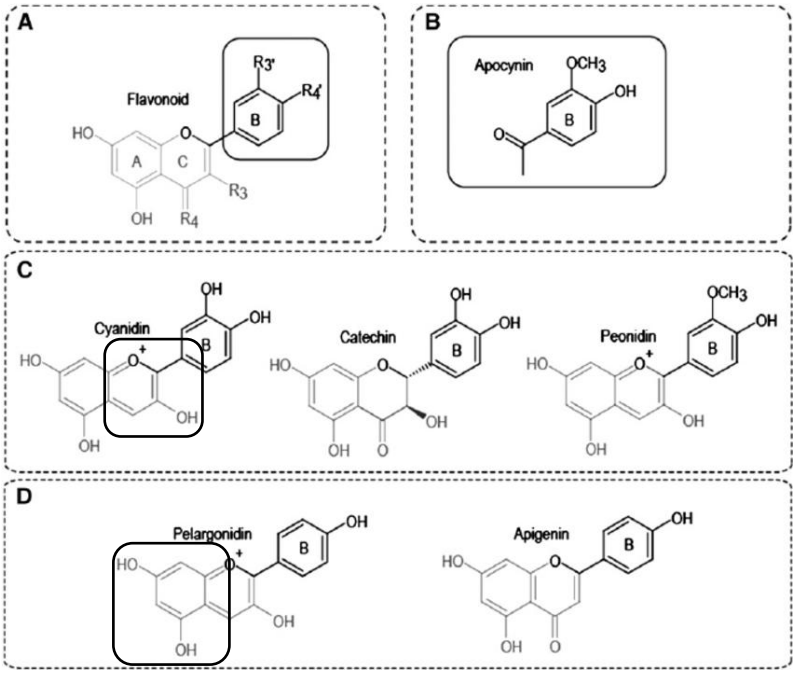

Figure 29. Particularity of flavonoid chemical structure that confer the antioxidant properties: (i) the catechol structure in the B-ring (panel A and B); (ii) the 2,3-double bond, in conjugation with the 4-oxo function in the C-ring (panel C); (iii) the 3- and 5-OH groups in the A-ring (panel D) (Jurasekova et al. 2014).

Flavonoids play a significant role in temperature acclimation. It is established that temperature acclimation results from a complex process involving a number of physiological and biochemical changes, including changes in membrane structure and function, tissue water content, global gene expression, protein, lipid, and primary and secondary metabolite composition.

During cold acclimation and freezing, flavonoids and especially quercetin may scavenge ROS and act as potent antioxidants. Under freezing conditions, large amount of water is removed from the cell into intercellular ice crystal; in these circumstances flavonoids are expected to partition even more strongly into lipid phase of cell membranes and thus stabilize them (Samanta, Das, and Das 2011).

The photosynthetic electron transport system in plant is the major source of active oxygen species (Møller 2001). Chloroplasts have evolved a highly developed ascorbate-glutathione cycle, i.e. a detoxification system to avoid oxygen-mediated toxicity. Flavonoids may scavenge photo-produced active oxygen species in the chloroplast. The superoxide anion radical can not readily diffuse into vacuoles where flavonoids are localized away from chloroplast, but H_2O_2 can diffuse across membranes. Efficient scavenging of ROS by phenolic compounds has been found to

reduce ultraviolet radiation stress. The antioxidant ability of flavonoids depends on the molecular structure and position of hydroxyl groups.

As plants are generally static organisms, they have developed mechanisms to protect themselves against many different abiotic environmental stressors. Water stress (drought and waterlogging) for instance, represents one of the most frequent stressors. It adversely impacts many aspects of plants physiology, especially photosynthetic capacity (Nakabayashi, Mori, and Saito 2014). Plants have evolved complex physiological/ biochemical adaptations to face this adverse conditions and the molecular/ physiological mechanisms associated with water-stress tolerance and water-use efficiency, included the role of secondary metabolites, have been extensively studied (Hassan et al. 2015). Water deficit strongly affects plant secondary metabolism, enhancing flavonoid production in ripening fruit and berries, and in cell suspension cultures of *Glycyrrhiza inflata Batal* and *Ligustrum vulgare*. Expression levels of PAL and CHS, two key genes in the biosynthesis of flavonoids, were also elevated by water deficit. Total isoflavonoid content in portions of soybean primary root increases during water too. This induction in flavonoid production find a logic explanation since these stress conditions induce an increase of ROS: in response to stress, plants activate powerful antioxidant systems, both enzymatic (e.g., superoxide dismutase, catalase, glutathione reductase, several peroxidades) and non-enzymatic (vitamins C and E, carotenoids, flavonoids and other phenolic compounds) (Yuan et al. 2012).

Thanks to their chelation mechanism, flavonoids used to be accumulated by the plants in response to toxic metals stress. For cell cultures of *Ginkgo biloba*, it was reported that flavonoids accumulated in response to heavy metal stress up to 12 fold, when treated with copper sulphate. The chelating action of these compounds may be due to high nucleophilic character of the aromatic rings.

It is also reported that flavonoids may alter peroxidation kinetics by chelating the lipid packing order and thus they stabilize the membranes, preventing the diffusion of free radicals and stopping peroxidation. Flavonoids can interact with membrane phospholipids by hydrogen bond too. *In vitro* study reveals that flavonoids can directly scavenge $O_2^{\cdot -}$, H_2O_2, ·OH, singlet oxygen or peroxyl radical. Their antioxidant capacity is due to the donation of electrons or hydrogen atom and to structural features, such as 3′4′″dihydroxy structure in the B-ring such as quercetin. Reducing activity also relies in the 2, 3- double bond in C-ring (which allows electron delocalization) and presence of 3-OH (most significant electron donating ability) and 5-OH group in C-ring and A-ring, respectively (Samanta, Das, and Das 2011).

Flavonoids beyond the plant system

Nanomaterials and nanoparticles

Nanoscience is the study of nano-scale matter and represents a rapidly growing, cross-disciplinary field. The importance of this new field is underlined by the growing interests of industries in nano-products: in USA for instance, the number of nano-materials-based goods and the national funding used for this propose have grown quite three times in the last decade (Metz et al. 2014).

So, during the last decade, nanotechnology has become a cutting edge and highly interdisciplinary research area including environmental/basic/material and medical science. Due to particular physical characteristics, nanomaterials present considerable changes in physical, mechanical, chemical, electrical, magnetic, optical, and biological properties. Latest innovations in nanotechnology have resulted in the synthesis of nanomaterials with different shapes, such as wires, tubes, and particles for doable applications in different fields (Razavi et al. 2015).

Among the different utilizations, the use of nanoparticles (NPs) in medicine represents the most important, innovative and promising application of this material (Figure 30).

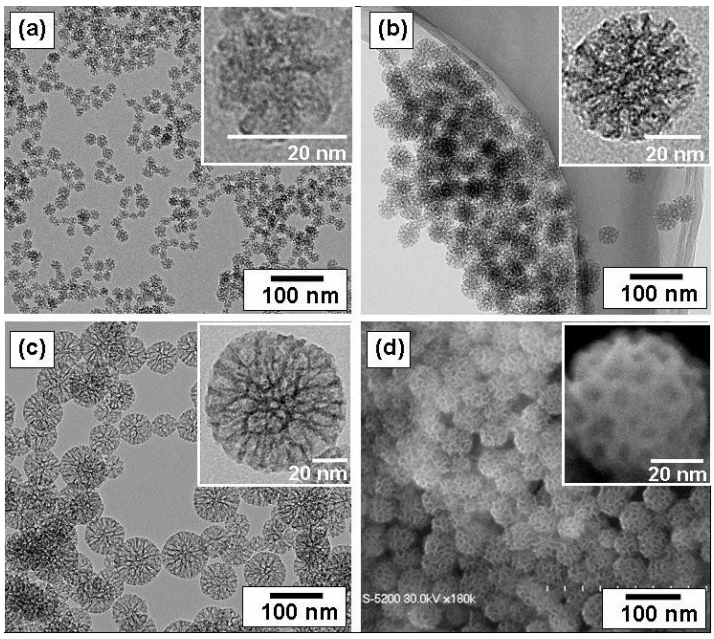

Figure 30. TEM images of golden NPs used for medical purpose (http://www.uh.edu/engines/epi2861.htm).

In general, the size of a NP spans the range between 1 and 100 nm and its biological properties depend very much on its physical properties. Metallic NPs have different

physical and chemical properties from bulk metals (e.g., lower melting points, higher specific surface areas, specific optical properties, mechanical strengths, and specific magnetizations), properties that might prove attractive in various industrial applications. One of the most important and easy to detect characteristic is the optical property of a NP. For example, 20-nm gold NPs has a characteristic red-wine color. Silver NPs is yellowish gray. Platinum and palladium NPs are black. Not surprisingly, the optical characteristics of NPs have been used from immemorial time in sculptures and paintings, dating back even before the 4th century AD. Nanotechnology is also easily evident in various old churches. A well-known application of early nanotechnology is the color that was used for stained glass windows during the Middle Ages. Beautiful examples of these applications can be found in glass windows of many Gothic European cathedrals (Figure 31). But the real industrial production of nanomaterials saw its origins only in the twentieth century: NPs of carbon black (tire soot) have been used in the fabrication of rubber tires of automobiles from the beginning of the twentieth century.

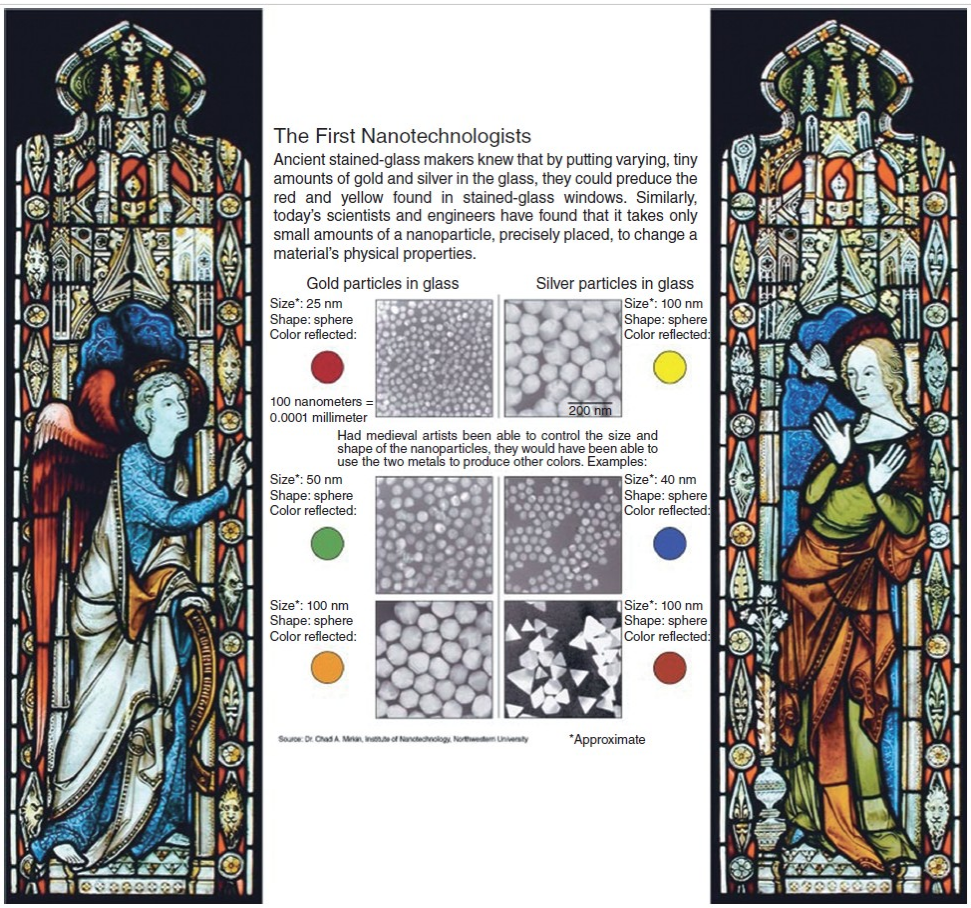

Figure 31. Example of optical properties of NPs present into different gothic glass colorations (Horikoshi and Serpone 2013).

Two approaches have been known in the preparation of ultrafine particles. The first one is the breakdown (top-down) method by which an external force is applied to a solid that leads to its break-up into smaller particles. The second is the build-up (bottom-up) method that produces NPs starting from atoms of gas or liquids based on atomic transformations or molecular condensations. The top-down method is the method of breaking up a solid substance. The solid substance is ground as a result of shock, compression, or friction. A feature of particles in grain-refining processes is that their surface energy increases, which causes the aggregation of particles too. Since condensation of small particles also takes place simultaneously with pulverization, it is difficult to obtain particles having sizes less than 3 μm by grain refining (Figure 32).

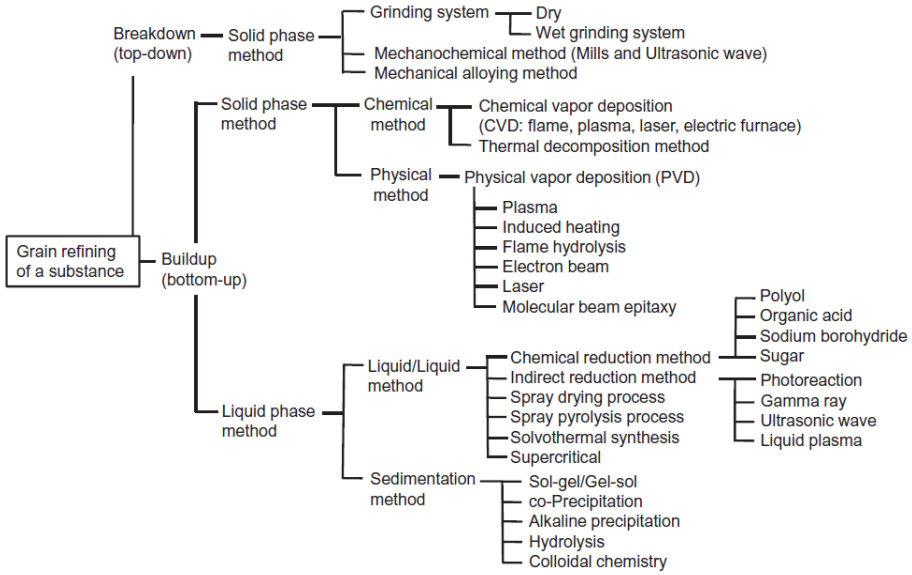

Figure 32. Scheme of different physical/chemical/biological procedures to obtain NPs (Horikoshi and Serpone 2013).

Liquid phase methods have been the major "bottom-up" preparation methods of NPs. By the chemical reduction method it is possible to fine-tune the form (shape) and size of the NPs by changing the reducing agent, the dispersing agent, the reaction time and the temperature. The chemical reduction method carries out chemical reduction of the metal ions to their 0 oxidation states (i.e., $Mn^{+} \rightarrow Mn^{0}$); the process uses non-complicated equipment or instruments, and can yield large quantities of NPs at a low cost in a short time. Besides the chemical reduction method that quite often requires dangerous and toxic compounds, other reduction methods, such as ultrasonic waves, liquid plasma and "green" biosynthesis can be used (Horikoshi and Serpone 2013).

Implications of nanotechnology on plant

The developments in nanotechnology and nanotechnology-based industries and products are tremendously growing. Until October 2013, the nanotechnology-based consumer products inventory has been grown more than ten times in less than 10 years. The use of nanomaterials in biomedicine and in agriculture is one of the most intensely studied areas in nanotechnology. In agriculture, this new area of research affords broad advantages, such as disease prevention, nutrient management and soil detoxification. Various kind of nanomaterials such as metal NPs, carbon nanotubes, quantum dots, magnetic particles and polymers have been studied for their use and possible effect in different areas (Thul and Sarangi 2015; Ditta, Arshad, and Ibrahim 2015).

Concerning the plant capability of metals detoxification, of particular interest is the ability of plant extracts to reduce metal ions to NPs, performing the so called "green-biosynthesis". This plant-specific activity has been known since the early 1900s, although the nature of the reducing agents involved in these extracts, is not well understood. Using plant extracts as source for reducing agents to make metal NPs has attracted considerable attention in the last 3 decades. Plant extracts may act both as reducing agents and stabilizing agents in the synthesis of NPs, because different extracts contain different concentrations and combinations of organic reducing agents (Figure 33).

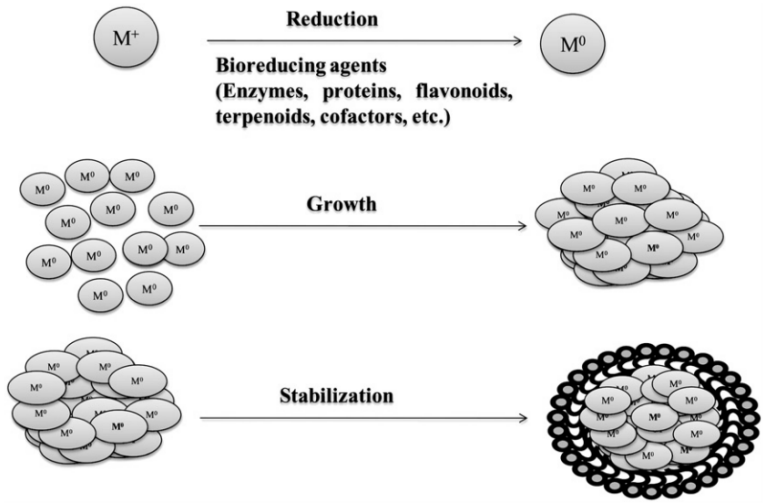

Figure 33. Mechanisms of NPs synthesis, involving three different steps: (i) reduction, (ii) growth and (iii) stabilization (M^+-metal ion) (Mittal, Chisti, and Banerjee 2013).

The entire process of NPs formation is usually complete within minutes, depending mainly on the nature of the plant extract, its concentration, the concentration of the metal salt, the pH, temperature and contact time. All these parameters seem to affect

the rate of production, the quality/ quantity and other characteristics of the NPs. Table 2 summarizes some of the reports pertaining to NPs synthesis mediated by extracts of various plants (Mittal, Chisti, and Banerjee 2013). The UV–visible spectroscopy is a commonly used technique. Light wavelengths in the 300–800 nm are generally used for characterizing various metal NPs in the size range of 2 to 100 nm. Spectrophotometric absorption measurements in the wavelength ranges of 400–450nm and 500–550 nm are used in characterizing the silver and gold nanoparticles, respectively (Figure 34).

Plant	Type of nanoparticle	Size and shape
Acalypha indica	Ag	20–30 nm; spherical
Allium sativum (garlic clove)	Ag	4–22 nm; spherical
Aloe vera	Au, Ag	50–350 nm; spherical, triangular
Aloe vera (*Aloe barbadensis* Miller)	Indium oxide	5–50 nm; spherical
Anacardium occidentale	Au/Ag bimetallic	~6 nm at 27 °C; 17 nm at 100 °C
Apiinextracted from henna (*Lawsonia inermis*) leaves	Au, Ag	7.5–65 nm; spherical, triangular, quasispherical
Azadirachta indica (neem)	Ag/Au bimetallic	50–100 nm
Boswellia ovalifoliolata	Ag	30–40 nm
Calotropis procera	Ag	150–1000 nm
Camelia sinensis	Ag, Au	30–40 nm
Carica papaya	Ag	25–50 nm
Catharanthus roseus	Ag	48–67 nm
Chenopodium album	Ag, Au	10–30 nm; quasi-spherical shape
Cinnamomum camphora	Ag, Au	55–80 nm
Cinnamomum camphora	Au, Pd	3.2–20 nm; cubic hexagonal crystalline
Citrus sinensis peel	Ag	35 ± 2 nm (at 25 °C), 10 ± 1 nm (at 60 °C); spherical
Coleus amboinicus Lour	Ag	25.8 ± 0.8 nm
Coleus aromaticus	Ag	44 nm
Curcuma longa	Ag	–
Cymbopogon sp. (lemongrass)	Au	200–500 nm; spherical, triangular
Datura metel	Ag	16–40 nm; quasilinear superstructures
Desmodium triflorum	Ag	5–20 nm
Diopyros kaki	Pt	15–19 nm
Dioscorea bulbifera	Au	11–30 nm spheres
Eclipta prostrate	Ag	35–60 nm; triangles, pentagons, hexagons
Emblica officinalis	Ag, Au	10–20 nm Ag; 15–25 nm Au
Eucalyptus hybrid	Ag	50–150 nm
Euphorbiaceae latex	Cu/Ag	18 nm Ag, 10.5 nm Cu
Garcinia mangostana (mangosteen leaf)	Ag	35 nm
Gelidiella acerosa	Ag	22 nm
Geranium leaf	Au	16–40 nm
Jatropha curcas L. latex	Pb	10–12.5 nm
Memecylon edule	Ag, Au	20–50 nm; triangular, circular, hexagonal
Melia azedarach	Ag	–
Mentha piperita (peppermint)	Ag, Au	5–150 nm; spherical
Moringa oleifera	Ag	57 nm
Mucuna pruriens	Au	6–17.7 nm; spherical
Musa paradisiacal	Ag	20 nm
Nelumbo nucifera (lotus)	Ag	25–80 nm; spherical, triangular
Parthenium leaf	Au	50 nm; face-centered cubic
Psidium guajava	Au	25–30 nm; spherical
Pyrus sp. (pear fruit extract)	Au	200–500 nm; triangular, hexagonal
Rhododedendron dauricam	Ag	25–40 nm; spherical
Rosa rugosa	Ag, Au	30–60 nm Ag; 50–250 nm Au
Sesuvium portulacastrum	Ag	5–20 nm; spherical
Swietenia mahogani (mahogany)	Ag/Au bimetallic	50 nm Ag at pH 7; 20 nm Ag and 100 nm Au at pH 12.5; 50 nm Au/Ag bimetallic at pH 12.5
Syzygium cumini	Ag	29–92; spherical
Tanacetum vulgare (tansy fruit)	Ag, Au	16 nm Ag, 11 nm Au
Terminalia catappa	Au	10–35 nm
Trachyspermum copticum	Ag	6–50 nm
Vitex negundo L	Au	10–30 nm; face centered cubic

Table 2. Biosynthesis of NPs using plant extracts (Mittal, Chisti, and Banerjee 2013).

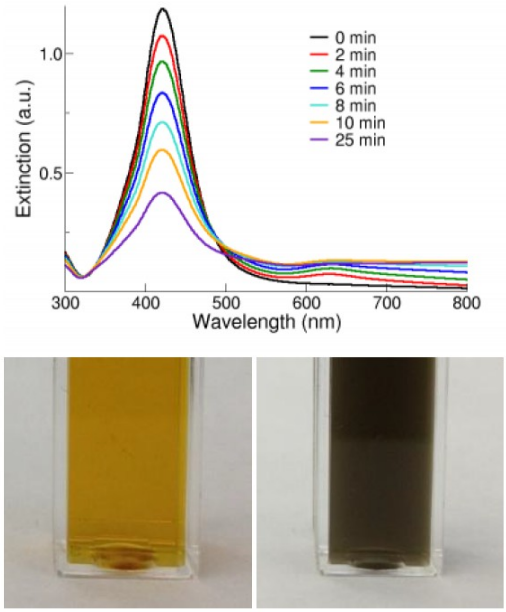

Figure 34. The absorption spectrum (upper) of silver NPs chemical synthesis followed in 25 minutes. Color change during the NPs formation (down) (http://nanocomposix.eu/pages/silver-nanoparticles-optical-properties).

Plant extracts contain alkaloids, proteins, enzymes, amino acids, alcoholic compounds, and polysaccharides responsible for the reduction of the silver ions to NPs (Kesharwani et al., 2009). Quinol and chlorophyll pigments present in the extract also contributed to the reduction of silver ions and stabilization of the NPs (Figure 35) (Mittal, Chisti, and Banerjee 2013).

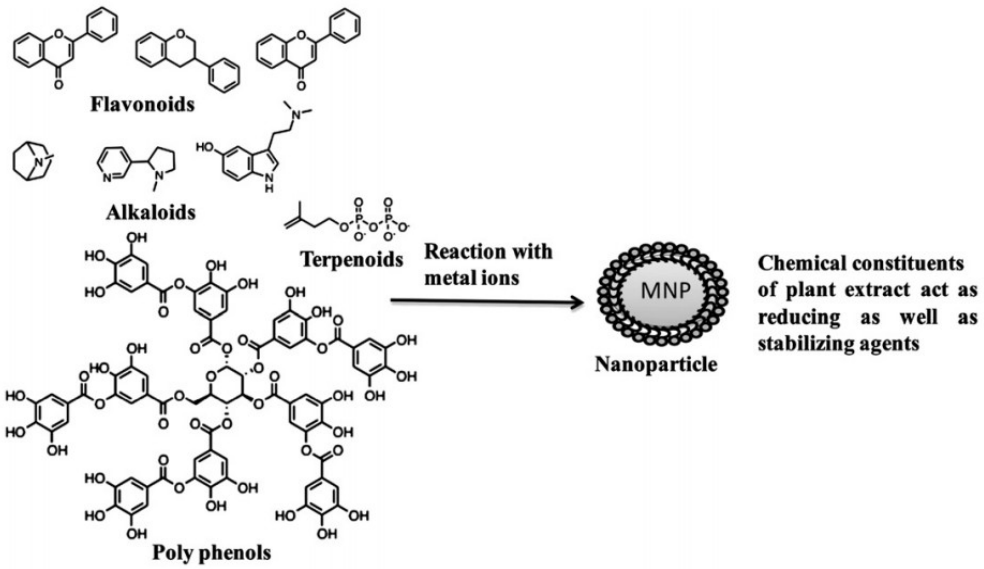

Figure 35. Probable chemical constituents present in the plant extract responsible for the reduction of metal ions in metal NPs (MNP) (Mittal, Chisti, and Banerjee 2013).

NPs synthesized by the various methods have been used in diverse *in vitro* diagnostic applications. Both gold and silver NPs have been commonly found to have a broad spectrum of antimicrobial activity against human and animal pathogens. Silver NPs are already widely used as antimicrobial agents in commercial medical and consumer products (Figure 36).

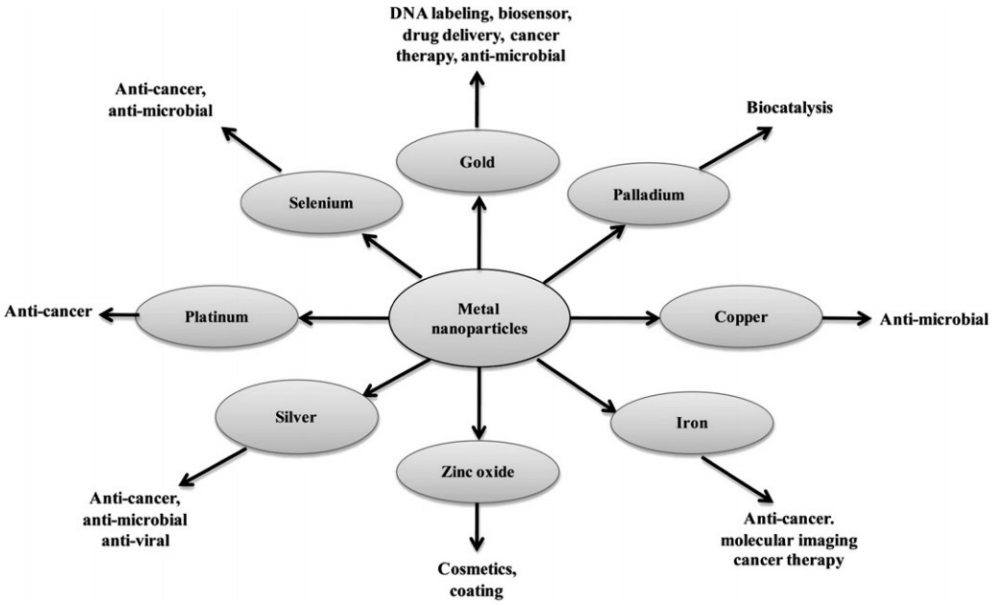

Figure 36. Types of metal NPs and their applications in biotechnology (Mittal, Chisti, and Banerjee 2013).

Extensive literature exists on the mechanisms of antimicrobial action of NPs: silver NPs, in particular, are larvicidal against *filariasis* and malaria vectors, they are active against plasmodial pathogens, cancer cells and posses antifungal effects. The toxic effects of silver NPs depends mainly on their slow release of silver ions via oxidation of the NPs structure and thanks to their interactions with membranes, enzymes and with the DNA replication system. They can be applied to crop protection, agriculture, food packaging/ production and wastewater treatment (Mittal, Chisti, and Banerjee 2013).

Nutraceutical action

"Nutraceutical" is a term coined in 1979 by Stephen DeFelice. It is defined "as a food or parts of food that provide medical or health benefits, including the prevention and treatment of disease." The major active nutraceutical ingredients in plants are flavonoids and approximately 2000 of this kind of compounds have been described, although many others are still totally un-known (Figure 37) (Lin and Weng 2006).

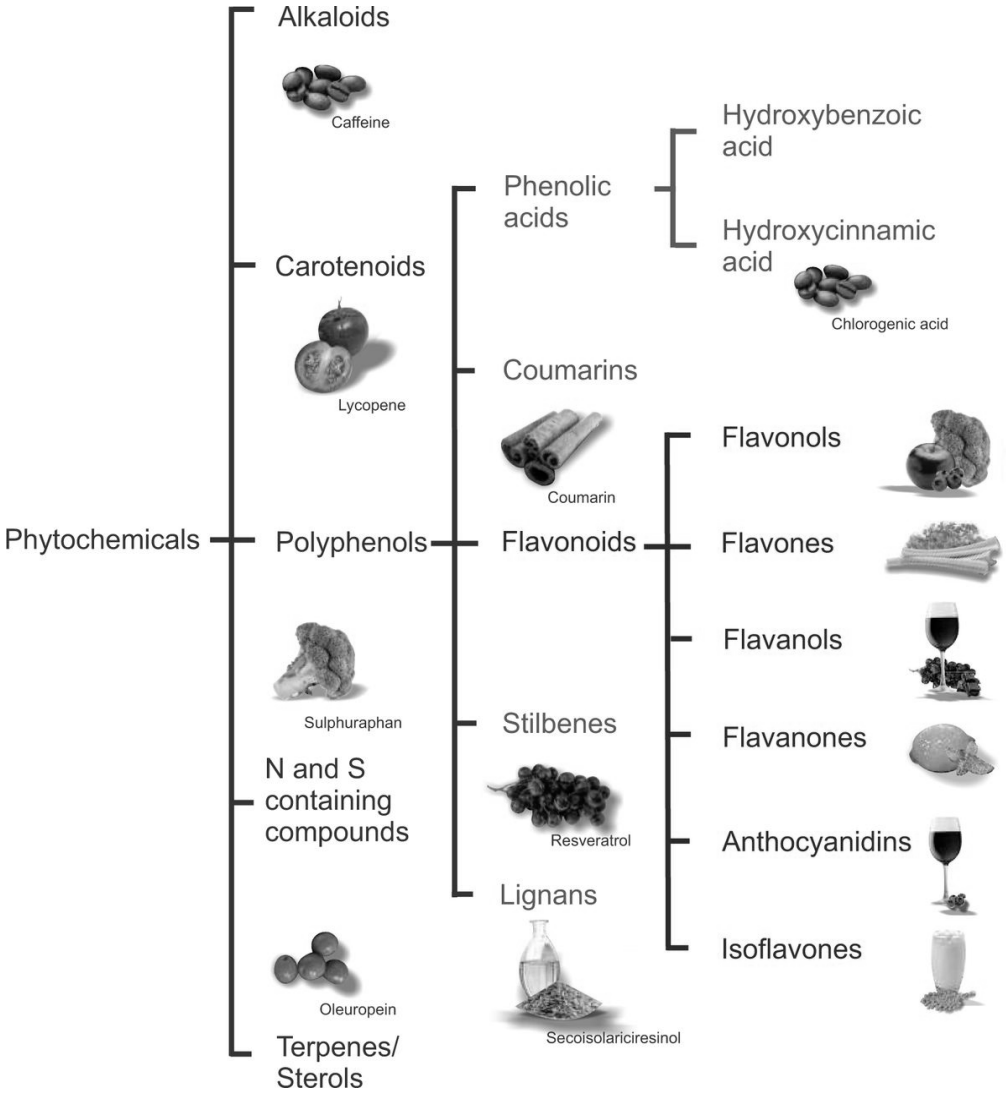

Figure 37. Scheme of the most abundant phytochemicals present in plant edible products (Bondonno et al. 2015).

Flavonoids are the most common and widely distributed group of plant phenolic compounds, present in all parts of the plant (in particular in the photosynthetic tissues). Being phytochemicals, flavonoids cannot be synthesized by humans and must be absorbed by the diet.

Although their biological importance was scientifically well known, only recently the health effects of dietary polyphenols in humans have come to the attention of nutritionists. Current scientific evidences strongly supports the common hypothesis that flavonoids contribute to the prevention of cardiovascular diseases, cancers and osteoporosis. A considerable body of literature supports also their positive contribution in solving human age-related oxidative stress damages. For many years, polyphenols like flavonoids were considered good candidates to protect cell constituents against oxidative damage through scavenging of free radicals. However, this concept now appears too poor and simple and recent evidences seem to explain how cells respond to polyphenols mainly through direct interactions with receptors or enzymes involved in signal transduction, which may result in modification of the redox status of the cell and may trigger a series of redox-dependent reactions (Scalbert, Johnson, and Saltmarsh 2005).

Particularly regarding neurodegenerative diseases located into the brain, this classical hydrogen-donating antioxidant activity theory seems to do not take in account the entire bioactivity of flavonoids *in vivo*, where they are usually found at only very low concentrations. Instead, it has been postulated that the effects of flavonoids in this organ are mediated by an ability to protect vulnerable neurons, enhance existing neuronal function, stimulate neuronal regeneration and induce neurogenesis. Indeed, it has become evident that flavonoids are able to exert neuroprotective actions (at low concentration) via their interactions with critical neuronal intracellular signalling pathways pivotal in controlling neuronal survival and differentiation, long-term potentiation (LTP) and memory (Spencer 2009).

Unfortunately, one of the major difficulties of elucidating all these polyphenols health effects is the large number of phenolic compounds found in food, yielding differing biological activities, depending on their chemical structure (Scalbert, Johnson, and Saltmarsh 2005).

The key point that mostly affects the beneficial action of these molecules regards their absorption once ingested, their so called "bioavailability". The absorption of the dietary flavonoids released from the food will depend on their physical and chemical properties such as molecular size, configuration, lipophilicity, solubility, and pKa. Strong influence on flavonoid absorption may depend upon structure of flavonoid aglycones and modification by glycosylation. Most flavonoids, except for the subclass of catechins, are present in plants bound to sugars. Unfortunately, flavonoid glycosides are not well absorbed; however, they can be converted into aglycone forms that are better absorbed by the small intestine. The hydrophilic flavonoid glucoside such as quercetin glucoside is transported across the small intestine by the intestinal Na^+-dependent glucose cotransporter (SGLT1). An alternative mechanism suggests

that flavonoid glucosides are hydrolyzed by lactase phloridzin hydrolase (LPH), a alpha-glucosidase on the outside of the brush border membrane of the small intestine. Subsequently, the free aglycone can be absorbed across the small intestine. The glycosides which are not substrates for these enzymes are transported toward the colon where bacteria have ability to hydrolyze flavonoid glycosides, but simultaneously they will also degrade the liberated flavonoid aglycones.

The site of deglycosylation and transport across the intestinal cells depends therefore on the nature of the flavonoid moiety and nature/ position of the attached sugar. For example, the pharmacokinetics of quercetin-3-glucoside and quercetin-3-rhamnoglucoside illustrate how strongly relevant could be the structural differences on the site of absorption. Quercetin glucoside may be readily deglycosylated in the small intestine, whereas small intestinal β-glucosidases appear inactive against quercetin rhamnoglucoside (Day et al. 2003).

Since absorption capacity of the colon is far less than that of the small intestine, only negligible absorption of these glycosides has to be expected. After absorption, the flavonoids are conjugated in the liver by glucuronidation, sulfation, or methylation or metabolized to smaller phenolic compounds. Due to these conjugation reactions, no free flavonoid aglycones can be found in plasma or urine, except for catechins. The flavonoids secreted with bile in intestine and those that cannot be absorbed from the small intestine are degraded in the colon by intestinal microflora which also breaks down the flavonoid ring structure (Figure 38) (Kumar and Pandey 2013; Bondonno et al. 2015).

So, only a small amount of flavonoids is able to reach the blood system and be bioavailable to exert biological functions, like reducing blood lipids and glucose, enhancing human immunity, playing important roles in protecting biological systems against the harmful effects of oxidative processes and exerting a direct antimicrobial activity. Furthermore, flavonoids are able to inhibit aldose reductase enzyme (that converts sugars to sugar alcohols) and is implicated with diabetic complications, such as neuropathy, heart disease and retinopathy. Many other biological activities of phenolic acids were reported: antidiabetic activity, increasing of bile secretion, reduction of blood cholesterol and lipid levels, antiulcer, anti-inflammatory, antioxidant, cytotoxic and antitumor effects, antispasmodic and antidepressant actions.

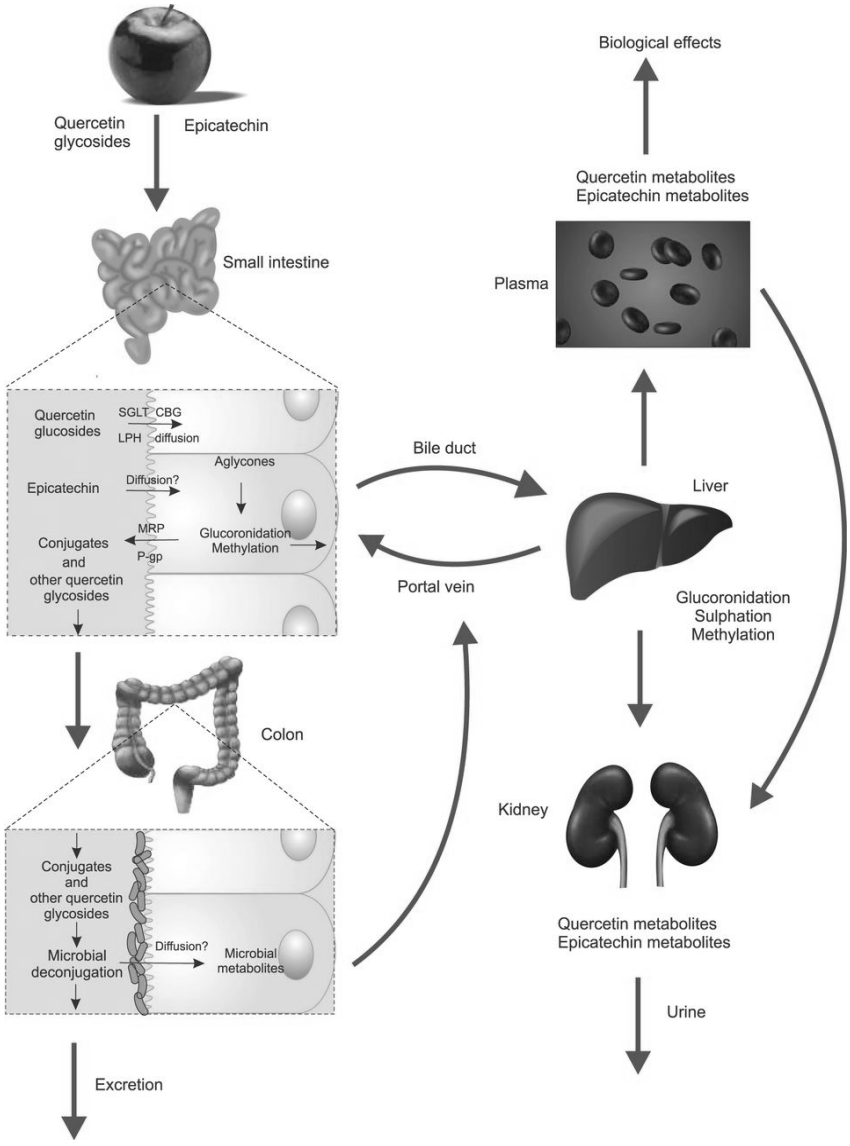

Figure 38. Scheme of flavonoid absorption and metabolism within human digestive (Bondonno et al. 2015).

Dietary polyphenolic compounds, with emphasis on quercetin, were shown to inhibit collagen-stimulated platelet activation through different components of the glycoprotein VI signaling pathway and also flavonoid antiviral activity have been recognized since the 1940s and many reports on this property are available (Ghasemzadeh and Ghasemzadeh 2011).

Although they possess all these biological activities of medical interest, the most important and under strictest study remains the biological influence on tumor cell proliferation. Consumption of onions and/or apples, two major sources of the flavonol quercetin, is inversely associated with the incidence of cancer of the prostate, lung, stomach, and breast. In addition, moderate wine drinkers also seem to have a lower

risk to develop cancer of the lung, endometrium, esophagus, stomach, and colon. Several mechanisms have been proposed for the effect of flavonoids on the initiation and promotion stages of the carcinogenicity including influences on development and hormonal activities. Major molecular mechanisms of action of flavonoids are given as follows:

(1) down-regulation of mutant p53 protein;
(2) cell cycle arrest;
(3) tyrosine kinase inhibition;
(4) inhibition of heat shock proteins;
(5) estrogen receptor binding capacity;
(6) inhibition of expression of Ras proteins.

It has been proposed that each flavonoid exerts a quite specific biological action when present into a mammalian system. Recently it has been shown that the flavanol epigallocatechin- 3-gallate inhibited fatty acid synthase (FAS) activity (expression of FAS is markedly increased in various human cancers) and lipogenesis in prostate cancer cells, an effect strongly associated with growth arrest and cell death. Quercetin is known to arrest cell cycle in proliferating lymphoid cells. In addition to its anti-neoplastic activity, quercetin exerted *in vitro* growth-inhibitory effects on several malignant tumor cell lines in vitro like P- 388 leukemia cells, gastric cancer cells (HGC-27, NUGC-2, NKN-7, andMKN-28), colon cancer cells (COLON320DM), human breast cancer cells, human squamous cell carcinoma, and ovarian cancer cells. It has been also proposed that tumor cell growth inhibition by quercetin may be due to its interaction with nuclear type II estrogen binding sites. It has been experimentally proved that the increased signal transduction in human breast cancer cells is markedly reduced by quercetin, acting as an anti-proliferative agent (Kumar and Pandey 2013).

In cerebral ischemia, the elevated permeability of the blood brain barrier (BBB) leads to many different physiological damages: green tea polyphenols may decrease the BBB permeability and thus leading to considerable amelioration of the clinical picture in the damaged tissues. Also in endothelial cells, the downregulation of caveolin-1 expression exerted by green tea polyphenols may protect the aorta against the pathological changes induced by a high-fat diet. The protective antiatherosclerotic effect of catechins is exerted by their anti-inflammatory influence on vascular endothelial. It is demonstrated that epigallocatechin gallate can regulate invasion and metastasis of liver cancer cells by preventing the phosphorylation of the receptor of hepatocyte growth factor HGF (c-Met) (Tarahovsky et al. 2014).

CHAPTER 1

In vivo assay to monitor flavonoid uptake across plant cell membranes

FEBS Open Bio 5 (2015) 748–752

journal homepage: www.elsevier.com/locate/febsopenbio

Method

In vivo assay to monitor flavonoid uptake across plant cell membranes

Antonio Filippi, Elisa Petrussa, Carlo Peresson, Alberto Bertolini, Angelo Vianello, Enrico Braidot *

Department of Agricultural and Environmental Sciences, Plant Biology Unit, via delle Scienze 91, I-33100 Udine, Italy

ARTICLE INFO

Article history:
Received 26 May 2015
Revised 31 July 2015
Accepted 21 August 2015

Keywords:
Flavonoid transport
2-Aminoethoxydiphenyl borate
Paraformaldehyde
Grape cell cultures
Quercetin

ABSTRACT

Flavonoids represent one of the most important molecules of plant secondary metabolism, playing many different biochemical and physiological roles. Although their essential role in plant life and human health has been elucidated by many studies, their subcellular transport and accumulation in plant tissues remains unclear. This is due to the absence of a convenient and simple method to monitor their transport. In the present work, we suggest an assay able to follow *in vivo* transport of quercetin, the most abundant flavonoid in plant tissues. This uptake was monitored using 2-aminoethoxydiphenyl borate (DPBA), a fluorescent probe, in non-pigmented *Vitis vinifera* cell cultures.

1. Introduction

Flavonoids are a group of plant polyphenolic secondary metabolites with a common three ring chemical structure (C_6–C_3–C_6, named A, C and B ring, respectively). The major classes of flavonoids are anthocyanins (red to purple pigments), flavonols (colourless to pale yellow pigments), flavanols (colourless pigments that become brown after oxidation), and proanthocyanidins or condensed tannins. These compounds are widespread in plants, in various amounts, dependent on the plant species, organ, developmental stage and growth conditions. They are involved in several physiological functions, such as antioxidant activity, UV-light protection, defence against phytopathogens, regulation of legume nodulation, male fertility, pollinator attraction and control of auxin transport [1].

Flavonoids play all these crucial roles thanks to a finely regulated transport and accumulation system allowing entrance into different subcellular compartments. Nevertheless a comprehensive view of the phenomenon has not yet been proposed and the process is still under investigation. The chemical nature of flavonoids and their activities depend on their structural class, degree of hydroxylation, other substitutions and conjugations. Spectral characteristics of most flavones and flavonols show two major absorption bands: Band I (320–385 nm) represents the B ring absorption, while Band II (250–285 nm) corresponds to the A ring absorption [2]. It has to be stressed that several flavonoids behave as pH indicators and their spectra could be strongly affected by the pH value of the assay medium [3]. This feature limits the utilization of the usual spectrophotometric and spectrofluorimetric transport assays.

Quercetin (QC) is a widely distributed natural flavonoid, found in many fruits, leaves and grains. It is able to modulate cell proliferation and apoptosis in different human cells. A high amount of QC is contained (values indicated in parentheses as mg/100 g FW) in the leaves of green (256) and black tea (205), cowberry (21), cranberries (14), apples (4) and red grapes (4) [4]. It is generally known that QC, like most other flavonoids, is poorly fluorescent in aqueous solutions, but exhibits an increased fluorescence when bound to specific probes such as 2-aminoethoxydiphenyl borate (DPBA) [5].

DPBA is an esterified moiety commonly used in microscopy for flavonoid localization [6], able to form a spontaneous complex with most represented flavonoid compounds [7]. Accordingly, it has already been used in tissue microscopy analysis to describe flavonoid accumulation inside specific plant compartments [8,9]. Similarly to flavonoids, the fluorescence of the probe/ligand complex seems to be very sensitive to the assay buffer and pH [10].

The present work was aimed at assessing a new methodological protocol to follow *in vivo* flavonoid transport, utilizing DPBA as a probe, in non-pigmented cell (NPC) cultures from *Vitis vinifera*, grown in the dark, which represent a reliable and easy-to-manage experimental model.

Abbreviations: DPBA, 2-aminoethoxydiphenyl borate; MS, Murashige and Skoog; NPC, non-pigmented cell; PFA, paraformaldehyde; QC, quercetin

* Corresponding author. Tel.: +39 432 558792.
E-mail address: enrico.braidot@uniud.it (E. Braidot).

http://dx.doi.org/10.1016/j.fob.2015.08.009

2. Materials and methods

2.1. Cell culture

Grapevine cell cultures (*Vitis vinifera* L. cv. Limberger) were grown on solid Murashige and Skoog medium (MS) [11] for 21 days and incubated at 25 °C in the dark, as described by Repka et al. [12]. Seven-day-old cultured cells were used for the uptake experiments.

2.2. Reagents

All reagents were purchased from Sigma–Aldrich. DPBA and QC were solubilized in pure ethanol to reach the desired concentration.

2.3. Spectrofluorimetric analysis of QC uptake in NPC cultures by DPBA

Three grams (FW) of 7 day-old cells were mixed in 20 ml of fresh MS medium and shaken to disrupt all the clusters. During the experiments, cells were maintained at constant shaking (110 rpm), at room temperature and shaded to avoid light exposure. Aliquots of the cell suspension were incubated with DPBA for 20 min, at a final concentration of 0.05% (w/v), corresponding to 2.2 mM (exceeding the QC concentrations used). The cells were then washed by centrifuging at about 400 *g* for 2 min, using a 50 μm nylon gauze, to eliminate all the liquid fraction. After filtration, the cells were collected by a gauze, resuspended in the same starting volume of fresh MS medium and maintained at constant shaking until the fluorimetric assay. Cells were then diluted (1:3 v/v) with fresh MS medium just before the analysis with spectrofluorimeter (Perkin Elmer, model LS50B). The reaction was started by addition of different concentrations of QC (ranging from 0.1 to 50 μM). The reading set up was: 461 nm for the excitation and 520 nm for the emission, using slit width of 5 and 10 nm for excitation and emission, respectively.

Transport inhibition was performed by incubating cells, preloaded with 0.05% DPBA for 10 min, with 0.1 or 0.3% (w/v) of paraformaldehyde (PFA) for further 10 min. The cells were then washed as described above and the inhibitory effect could be evaluated by comparing the initial rate of treated and untreated samples after the addition of 0.5 μM QC.

Sonication treatment, using 1 pulse for 20 s with 400 W of power, was applied to disrupt cell wall and cell integrity, to obtain vesicles more easily prone to detergent action. The protocol differed slightly from the one proposed by Pereira-Lachataignerais et al. [13] because one single pulse was sufficient to disrupt the cell wall and necessary to obtain bigger vesicles able to be kept into the nylon gauze. After sonication, the vesicles were washed and resuspended in a double volume of starting MS medium, and subsequently diluted (1:3 v/v) in MS medium, before the spectrofluorimetric analysis. SDS (0.3% w/v, final concentration) was added to allow the release of DPBA from the cells.

2.4. Total QC evaluation in cell extracts by DPBA

The analysis was performed according to the method described by Lee et al. [7], with minor changes. Briefly, 4 g (FW) of cells were diluted in 16 ml of MS medium, split into four 4 ml-flasks and then incubated for 1 h at different QC concentrations (0, 0.5, 5 and 50 μM). Cells were collected and washed as reported previously. The filtered cells were resuspended in 4 ml of cold methanol and, after disruption by 3 pulses of sonication for 20 s at 400 W, the homogenates were incubated overnight in the dark at room temperature and at constant shaking. Two centrifugations at 27,000 *g* for 5 min were performed in sequence on the supernatant to discard all the cell debris. A continuous nitrogen flux was used to dry the solvent and the powder was resuspended in 400 μl of cold methanol.

DPBA (0.05%, w/v) and samples were mixed 1:2 and fluorescence signal was measured using a Multilabel Counter (WALLAC, model 1420, Perkin–Elmer) set at 465 ± 10 nm (excitation filter) and 535 ± 10 nm (emission filter), respectively.

3. Results

3.1. Emission spectra of DPBA and DPBA/QC complex

With the aim to determine the appropriate wavelength range for slit setting, the emission spectrum of DPBA and QC-bound DPBA was evaluated (Fig.1). The figure shows a rather large spectrum (between 500 and 590 nm), where the emissions of bound and unbound DPBA differ from each other. An emission value of 520 nm was, therefore, chosen for spectrofluorimetric analysis, according to Murphy et al. [14]. Instead, an emission value of 535 nm was used for the detection, using Multilabel Counter.

3.2. In vivo QC uptake in grapevine suspension cell cultures

The assay was carried out aiming to follow the QC uptake in a plant cellular system. Grapevine suspension cell cultures were loaded with DPBA (0.05% w/v) and then different QC concentrations (ranging from 0.1 to 50 μM) were added. The formation of the fluorescent complex between the probe and the flavonoid was demonstrated by a microscope under fluorescent light (Fig. 2). Panel a shows that, in the presence of DPBA only, grapevine NPC exhibited a low fluorescence, which strongly increases after the addition of QC (panel b). In agreement, during spectrofluorimetric assay cells showed rising fluorescence values at increasing concentration of the added flavonoid (panel c). When the initial rates of QC uptake into cells were plotted *versus* QC concentration, a hyperbolic regression curve, describing the kinetic features of *in vivo* QC uptake through the plasma membranes, was obtained. Both the washing step and the DPBA loading treatment did not alter the cell viability (data not shown).

3.3. Spectrofluorimetric analysis of DPBA/QC uptake

To verify if the complex DPBA/QC was not specifically bound to cell outer components and could be released by cells, suspension

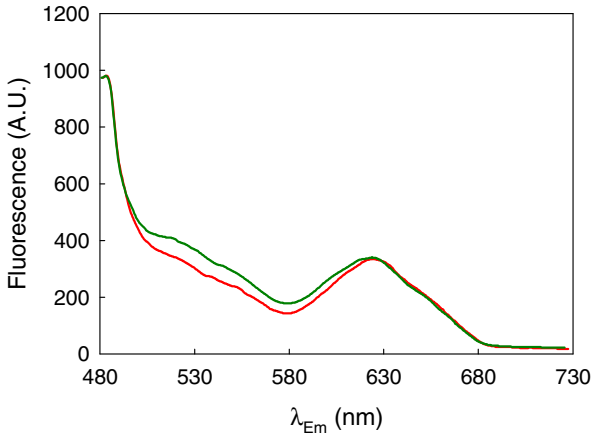

Fig. 1. Emission spectra of DPBA (red trace) and DPBA/QC complex (green trace) in MS medium. DPBA and QC were 0.05% and 0.5 μM, respectively.

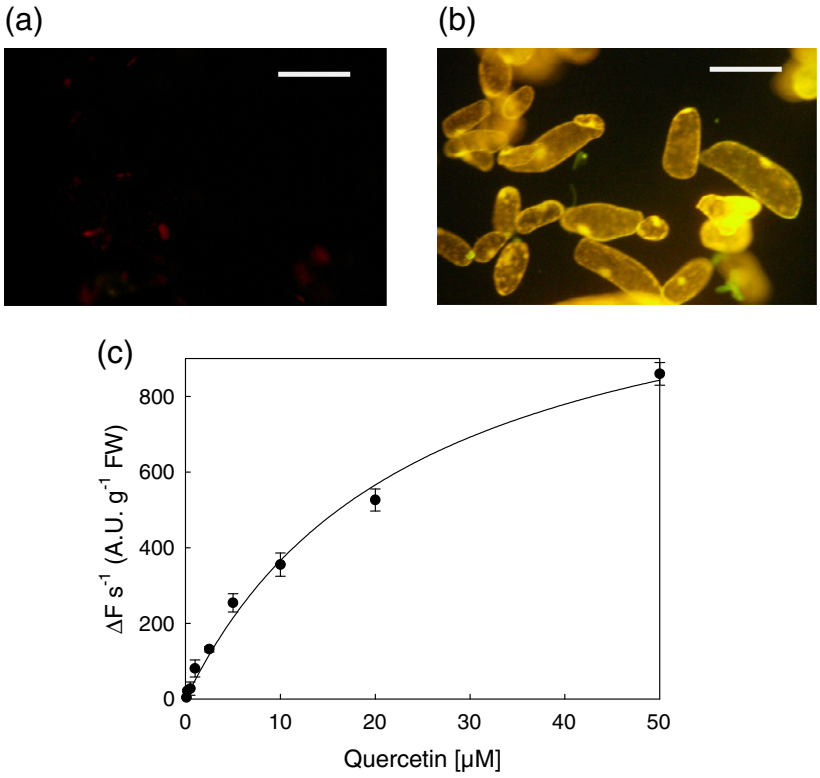

Fig. 2. Panels (a) and (b): images under fluorescent light of grapevine NPC cultures treated either with DPBA (a) or with both DPBA and QC (b). Scale bars = 50 μm. Panel (c): *in vivo* QC uptake in grapevine NPC cultures, measured by means of DPBA fluorescence. Values represent a mean of five independent replicates ± SD. Regression curve (single rectangular hyperbola) was obtained using the following equation: $y = a^*x/(b + x)$; a = 1250 ± 87 $\Delta F\ s^{-1}$ and b = 24.2 ± 3.5 μM.

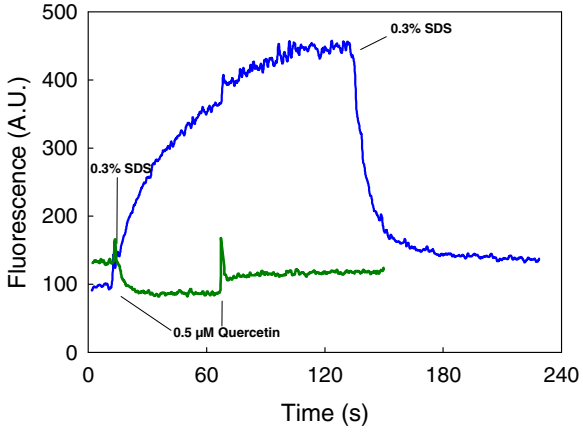

Fig. 3. Spectrofluorimetric analysis of DPBA/QC uptake in grapevine suspension cell cultures. Traces are representative of at least three independent replicates. Sonicated cells were used to check DPBA/QC movement within the vesicles, by firstly adding 0.5 μM QC (blue line) or 0.3% SDS (green line), respectively.

cell cultures were treated with DPBA, sonicated (to obtain vesicles with broken cell wall) and washed (Fig. 3). The addition of QC determined an increase of fluorescence, which was completely reversed by the subsequent addition of 0.3% SDS (blue trace). This suggests that the DPBA/QC complex entered the vesicles, to a greater extent when compared to intact cells. In agreement, the uptake was prevented if the vesicles were pre-treated with 0.3% SDS (green trace). However, the addition of SDS, before QC, still induced a small decrease in the fluorescence signal. This result indicates that vesicles already possessed a low, but detectable amount of endogenous flavonoids, of which the presence could be evaluated by DPBA.

Experiments performed with intact cells revealed the inability of SDS to solubilize plasma membranes, if the cell wall was still present (result not shown). SDS added to the assay was not able to alter the permeability of the cell wall in grape suspension cell cultures. Indeed, only after sonication and cell wall breaking, SDS effectively disrupted the phospholipid bilayer, thus allowing the release of the fluorescent complex DPBA/QCQuercetin. The phenomenon was visualized by fluorescence quenching of DPBA/QC complex, caused by its dilution into assay medium.

3.4. PFA inhibition of QC transport in grapevine suspension cell cultures

PFA is the smallest poly-oxymethylene (the polymerization product of formaldehyde), largely used in microscopy to fix the cells to preserve the membrane integrity. The PFA's aldehyde group can form a methylene bridge (–CH2–) between two reactive atoms of a protein. The reaction involves nitrogen and another reactive atom very similar to it in protein structure. Therefore, PFA has proven to be an excellent protein cross-linker, maintaining membrane structure and thus cellular compartmentation. To verify if the QC transport could be a protein-mediated phenomenon, the uptake of QC was studied after the addition 0.1 and 0.3% PFA to the assay medium (Fig. 4). After DPBA loading and incubation with different PFA concentrations, QC uptake was evaluated as the initial rate of fluorescence increase. In the presence of PFA, the uptake showed an inhibition of more than 30% (0.1% PFA, ΔF/min = 299) and more than 70% (0.3% of PFA, ΔF/min = 86), when compared to the control (ΔF/min = 583). This result supports and confirms the hypothesis that QC could be transported by membrane proteins. Accordingly, DPBA transport, occurring during previous loading, was also

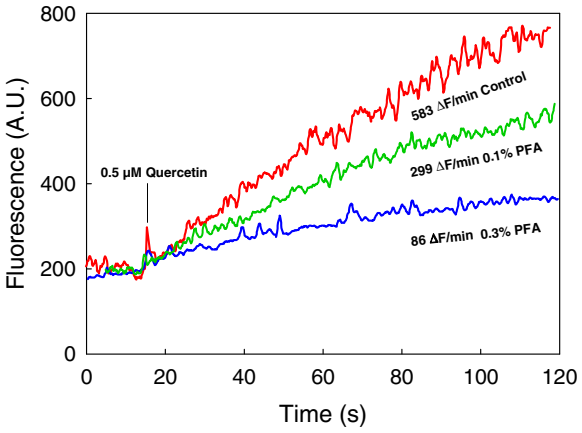

Fig. 4. PFA inhibition of QC transport in grapevine suspension cell cultures. The percentages of PFA used for conditioning grape suspension cell cultures were, respectively, 0% (blue line), 0.1% (green line) and 0.3% (red line). Each curve is representative of three different experiments.

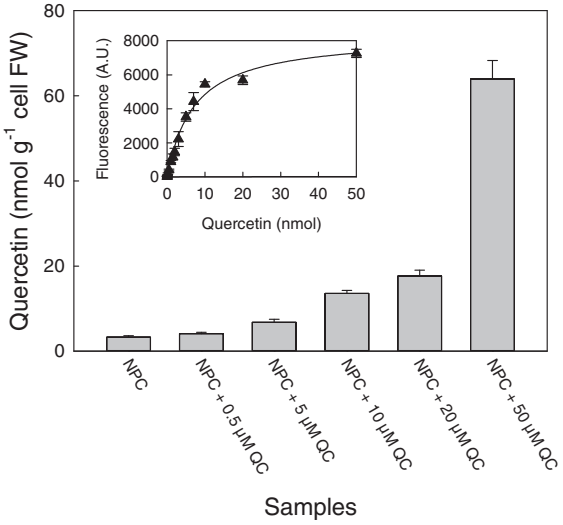

Fig. 5. QC determination in cell methanolic extracts. Different QC concentrations (0.5, 5, 10, 20 and 50 µM, respectively) were added to grapevine suspension cell cultures. The inset plot shows the calibration curve of fluorescence intensity obtained with different amounts of QC, ranging from 0 to 50 nmol. Values are means of three independent replicates ± SD.

slowed by the PFA treatment, indicating again the possible involvement of a protein-mediated transport (data not shown).

3.5. QC quantification in cellular extracts

The actual amount of QC taken up by the cells was quantified by DPBA reactions in methanolic extracts. The corresponding fluorescence values were converted by means of a calibration curve constructed using known QC concentrations. As shown in Fig. 5, NPC cultures without any QC addition contained a detectable amount of approx. 4 nmol/g FW of endogenous flavonoids, which then doubled (10 nmol/g FW) in the occurrence of incubation with 5 µM of QC. When incubated with a large concentration of the flavonoid (50 µM), the cells were able to accumulate a greater amount, reaching a level of approx. 71 nmol/g FW. Considering that the concentration of 50 µM QC corresponds to 200 nmol of QC g^{-1} FW of cells, it can approximately be estimated that cells were able to take up to 30% of the added QC in the assay medium.

4. Discussion

Currently, methodologies to monitor plant flavonoid transport *in vivo* are lacking, since spectrophotometric and fluorimetric assays are not easily applicable to these molecules. Previously, the transport of flavonoids in plant cells was evaluated with regard to the accumulation of these metabolites in the cells. To do this, analytical [15], biochemical [16,17] and indirect genomic approaches [18] were applied, mainly based on flavonoid quantification and identification by HPLC.

For these reasons, the fluorimetric method described in this paper can be viewed as a new tool useful to study flavonoid uptake into *in vivo* plant cells. The dye (DPBA) has been originally used for histological analysis of flavonoids by microscopic techniques, but recently Lee et al. [7] applied it also for rapid quantification of flavonoids in methanol extracts from animal cells. The method here described allows the detection and characterization of biochemical parameters linked to flavonoid transport into plant cells, an uptake probably mediated by membrane carriers. This protocol appears to be reliable even in the presence of cell wall, which could be an interfering structure in the case of plant systems. Indeed, it seems to be stable during long-lasting experiments, allowing an easy-to-use, fast and, moreover, direct method to evaluate flavonoid accumulation.

The spectrum analysis of QC-bound and free DPBA in a cell-free medium revealed that the complex shows high emission fluorescence, ranging from 500 to 600 nm, which allows a wide selection of the proper analytic setup (Fig. 1). After the loading of DPBA in NPC of grapevine and the washing of external dye in excess (Fig. 2, panel a), cells exhibited an increase of fluorescence intensity when QC was added (Fig. 2, panel b). The signal was confined within the cells and, in particular, was localized in the nucleus and cytoplasm, in agreement with Saslowsky et al. [8].

In addition, Fig. 2 panel c shows that the probe was not yet saturated by QC concentration (50 µM), thus permitting a good flexibility and a wide range of detection.

In previous papers, it was shown that pH conditioning is essential, according to the reversible chemical transformation of phenolic compounds under different pH conditions [19], and that the fluorescence increase of DPBA/flavonoid complexes are related to increasing pH [20]. This pH-dependent reaction, possibly due to DPBA/flavonoid complex entry in the cell, could explain the increase in fluorescence, detected in grapevine suspension cell cultures, which could reflect a true kinetic within a living system and not an unspecific effect or artefact. In addition, Fig. 3 shows that, after cell integrity disruption by mild sonication and microsomal vesicle formation, the QC uptake was higher than that observed in intact cells. This difference can be explained by these observations: i) the small volume of vesicles formed during sonication affects the fluorescence signal intensity, particularly if one considers that a plant cell (with a diameter approximately around 100 µm) possesses a volume 8-fold larger than that of vesicles (calculated on the basis of mesh size of the 50 µm nylon gauze); such condition allowed DPBA to be more easily saturated by QC inside the vesicles; ii) during sonication, vesicles can directly and quickly internalize greater amounts of DPBA, present in the assay buffer, with respect to intact cells; iii) the microsomal membrane system represents an environment more freely permeable for the probe (dye) and flavonoids in comparison to the intact cell, where different compartments and metabolites could inhibit the uptake, thus decreasing the associated fluorescence. Moreover, the QC uptake seems to be a process mediated by protein(s), since increasing concentrations of PFA, a known protein-linker, were able to inhibit it (Fig. 4).

The percentage of QC taken up into the cell actually represents a little part of the entire QC added to the assay mixture (Fig. 5). The amount of QC capable of entering the cells was about 30% of the total amount supplied, namely more than a double, if compared to similar experiments in animal cell systems (12%) [7]. On the other hand, plant cell systems should be more efficient and specialized to translocate QC and secondary metabolites. In this system, the DPBA is also able to detect endogenous flavonoids, present at nano-scale concentrations, within NPC of grapevine, as demonstrated by the fluorescence, monitored even in the absence of any external QC addition (Figs. 3 and 5). These data, therefore, confirm that flavonoids could be detectable by means of DPBA fluorescence also in plant cell extracts, aligning with previous results obtained in mammalian cells [21], and suggesting that this method is highly sensitive.

Hence, this new methodology can be considered as a initial approach that could then be applied to study the uptake of other flavonoids [22]. Further steps could involve the assessment of experimental conditions suitable for different polyphenolic moieties. Another application field would be the use of this method in a number of cell systems, aiming at defining a more general protocol for different organisms. In particular, dietary flavonoids, which are known to be transported at low concentration in mammalian cells, could be the next suitable candidates for their uptake detection by the DPBA fluorimetric method, considering also their essential role on human health and cancer proliferation [23].

Acknowledgements

This work was supported by the Italian Ministry of Education, University and Research (National Research Program PRIN2010CSJX4F).

AF and EB conceived the project, AF acquired the data, AF and EB analyzed and interpreted the data, AF, EB and EP wrote the paper, AV, CP and AB reviewed the manuscript.

References

[1] Petrussa, E., Braidot, E., Zancani, M., Peresson, C., Bertolini, A., Patui, S. and Vianello, A. (2013) Plant flavonoids-biosynthesis, transport and involvement in stress responses. Int. J. Mol. Sci. 14, 14950–14973.

[2] Kumar, S. and Pandey, A.K. (2013) Chemistry and biological activities of flavonoids: an overview. Sci. World J.

[3] Mezzetti, A., Protti, S., Lapouge, C. and Cornard, J.P. (2011) Protic equilibria as the key factor of quercetin emission in solution. Relevance to biochemical and analytical studies. Phys. Chem. Chem. Phys. 13, 6858–6864.

[4] Dmitrienko, S.G., Kudrinskaya, V.A. and Apyari, V.V. (2012) Methods of extraction, preconcentration, and determination of quercetin. J. Anal. Chem. 67, 299–311.

[5] Baran, I., Ganea, C., Ursu, I., Baran, V., Calinescu, O., Iftime, A., Ungureanu, R. and Tofolean, I.T. (2011) Fluorescence properties of quercetin in human leukemia jurkat T-cells. Rom. J. Phys. 56, 388–398.

[6] Hsieh, K. and Huang, A.H.C. (2007) Tapetosomes in Brassica tapetum accumulate endoplasmic reticulum-derived flavonoids and alkanes for delivery to the pollen surface. Plant Cell 19, 582–596.

[7] Lee, J.H., Kim, Y., Hoang, M.H., Jun, H.J. and Lee, S.J. (2014) Rapid quantification of cellular flavonoid levels using quercetin and a fluorescent diphenylboric acid 2-amino ethyl ester probe. Food Sci. Biotechnol. 23, 75–79.

[8] Saslowsky, D.E., Warek, U. and Winkel, B.S.J. (2005) Nuclear localization of flavonoid enzymes in Arabidopsis. J. Biol. Chem. 280, 23735–23740.

[9] Buer, C.S., Muday, G.K. and Djordjevic, M.A. (2007) Flavonoids are differentially taken up and transported long distances in Arabidopsis. Plant Physiol. 145, 478–490.

[10] Karabourniotis, G., Kofidis, G., Fasseas, C., Liakoura, V. and Drossopoulos, I. (1998) Polyphenol deposition in leaf hairs of *Olea europaea* (Oleaceae) and *Quercus ilex* (Fagaceae). Am. J. Bot. 85, 1007–1012.

[11] Owen, H.R. and Miller, A.R. (1992) An examination and correction of plant-tissue culture basal medium formulations. Plant Cell Tissue Organ Cult. 28, 147–150.

[12] Repka, V., Kubikova, J. and Fischerova, I. (2000) Immunodetection of PR-1-like proteins in grapevine leaves infected with *Oidium tuckeri* and in elicited suspension cell cultures. Vitis 39, 123–127.

[13] Pereira-Lachataignerais, J., Pons, R., Panizza, P., Courbin, L., Rouch, J. and Lopez, O. (2006) Study and formation of vesicle systems with low polydispersity index by ultrasound method. Chem. Phys. Lipids 140, 88–97.

[14] Murphy, A., Peer, W.A. and Taiz, L. (2000) Regulation of auxin transport by aminopeptidases and endogenous flavonoids. Planta 211, 315–324.

[15] Merken, H.M. and Beecher, G.R. (2000) Measurement of food flavonoids by high-performance liquid chromatography: a review. J. Agric. Food Chem. 48, 577–599.

[16] Francisco, R.M. et al. (2013) ABCC1, an ATP binding cassette protein from grape berry, transports anthocyanidin 3-O-glucosides. Plant Cell 25, 1840–1854.

[17] Tommasini, R., Evers, R., Vogt, E., Mornet, C., Zaman, G.J.R., Schinkel, A.H., Borst, P. and Martinoia, E. (1996) The human multidrug resistance-associated protein functionally complements the yeast cadmium resistance factor 1. Proc. Natl. Acad. Sci. USA 93, 6743–6748.

[18] Kim, C.K. et al. (2013) Multi-layered screening method identification of flavonoid-specific genes, using transgenic rice. Biotechnol. Biotechnol. Equip. 27, 3944–3951.

[19] Lee, J., Durst, R.W. and Wrolstad, R.E. (2005) Determination of total monomeric anthocyanin pigment content of fruit juices, beverages, natural colorants, and wines by the pH differential method: collaborative study. J. AOAC Int. 88, 1269–1278.

[20] Matteini, P., Agati, G., Pinelli, P. and Goti, A. (2011) Modes of complexation of rutin with the flavonoid reagent diphenylborinic acid 2-aminoethyl ester. Monatshefte Fur Chemie 142, 885–893.

[21] Lee, J.H., Lee, J.E., Kim, Y., Lee, H., Jun, H.J. and Lee, S.J. (2014) Multidrug and toxic compound extrusion protein-1 (MATE1/SLC47A1) is a novel flavonoid transporter. J. Agric. Food Chem. 62, 9690–9698.

[22] Kartnig, T. and Gobel, I. (1996) Effect of fluorescence intensifiers on the fluorodensitometric determination of flavones and flavonols after detection with diphenylboric acid 2-aminoethyl ester. J. Chromatogr. A 740, 99–107.

[23] Batra, P. and Sharma, A.K. (2013) Anti-cancer potential of flavonoids: recent trends and future perspectives. 3 Biotech 3, 20.

CHAPTER 2

Flavonoid facilitated/ passive transport:
characterization of quercetin microsomial uptake

Paper under revision

Flavonoid facilitated/ passive transport in plants: characterization of quercetin microsomal uptake

Antonio Filippi[1], Elisa Petrussa[1] and Enrico Braidot[1]

[1] Depart. of Agricultural, Food, Animal and Environmental Sciences, University of Udine, Via delle Scienze 91, 33100 Udine, Italy.

ABSTRACT

Flavonoids consist of a large group of hydroxylated phenolic substances, ubiquitously present in plants, synthesized on the cytosolic side of endoplasmic reticulum. To fulfil their physiological roles in plants, the site of flavonoid biosynthesis, the compartment of storage and their cellular activity require an efficient membrane transport. In addition to the well-known primary and secondary transporters mechanisms (e.g. ABCC1 and MATE) and vesicle-mediated traffic, a new hypothesis on a facilitated/passive transport of flavonoids through membrane, has been recently proposed. With this work we tried to better characterize a facilitated/passive transport of quercetin (QC) in *Pisum sativum* microsomes, by using for the first time a new *in vitro* application of DPBA-dependent methodology. Further characterization was carried out using modulators of protein redox state, evidencing the role of reducing moieties in increasing passive protein-mediated transport.

1. INTRODUCTION

Flavonoids are a group of plant secondary metabolites with a phenolic structures, chemically based upon a fifteen-carbon skeleton, consisting of two benzene rings (A and B) linked via a heterocyclic pyran ring (C). They can be divided into a variety of classes, depending on the position of the benzene ring (B ring) respect to the benzopyran moiety (A,C rings). According to substituents in position 2, 3 or 4 we can distinguish (i) flavones, flavanols (flavan-3-ols) and anthocyanidins, (ii) isoflavonoids (3-benzopyrans) and (iii) 3-neoflavonoids (4-benzopyrans) respectively. The various classes of flavonoids differ in the level of oxidation and pattern of substitution of the C ring, while individual compounds within a class differ in the pattern of substitution of the A and B rings. Although studies on flavonoids have revealed that most flavones and flavonols exhibit two major absorption bands (320-385nm for B ring, and 250-285 nm for A ring), their spectrophotometric properties are far from being elucidated in a clear manner due to their chemical structure that leads different (several) physical and chemical properties (Kumar and Pandey 2013).

Over the 4000 different widely distributed plant polyphenolic metabolites, the flavonol

quercetin (QC) is an interesting lead compound for further pharmaceutical research, and has been discussed in over 6000 journal publications (Wang et al. 2011).

In plants the different flavonoids play specific biological functions, including protection against ultraviolet (UV) radiation and phytopathogens, signaling during nodulation, male fertility, auxin transport, as well as the coloration of flowers and fruits as a visual signal that attracts pollinators and seed dispersing animals. Flavonoids are also responsible for the display of colors in many deciduous plants, which may protect leaf cells from photo-oxidative damage, enhancing the efficiency of nutrient retrieval during senescence. Flavonols are probably the most important flavonoids participating in stress responses. From an evolutionary point of view, they are the most ancient and widespread flavonoids, having a wide range of relevant physiological activities (Falcone Ferreyra, Rius, and Casati 2012).

In plants, flavonoids are synthesized on the cytosolic side of the endoplasmic reticulum (ER) and then stored into the vacuole or transported to other destinations (like nucleus or cell wall), where they can act as bioactive molecules (Pérez-Díaz et al. 2014).

To fulfill their biological roles, flavonoids have to move from the site of biosynthesis to the storage compartments and metabolic targets, so they require a fine and efficient transport mechanism. However, evidence of flavonoid subcellular distribution, transport and storage has only recently emerged, due to methodological and analytical difficulties in tracking them. Four distinct, but potentially non-exclusive mechanisms for flavonoid transport in plant cells have been proposed: vesicle trafficking, membrane and GST-mediated transport, and facilitated/passive transport. According to the first mechanism, biological studies have illustrated that anthocyanins (the aglycone of anthocyanidins) can be transported into the central vacuole via vesicle trafficking in a Golgi-dependent or independent manner (Poustka et al. 2007).

Other recent observations, in *Vitis* hairy roots and *Arabidopsis* seed endothelium cells, further demonstrated that ER-derived small vesicles filled with anthocyanins are transported toward the central vacuole. The first committed step required for vesicle trafficking is loading flavonoids into the ER lumen or into small vesicles budding from it, using a protein-mediated system; however, little is known about this mechanism. Three flavonoid-loading processes have been proposed:

(i) the traffic among the ER and Golgi secretory vesicles involved transporters localized on the small vesicle or the Golgi membranes;

(ii) the glutathione-*S*-transferase GST-flavonoid complex that can be associated with ER membranes and it may facilitate flavonoids loading into ER vesicles;

(iii) flavonoids may be loaded into the ER as soon as they are synthesized on the ER via other unknown mechanisms (Zhao 2015).

Concerning the second mechanism (membrane transporter model), biochemical, molecular, and genetic evidences support the involvement of both multidrug and toxic extrusion (MATE) and the ATP binding cassette (ABC) proteins. The establishment of a proton gradient between the cytosol and the vacuole (or the cell wall) by H^+-ATPases (and H^+-PP_iases in the tonoplast) has been proposed as the main driving force for the vacuolar transport of some flavonoids by MATE proteins. Once these compounds are in the vacuoles, the acidic pH inside the vacuolar compartment and the acylation of flavonoids are both necessary for the induction of a conformational modification, responsible for the appropriate trapping and retention of the metabolites (Petrussa et al. 2013).

Empirical evidences showed in fact the presence of many anthocyanin vacuolar inclusions (AVIs) within the tonoplast. Vacuolar localization prevents anthocyanin oxidation and the low pH environment confers the typical intense coloration, helping them to condensate into a compact, crystal form too (Chanoca et al. 2015).

MATE transporters comprise a large family of transporters, widely distributed in all living organisms. The first experimental evidence for the involvement of a MATE transporter in flavonoid transport came from a genetic screening in *Arabidopsis thaliana*, aiming at identifying the different steps of flavonoid biosynthesis (Francisco et al. 2013).

ABC proteins have also been claimed to play a role in sequestration of flavonoids into the vacuole. The ABC transporter family is very large (79 members in *Escherichia coli*, 29 in *Saccharomyces cerevisiae*, and 131 in *Arabidopsis*) and its members are found in all organisms. However, functionally the subfamily C of ABC transporters is only marginally characterized and ABCC transporters might be responsible for several so far unknown functions. These proteins are capable to coupling the ATP hydrolysis to a direct translocation, through the membranes, of many substrates (lipids, heavy metal ions, inorganic acids, glutathione conjugates, sugars, amino acids, peptides, secondary metabolites, and xeno-(molecules)biotics, used as drugs) after their conjugation with glutathione (GSH), by a reaction catalyzed by GST. Genetic studies have shown that multidrug resistance-associated protein (MRP)/C-type of ABC (ABCC) transporters, such as maize MRP1, are involved in vacuolar flavonoid accumulation, postulating that they are able to transport flavonoid conjugates with glutathione (GSH). However, this assumption has not been so far demonstrated, since no glutathionylated flavonoid moiety has been found inside vacuolar compartment. Recently, Francisco et al. (2013) suggested that the GSH was essential for ABCC1-mediated anthocyanin transport in grapevine, since it was co-transported with the flavonoid.

The third mechanism involves GSH as a hypothetical flavonoid-ligand peptide. The involvement of GST/GSH is under investigation since the exact role of both the

enzyme and the peptide is still unclear. A GSH-deficient mutant of *Arabidopsis thaliana*, *gsh2*, displayed in fact defective secretory trafficking with the appearance of small vacuole-like vesicles and disappearance of the large vacuole. The GSTs enzymes from various plants are essential for anthocyanin and PA accumulation, and free GSH is strictly required for transport of the anthocyanin malvidin 3-O-glucoside, into yeast vacuoles by *Vitis vinifera* ABCC1. Nevertheless GSTs that are involved in flavonoid accumulation may not catalyze the link between flavonoid and GSH, but rather they physically bind to flavonoids and act as flavonoid carrier proteins that facilitate flavonoid translocation from the cytoplasm into the vacuole. In plant cells that produce high levels of anthocyanins GSTs were also associated with membranes, likely the ER and the vacuole (Zhao 2015).

To facilitate flavonoid membrane crossing, the above-mentioned mechanisms need to be energized by ATP consumption. In addition, it could be also considered another energy independent mechanism responsible for flavonoid accumulation: the facilitated/passive transport. Unlike simple diffusion where moieties pass through a membrane along the concentration gradient without the involvement of proteins (passive transport), facilitated transport allows molecules to diffuse across the membrane through a trans-membrane polypeptide structure (Bienert and Chaumont 2014).

As additional modality of the above mentioned passive mechanism, recently an innovative idea has been proposed, based on a vesicle system closely related to the auto-phagy process. The theory raised from an observation: the standard model of anthocyanin transport predicts that anthocyanin vacular inclusions (AVIs) should not be bound by membranes, thanks to a protein-mediated transport, but fluorescence microscopy observations show that the AVIs are surrounded by a single membrane, compelling them to rethink current models and proposing the auto-phagy system (Bassham 2015).

Also, the presence of many large intra-vacuolar bodies, including membranous ones, named neutral red stained bodies (NRSBs), are considered to originate by autophagy processes. NRSBs are much larger in the anthocyanin accumulating cells indicating that these bodies are related to anthocyanin vesicular inclusions (AVIs). Accordingly, *Arabidopsis* vesicle tethering complex subunit exo70B1-2 mutant, lacking in vacuolar anthocyanins presence, display decreased accumulation of NRSBs too (Kulich and Žárský 2014).

Considering the facilitated transport, the main members of integral membrane proteins involved in the transport of ions and polar molecules not diffusible through the hydrophobic layer, are: i) carriers able to bind a molecule and, consequently, trigger a change of their own structure, moving the bound molecule from one side to

the other; ii) channel proteins able to create a pore through the membrane hydrophobic region for the transport of molecules and ions at high speed rate (Boundless 2016).

There are several example of this process in mammalian cells and particularly it is well known in the kidney, where glucose, water, salts, ions, and aminoacids' channels are needed to filter the blood. A large family of sugar facilitate-transport proteins exists in mammalian tissues, such as in the brain, where the tissue has a constitutively high glucose requirement and has been endowed with transporters that are constitutively targeted to the cell surface (for example, GLUTs 1–3) (Bryant, Govers, and James 2002).

In this huge scenario, the study of flavonoids has required many techniques and methodological approaches to understand the mechanisms involved in the regulation of their transport. The use of fluorescent probes has been recently re-evaluated, as well as the innermost fluorescent properties of the flavonoids themselves.

2-aminoethoxydiphenyl borate (DPBA) is an esterified moiety largely used in microscopy for flavonoid localization, due to its ability to form a spontaneous complex with many different flavonoid compounds. It has already been used in mammalian tissue microscopy analysis to describe flavonoid accumulation inside specific compartments. Accordingly, the complex between DPBA and flavonoids highly increases the inner fluorescent properties of the DPBA, allowing a better detection under spectro-fluorimetric analysis. DPBA has been recently used to detect flavonoid concentration within mammalian cells and to characterize the *in vivo* QC transport in a plant cell system (Filippi et al. 2015).

For this reason we aimed to validate and implement the use of this fluorescent probe in an *in vitro* assay of QC transport, in isolated pea stem microsomial vesicles. Nevertheless, since large interest has been developed on the characterization of flavonoid transport requiring ATP-generated electrochemical gradient (active transport), considered as the main driver of the secondary metabolites movement within the cell, in this work we have instead characterized and evaluated the role of QC facilitated-passive transport across plant membranes.

2. MATERIAL AND METHODS

2.1 Plant material

Etiolated pea (*Pisum sativum* L., cv. Meraviglia d'Italia, Ingegnoli) stems were obtained by growing plants on sand for 7 days, in the dark, at 25°C and 60% relative humidity.

2.2 Microsome isolation

To obtain competent microsomes from *P. sativum* stems, the protocol of Macrì et al.

(1991) has been used, with minor changes: in the washing buffer the BSA concentration was 0.05% and final resuspension buffer was 20 mM MES/KOH (pH 5.5), 0.25 M sucrose, 5 mM DTT.

2.3 Acridine orange (AO) measurement

The generation of proton gradient mediated by ATPase in pea microsomes was monitored as uptake of AO, at room temperature, following the quenching of AO fluorescence by a Perkin-Elmer spectrofluorimeter (model LS50B). The assay was described in Macrì et al. (1991).

2.4 Spectrofluorimetric analysis of QC uptake in microsomes suspension by DPBA

The reaction was performed in 2 ml of the microsome resuspension buffer after the addition of 50 mM KCl and 100 μg protein of competent microsomes. The reaction started after the addition of 0.0001% DPBA and the desired concentration of QC (0.1-1 μM). Modulators of different transport proteins were incubated 5 min at room temperature with microsomes, before starting the reaction, into a resuspention buffer without DTT. The reading set up was: 461 nm for the excitation and 520 nm for the emission wavelength, respectively, using slit width of 15 nm for both excitation and emission.

3. RESULTS

3.1 QC uptake into pea stem microsomes

In order to study QC uptake in microsomal vesicles obtained by pea etiolated stem, the first step was to assess if membrane vesicles were intact and sealed enough to sustain a flavonoid transport through membrane bilayer. This condition was essential in order to perform the transport assay by means of changes in fluorescence of DPBA, when complexed by QC. For this reason, competence of microsomes was assessed by AO fluorescence quenching (paragraph 2.3) induced by proton pumping activities of ATPases (data not shown) just before QC transport experiments. This procedure allows to validate an efficient membrane system for the internal accumulation of the transported amount of QC. In addition, a similar concentration of diluted DPBA solution (0.0001%) was added after the formation of the proton gradient, aiming to verify that this compound would not collapse pH gradient or affect the membrane intactness. DPBA addition was similar to what used in the subsequent transport assay.

The transport assay was performed in resuspension buffer within few minutes, as shown in the representative kinetic curve of Figure 1. After the addition of microsomes

and DPBA probe, when added to the resuspension buffer at low micromolar concentration, a kinetic curve is recorded as transport of QC within the lumen of the microsomes. The transport kinetic was followed as an instantaneous, real-time increase of fluorescence, which reached a steady state level after approx. 2 min. The initial speed rate of the kinetic curve was measured and expressed as fluorescence absolute units (A.U. s^{-1}). This value was considered to be the actual measurement of QC transport rate through vesicle bilayer. It was believed that DPBA probe should be enough small to pass quickly pea microsomal membranes and, once inside, it could be complexed only by the QC transported in the interior of the vesicle, causing the change in fluorescence observed at the fluorimeter. The actual transport of QC inside of the vesicles was validated by a parallel control experiment, performed in the absence of microsomes, when the addition of QC to the DPBA-buffer assay caused only a lower postitive jump without kinetics (result not shown).

As shown in Figure 1, a steady line was obtained after QC transport, due to a probable dinamic equilibrium between the QC migrating inside microsomal lumen and bound to DPBA probe and that one leached outside the vesicles.

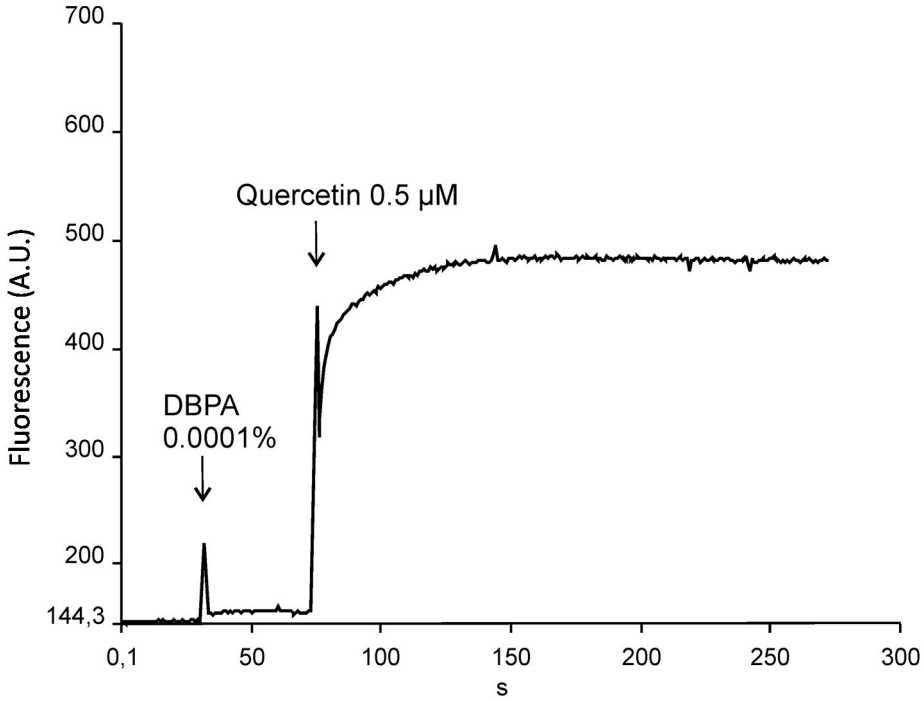

Figure 1. Kinetic curve of QC transport into pea stem microsomal vesicles. Representative curve of QC transport assay. Pea stem microsome vesicles (100 µg protein) were incubated in the assay buffer with 0.0001% DPBA, as described in paragraph 2.4. Transport of QC was evaluated as the initial rate of fluorescence increase.

3.2 Characterization of QC transport into pea stem microsome vesicles by modulators of passive facilitated-diffusion channels

As the observed transport of QC into microsomes preincubated with DPBA occurred in the absence of energy supply and it didn't require any proton gradient built across membranes, it was suggested the possible involvement of one/some facilitated/passive-like transporter(s). The measurement of the effect of different well-known modulators of membrane channels and/or transporters was revealed on the initial rate of QC uptake by pea microsomes (Table 1). Appreciable effects of oxidant and reducing agents were detected: diamide, a potent oxidant agent able to affect carrier-mediated transport produced a decrease in the initial speed of QC uptake, while the reducing agent ditiothreitol (DTE) stimulated significantly the QC transport, causing a stimulation of the initial rate by a 67%, when compared to the control.

Moreover, it was interesting to observe that the N-ethyl maleimide agent (NEM), able to irreversibly block the sulphydryl groups of proteins, did not inhibit the transport mechanism, but it slightly stimulated the activity at 40 μM. Formaldehyde, a crosslinker routinely employed for detection of protein-DNA and protein-protein interactions, showed a maximum reduction of 50% when used at 0.1%. The bounds between different functional groups of the same/different proteins made by this molecule are able to inactivare or at least reduce the biological functions of the proteins keeping the membranes intact.

	Dose	Initial rate		
NEM	0	4.58±0.98 a	F	4.268
	0.1 μM	5.44±1.23 ab	P	0.017*
	1 μM	6.06±0.97 abc		
	10 μM	6.95±1.33 bc		
	40 μM	7.52±1.10 c		
DTT	0	6.58±0.61 a	F	13.65
	5 mM	9.19±1.14 b	P	0.007**
Diamide	0	6.21±0.92 a	F	5.745
	0.5 mM	5.16±0.46 ab	P	0.011*
	5 mM	4.77±0.85 b		
	15 mM	4.27±0.33 b		
Formaldehyde	0	6.28±0.48 a	F	25.39
	0.01%	5.79±0.67 a	P	0.000***
	0.05%	4.66±0.58 b		
	0.10%	3.13±0.46 c		

Table 1. Effect of different modulators of proteins on the initial rate of QC transport into pea stem microsome vesicles. Transport modulators at different concentrations were preincubated in the assay medium in the presence of microsome vesicles and then DPBA and 0.5 μM QC were added and the actual initial rate was calculated as above described. Values of the initial speed are means of at least three independent replicates ± SD. F- Fisher-Snedecor value, P- probability

3.3 Evidence of QC entrance into microsome vesicles

With the aim of demonstrating that QC actually entered into the microsome vescicles and the reaction of magnification of the signal shown in Figure 1 was not only related to unspecific binding of QC to proteins or phospholipids, we have considered a feature of the complex DPBA/QC, which exhibited different fluorescence intensity depending on buffer pH. Microsomes were prepeared as explained into Materials & Methods, with one minor change: the microsomes were conditioned in the resuspension buffer at two different pHs (4.5 and 6.5, respectively). The assay of QC transport was performed as usual, with an assay buffer at pH 5.5. Since fluorescence was less intense when the pH of the buffer is close to neutral values, we evaluated that the initial speed rate, strictly depending on fluorescence intensity, was significantly reduced when the microsomes were conditioned at the more basic buffer (pH 6.5), demonstrating that the complex of DPBA/QC formed inside of the vesicles caused the effect of pH on fluorescence intensity (Figure 3, inset).

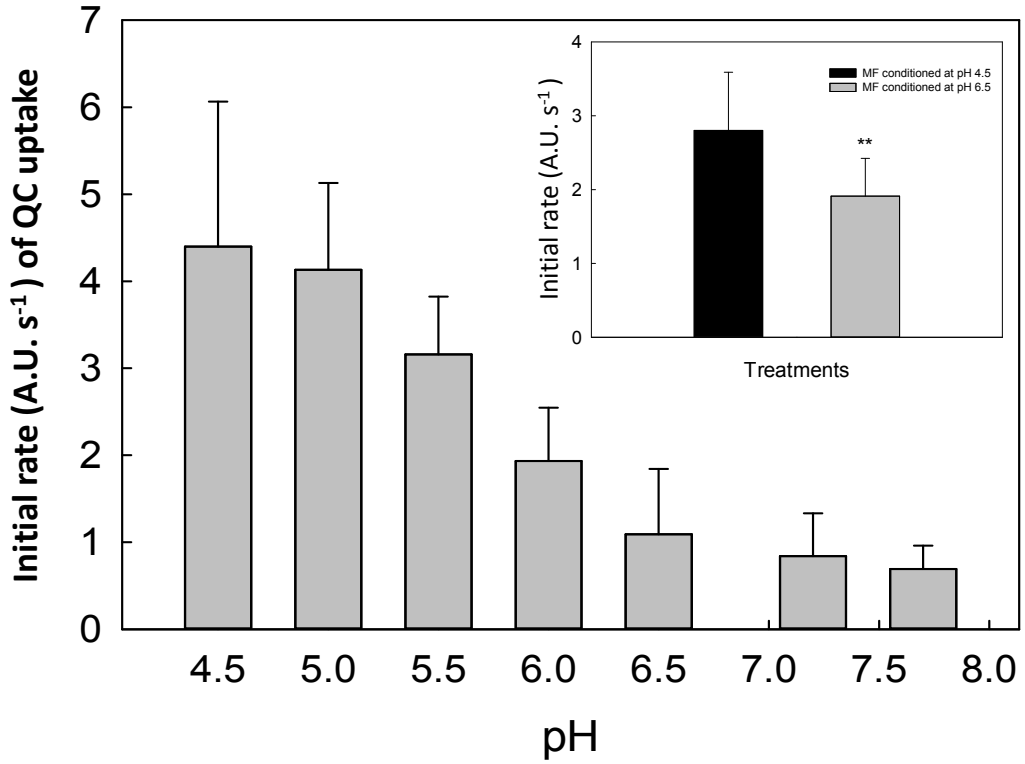

Figure 2. Effect of assay buffer pH on fluorescence intensity of DPBA/QC complex, in comparison to initial speed rate of QC transport within microsomes conditioned at two resuspension buffer pH. Microsomes were resuspended in buffer at pH 5.5 and then transport of QC was assayed by changing the pH of assay buffer (4.5-8.0). In the inset, two microsome samples, conditioned at pH 4.5 or 6.5, were used for transport assay at pH 5.5.

4. DISCUSSION

Flavonoids are among the most powerful bioactive plants metabolites, capable to interact both with plant and mammalian metabolism. They are present in terrestrial plants since their land colonization and they are part of mammalian diet since more than 4 million years. Flavonoids exert many different biological activities in plants (UV-protection, ROS scavenging, enzymatic activity modulation, flowers and fruits coloration, signalling and cellular communication) and in mammals (antioxidant activity, cancer cell proliferation inhibition, enzymatic activity modulation) (Falcone Ferreyra, Rius, and Casati 2012; Poór, Zrínyi, and Kőszegi 2016).

Flavonoid biological activities are very sensitive to pH and molar concentration and strongly connected to plant cellular capability to transport, store, excrete or to concentrate and sequestering them into specific cellular compartments. Particularly, the scientific community has debated upon flavonoid transport many times in the last 30 years, trying to obtain a complete overview of the production and transport systems, but up to date a full understanding of such a complicated mechanism is far from being elucidated (Chanoca et al. 2015).

From the literature, flavonoids are mainly translocated across membranes by energized protein systems, i.e. a primary transport with a direct ATP hydrolysis or a secondary transport using a proton gradient formed by H^+-ATPase pump activity. Other molecules are transported by a third common mechanism, the passive/facilitated transport. This system seems not to be involved in flavonoid transport, although considering the high molar concentration of flavonoid in light-exposed tissues, the only active transport appears to be insufficient and energetically unsustainable (Petrussa et al. 2013).

For this reason, in this work we want to evaluate the possible role of passive/facilitated transport of quercetin (QC) across a simplified plant membrane model (etiolated *P. sativum* microsomes), by means of a new *in vitro* methodology (Filippi et al. 2015). This methodology, based on a DPBA protocol set in a cellular system, was assessed upon microsomal membrane vesicles. A kinetic curve (Figure 1) was obtained when QC was added to *P. sativum* microsomes incubated with DPBA, indicating the entrance of the flavonoid within the structure of microsomes. The complex formation between the flavonoid QC and the probe DPBA within microsomes was followed as an increase of the fluorescence signal, which reached a plateau after few minutes (Figure 1). The kinetic curve is composed by an initial immediate jump, probably caused by the interaction between QC and membranes and a subsequent asymptotic curve, caused by QC entrance: the value of initial rate (interpolated within the first 10 seconds) was in fact considered representative of the entrance of QC within microsomes.

A possible artifact caused by unspecific bond between QC and the phospholipid

membrane, has been considered, although the experiment shown in Figure 2, demonstrated how keeping stable the pH value of the resuspension buffer (and so the protonation state of the flavonoid), the pH-dependent variation of fluorescence recorded as different initial speed rate, must be due to the different internal pH conditions only. So this is a proof that the measured fluorescence increase is related at least partially to the complex formed within microsomes, reducing the possibility that unspecific binding could affect the fluorescence signal.

To further investigate if proteins are involved in this passive transport of flavonoid across membranes, further assays were performed using thiol reacting (NEM- n-ethyl maleimide) reducing (DTE- dithiothreitol), oxidizing (diamide) and protein cross-linking (formaldehyde) agents, with the aim to modulate the uptake of QC within the microsomes. The Table 1 shows that DTE enhanced the initial rate of QC entrance, while diamide and formaldehyde induced a decrease in the initial rate. These results seem to confirm what has been described in literature so far about the essential role of reducing agents in maintaining structural and biological/enzymatic functions of the proteins, particularly when bound to or within membranes (Lundahl et al. 1981). On the contrary, oxidizing molecule and protein cross-linker lowered the initial rate as already known in liteature, although no strong effect of transport induction seems to have NEM (Kozlova et al. 2002).

In fact it is not easy to univocally describe the chemical action of this sulfhydryl reagent, known on one hand to inhibit vesicular transport and on the other to stimulate chloride-dependent K^+ transport (Berkowitz, Walstad, and Orringer 1987) or at least not to affect the hexose transport modulated by insulin activity (Czech 1976).

In the present study, we should consider the effect of modulators on a complex system in which more characters (DPBA, QC and membranes) play different roles in a net of interactions that is only recently under investigation and is still not fully understood. To the best of our knowledge, this is the first time the flavonoid-binding probe DPBA is used to detect an *in vitro* real time transport of flavonoid across biological membranes. Moreover, this methodology is applied to understand the possibility that facilitated/passive transport is involved in the translocation of flavonoid across membranes, as only recently hypothesized (Bassham 2015). Further experiments must be set to give a complete and real comprehension of the assay system, starting from an actual determination of the amount of QC loaded within microsoms (methanolic extraction of pre-loaded microsomes with different concentrations of QC) to a quantification of a putative free interaction between flavonoid and membrane, as well as evaluation of the permeability of QC through phospholipid bilayer using artificial membrane methodology (PAMPA) (Kerns et al. 2004). Such assays will allow to confirm the presence of a passive QC uptake into plant microsome vesicles and to

quantify the respective contribution to the overall transport by the passive membrane diffusion component in comparison to the protein mediated mechanism.

5. BIBLIOGRAPHY

Bassham, D. C. Plant biology: Pigments on the move. *Nature* **526,** 644–645 (2015).

Berkowitz, L. R., Walstad, D. & Orringer, E. P. Effect of N-ethylmaleimide on K transport in density-separated human red blood cells. *American Journal of Physiology - Cell Physiology* **253,** C7–C12 (1987).

Bienert, G. P. & Chaumont, F. Aquaporin-facilitated transmembrane diffusion of hydrogen peroxide. *Biochim. Biophys. Acta* **1840,** 1596–1604 (2014).

Boundless. Facilitated transport. *Boundless* (2016).

Bryant, N. J., Govers, R. & James, D. E. Regulated transport of the glucose transporter GLUT4. *Nat Rev Mol Cell Biol* **3,** 267–277 (2002).

Chanoca, A. *et al.* Anthocyanin Vacuolar Inclusions Form by a Microautophagy Mechanism. *Plant Cell* **27,** 2545–2559 (2015).

Czech, M. P. Current status of the thiol redox model for the regulation of hexose transport by insulin. *J. Cell. Physiol.* **89,** 661–668 (1976).

Falcone Ferreyra, M. L., Rius, S. P. & Casati, P. Flavonoids: biosynthesis, biological functions, and biotechnological applications. *Front Plant Sci* **3,** 222 (2012).

Filippi, A. *et al.* In vivo assay to monitor flavonoid uptake across plant cell membranes. *FEBS Open Bio* **5,** 748–752 (2015).

Francisco, R. M. *et al.* ABCC1, an ATP binding cassette protein from grape berry, transports anthocyanidin 3-O-Glucosides. *Plant Cell* **25,** 1840–1854 (2013).

Kerns, E. H. *et al.* Combined application of parallel artificial membrane permeability assay and Caco-2 permeability assays in drug discovery. *J. Pharm. Sci.* **93,** 1440–1453 (2004).

Kozlova, N. M. *et al.* [Effect of diamide on protein oxidation and physico-chemical properties of lipids in erythrocyte membranes]. *Biofizika* **47,** 500–505 (2002).

Kulich, I. & Žárský, V. Autophagy-related direct membrane import from ER/cytoplasm into the vacuole or apoplast: a hidden gateway also for secondary metabolites and phytohormones? *Int J Mol Sci* **15,** 7462–7474 (2014).

Kumar, S. & Pandey, A. K. Chemistry and Biological Activities of Flavonoids: An Overview. *The Scientific World Journal* **2013,** e162750 (2013).

Lundahl, P. *et al*. The stereospecific D-glucose transport activity of cholate extracts from human erythrocyte membranes. *Biochim Biophys Acta* **644,** 101–107 (1981).

Macri, F., Vianello, A., Braidot, E. & Zancani, M. Free fatty acids dissipate proton

electrochemical gradients in pea stem microsomes and submitochondrial particles. *Biochimica et Biophysica Acta (BBA) - Bioenergetics* **1058,** 249–255 (1991).

Pérez-Díaz, R. *et al.* VvMATE1 and VvMATE2 encode putative proanthocyanidin transporters expressed during berry development in Vitis vinifera L. *Plant Cell Rep.* **33,** 1147–1159 (2014).

Petrussa, E. *et al.* Plant Flavonoids—Biosynthesis, Transport and Involvement in Stress Responses. *International Journal of Molecular Sciences* **14,** 14950–14973 (2013).

Poór, M., Zrínyi, Z. & Kőszegi, T. Structure related effects of flavonoid aglycones on cell cycle progression of HepG2 cells: Metabolic activation of fisetin and quercetin by catechol-O-methyltransferase (COMT). *Biomed. Pharmacother.* **83,** 998–1005 (2016).

Poustka, F. *et al.* A trafficking pathway for anthocyanins overlaps with the endoplasmic reticulum-to-vacuole protein-sorting route in Arabidopsis and contributes to the formation of vacuolar inclusions. *Plant Physiol.* **145,** 1323–1335 (2007).

Wang, R. E., Hunt, C. R., Chen, J. & Taylor, J.-S. Biotinylated quercetin as an intrinsic photoaffinity proteomics probe for the identification of quercetin target proteins. *Bioorganic & Medicinal Chemistry* **19,** 4710–4720 (2011).

Zhao, J. Flavonoid transport mechanisms: how to go, and with whom. *Trends in Plant Science* **20,** 576–585 (2015).

CHAPTER 3

Flavonoid interaction with a chitinase from grape berry skin: protein identification and modulation of the enzymatic activity

molecules

MDPI

Article

Flavonoid Interaction with a Chitinase from Grape Berry Skin: Protein Identification and Modulation of the Enzymatic Activity

Antonio Filippi [1], Elisa Petrussa [1], Uros Rajcevic [2], Vladka Čurin Šerbec [2], Sabina Passamonti [3], Giovanni Renzone [4], Andrea Scaloni [4], Marco Zancani [1], Angelo Vianello [1] and Enrico Braidot [1,*]

1 Department of Agricultural, Food, Animal and Environmental Sciences, University of Udine, Via delle Scienze 91, 33100 Udine, Italy; antonio.filippi@uniud.it (A.F.); elisa.petrussa@uniud.it (E.P.); marco.zancani@uniud.it (M.Z.); angelo.vianello@uniud.it (A.V.)

2 Blood Transfusion Centre of Slovenia, Department of R&D, Šlajmerjeva 6, 1000 Ljubljana, Slovenia; uros.rajcevic@ztm.si (U.R.); vladka.curin@ztm.si (V.Č.Š.)

3 Department of Life Sciences, University of Trieste, via L. Giorgieri 1, 34127 Trieste, Italy; spassamonti@units.it

4 Proteomics and Mass Spectrometry Laboratory, ISPAAM, CNR, via Argine, 1085-80147 Napoli, Italy; giovanni.renzone@ispaam.cnr.it (G.R.); andrea.scaloni@ispaam.cnr.it (A.S.)

* Correspondence: enrico.braidot@uniud.it; Tel.: +39-0432-558792

Academic Editors: Celestino Santos-Buelga and Arturo San Feliciano
Received: 1 September 2016; Accepted: 22 September 2016; Published: 28 September 2016

Abstract: In the present study, an antibody raised against a peptide sequence of rat bilitranslocase (anti-peptide Ab) was tested on microsomal proteins obtained from red grape berry skin. Previously, this antibody had demonstrated to recognize plant membrane proteins associated with flavonoid binding and transport. Immuno-proteomic assays identified a number of proteins reacting with this particular antibody, suggesting that the flavonoid binding and interaction may be extended not only to carriers of these molecules, but also to enzymes with very different functions. One of these proteins is a pathogenesis-related (PR) class IV chitinase, whose in vitro chitinolytic activity was modulated by two of the most representative flavonoids of grape, quercetin and catechin, as assessed by both spectrophotometric and fluorimetric assays in grape microsomes and commercial enzyme preparations. The effect of these flavonoids on the catalysis and its kinetic parameters was also evaluated, evidencing that they determine a hormetic dose-dependent response. These results highlight the importance of flavonoids not only as antioxidants or antimicrobial effectors, but also as modulators of plant growth and stress response. Implications of the present suggestion are here discussed in the light of environment and pesticide-reduction concerns.

Keywords: catechin; chitinase; pathogenesis-related proteins; quercetin; *Vitis vinifera*

1. Introduction

Flavonoids are a group of plant polyphenolic secondary metabolites, including red to purple anthocyanins, colourless to pale yellow flavonols (e.g., quercetin: QC), colourless to brown flavanols (e.g., catechin: CA) and proanthocyanidins or condensed tannins [1,2]. They are involved in several physiological functions, such as antioxidant activity, UV-light protection and defence against bacterial and fungal phytopathogens [3]. The latter function is related to some specific activities, such as: (i) the polyphenol oxidase polymerizing activity on sinapyl and coniferyl derivatives, which generates a physical barrier to pathogen invasion [4]; (ii) the inhibitory properties against essential enzymes for pathogens, as in the case of tannins; iii) the direct antimicrobial/antifungal action, as in the case of phytoalexins [5]. The antibiotic activity of flavonoids and of their brown derivatives may also depend,

in part, on their antioxidant properties, either by acting as free radical scavengers or by preventing their formation by chelating metals.

To exert antibiotic action, flavonoids have to be either transported from the source tissue to the site of infection or increasingly produced by infected cells, where they induce the hypersensitive reaction against biotrophic pathogens, leading to a fast and localized programmed cell death [6]. This response is particularly important during fruit ripening, because such organ accumulates sugars and attractive molecules, so becoming more prone to biotic attack. Thus, plant cells start to synthesize pathogenesis-related (PR) proteins and flavonoids, whose efficiency seems to depend on the activation rate of the corresponding biosynthetic pathways [7], as shown by the finding that polyphenols exert antifungal activity, so inducing resistance [7].

Regarding the general ability of flavonoids to interact with proteins, relative binding properties and effect on the corresponding enzyme activities may depend on their molecular structure and oxidation state. In this context, examples have been reported for different enzymes, including NADH oxidases, polyphenol oxidases and peroxidases [4], lipoxygenases [8], cellulases, xylanases, pectinases, glutathione-*S*-transferases (GST) and glycoproteins and protein kinases involved in the polar auxin transport [6]. Indeed QC and kaempferol could inhibit the activity of auxin transport proteins through the interaction of their catechol group in the B-ring of the flavonoid skeleton [2,9].

Grapevine (*Vitis vinifera* L.) is one of the richest sources of polyphenols among fruits, and it is a common food in the human diet. Flavonoids are the most abundant phytonutrients with biological activity; actually, they possess cardio-protective, neuro-protective, antimicrobial and anti-aging properties [10]. Most flavonoids are found primarily in the outer epidermal cells of red grape skin, whereas ca. 60%–70% of total polyphenols are stored in seeds. Flavanols, one of the most abundant class of flavonoids found in grapevine, are present mainly in the form of (+)-CA, (−)-epicatechin, and proanthocyanidins [11]. In white grape varieties, flavanols represent 46%–56% of total phenolics, whereas in red grapes their concentration is in the 13%–30% range. Although flavonols are present only as 3-*O*-glycosides in grape skin, they can be found also as aglycones (QC, kaempferol, myricetin and isorhamnetin) in wines and juices, as a result of acid hydrolysis during their processing and storage. Although the profile of flavonols strongly depends on grape cultivars, QC, kaempferol and isorhamnetin derivatives are found in both red and white grapes [12].

Due to their extensive cultivation, grapevine varieties are sensitive to a great number of pathogens. These infections provoke heavy damages and yield losses, finally affecting wine quality. The spread of diseases are generally controlled by the application of chemical pesticides. To limit environment pollution, alternative strategies involve the activation of plant defence mechanisms by natural elicitors. This type of resistance, characterized by a systemic accumulation of PR-proteins, is mainly associated with the induction of systemic acquired resistance (SAR) induced by pathogens [13]. This resistance to biotic stress is generally based on multiple biochemical factors and involves PR-proteins (chitinases, peroxidases, and β-1,3-glucanases), several elicitor-induced defence responses (e.g., the lignification of cell walls), and production of flavonoid phytoalexins [14] that inhibit fungi growth [15,16].

In this complex scenario, the complete role of flavonoids is still under study, because they are both ubiquitous in plant cells and involved in several biological activities [10]. Depending on their multiple physiological roles and localization, flavonoids need to be efficiently transported to short- and long-distance sites. A number of transporters with this putative function have been identified, which may perform both facilitated-passive and active transport, sometimes overlapping in a synergistic manner. In particular, active transport seems to involve different enzymes, such as ABC (ATP-binding cassette) proteins, MATE (multidrug and toxic extrusion) proteins, GST and a bilitranslocase-like protein [17]. The latter protein was assigned on the basis of its recognition by an antibody raised against a peptide sequence of rat bilitranslocase (anti-peptide Ab) [18]. This study was undertaken to further characterize the nature of grape berry skin proteins reacting with anti-peptide Ab, and in particular the putative modulation of flavonoids on their enzymatic activities.

The analysis could provide further information on the regulative activities exerted by flavonoids on plant cell metabolism, in particular on those pathways involved in biotic stress responses.

2. Results

2.1. Western Blot on Microsomal Fraction from Red Grape Skin

Antibodies produced against the peptide 235–246 (EFTYQLTSSPTC) from bilitranslocase have been previously used to detect flavonoid membrane transporters in both human and plant materials [17,19]. In this context, preliminary experiments were performed on pulp and skin of grape fruits aimed at identifying putative flavonoid-binding proteins [17]. To further investigate this issue in grape, we used a novel mouse antibody (Ab), generated according to the method described before [20], which was utilized to assay grape skin microsomes. Western blot (WB) experiments demonstrated the presence of at least 5 bands migrating at 22, 25, 27, 37 and 50 kDa, respectively (Figure 1). We focused on the bands in the mass range of 25–27 kDa, since a quantitative correlation between signal intensity and protein concentration was obtained (A and B for 15 and 30 μg protein, respectively).

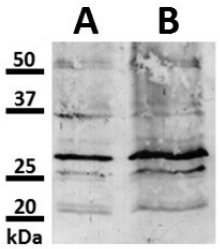

Figure 1. WB of proteins from RGSM revealing candidates for anti-peptide Ab interaction. RGSM proteins from cv. Merlot (15 and 30 μg, (**A**) and (**B**) respectively) were loaded onto 12% polyacrylamide gel. Western blotting was performed using mouse anti-peptide Ab at the concentration of 5 $\mu g \cdot mL^{-1}$. Anti-mouse IgM (dilution 1:15,000) was used as secondary antibody. Protein molecular mass markers are shown on the left.

2.2. Proteomic Analysis

Two protein bands occurring in the range of 25–27 kDa were subjected to an integrated proteomic approach based on combined SDS-PAGE, 2-DE, WB and nLC-ESI-LIT-MS/MS analysis. These proteins were preliminarily purified by SDS-PAGE, thus reducing the complexity of the plant samples. Their resolution by isoelectric focusing within the 3.0–11.0 pH range allowed for a better visualization of the protein components recognized by the anti-peptide Ab. At the same time, it limited the occurrence of contaminants in the gel spots to be further subjected to mass spectrometric analysis for protein identification.

Figure 2 shows two representative gel images resulting from WB (Panel A) and silver nitrate staining (Panel B) of gel of the same protein sample after its preliminary purification by SDS-PAGE. A number of protein spots (A,B,C with numbering 1–4) was evident after WB with the anti-peptide Ab (Figure 2A); their counterparts within the silver nitrate stained gel were identified by software-assisted comparison of the corresponding 2-D images (Figure 2B). The limited number of spots detected by WB, with respect to that visualized by silver staining, demonstrated that only a very small portion of the proteins present within the samples was recognized by Ab (Figure 2).

In particular, they consisted in a "train" of four spots (spots A1-4) migrating in the pI range 4.0–5.5 and with an apparent mass of 25 kDa, a "train" of four spots (spots C1-4) migrating in the pI range 6.0–8.0 and with an apparent mass of 25 kDa, and a "train" of three spots (spots B1-3) migrating in the pI range 6.0–7.0 and with an apparent mass of 27 kDa. These spots were further digested with trypsin and the resulting digests were analyzed by nLC-ESI-LIT-MS/MS. The results of database searching are reported in Table 1.

Table 1. Grape berry skin proteins recognized by the anti-peptide Ab. Spot number, UniProtKB/NCBI accession, protein description, MASCOT score, theoretical Mr and pI values, matched and unique peptides observed by MS analysis and sequence coverage (%) are given.

Spot	UniProtKB/NCBI Accession	Protein Description	MASCOT Score	Theor. Mass (kDa)	Theor. pI	Matched Peptides	Unique Peptides	Protein Coverage (%)
A1	Q7XAU6_VITVI/33329392	Class IV chitinase [*V. vinifera*]	82	25.6	5.15	2	1	6.6
A2	Q7XAU6_VITVI/33329392	Class IV chitinase [*V. vinifera*]	298	25.6	5.15	6	4	24.2
A3	Q7XAU6_VITVI/33329392	Class IV chitinase [*V. vinifera*]	338	25.6	5.15	5	4	24.2
A4	Q7XAU6_VITVI/33329392	Class IV chitinase [*V. vinifera*]	358	25.6	5.15	8	4	24.2
B1	F6HLL9_VITVI/225441373	Glucan endo-1,3-β-glucosidase [*V. vinifera*]	227	33.3	7.06	10	3	17.8
B2	F6HLL9_VITVI/225441373	Glucan endo-1,3-β-glucosidase [*V. vinifera*]	278	33.3	7.06	24	5	28.7
B3	F6HLL9_VITVI/225441373	Glucan endo-1,3-β-glucosidase [*V. vinifera*]	476	33.3	7.06	24	8	49.4
C1	A5BV65_VITVI/147784332	Triose phosphate isomerase [*V. vinifera*]	190	27.2	6.35	6	4	15.4
C2	731394960	Vicilin-like antimicrobial peptides 2-3 [*V. vinifera*]	338	97.0	6.95	11	8	10.0
	A5BV65_VITVI/147784332	Triose phosphate isomerase [*V. vinifera*]	113	27.2	6.35	2	2	10.2
C3	731394960	Vicilin-like antimicrobial peptides 2-3 [*V. vinifera*]	254	97.0	6.95	5	5	10.7
C4	731394960	Vicilin-like antimicrobial peptides 2-3 [*V. vinifera*]	338	97.0	6.95	11	8	10.0
	A5BV65_VITVI/147784332	Triose phosphate isomerase [*V. vinifera*]	113	27.2	6.35	2	2	10.2

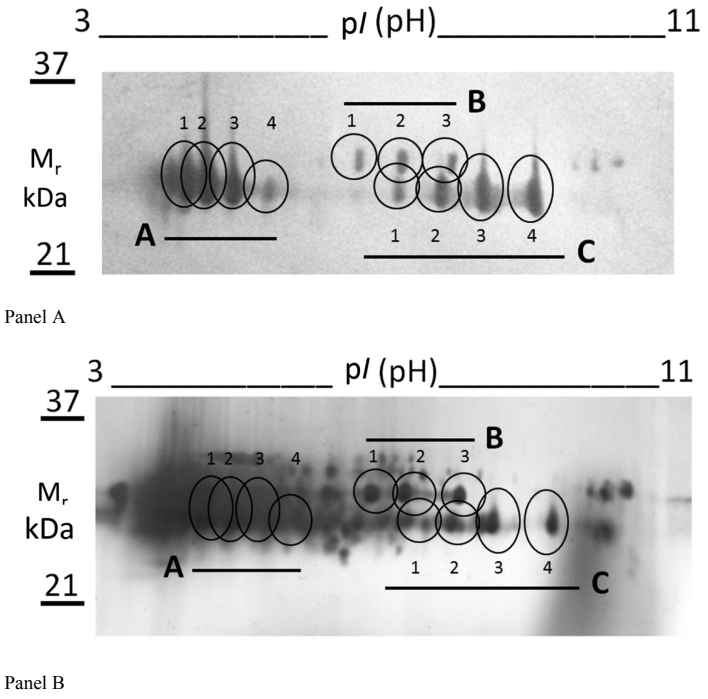

Figure 2. Immuno-proteomic analysis of grape skin proteins with a mass in the range 25–27 kDa. Thirty μg of RGSM proteins with a mass 25–27 kDa (Figure 1) was extracted from SDS-PAGE and subjected to 2-D electrophoresis, as described in the Materials and Methods section. Gels run in parallel were subjected to WB with anti-peptide Ab (Panel A) or to silver staining (Panel B). The "trains" of spots showing immuno-reactive signals were matched to counterparts in the silver-stained gel, and are labelled as A1-4, B1-3 and C1-4 in both panels. Spots of interest were digested with trypsin and subjected to MS analysis.

Spots A1-4 and B1-3 corresponded to class IV chitinase (Q7XAU6) and glucan endo-1,3-β-glucosidase (XP_002277446), respectively. Otherwise, spots C1-4 contained a mixture of vicilin-like antimicrobial peptides 2-3 (XP_003632318) and triose phosphate isomerase (CAN70587) that migrated together within the gel as result of their almost identical pI and mass values. The observation that the theoretical mass of vicilin-like antimicrobial peptides 2-3 is 97 kDa suggested that a fragment of this protein was identified in this study.

In order to rationalize the reaction of the above-mentioned proteins with the anti-peptide Ab, in silico sequence alignment of class IV chitinase, glucan endo-1,3-β-glucosidase, vicilin-like antimicrobial peptides 2-3, and triose phosphate isomerase with the peptide 235-246 of rat bilitranslocase was performed by using the L-Align program. These alignments provided evidence that all these proteins contain certain sequence similarities with that of the peptide 235-246 (Table 2) used to generate the anti-peptide Ab.

In fact, alignments exhibited an acceptable Eigen value, which was always under the limit of 0.5; it is also noteworthy the constant occurrence of Q, S and P residues at positions 5, 9 and 10, respectively. Furthermore, the structural analysis of the tertiary structure of chitinase C from *S. griseus* (pdb 1WVU_A), which shares 69.4% identity and 83.8% similarity with chitinase from *S. griseus* (WP_044369170) and 41.0% identity and 74.2% similarity with class IV chitinase protein from grape (Q7XAU6), showed that the putative sequence recognized by the anti-peptide Ab is located at C-terminus of the protein and exposed to the aqueous environment.

Table 2. Sequence alignment of proteins detected as reacting with the Ab raised against the peptide 235–246 of bilitranslocase. The rat enzyme is reported at the bottom of the each sequence alignment, while the target one is shown at the top.

Protein Description	Apparent Mass	Alignment	L-Align E Value
Class IV chitinase Accession n.: Q7XAU6	27.5 kDa 264 aa	250 DYCSQLGVSP .. :: :: EFTYQLTSSP 10	E < 0.29 60% similarity 40% identity
Chitinase (from *S. griseus*) Accession n.: WP_044369170	31.3 kDa 289 aa	280 QFTQILGTTP .:: : ..: EFTYQLTSSP 10	E < 0.13 70% similarity 40% identity
Glucan endo-1,3-β-glucosidase Accession n.: XP_002277446	36.7 kDa 340 aa	220 NLNYALFTAP ...: : ..: EFTYQLTSSP 10	E < 0.18 80% similarity 30% identity
Triose phosphate isomerase Accession n.: CAN70587	27.2 kDa 254 aa	240 FQANTSP .: ..:: YQLTSSP 10	E < 0.046 86% similarity 43% identity
Vicilin-like antimicrobial peptides 2-3 Accession n.: XP_003632318	97.0 kDa 843 aa	470 YQRLSSP :: ::: YQLTSSP 10	E < 0.14 71% similarity 71% identity

2.3. Reaction of a Chitinase from S. griseus with Anti-Peptide Ab

With the aim of investigating whether the anti-peptide Ab was able to recognize a chitinase from an alternative source, a WB experiment was performed using a commercial enzyme from *S. griseus*. In this case, notwithstanding the low purification grade of the enzyme preparation, as evidenced by Coomassie-stained gel (Figure 3), the immuno-reaction showed a strong band, with an apparent mass of about 23 kDa.

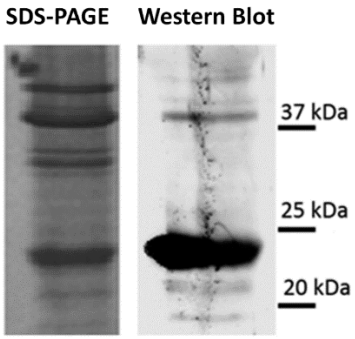

Figure 3. Reaction of a chitinase from *S. griseus* with anti-peptide Ab. Three micrograms of *S. griseus* chitinase was loaded onto 12% SDS-PAGE. Monoclonal anti-peptide Ab (5 μg IgM·mL^{-1}) was used to detect the reaction with *S. griseus* chitinase. A Coomassie-stained gel corresponding to the counterpart challenged with Ab is also shown for comparison. Protein molecular mass markers are shown on the right.

This mass value was slightly lower than that predicted on the basis of the protein sequence and that measured in the case of red grape skin microsomes (RGSM) samples (Figure 1); accordingly, the enzyme was ascribed to family 19 bacterial chitinase C. This subtle difference may be due to the

different mass value of the two chitinases, based on their amino acid sequence, or the occurrence of still unknown post-translational modifications. In this context, various enzymes belonging to the family of chitinases, with different mass values have already been identified in grape berries [21].

2.4. Acetazolamide Inhibition of Chitinase Activity

To further validate the occurrence of chitinase activity in berry skin extracts, samples of chitinase from RGSM and *S. griseus* were incubated with a specific inhibitor of this enzyme. Since various chitinase inhibitors of plant and animal chitinase isoforms have been described [22], acetazolamide was chosen, because of its effective inhibitory properties with both bacterial enzyme and plant extracts. Table 3 shows that the inhibitory effect of acetazolamide on the chitinase activity in RGSM extracts and *S. griseus* enzyme was 15.2% and 20.9%, respectively, confirming the presence of an active form of this enzyme in grape berry skin.

Table 3. Inhibition of the chitinase activity of RGSM and *S. griseus* by acetazolamide. The inhibitory effect of acetazolamide was tested according to the protocol of Schuttelkopf et al. [23].

	***S. griseus* (Fluorescence, A.U. h^{-1})**	**RGSM (Fluorescence, A.U. h^{-1})**
Control	78,202 ± 3899 (100%)	40,397 ± 1654 (100%)
Acetazolamide (32 μM)	61,859 ± 2027 (79.1%)	34,091 ± 1152 (84.8%)

2.5. Inhibition of Chitinase Activity by Anti-Peptide Ab

To investigate the interaction between the anti-peptide Ab and the chitinase present in RGSM, the inhibitory effect of this antibody on the chitinase activity in RGSM extract and the *S. griseus* enzyme was assessed by two independent methods, which are based on absorbance [13] and fluorescence [23] measurements, respectively.

Both assays showed similar results, being Ab inhibitory on both chitinase samples. Figure 4 shows the data obtained by the fluorimetric method, which was preferred because of its accuracy, sensitivity and simplicity. In particular, addition of increasing amounts of the anti-peptide Ab determined an inhibition of the *S. griseus* chitinase enzymatic activity. Accordingly, a direct effect of the Ab on the catalytic properties of the enzyme was hypothesized as result of its interaction with protein regions involved in catalysis. A similar inhibitory response was obtained in the case of RGSM extracts, although with a less pronounced extent.

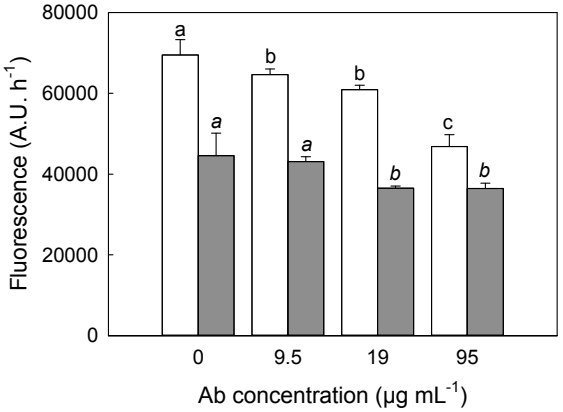

Figure 4. Inhibition of the chitinase activity of *S. griseus* and RGSM chitinase by anti-peptide Ab. Chitinolytic activity was measured as described in Schuttelkopf et al. [23]. 0.2 μg·μL^{-1} of *S. griseus* chitinase (white bars) and 30 μg of RGSM (grey bars) were assayed in the presence of increasing concentrations of anti-peptide Ab. Different letters assigned to means designate a statistical difference regarding data from *S. griseus* (not italic letters), or from RGSM samples (italic letters).

2.6. Modulation of Chitinase Activity by QC and CA

Since the anti-peptide Ab, developed to recognize a flavonoid-binding domain of bilitranslocase, reacted with a class IV chitinase from grape berry skin, it could be argued that chitinase activity may be modulated by flavonoids. Thus, flavonoids belonging to flavonol and flavan-3-ol classes (QC and CA, respectively), were incubated at different concentrations with *S. griseus* chitinase in order to characterize their effect on the kinetic parameters (Table 4).

Commercial chitinase activity was evaluated using fluorimetric assay. The modulatory effect of QC in the range of 0–20 μM was bi-phasic (Table 4, left values). In the range 0–3 μM, both Vmax and KM increased; however, they decreased at higher concentrations up to 20 μM QC. The combined effect of this uncompetitive modulation is that the catalytic performance of chitinase improves at low concentrations of QC. In fact, the increased KM implies a wider range of substrate concentrations, where reaction rate increases linearly. In addition, the substrate-saturated enzyme has a higher Vmax than the control one.

Table 4. QC and CA modulation of the chitinase activity of *S. griseus*. Chitinolytic activity by chitinase from *S. griseus* was measured using 4-methyl-umbelliferyl β triacetyl chitotrioside as a substrate, as described in the Material and Methods section. The enzyme activity was assayed in the absence and in the presence of different concentrations of QC and CA. The apparent Michaelis-Menten parameters were obtained at each substrate concentration, by fitting data to the Michaelis-Menten equation.

Flavonoid (μM)	K_M (μM) Quercetin	V_{max} (nmol 4-4-Methyl-umbelliferone (mg prot h)$^{-1}$) Quercetin	R^2	K_M (μM) Catechin	V_{max} (nmol 4-4-Methyl-umbelliferone (mg prot h)$^{-1}$) Catechin	R^2
0	35.42 ± 4.18	802 ± 41	0.996	48.89 ± 4.72	972 ± 46	0.998
0.5	42.05 ± 4.50	976 ± 48	0.997	68.81 ± 8.76	1190 ± 85	0.997
3	58.67 ± 2.91	1077 ± 28	0.999	78.33 ± 16.66	1183 ± 148	0.994
10	28.86 ± 4.94	598 ± 40	0.991	93.27 ± 7.60	1494 ± 76	0.999
20	28.70 ± 3.54	472 ± 23	0.995	53.21 ± 2.07	1007 ± 20	0.999

Conversely, higher concentrations of QC reversed this gain of function, with a lower KM going along with a lower Vmax. A similar hormetic modulation was observed with CA (Table 4, right values). The peculiar response of commercial chitinase activity to increasing QC and CA concentrations was shown also in Figure 5 (panel A) and in supplementary Figure S1, where 0.1–100 μM range was used. CA (black bars) and QC (grey bars) showed a biphasic pattern described by a sort of hormetic dose-response effect. This phenomenon has already been reported in pharmacology, where low concentrations of a molecule exhibit an opposite effect on a certain enzymatic activity, when compared to high concentrations. Although the hormetic response was observed for both flavonoids, QC induced the strongest modulation; in particular, it determined a 60% increment of the chitinase activity when tested at 1 μM concentration, and a 20% decrement when assayed at 100 μM concentration (Figure 5, Panel A). At the same concentrations, CA stimulated the activity by about 5% and reduced it by almost 13%, respectively.

In the case of RGSM (Panel B), the effects of CA and QC were not as strong as in the case of *S. griseus* chitinase. In particular, no significant modulation was observed when RGSM were treated with CA. In contrast, an evident and linear inhibition was observed when QC was used. The apparent contrasting effect of CA and QC on the chitinase activity of RGSM, when compared to that of *S. griseus* enzyme, was rationalized hypothesizing the presence of endogenous flavonoids in the microsome extract, which might have masked and reduced the modulatory effect due to the external addition of CA and QC.

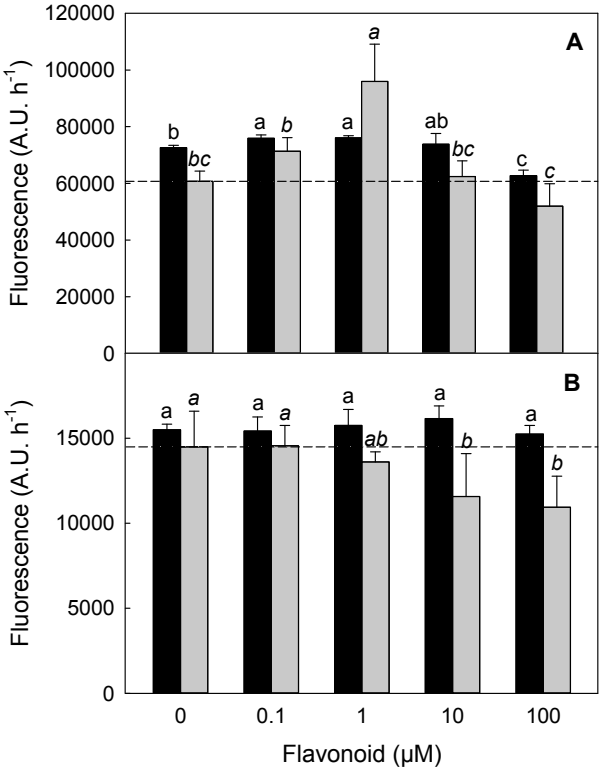

Figure 5. QC and CA modulation of the chitinase activity of *S. griseus* and RGSM enzyme. Chitinolytic activity was measured as described in Schuttelkopf et al. [23]. Different concentrations of CA (black bars) and QC (grey bars) were tested on chitinase from *S. griseus* (Panel A) and on RGSM (Panel B). Different letters assigned to means designate a statistical difference regarding data from CA (not italic letters), or from QC (italic letters).

3. Discussion

Chitinases (EC 3.2.1.14) belong to a widely studied family of enzymes present in plant, animal and bacteria kingdoms [24]. These enzymes catalyze the hydrolytic cleavage of the β-1,4-glycosidic bond in *N*-acetylglucosamine-based biopolymers, mainly in chitin. Chitin is found in the cuticle of insect and crustacean shells, as well as in the cell walls of many fungi; accordingly, chitin is the second most abundant polysaccharide in nature after cellulose. Chitinases are the most studied PR-proteins, belonging to the families 18 and 19 of glycosyl hydrolases, which differ in amino acid sequence, structure and mechanism. While family 18 contains chitinases from many organisms, family 19 includes only highly conserved plant enzymes, typically endo-chitinases [22]. In bacteria, chitinases are mainly involved in nutrition processes; in yeast and various fungi, they participate in morphogenesis and some pathogenesis processes; in animals and plants, they mainly play a role in the defence against pathogen attack, as components of the innate immunity [25–27]. In the latter context, worth mentioning is the fact that different isoforms of chitinases can be induced by developmental signals regulating fruit ripening [21,28]. Specifically in the skin of grape berry, chitinase isoforms were over-expressed at maturation and the enzymatic activity correspondingly increased during ripening, even in the absence of any pathogen attack [28]. In grape berry from different cultivars, proteomic analysis evidenced that a class IV chitinase (CTG1027246) was strongly transcripted during post-veraison stage, where this PR protein is presumed to be involved in disease and pest resistance [29]. By generating or degrading signal metabolites, chitinases also participate to signalling pathways, including hormonal (ethylene) interaction [30]. This phenomenon is confirmed by the observation that chitinases and PR-proteins increase their activity during plant senescence [31]. Their involvement in programmed cell death has been hypothesized in *Arabidopis* and *Brassica napus* [30].

In the present work, a class IV chitinase (family 19) was identified in microsomes from red grape berry teguments as the main protein reacting with a mouse IgM Ab raised against the peptide 235-246 of rat bilitranslocase. The latter protein was chosen as a probe species being a flavonoid translocator [32]; peptide 235-246 was selected being present in the bilitranslocase region involved in the flavonoid binding [33]. Class IV chitinase identification was obtained by a combination of SDS-PAGE, 2-DE, WB and nLC-ESI-LIT-MS/MS experiments (Figure 2). Evidence of the existence of a protein similar to that identified here as reacting with this antibody derived from a previous work, where bilitranslocase-like proteins were characterized in grape berry skin microsomes by using rabbit IgG polyclonal Ab raised against the same peptide [18,19]. Although the immune-chemical assays were performed on similar plant extracts, the two antibodies exhibited a slightly different cross-reactivity. Mouse IgM Ab was able to cross-react with about five proteins (Figure 1), while rabbit IgG Ab detected only two polypeptides having similar molecular mass values (28–30 kDa). Mouse IgM Ab also reacted with a chitinase having bacterial origin (from *S. griseus*), which was used as a positive control (Figure 3). The latter is a bacterial member of the family 19 chitinases sharing sequence similarities with plant counterparts. In particular, family 19 chitinases are widely observed in the plant kingdom and, specifically, in grapevine [34], but they have also been characterized in bacteria. In this context, chitinase C from *S. griseus* HUT6037 was the first example of a bacterial member of family 19 chitinase that was identified [35]. Thus it is a good candidate to accomplish an evolutionary linkage between Actinobacteria and Viridiplantae [36,37].

The presence of a chitinase in grape extracts was confirmed by using acetazolamide, a well-known broad-spectrum chitinase inhibitor, which was able to inhibit the chitinolytic activity of both RGSM and *S. griseus* enzyme (Table 1). This is a remarkable result since it is well-known that members of the chitinase family 19 are heterogeneous. Although its inhibitory effect on RGSM extracts was low, acetazolamide resulted to be effective with both plant and bacterial enzymes. Accordingly, it can be suggested as a suitable inhibitor of chitinases from organisms of different kingdoms.

Aiming at better understanding why an Ab, raised toward a flavonoid binding sequence, can also recognize plant PR-proteins, the interaction among flavonoids and class IV chitinase was further investigated. In particular, the possible connection between chitinases and flavonoids was elucidated by assaying the effect of two of the most representative flavonoids present in grape, namely CA and QC on chitinase activity [12]. The functional assay was performed on both *S. griseus* chitinase and on a RGSM extracts containing class IV chitinase (supplementary Figure S1 and Figure 5). In either cases, a sort of hormetic effect was observed, thus indicating that flavonoids may actually act as modulators, rather than mere inhibitors, with a typical kinetics already observed in the case of other derivatives having pharmacological properties [38]. This effect was confirmed by two different assays, thus excluding any possible artefact; for sake of brevity, only one has been shown in this study. The functional comparison between the bacteria and RGSM chitinase showed that the modulation was strong and significant in the first case, while was less pronounced in the remaining one. This was ascribed to the flavonoids, already present in RGSM preparations, which probably acted as inner modulators, reducing any further possible measurable effect.

The results reported above on the modulation of the chitinase activity exerted by QC, CA and on the inhibition by anti-peptide Ab, let us to speculate that all these molecules may interact with the enzyme region devoted to binding of flavonoids. Moreover, the hormetic effects reveal that the enzyme has a conformational flexibility, controlled by flavonoid binding. Also in the case of the measurements of the effect of the anti-peptide Ab, on chitinase activity (Figure 4), experiments were performed by two independent assays to exclude any possible artefact. Since sequence comparisons with bilitranslocase (Table 2 and data not shown) have suggested that the site recognized by the anti-peptide Ab site is located in a highly accessible C-terminus region of both class IV and *S. griseus* chitinase, it is tempting to hypothesize that this structural portion may be involved in the interaction with flavonoids. In particular a biochemical analysis of kinetic features of the microbial chitinase (Figure 5 and Table 4) showed a hormetic effect both on KM and Vmax parameters, which were

increased at low flavonoid doses, while higher treatments caused a decrease under the control level. The possible explanation about the hormetic behaviour of chitinase activity modulated by flavonoids is clearly merely speculative. As already claimed by Vargas and Burd [39], flavonoids, and quercetin in particular, show a biphasic effect on metabolic processes and catalytic activities depending on concentration, since at low concentration they act as reducing agents, while at high concentration they exert a pro-oxidative action. In the case of other auto-oxidizable molecules such as methylene blue, it has also been shown that their electron reduction-oxidation capacity was related to their in vitro hormetic dose-response modulation of the enzymatic activity [40]. Actually, there is evidence about redox status regulation on chitinolytic activity [41,42] and that plant chitinases and β-glucanases respond to UV-C treatment with a hormetic concentration-dependent manner [43].

All these modulatory effects showed by flavonoids support the dual action of these secondary metabolites, by having a complex regulatory role, depending on their concentration and redox state, in maintaining the homeostatic equilibrium among different cell metabolic processes. In addition, polyphenols often play also an ecological role as allelo-chemicals, being released in the environment to affect neighboring plant species. These physiological responses are themselves hormetic phenomena, which are described by complex mathematical models [44]. At the molecular level, hormesis probably results from the presence of multiple binding domains on the chitinase catalytic site, each of them characterized by a different binding affinity with both substrate and flavonoid. Such a complex interaction has already been proposed to explain hormetic response, for example in the case of mono-amine oxidase [45]. In our system, chitinase appeared to be not allosterically modulated, since the best regression curve for our data was a rectangular hyperbolic curve and not a sigmoid curve, as expected in the case of allosteric regulation.

In conclusion, the results reported in this study on the modulatory effect exerted by flavonoids on chitinase activity are in good agreement with recent literature, which evidenced that further physiological functions can be claimed for these secondary metabolites, in addition to the antioxidant and/or antimicrobial ones [6,46]. In fact, flavonoids have been demonstrated to act as developmental regulators and signals by a direct interaction with target proteins and modulation of activity [6,8,47]. Moreover, it has also been suggested that flavonoid localization in the nucleus may be associated to their role as activators/repressors of transcriptional factors [48].

During plant defence response to pathogen attack, flavonoid biosynthesis is induced in parallel with the activation of the expression of PR proteins, including chitinases. The results reported in this study on the modulation in vitro of chitinase activity by flavonoids, suggest that secondary metabolites may also exert such biological effects in vivo. These results may be useful for a better understanding of the intricate picture describing the various mechanisms underlying the plant response to biotic stresses. The modulatory effect of flavonoids on chitinase activity, together with PR protein expression, may be considered as an example of a regulatory convergence of two independent mechanisms of plant response to pathogens. This flavonoid property may also have practical consequences due to its possible impact on the augmentation of plant resilience. In fact, the use of flavonoids may be hypothesized to induce plant defence to pathogens by modulating the activity of PR-related proteins, in a similar way as other natural products regulate protective metabolic reactions/pathways [49,50]. Additional experiments have to be performed in this direction, together with a more detailed description of the structural basis regulating flavonoid-chitinase interaction.

4. Materials and Methods

4.1. Isolation of Microsomes from Berry Skin

Approximately 30 g (FW) of red grapevine (*Vitis vinifera* L., cv. Merlot) berry skin was homogenized as described in Braidot et al. [18], with minor changes: grape berries were pressed through 100 μm nylon gauze and the seeds were separated by floating into 10 mM Tris-HCl buffer at pH 7.5. The skins obtained were used to extract microsomes as described in the above-mentioned

paper. For chitinase activity determination, microsomes were finally resuspended in 200 mM sodium acetate buffer, pH 5.0.

4.2. Anti-Peptide Antibody Production

Mice were immunized with a peptide corresponding to segment 235-246 (EFTYQLTSSPTC) of the primary structure of the mammalian bilitranslocase carrier [51]. Mouse antibody (Ab) was generated by cell fusion of mouse spleen lymphocytes and mouse myeloma NS1 cells, as described before [20]. Ab was purified from the growth medium by affinity FPLC on protein G column (General Electric, Healthcare, Little Chalfont, UK). Purified Ab was used for immunodetection at a concentration of 5 μg·IgM·mL^{-1}.

4.3. SDS-PAGE and Subsequent Protein Extraction from Polyacrylamide Gel

Aiming at enriching the protein samples, 0.5 mg of protein from red grape skin microsomes (RGSM), conditioned in 62.5 mM Tris-HCl pH 6.8, 2.5% (*v*/*v*) SDS, 0.002% (*v*/*v*) bromophenol blue, 0.71 M β-mercaptoethanol, 10% (*v*/*v*) glycerol, were loaded onto a large SDS-PAGE 3 × 50 μL-volume well, with lateral wells for standard molecular markers. Proteins from RGSM were separated by SDS-PAGE (12%), as described in Braidot et al. [18]. After running, selected gel slices, corresponding to the band of interest able to cross react with antipeptide Ab (see also Section 4.5. Western Blotting), were cut and crushed in 4 mL of 25 mM Tris/250 mM glycine (Tris-glycine 1×). After centrifugation at 5000× *g* for 5 min, solubilized proteins were collected and concentrated using a Vivaspin filter (with 10 kDa molecular mass cut off), after 3 washing steps with 1 mL of Tris-glycine 1× to remove SDS.

4.4. Two-Dimensional Electrophoresis

Proteins recovered from SDS-PAGE were loaded on two-dimensional electrophoresis (2-DE); experiments were always performed in duplicate for further western blotting (WB) (30 μg protein loaded/strip) and silver staining analyses (3 μg protein loaded/strip). In the first dimension, isoelectric focusing of samples was performed on 3–11 NL strips (GE Healthcare), using an Ettan IPGphor 3 Isoelectric Focusing System unit (GE Healthcare), according to manufacturer's instructions. Focused strips were equilibrated with dithiothreitol (DTT) and iodoacetamide, according to manufacturer's instructions. Second dimension was performed by positioning the strips at the top of the running gels and performing SDS-PAGE as reported above (Section 4.3). After running, one gel was used for WB, which was carried out as reported below; the other gel was subjected to silver staining, as reported in Bortolussi et al. [52]. In both cases, gel images were acquired, analyzed and matched, as described by the same authors. Silver-stained gel spots corresponding to those detected by WB were excised, and further treated for protein identification.

4.5. Western Blotting

Gels from mono- and 2-D analyses were transferred onto nitrocellulose membranes and subjected to immunoblotting according to the protocol described in Braidot et al. [18]. In this case, the primary anti-peptide Ab (see the Section 4.2 on antibody production) was used at a final concentration of 5 μg·mL^{-1}. Secondary antibody against mouse IgM (product A9044, Sigma Aldrich, Milan, Italy) was used at final dilution of 1:15,000.

4.6. Protein Identification

Gel spots of interest were triturated, washed with water, in-gel reduced with DTT, *S*-alkylated with iodoacetamide, and then in-gel digested with trypsin. Resulting peptide mixtures were desalted by μZip-TipC18 using 50% (*v*/*v*) acetonitrile and 5% (*v*/*v*) formic acid as eluents. Recovered peptides were then analyzed for protein identification by nano-liquid electrospray-linear ion trap-tandem mass spectrometry (nLC-ESI-LIT-MS/MS), using an LTQ XL mass spectrometer (Thermo Fisher Scientific,

Waltham, MA, USA) equipped with a Proxeon nanospray source connected to an Easy-nanoLC (Proxeon, Odense, Denmark). Peptides were separated on an Easy C18 column (100 mm × 0.075 mm, 3 μm) (Proxeon). Mobile phases were 0.1% (*v*/*v*) formic acid (solvent A) and 0.1% (*v*/*v*) formic acid in acetonitrile (solvent B), running at a total flow rate of 300 nL·min^{-1}. Linear gradient was initiated 20 min after sample loading; solvent B ramped from 5% to 35% over 45 min, from 35% to 60% over 10 min, and from 60% to 95% over 20 min. Spectra were acquired in the range m/z 400−2000. Peptide samples were analyzed under collision-induced dissociation (CID)-MS/MS data-dependent product ion scanning procedure, enabling dynamic exclusion (repeat count 1 and exclusion duration 60 s) over the three most abundant ions. Mass isolation window and collision energy were set to m/z 3 and 35%, respectively [53].

Raw data from nLC-ESI-LIT-MS/MS analysis were compared by MASCOT search engine (version 2.2.06, Matrix Science, London, UK) against a database containing protein sequences from *Vitis vinifera*, which were downloaded from the National Center for Biotechnology Information and UniProtKB database. Database searching was performed by using Cys carbamidomethylation and Met oxidation as fixed and variable modifications, respectively, a mass tolerance value of 1.8 Da for precursor ion and 0.8 Da for MS/MS fragments, trypsin as proteolytic enzyme, and a missed cleavage maximum value of 2. Other MASCOT parameters were kept as default. Protein candidates assigned on the basis of at least 2 sequenced peptides with an individual peptide expectation value <0.05 (corresponding to a confidence level for peptide identification >95%) were considered confidently identified. Definitive assignment was always associated with manual spectra visualization and verification.

4.7. Chitinase Activity Assays

Two different assays were used to evaluate the chitinase activity of both commercial enzyme from *Streptomyces griseus* (Sigma Aldrich) and RGSM preparation, following, respectively, the protocol of Magnin-Robert et al. [13] (data presented in Figure S1) and the protocol of Schuttelkopf et al. [23], with minor changes. Briefly, 2 μg of enzyme were mixed with the desired amount of the antibody in McIlvain's buffer, pH 5.5 (100 μL-final volume) and pre-incubated in a black 96-well plate for 15 min (data presented in Figure 5 refer to the latter protocol). The fluorescent substrate 4-methylumbelliferyl β-d-*N*,*N*′,*N*′-tri-acetyl-chitotrioside (Sigma Aldrich) was dissolved in McIlvain's buffer, pH 5.5, added to the mixture as substrate at final concentration of 0.5–100 μM, and then incubated at 37 °C, for 1 h. Finally, 100 μL of 1 M Na_2CO_3 was added to each well and the fluorescence was measured by means of a Multilabel Counter (WALLAC, model 1420, Perkin-Elmer, Waltham, MA, USA) set at 340 nm (20 nm excitation filter bandwidth) and at 465 nm (20 nm emission filter bandwidth). The same protocol was applied when 30 μg of RGSM was used instead of pure chitinase. For modulation experiments by the inhibitor acetazolamide, 1 μg of enzyme was pre-incubated for 30 min.

4.8. Statistical Data Analysis

All the experiments were carried out with at least three biological replicates, unless differently stated. In the case of chitinase activity determinations, treatment means were compared by Least Significant Difference (LSD), according to Fisher's statistical test, and different letters assigned to means designate a statistical difference at $p \leq 0.05$.

5. Conclusions

The identification of a chitinase in microsomes from grape berry skin was assessed by an antibody raised against a sequence of rat bilitranslocase. The antigen sequence of the mammalian protein is also a flavonoid binding domain. Consistently, the putative chitinase activity was found to be modulated by flavonoids. Such evidence was obtained in both grape extracts and pure commercial preparation from *S. griseus*.

These findings are noteworthy, because chitinase family plays a pivotal role as pathogen-related (PR) proteins, a class of enzymes involved in both plant responses to biotic and pollution stress, as well as in senescence. The modulation exerted by flavonoids on this activity opens new possibilities to increase plant resilience towards environmental strains. In particular, recent researches have been developed in the field of plant induced resistance, by means of activation of plant immune system. It has been demonstrated that treatments with peptones or chitosans are able to strengthen plant defense, acting as activators of PR protein. In this view, flavonoids could further stimulate the induced resistance, thus minimizing the use of pesticides. Actually, this is a critical issue that needs to be developed, in particular in the case of viticulture practices.

Supplementary Materials: Supplementary materials can be accessed at: http://www.mdpi.com/1420-3049/21/10/1300/s1.

Acknowledgments: This work was partially supported from the Italian Ministry of Education, University and Research (National Research Program PRIN2010CSJX4F), the Cross-Border Cooperation Programme Italy-Slovenia 2007–2013 (European Regional Development Fund and national funds-TRANS2CARE project) and the Regione Campania for the Project "BenTeN—Nuovi Processi e Prodotti per la Nutraceutica, la Cosmeceutica e la Nutrizione Umana" (P.O.R. 2007/2013, objectives 2.1).

Author Contributions: E.B. and E.P. conceived and designed research; A.F. conducted all the experiments, unless differently stated; G.R. performed the experiments regarding proteomic analysis and identification; V.Č.Š. and U.R. contributed with immunochemical devices and antibodies; M.Z. performed the in silico protein analysis; A.S., E.P., A.F., S.P., A.V. and E.B. wrote the manuscript; A.S., A.V., U.R., M.Z., E.P. and S.P. critically revised the manuscript and gave suggestions for result interpretation. All authors read and approved the manuscript.

Conflicts of Interest: The authors declare no conflict of interest.

References

1. Agati, G.; Azzarello, E.; Pollastri, S.; Tattini, M. Flavonoids as antioxidants in plants: Location and functional significance. *Plant Sci.* **2012**, *196*, 67–76. [CrossRef] [PubMed]
2. Brunetti, C.; di Ferdinando, M.; Fini, A.; Pollastri, S.; Tattini, M. Flavonoids as antioxidants and developmental regulators: Relative significance in plants and humans. *Int. J. Mol. Sci.* **2013**, *14*, 3540–3555. [CrossRef] [PubMed]
3. Treutter, D. Significance of flavonoids in plant resistance and enhancement of their biosynthesis. *Plant Biol.* **2005**, *7*, 581–591. [CrossRef] [PubMed]
4. Pourcel, L.; Routaboul, J.M.; Cheynier, V.; Lepiniec, L.; Debeaujon, I. Flavonoid oxidation in plants: From biochemical properties to physiological functions. *Trends Plant Sci.* **2007**, *12*, 29–36. [CrossRef] [PubMed]
5. Vercauteren, J; Groupe Polyphénols; International Conference on Polyphenols. *Proceedings 96: 18th International Conference on Polyphenols, Bordeaux Cedex, France, 15–18 July 1996;* Vercauteren, J., Cheze, C., Triaud, J., Eds.; INRA: Paris, France, 1998.
6. Mierziak, J.; Kostyn, K.; Kulma, A. Flavonoids as important molecules of plant interactions with the environment. *Molecules* **2014**, *19*, 16240–16265. [CrossRef] [PubMed]
7. Benouaret, R.; Goujon, E.; Trivella, A.; Richard, C.; Ledoigt, G.; Joubert, J.M.; Mery-Bernardon, A.; Goupil, P. Water extracts from winery by-products as tobacco defense inducers. *Ecotoxicology* **2014**, *23*, 1574–1581. [CrossRef] [PubMed]
8. Harborne, J.B.; Williams, C.A. Advances in flavonoid research since 1992. *Phytochemistry* **2000**, *55*, 481–504. [CrossRef]
9. Hernandez, I.; Alegre, L.; van Breusegem, F.; Munne-Bosch, S. How relevant are flavonoids as antioxidants in plants? *Trends Plant Sci.* **2009**, *14*, 125–132. [CrossRef] [PubMed]
10. Ferreyra, M.L.F.; Rius, S.P.; Casati, P. Flavonoids: Biosynthesis, biological functions, and biotechnological applications. *Front. Plant Sci.* **2012**, *3*, 222. [CrossRef]
11. Yilmaz, Y.; Toledo, R.T. Major flavonoids in grape seeds and skins: Antioxidant capacity of catechin, epicatechin, and gallic acid. *J. Agric. Food Chem.* **2004**, *52*, 255–260. [CrossRef] [PubMed]
12. Georgiev, V.; Ananga, A.; Tsolova, V. Recent advances and uses of grape flavonoids as nutraceuticals. *Nutrients* **2014**, *6*, 391–415. [CrossRef] [PubMed]

13. Magnin-Robert, M.; Trotel-Aziz, P.; Quantinet, D.; Biagianti, S.; Aziz, A. Biological control of *Botrytis cinerea* by selected grapevine-associated bacteria and stimulation of chitinase and β-1,3-glucanase activities under field conditions. *Eur. J. Plant Pathol.* **2007**, *118*, 43–57. [CrossRef]
14. Fofana, B.; Benhamou, N.; McNally, D.J.; Labbe, C.; Seguin, A.; Belanger, R.R. Suppression of induced resistance in cucumber through disruption of the flavonoid pathway. *Phytopathology* **2005**, *95*, 114–123. [CrossRef] [PubMed]
15. Repka, V.; Kubikova, J.; Fischerova, I. Immunodetection of pr-1-like proteins in grapevine leaves infected with *Oidium tuckeri* and in elicited suspension cell cultures. *Vitis* **2000**, *39*, 123–127.
16. Schlumbaum, A.; Mauch, F.; Vogeli, U.; Boller, T. Plant chitinases are potent inhibitors of fungal growth. *Nature* **1986**, *324*, 365–367. [CrossRef]
17. Braidot, E.; Zancani, M.; Petrussa, E.; Peresson, C.; Bertolini, A.; Patui, S.; Macrì, F.; Vianello, A. Transport and accumulation of flavonoids in grapevine (*Vitis vinifera* L.). *Plant Signal. Behav.* **2008**, *3*, 626–632. [CrossRef] [PubMed]
18. Braidot, E.; Petrussa, E.; Bertolini, A.; Peresson, C.; Ermacora, P.; Loi, N.; Terdoslavich, M.; Passamonti, S.; Macri, F.; Vianello, A. Evidence for a putative flavonoid translocator similar to mammalian bilitranslocase in grape berries (*Vitis vinifera* L.) during ripening. *Planta* **2008**, *228*, 203–213. [CrossRef] [PubMed]
19. Bertolini, A.; Peresson, C.; Petrussa, E.; Braidot, E.; Passamonti, S.; Macri, F.; Vianello, A. Identification and localization of the bilitranslocase homologue in white grape berries (*Vitis vinifera* L.) during ripening. *J. Exp. Bot.* **2009**, *60*, 3861–3871. [CrossRef] [PubMed]
20. Montanic, S.; Terdoslavich, M.; Rajcevic, U.; de Leo, L.; Bonin, S.; Serbec, V.C.; Passamonti, S. Development and characterization of a novel mab against bilitranslocase—A new biomarker of renal carcinoma. *Radiol. Oncol.* **2013**, *47*, 128–137. [CrossRef] [PubMed]
21. Robinson, S.P.; Jacobs, A.K.; Dry, I.B. A class IV chitinase is highly expressed in grape berries during ripening. *Plant Physiol.* **1997**, *114*, 771–778. [CrossRef] [PubMed]
22. Andersen, O.A.; Dixon, M.J.; Eggleston, I.M.; van Aalten, D.M.F. Natural product family 18 chitinase inhibitors. *Natl. Prod. Rep.* **2005**, *22*, 563–579. [CrossRef] [PubMed]
23. Schuttelkopf, A.W.; Gros, L.; Blair, D.E.; Frearson, J.A.; van Aalten, D.M.F.; Gilbert, I.H. Acetazolamide-based fungal chitinase inhibitors. *Bioorgan. Med. Chem.* **2010**, *18*, 8334–8340. [CrossRef] [PubMed]
24. Collinge, D.B.; Kragh, K.M.; Mikkelsen, J.D.; Nielsen, K.K.; Rasmussen, U.; Vad, K. Plant chitinases. *Plant J.* **1993**, *3*, 31–40. [CrossRef] [PubMed]
25. Nurnberger, T.; Brunner, F.; Kemmerling, B.; Piater, L. Innate immunity in plants and animals: Striking similarities and obvious differences. *Immunol. Rev.* **2004**, *198*, 249–266. [CrossRef] [PubMed]
26. Sharma, V. Pathogenesis related defence functions of plant chitinases and β-1,3-glucanases. *Vegetos* **2013**, *26*, 205–218. [CrossRef]
27. Grover, A. Plant chitinases: Genetic diversity and physiological roles. *Crit. Rev. Plant Sci.* **2012**, *31*, 57–73. [CrossRef]
28. Deytieux, C.; Geny, L.; Lapaillerie, D.; Claverol, S.; Bonneu, M.; Doneche, B. Proteome analysis of grape skins during ripening. *J. Exp. Bot.* **2007**, *58*, 1851–1862. [CrossRef] [PubMed]
29. Da Silva, F.G.; Iandolino, A.; Al-Kayal, F.; Bohlmann, M.C.; Cushman, M.A.; Lim, H.; Ergul, A.; Figueroa, R.; Kabuloglu, E.K.; Osborne, C.; et al. Characterizing the grape transcriptome. Analysis of expressed sequence tags from multiple vitis species and development of a compendium of gene expression during berry development. *Plant Physiol.* **2005**, *139*, 574–597. [CrossRef] [PubMed]
30. Kasprzewska, A. Plant chitinases—Regulation and function. *Cell. Mol. Biol. Lett.* **2003**, *8*, 809–824. [PubMed]
31. Quirino, B.F.; Noh, Y.S.; Himelblau, E.; Amasino, R.M. Molecular aspects of leaf senescence. *Trends Plant Sci.* **2000**, *5*, 278–282. [CrossRef]
32. Passamonti, S.; Terdoslavich, M.; Franca, R.; Vanzo, A.; Tramer, F.; Braidot, E.; Petrussa, E.; Vianello, A. Bioavailability of flavonoids: A review of their membrane transport and the function of bilitranslocase in animal and plant organisms. *Curr. Drug Metab.* **2009**, *10*, 369–394. [CrossRef] [PubMed]
33. Passamonti, S.; Cocolo, A.; Braidot, E.; Petrussa, E.; Peresson, C.; Medic, N.; Macri, F.; Vianello, A. Characterization of electrogenic bromosulfophthalein transport in carnation petal microsomes and its inhibition by antibodies against bilitranslocase. *FEBS J.* **2005**, *272*, 3282–3296. [CrossRef] [PubMed]
34. Vincenzi, S.; Bierma, J.; Wickramasekara, S.I.; Curioni, A.; Gazzola, D.; Bakalinsky, A.T. Characterization of a grape class iv chitinase. *J. Agric. Food Chem.* **2014**, *62*, 5660–5668. [CrossRef] [PubMed]

35. Hoell, I.A.; Dalhus, B.; Heggset, E.B.; Aspmo, S.I.; Eijsink, V.G.H. Crystal structure and enzymatic properties of a bacterial family 19 chitinase reveal differences from plant enzymes. *FEBS J.* **2006**, *273*, 4889–4900. [CrossRef] [PubMed]
36. Kawase, T.; Saito, A.; Sato, T.; Kanai, R.; Fujii, T.; Nikaidou, N.; Miyashita, K.; Watanabe, T. Distribution and phylogenetic analysis of family 19 chitinases in actinobacteria. *Appl. Environ. Microbiol.* **2004**, *70*, 1135–1144. [CrossRef] [PubMed]
37. Neuhaus, J.M. *Pathogenesis-Related Proteins in Plants*; CRC Press: Boca Raton, FL, USA, 1999; pp. 77–98.
38. Calabrese, E.J. Hormesis and homeopathy: Introduction. *Hum. Exp. Toxicol.* **2010**, *29*, 527–529. [CrossRef] [PubMed]
39. Vargas, A.J.; Burd, R. Hormesis and synergy: Pathways and mechanisms of quercetin in cancer prevention and management. *Nutr. Rev.* **2010**, *68*, 418–428. [CrossRef] [PubMed]
40. Bruchey, A.K.; Gonzalez-Lima, F. Behavioral, physiological and biochemical hormetic responses to the autoxidizable dye methylene blue. *Am. J. Pharmacol. Toxicol.* **2008**, *3*, 72–79. [CrossRef] [PubMed]
41. Pel, R.; Gottschal, J.C. Mesophilic chitin-degrading anaerobes isolated from an estuarine environment. *FEMS Microbiol. Ecol.* **1986**, *38*, 39–49. [CrossRef]
42. Pel, R.; Gottschal, J.C. The effect of oxygen and sulfhydryl-reagents on the hydrolysis and the fermentation of chitin by *clostridium*-9.1. *FEMS Microbiol. Lett.* **1987**, *44*, 59–62. [CrossRef]
43. Pombo, M.A.; Rosli, H.G.; Martinez, G.A.; Civello, P.M. UV-C treatment affects the expression and activity of defense genes in strawberry fruit (*Fragaria* × *ananassa*, Duch.). *Postharvest Biol. Technol.* **2011**, *59*, 94–102. [CrossRef]
44. Liu, Y.; Chen, X.; Duan, S.; Feng, Y.; An, M. Mathematical modeling of plant allelopathic hormesis based on ecological-limiting-factor models. *Dose Response* **2010**, *9*, 117–129. [CrossRef] [PubMed]
45. Holt, A.; Smith, D.J.; Cendron, L.; Zanotti, G.; Rigo, A.; di Paolo, M.L. Multiple binding sites for substrates and modulators of semicarbazide-sensitive amine oxidases: Kinetic consequences. *Mol. Pharmacol.* **2008**, *73*, 525–538. [CrossRef] [PubMed]
46. Landi, M.; Tattini, M.; Gould, K.S. Multiple functional roles of anthocyanins in plant-environment interactions. *Environ. Exp. Bot.* **2015**, *119*, 4–17. [CrossRef]
47. Taylor, L.P.; Grotewold, E. Flavonoids as developmental regulators. *Curr. Opin. Plant Biol.* **2005**, *8*, 317–323. [CrossRef] [PubMed]
48. Saslowsky, D.E.; Warek, U.; Winkel, B.S.J. Nuclear localization of flavonoid enzymes in *arabidopsis*. *J. Biol. Chem.* **2005**, *280*, 23735–23740. [CrossRef] [PubMed]
49. Burketova, L.; Trda, L.; Ott, P.G.; Valentova, O. Bio-based resistance inducers for sustainable plant protection against pathogens. *Biotechnol. Adv.* **2015**, *33*, 994–1004. [CrossRef] [PubMed]
50. Wiesel, L.; Newton, A.C.; Elliott, I.; Booty, D.; Gilroy, E.M.; Birch, P.R.J.; Hein, I. Molecular effects of resistance elicitors from biological origin and their potential for crop protection. *Front. Plant Sci.* **2014**, *5*, 655. [CrossRef] [PubMed]
51. Battiston, L.; Passamonti, S.; Macagno, A.; Sottocasa, G.L. The bilirubin-binding motif of bilitranslocase and its relation to conserved motifs in ancient biliproteins. *Biochem. Biophys. Res. Commun.* **1998**, *247*, 687–692. [CrossRef] [PubMed]
52. Bortolussi, G.; Codarin, E.; Antoniali, G.; Vascotto, C.; Vodret, S.; Arena, S.; Cesaratto, L.; Scaloni, A.; Tell, G.; Muro, A.F. Impairment of enzymatic antioxidant defenses is associated with bilirubin-induced neuronal cell death in the cerebellum of Ugt1 KO mice. *Cell Death Dis.* **2015**, *6*, e1739. [CrossRef] [PubMed]
53. Renzone, G.; Arena, S.; Scaloni, A. Proteomic characterization of intermediate and advanced glycation end-products in commercial milk samples. *J. Proteom.* **2015**, *117*, 12–23. [CrossRef] [PubMed]

Sample Availability: Samples of the compounds are not available from the authors.

CHAPTER 4

Green synthesis of silver nanoparticles: analysis of the role of flavonoid quercetin

Paper submitted to AIP Conference Proceedings

Green synthesis of Ag nanoparticles using plant metabolites

Filippi A., Mattiello A., Musetti R., Petrussa E., Braidot E., Marchiol L.[a)]

DI4A - Department of Agriculture, Food, Environment and Animal Sciences, University of Udine, via delle Scienze 2068, I-33100 Udine, Italy

[a)]*Corresponding author: marchiol@uniud.it*

Abstract. Nano-biotechnology is one of the most promising areas in modern nanoscience and technology. In this emerging area of research, nanoparticles (NPs) play an important role since the large-scale production and huge numbers of utilization. Gold and silver nanoparticles are among the most extensively studied nanomaterials, since they show high stability and low chemical reactivity in comparison to other metals. They are commonly synthesized using toxic chemical reducing agents able to reduce metal ions into less charged NPs and/or high energy supplied procedures. The most commonly used method for the synthesis of NPs requires toxic chemicals like N,N-dimethyl formamide (DMF) or trisodium citrate, but recently a "green" technique, based on natural reducing agents, has been suggested to substitute the nature-unfriendly chemical methods. Many scientific works put in evidence the efficacy of plant extracts to reduce metal salts into the respective NPs, but this process lacks a clear control of NPs shapes and dimensions, since many different metabolites present into the extracts could participate to the process. This paper aims to clarify the reducing action of single pure natural compounds usually present in plant tissues and to obtain a stable and reproducible protocol for NPs synthesis.

INTRODUCTION

Nanoscience is the study of matter with at least one dimension between 1 and 100 nm that displays properties different from its bulk counterpart and it represents one of the most rapidly growing and cross-disciplinary field in science. The relevance of nanoscale researches is underlined by USA federal funding through the National Nanotechnology Initiative, which has grown from $464 million in 2004 to $1.85 billion in 2011. Also the number of consumer goods that self-report the inclusion of nanomaterials has risen from 54 in 2005 to 1317 in 2010, as an

indicator of the economic importance of nanoscience through commercialization (Metz et al., 2014).

In particular, during the last decade, nanotechnology has become a cutting edge application in interdisciplinary research area of strong interest, including basic / environmental / material and medical sciences. Nanomaterials present unique physical (wider surface) and structural (shape and dimensions) characteristics that give them peculiar mechanical, chemical, electrical, magnetic, optical, and biological properties (Razavi et al., 2015).

For these reasons, the use of nanomaterials and in particular nanoparticles (NPs) is getting an even more relevant and promising areas in biological science.

NPs are usually ≤100 nm in each spatial dimension and are commonly synthesized using top-down and bottom-up strategies. In top-down approach, the bulk materials are gradually broken down to nano-sized materials, whereas in bottom-up approach, atoms or molecules are assembled to molecular structures in the nanometer range. Bottom-up approach is commonly used for chemical and "green" biological synthesis of nanoparticles.

Different organic and inorganic reducing agents, such as sodium borohydride ($NaBH_4$), sodium citrate, ascorbate, elemental hydrogen, Tollen's reagent, N,N-dimethyl formamide (DMF) and poly-ethylene glycol (PEG) block copolymers are used for reduction of ions in aqueous or non-aqueous solutions. Capping agents are also used for size stabilization of the nanoparticles. Although the amount of NPs produced by physicochemical treatments is larger if compared to "green" synthesis, on the other hand the use of toxic chemicals to carry on the reduction step represents a great concern on this strategy that leads to eco-unfriendly by-products. The advancement of "green" syntheses over chemical methods is: environment friendly, cost effective and easily scaled up for large scale syntheses of NPs. A lot of data has been reported in literature on "green" syntheses of NPs using bacteria, fungi and in particular plants, thanks to their extracts rich in antioxidant and reducing agents, responsible for the reduction of metal salts in their respective NPs (Ahmed et al. 2016).

Among all the metals, silver nanoparticles (AgNPs) represent one of the most used NPs exhibiting intrinsic medical (bactericidal action) and optical (yellowish color in water) peculiar characteristics. Thanks to excitation of surface plasmon vibrations in the metal nanoparticles, the UV-Visible spectra recorded from the aqueous solution of AgNPs shows a strong characteristic absorbance peak around at 420 nm (Kesharwani et al., 2009).

The capability of plant extracts to reduce metal ions has attracted considerable attention within the last 30-years, although the role of the involved single reducing agents has not well understood. Plant extracts may act as both reducing and stabilizing agents in the synthesis of NPs and the different metabolites present at various concentrations in several plant tissues enhance even more the capability of the extract to reduce and stabilize the NPs. Typically, a plant extract-mediated bio-reduction occurs at room temperature and is generally complete within a few minutes. In view of the number of different molecules involved, the bio-reduction process is relatively complex and not well controlled: shape and dimensions of the NPs can vary widely from one extract to the other and different plants can produce different type of the same metal NPs. In addition, dimensional distribution is rather wide and this is a generally undesired feature in terms of biotechnological applications (Mittal et al., 2013).

Many different molecules seem to participate to the reduction power of plant extracts, but only one group of moieties possess all the appropriate characteristic like sufficient molar concentration, high antioxidant/reducing power, direct involvement in heavy metal plant detoxification mechanism: this group is the polyphenol family. They are a large class of molecules characterized by the presence of multiples phenol structural units. The most abundant polyphenols are the condensed tannins, found in virtually all families of plants. Another important sub-class of polyphenols is represented by flavonoids. In plants the different flavonoids have diverse biological functions, including protection against ultraviolet (UV) radiation and phytopathogens, flower and fruit coloration, as well as a strong antioxidant activity (Falcone Ferreyra et al., 2012).

Quercetin (QC) represents the most abundant flavonoid present in plant kingdom. Flavonoids share a common aromatic chemical structure that allows them to perform many different chemical reactions that involve sharing and exchanging of electrons.

Since the physical characteristics of the NPs seem to be the most important desired features, the aim of this work is to characterize the role played by a flavonoid such as QC in NPs formation and clarify the characteristics of the synthesized NPs by comparing the effect of flavonoid concentration and different pHs of incubation buffer.

MATERIALS AND METHODS

Materials

All the reagents (buffer salts, quercetin and $AgNO_3$) were purchased by Sigma. Three different 10 mM buffer solutions were used based on MOPS and Borax salts.

Green NPs synthesis

The reduction step of $AgNO_3$ to the respective NPs has been conducted mixing a fixed concentration of $AgNO_3$ (25 μM) with two different concentrations of QC as reducing agent (0.1 mM and 0.01 mM). The experiments were performed in 10 mM MOPS/KOH solution at pH 7.5 and 8.5 or 10 mM Borax solution at pH 9.2. The reaction took place at room temperature for 30 minutes, in dark round bottles, in constant shaking. After the synthesis the samples were kept at 4°C. The following data was the results of 3 independent replicates. Preliminary evidence of AgNPs formation was appreciated observing the color of QC 0.1 mM solution which turned from light yellow to brown color (Fig. 1).

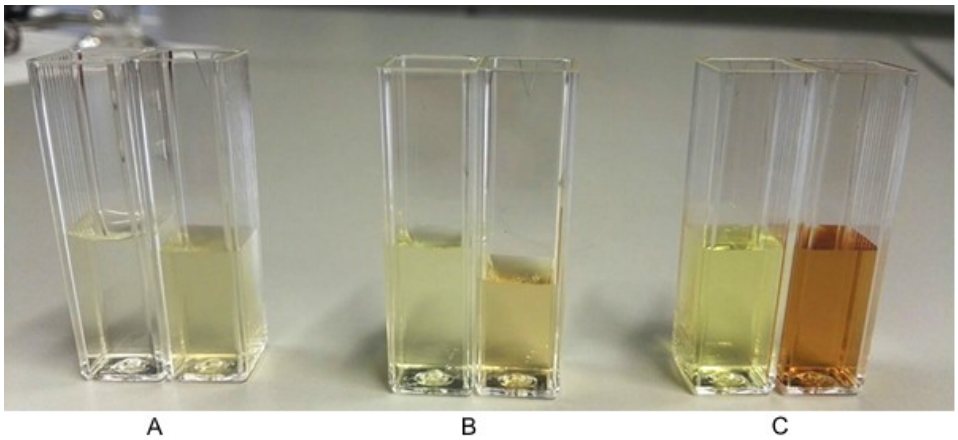

FIGURE 1. Preliminary evidences of AgNPs formation in response to pH variations (A=pH 7.5, B=pH 8.5, C=pH 9.2) are demonstrated by color change of the solution. The left-side cuvettes contained 0.1 mM QC and the buffer solution at different pH, while the right-side cuvettes were further added by 25 μM $AgNO_3$.

Spectrophotometric and dynamic light scattering (DLS) characterization

The different solutions obtained in the previous paragraph were centrifuged at 100.000 *g* for 2 hours and the pellet resuspended in few ml of the same buffer solution. This resuspension was sonicated during 5 minutes and analyzed with Agilent 8453 UV-visible Spectroscopy System for the spectrophotometric analysis, and with Zeta Potential/Particle Sizer NICOMPTM 380ZLS for DLS analysis.

Single Particle Inductively Coupled Plasma Mass Spectrometry (spICP-MS)

The solutions obtained from the previous step were analyzed by spICP-MS (NexIon 350X, Perkin Elmer, USA). The solutions were sonicated during 5 minutes and diluted in order to obtain a final concentration of NPs in the range of 100.000 and 200.000 particles per ml. The spICP-MS parameters were set as follow: Dwell Time 100 μs, Sample Time 100 s, the Sample Flow Rate and the Transport Efficiency were daily calculated. The sample flow rate was obtained by sucking MilliQ water for 5 minutes and checking the weight difference while the transport efficiency by using gold nanoparticles standards (AuNPs) of 30 and 60 nm size and gold dissolved solutions at 1, 2, 4 and 10 ppb, respectively.

Transmission electron microscopy (TEM)

The TEM samples were prepared by deposition of a single drop, almost 10 μl, of the solutions as it is on TEM Formvar/Carbon coated copper grid with 200 mesh and they were left to dry covered overnight.

RESULTS

TEM and DLS analysis

A first validation of the presence of silver NPs obtained using QC as reducing agent was obtained by TEM analysis. A blank sample with a representative concentration of reducing agent (QC 0.1 mM) was used to validate the presence of silver NPs at the three pHs (Fig. 2). Irrespective of the used pH, NPs were observed, although in different concentration and with different dimensional classes.

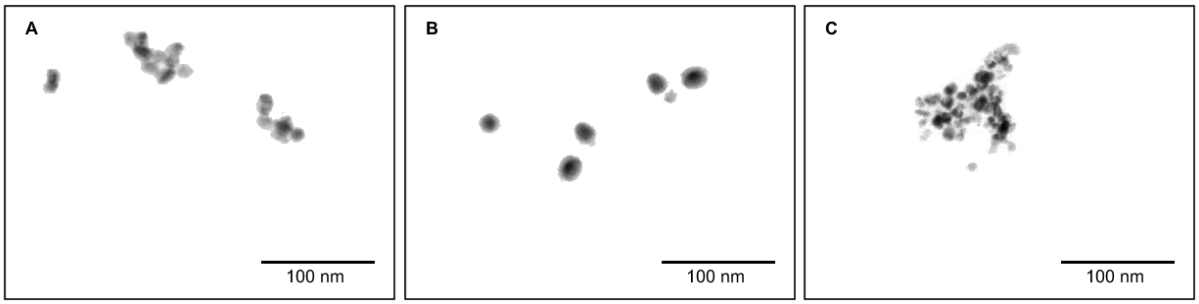

FIGURE 2. Representative TEM images of silver NPs obtained with QC (0.1 mM) at pH 7.5 (A), 8.5 (B) and 9.2 (C).

With regard to DLS analysis, at each pH two or three distinct groups of nanostructures are observed (Fig. 3). The information about each group of nanostructures are reported on Table 1.

The data show the presence of nanostructures with huge diameter, in particular 1180 nm, 191 nm and 106.1 nm at pH 7.5, 8.5 and 9.2 respectively. These nanostructures could be formed by polymerization of QC and not by AgNPs formation (as later explained).

The DLS analysis puts on evidence the presence of one/two smaller groups of NPs, in particular 15.4 nm, 12/54 nm and 11.9 nm at pH 7.5, 8.5 and 9.2 respectively, where these nanostructures exhibit a percentage of frequency lower than the bigger aggregates. From these data, in agreement with that shown at TEM, we observed that the smallest NPs (with a dimensional average of approx. 12 nm) increase from 3% to 14.8% when the pH value increased from 8.5 to 9.2. This group of small NPs was not detected at pH 7.5, although DLS analysis showed a clear limitation in the detection of NPs under a certain level of intensity.

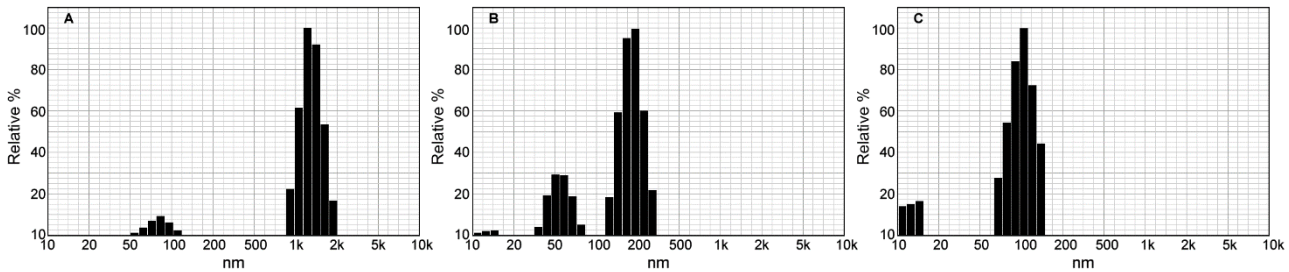

FIGURE 3. DLS analysis of silver NPs obtained with QC (0.1 mM) at pH 7.5 (A), 8.5 (B) and 9.2 (C).

TABLE 1. DLS analysis data for each group of nanostructure observed.

	Parameter	1° group	2° group	3° group
pH 7.5	Diameter Av.	89.4 nm	1180 nm	
	St. Dev.	15.4nm (17.3%)	239.9nm (20.3%)	
	% of total	8.5%	91.5%	
pH 8.5	Diameter Av.	12 nm	54 nm	191 nm
	St. Dev.	1.6 nm (13%)	9.2nm (17.1%)	33.5nm (17.5%)
	% of total	3%	22%	75%
pH 9.2	Diameter Av.	11.9 nm	106.1 nm	
	St. Dev.	1.6 nm (13.4%)	23.8 nm (22.5%)	
	% of total	14.8%	85.2%	

Spectrophotometer analysis of AgNPs

After the AgNPs synthesis, 2 ml of silver NPs suspension were analyzed using a spectrophotometer to obtain spectra that indicate the formation of Ag NPs (Fig. 4). A previous spectrophotometric screening has been performed to obtain information regarding the best range of pH and $AgNO_3$/QC concentration upon which to perform the further experiments. As it can be observed, low concentration of QC (0.01 mM) was able to induce acceptable amount of AgNPs similarly to that formed by the high concentration of QC (0.1 mM), at all tested pH except for 9.2 (panel C). Conversely, at this pH, NPs formation was strongly stimulated by 0.1 mM QC. The synthesis reaction was associated to the development of a yellow/brown coloration, whose intensity depended on QC concentration.

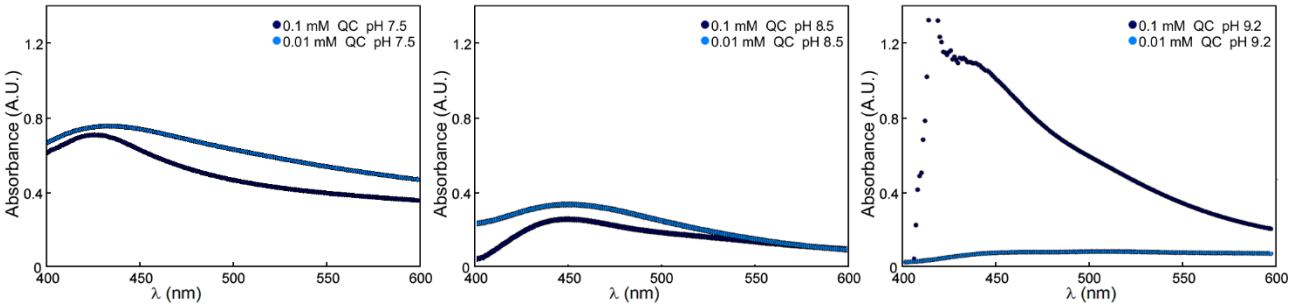

FIGURE 4. Absorption spectra of 0.1 and 0.01 mM QC at three different pHs. The synthesis of the AgNPs in buffer solution was monitored by recording the absorption spectra at a wavelength range of 400-600 nm.

spICP-MS analysis

An aliquot of AgNPs suspension was analyzed using spICP-MS to obtain the size distribution of the most abundant dimensional class of AgNPs present into each sample (Fig. 5). NPs formation has been observed at all the different pHs, although with little difference in the medium size dimension. The solution with 0.01 mM QC appears to be the best reducing agent concentration, since the medium size of NPs was smaller than 31 nm, whereas in the 0.1 mM concentration solution larger NPs (approx. > 31 kDa) were present.

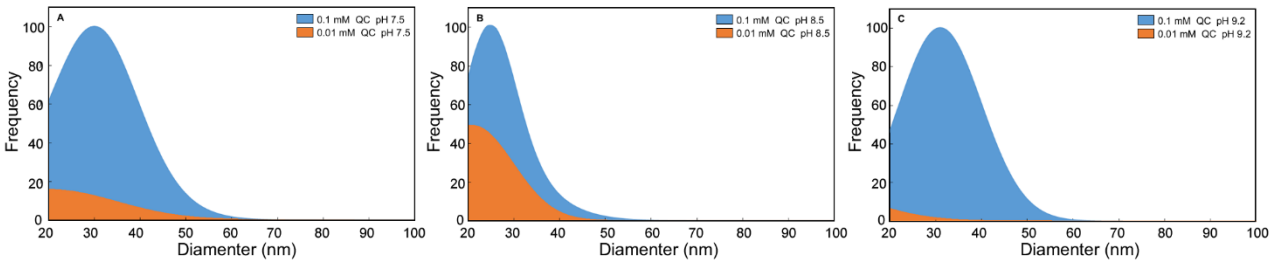

FIGURE 5. Frequency and diameters of AgNPs produced by 0.1 and 0.01 mM QC at respectively pH 7.5 (A), 8.5 (B) and 9.2 (C) and observed at spICP-MS.

DISCUSSION

Nanotechnology is a rapid growing field regarding nanoproducts and nanoparticles (NPs) that possess relevant size-related physicochemical properties, different from the respective larger matter. Among all the metal NPs, AgNPs have attracted increasing interest due to their unique physical/ chemical/ biological properties: high electrical and thermal conductivity, surface-enhanced Raman scattering, chemical stability, catalytic activity and nonlinear optical behavior. The AgNPs optical properties allow them to be easily detected by spectrophotometric analysis, recording the absorption spectra at a wavelength range of 400-600 nm, and focusing on a peak around 420 nm that indicates the AgNPs presence (Jyoti et al., 2016). These properties confer them a huge potential value in engineering (inks and microelectronics), medicine (bactericidal and fungicidal activity), and industry (plastics, soaps, pastes, food and textiles) and for the environment (air disinfection, water purification, soil detoxification). According to the Project on Emerging Nanotechnologies (PEN) among 1300 nanotechnology-enabled products within the global market, there are 313 nanosilver products (24% of products listed), making it the largest and fastest growing class of NPs in consumer products applications. Because of their widespread applications, the scientific community and industry has paid special attention to the research topic of AgNPs and in particular on “green” eco-friendly NPs synthesis. When AgNPs are produced by chemical synthesis, three main components are needed: a silver salt, a reducing agent to reduce ions to 0-charged molecules and a stabilizer or capping agent to control the growth of the NPs and prevent them from aggregation. In case of the “green” synthesis of

AgNPs, the reducing agent and the stabilizer are replaced by molecules produced by living organisms. These reducing and/or stabilizing compounds can be obtained from bacteria, fungi, yeasts, algae or plants (Tran et al., 2013).

Green chemistry principles maximize safety and efficiency and minimize the environmental and social impact of toxic raw materials. Green synthesis of NPs focuses on three important aspects i.e., (i) use of green solvents, (ii) use of an eco-friendly reducing agent, and (iii) use of a non-toxic material as a stabilizer (Nayak et al. 2016).

Plant extracts contains enzymes (hydrogenases, reductases) and phytochemicals, such as terpenoids, flavonoids, phenols, dihydric phenols and so on, acting both as reductants and capping agents in the presence of metal salt for NPs synthesis (Jyoti et al., 2016).

Although in literature is present a huge number of papers regarding hundreds of different plant extracts and there is plenty of information about the NPs characteristics (dimension, shape and quantity) for each extract, currently the knowledge on which molecules contribute to the process - and how - is quite poor (Logeswari et al., 2013; Kumar et al., 2017; Mittal et al., 2013).

With the aim to clarify this problem, we focused the attention on an ubiquitary class of secondary metabolites (flavonoids), known to be an essential part of the reducing/oxidizing system of plants. Among this class of potent antioxidant molecules, we consider quercetin (QC) as a good candidate, as it is the most naturally abundant and easy to extract flavonoid.

Since dimensions and quantity are two of the most important parameters to be considered during industrial synthesis, an initial screening using spectrophotometric analysis (data not shown) was performed to set the better conditions and the most correct parameters to obtain the larger amount of smaller NPs.

According to this preliminary assays, a fixed $AgNO_3$ concentration (25 μM), two QC concentrations (0.1 and 0.01 mM) and three different pH values (7.5-8.5-9.2) were used, performing the synthesis in round brown bottles, at room temperature for 30 minutes, with shaking. Once set the parameters, the highest concentration of reducing agent (QC 0.1 mM) was used as reference standard for the TEM and DLS analysis (Fig. 2-3), with the aim to colorimetrically visualize and characterize the formation of AgNPs. Considering the increasing solubility and color intensity of QC at higher pH, the synthesis shows a clear color change in all the three treatments. This change is typically due to AgNPs formation and the results are in agreement with the literature, which identifies the basic pH as the better for NPs synthesis (Ahmad et al. 2015). In fact, as showed, in our experiment the major color change occurred at pH 9.2.

In TEM images, each pH solution shows NPs formation although with different medium sizes: the smallest ones at pH 9.2 and the largest ones at 7.5 (data not shown). The same results are shown in DLS analysis data, although different distributions are presented. Although the DLS technique is widely used for particles characterization, there are some problems in case of measuring samples with large-size distribution or multimodal distributions (like in our case), particularly whether nothing is known about the actual AgNPs distribution. In case of polydisperse colloids, there is a risk that during the DLS measurement small objects can be screened by bigger ones and will not even be seen at all. In addition, a hydration/capping layer

must be considered to cause a general increase in particle diameter (Tomaszewska et al. 2013). For all these reasons, only general considerations can be formulated:

(i) At increasing pH, there is a parallel increase in the percentage of small NPs;

(ii) At increasing pH, there is a general decrease in total particle sizes;

(iii) Nothing can be deduced about the actual quantity of each single NPs, except that small NPs are less in percentage with respect to the total;

(iv) It is likely that in the sample with large aggregates (pH 7.5), small NPs are actually present and hidden.

According to the assumption that AgNPs possess a surface plasmon resonance peak around 420 nm (Jyoti et al., 2016), absorption spectra of AgNPs formation by 0.1 and 0.01 mM QC at different pH were obtained (Figure 4). In accordance with the results found at TEM and DLS analysis, the spectrophotometric analysis evidences the highest peak at 420 nm and the strongest difference between the two reducing agent concentrations at pH 9.2. At 7.5 and 8.5 pH values, sample analysis exhibits instead weak peak intensity at 420 nm, without a significant difference between the two concentrations. This effect is probably due to the poor solubility of QC at pH close to neutral (Srinivas et al. 2010).

Among the techniques of NPs characterization, the most commonly and easy to use are DLS and UV-Vis spectroscopy, although none of them are really capable to detect with precision the metal composition of the particle under analysis, giving only general information on the aggregate suspension of the solution. For this reason, spICP-MS was used to obtain more precise information regarding specific Ag nanomaterial. The Figure 5 reports that all the assayed pHs induce the AgNPs formation, although with a negligible difference in their average size, in accordance with the previous discussion. Taking in account that the sensitivity and the accuracy of spICP-MS have a NPs size distribution detection limit (denoted as Dmin) of approx. 20 nm for AgNPs (Lee et al. 2014), the small NPs observed in DLS analysis and TEM could not be detected by the spICP-MS output. Considering the 0.1 mM concentration, the spICP-MS analysis can however evidence that the aggregates bigger than 100 nm, observed with DLS, seemed not to be ascribed to silver metal. The frequency indicated into the graphics as percentage on the total (CPS) shows the distribution of the most frequent dimensional class of NPs contained into the sample volume, though not providing a true direct quantification of the NPs present into the sample.

These preliminary results need to be further corroborated with experiments to confirm, witha more accurate analysis by means of TEM images, the actual dimensional classes of AgNPsand also to extend the effects of different range of QC concentrations.

ACKNOWLEDGEMENTS

We are very grateful to Prof. Emilio Celotti and dr. Paola Ferraretto (DI4A, University of Udine) for collaboration in DLS analysis.

REFERENCES

1. N. Ahmad et al. Int. J. Nanomedicine 10, 7019–7030 (2015).
2. S. Ahmed et al. J. Adv. Res. 7, 17–28 (2016).
3. M.L. Falcone Ferreyra et al. Front. Plant Sci. **3,** 222 (2012).
4. K. Jyoti et al. J. Rad. Res. Appl. Sci. **9,** 217–227 (2016).
5. J. Kesharwani et al. J. Bionanosci. **3,** 39–44 (2009).
6. B. Kumar et al., Saudi J. Biol. Sci. 24, 45-50 (2017)
7. S. Lee et al. Environ. Sci. Technol. **48,** 10291–10300 (2014).
8. P. Logeswari et al. Scientia Iranica **20,** 1049–1054 (2013).
9. K.M. Metz et al. J. Chem. Educ. **91,** 264–268 (2014).
10. A.K. Mittal et al. Biotechnol. Adv. **31,** 346–356 (2013).
11. D. Nayak et al. *Mat. Sci. Eng. C* **58,** 44–52 (2016).
12. M. Razavi et al. "Green Chemical and Biological Synthesis of Nanoparticles and Their Biomedical Applications" in *Green Processes for Nanotechnology* edited by Basiuk, V. A. & Basiuk, E. V. (Springer International Publishing, 2015), pp. 207–235.
13. K. Srinivas et al. J. Food Eng **100,** 208–218 (2010).
14. E. Tomaszewska et al. J. Nanomat. e313081 (2013).
15. Q. Tran et al. Adv. Nat. Sci: Nanosci. Nanotechnol. **4**, 33001 (2013).

DISCUSSION

Flavonoids form one of the most studied classes of plant secondary metabolites, because of their chemical and biochemical properties, in addition to relevant physiological and pharmacological effects both in plants and humans (Pollastri and Tattini 2011; Scalbert, Johnson, and Saltmarsh 2005). The relevance of these molecules in plant biology is indicated by the fact that, in normal growth conditions, 20% of carbon fixed by plants flows through this pathway (Michalak 2006). Flavonoids encompass more than 10,000 molecules present into the plant tissues at different molar concentrations and differentially synthetised during all the developmental stages (Tsimogiannis and Oreopoulou 2006). Since most flavonoids are independently produced after environmental stress, individuals in different populations exposed to varying environmental conditions usually show variable accumulation of flavonoids (Valle et al. 2015). Under the pressure of natural selection, this impressive chemical diversity of metabolites has been selected for the high number of possible physiological functions, spanning from their crucial role in biotic and abiotic stress responses, to cellular communication mechanisms (Trantas et al. 2015). It is clear that these compounds can fulfill all these different biological functions, thanks to shared characteristics: (i) the double aromatic rings (A and C ring), (ii) the benzopyrane ring (B ring) that can be bound in three different positions to the C ring, often forming a planar structure; (iii) the many functional groups in all the three components of the molecules (A, B and C ring) that contribute to the antioxidant and linkage-specific properties (Tsimogiannis and Oreopoulou 2006) (Fig. 39).

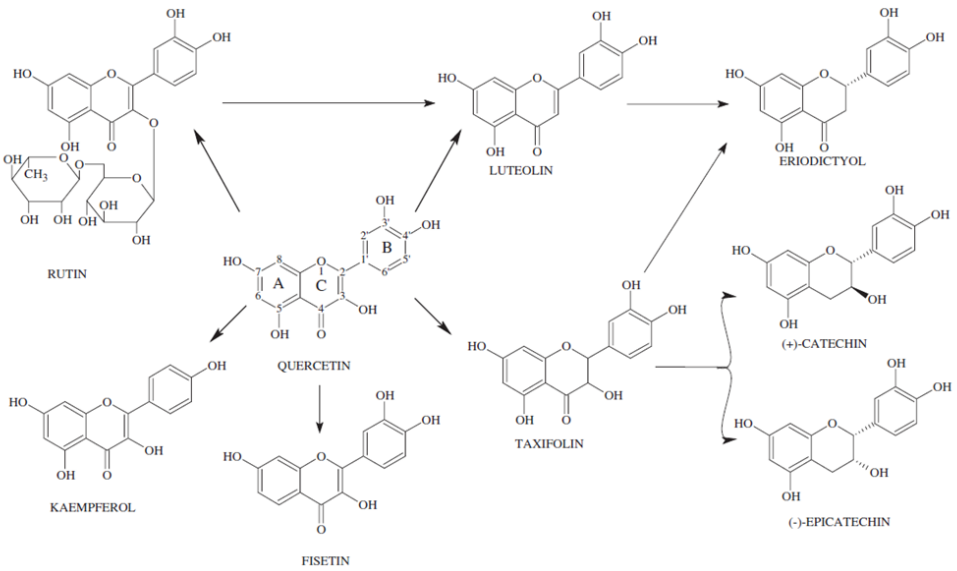

Figure 39. Chemical structure of different flavonoids: quercetin, kaempferol, fisetin (flavonols), rutin, luteolin (flavones), taxifolin (dihydroflavonol), eriodictyol (flavanone), (+)-catechin, ()-epicatechin (flavanols) (Tsimogiannis and Oreopoulou 2006).

Hence, their chemical structure appears to be a key factor in interactions with biological structures such as proteins and membranes (Tarahovsky et al. 2014). Although there is huge information in literature regarding flavonoid/protein interactions, only recently the scientific interest has been focused on their interaction with phospholipid membranes. Singh et al. (2016) proposed for the first time a model that predicts the possibility of free interaction between flavonoids (in particular quercetin and kaempferol) and micelle-like structure, made of anionic surfactant (AOT)/ NaDEHP able to mimic artificial biological membranes. Moreover, Srinivas et al. (2010) hypothesized the absorption of flavonoids in the outer portion of palisade layer of micelles, thanks to their planar amphipathic structure (with phenyl rings forming the hydrophobic part of the molecule and the hydroxyl groups constituting the polar portion) (Figure 40).

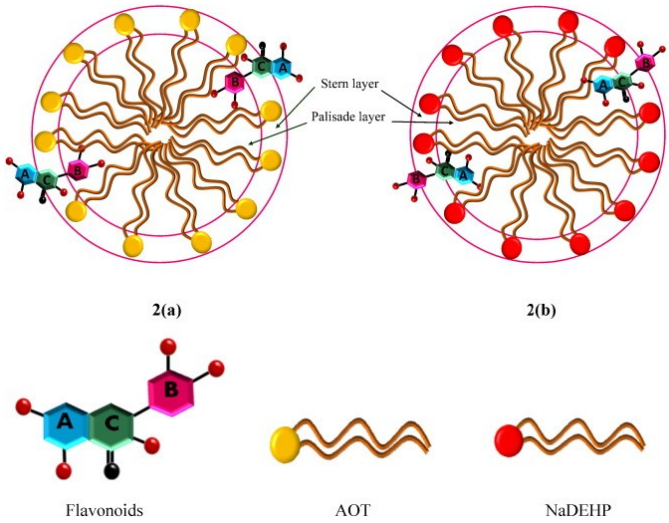

Figure 40. Possible location of flavonoids in (a) AOT micelles, (b) NaDEHP micelles (Srinivas et al. 2010).

Flavonoids contain a number of hydroxyl groups that confer polarity and weak acidic properties to the molecules. The interaction with the lipid bilayer depends on the pH, which determines the electrostatic charges of these groups and the (hydrophobic) interactions with lipid molecules (it is experimentally demonstrated an inverse correlation between the number of hydroxyl groups and the lipophilicity of flavonoids). Consequently, a lower pH results in a lower deprotonation of polar groups and thus a deeper penetration of flavonoids into the lipid bilayer. All these considerations do not take in account the glycosylation, a flavonoid modification that increases their water-solubility and decreases their absorption to the membrane (Tarahovsky et al. 2014).

Furthermore, since flavonoids exert their biological activity in close relationship with their cellular localization, the fine regulation of their transport within the cell appears

of primarily importance. In the literature, primary or secondary active transporter proteins are the most important players of flavonoid translocation across membranes, whereas the contribution of facilitated/passive transport mechanisms received less attention. Moreover, a large part of the research relies on genetic RNA expression studies or in time-consuming transport assay experiments involving both radiolabeled substrates or transporter-expressing transformed yeast vesicles.

The first approach of my work was in fact focused on setting a new *in vivo*/*in vitro* methodology to follow flavonoid transport across biological membranes: a first part concerned the QC uptake across membranes in a cell suspension culture of *V. vinifera* (work published in FEBS Open Bio, Filippi et al. 2015), while a second part focused on facilitated/passive QC transport characterization in a more simple system of microsome vesicles isolated from etiolated *P. sativum* seedlings. With these experiments I would like to characterize to a better extent the mechanism(s) involved in cellular flavonoid uptake. Aiming at performing a simple and rapid transport assay of QC, my attention has been devoted to the well-known technique able to evidence flavonoid accumulation in plant tissues by means of the fluorescence signal emitted by DPBA/flavonoid complex. This feature has been considered for implementing a transport assay on fluorimeter, where QC transport into suspension cells or into membrane vesicles could be followed as a time-dependent kinetic curve. In addition it should be argued that high energy demanding mechanisms are hardly compatible with phenological phases exhibiting intense flavonoid transport (e.g. senescence). The results, shown in the first part of the PhD project, demonstrated the validity of the DPBA-dependent assay to monitor flavonoid transport across both cellular and microsomal membranes. This new methodology appears cheap and fast, with no particular requirement of instruments and environmental precautions. This assay could be utilized for enzymatic characterization of different transporter(s) and carrier(s) mainly involved in this process, by choosing specific calibration curves and incubation medium conditions for each species and flavonoid. In the present study, specific modulators of protein functional groups caused an alteration on QC uptake, indicating a probable involvement of carriers/ channels into the transport process. It is noteworthy to further underline that QC uptake in pea microsome vesicles took place in the absence of ATP supply, thus suggesting the presence also of facilitated/ passive transporters of QC, currently not yet investigated. This observation needs a more extended experimental design in order to appreciate the possible contribution, if any, of energy-independent, concentration-dependent mechanisms of QC flux across membrane.

Considering their polycyclic structure and the huge number of functional groups characterizing different flavonoid molecules, it is also interesting to take into account

their interaction with specific proteins. There is great evidence on flavonoid modulation of enzymatic activities, such as protein kinases, ATPases, cyclooxygenase, aldose reductase (Pawlikowska-Pawlega et al. 2007; Graziani and Chayoth 1979; Ghasemzadeh and Ghasemzadeh 2011; Tarahovsky et al. 2014), and their interaction with several proteins like human serum albumin (Vachali et al. 2016), proline-rich salivary proteins (forming insoluble complexes responsible for the perception of astringency) (Gallo et al. 2013), low-density lipoproteins (Tarahovsky et al. 2014), or with other different proteins present in common beverages like beer and wine. In fact, polyphenols seem to interact preferably with globular proteins, causing structural and conformational changes, mainly depending on polyphenol molecular size and spatial conformation (Gallo et al. 2013).

Furthermore, in the second part of my thesis, I wanted to shed light on this interaction by using an antibody built upon a flavonoid binding sequence of an organic anion membrane carrier present in different rat (mammalian) membranes. This antibody was used as a tool aiming to select proteins from red grape berry skin microsomes that could interact with flavonoids (published in Molecules, Filippi et al. 2016). Among the proteins with a mass range of 25-27kDa, revealed by Western Blot analysis, a quantitative correlation between signal intensity and protein concentration was observed. Their sequence was obtained by nLC-ESI-LIT-MS/MS. The most promising protein identified was the IV group chitinase, since the assay of its activity was easy and sensible, for its ubiquitous presence in living organisms and also for its role as pathogen-related protein during plant defense against fungi and insect attack. As a confirmation of the hypothesized flavonoid/chitinase interaction, QC and CA, although to a lower extent, were discovered as able to modulate the activity of chitinase, according to a hormetic response curve. This evidence gives more strength to the role of flavonoids as enzyme modulators; to the best of my knowledge, this role has been considered only as marginal in plants so far.

Flavonoids are not only important for their 3-ring structure, thanks to which they are able to interact with membranes and proteins, but they are also characterized by many different functional groups that confer fundamental antioxidant properties. This ability to reduce reactive oxygen species (ROS) during stress is directly connected to their molecular ability to donate electrons to highly oxidized molecules. This property mainly depends on hydroxyls groups and phenolic rings present in their chemical structure: flavonoids and tannins (all generally grouped into phenolic compounds) are plant secondary metabolites with several of these aromatic rings (Mittal, Chisti, and Banerjee 2013). In addition to their antioxidant features, flavonoids possess chemical structure and functional groups able to chelate metal ions and form different

complexes with them too (Jabeen et al. 2017), avoiding metal to induce harmful catalysis reactions (Figure 41).

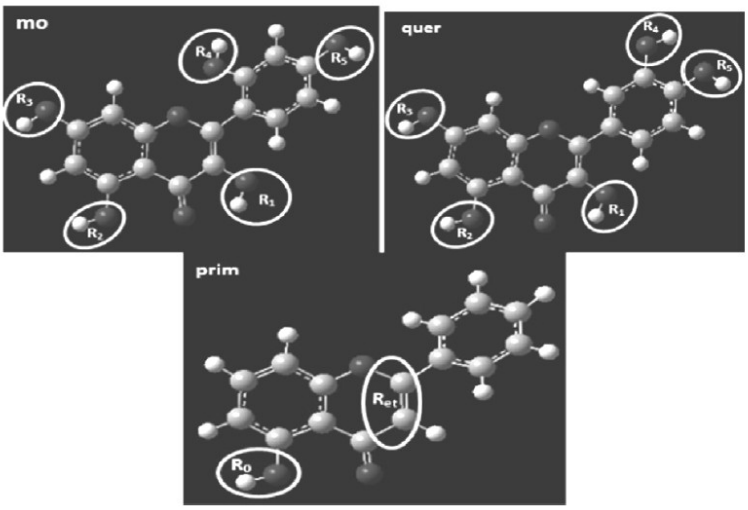

Figure 41. Possible site of attack by radicals in three model flavonoids: (mo) morin; (quer) quercetin; (prim) primuletin (Jabeen et al. 2017).

Thanks to their structure, flavonoids are essential in plant responses of soil metal starvation (Jin et al. 2007; Selvaraj et al. 2014) and in plants inactivation and transformation of heavy metal salts into a physiologically tolerable form, by the synthesis of NPs, starting from metal salt. This phenomenon is mainly due to the presence of many reducing and stabilizing cellular metabolites (Mittal, Chisti, and Banerjee 2013) and recent findings also include flavonoids among these. Although the flavonoid involvement was not evaluated, Mattiello et al. (2015) demonstrated in a recent work (see Appendix 2) that particularly cerium oxide NPs were able to enter into barley plantlets, inducing physiological modification in ROS and ATP content, two molecules regulated by flavonoid content too.

The presence of the OH group in the 3-position of the flavonoid skeleton C ring (Figure 42) is an important structural feature responsible for the specific ability of flavonols to chelate transition metal ions. Also the presence of a catechol group in the B-ring seems to be responsible for a high capacity to chelate transition metal ions and for the reduction of various forms of ROS (Pollastri and Tattini 2011).

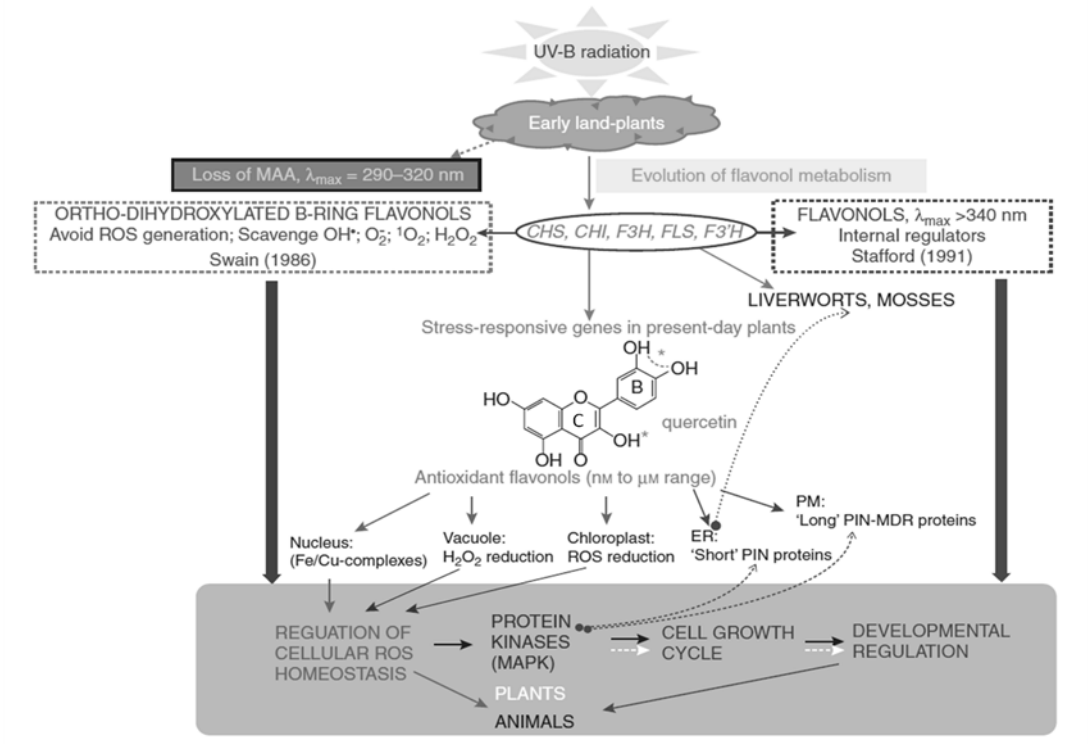

Figure 42. A schematic diagram showing the functional roles hold by flavonols in evolutionarily oldest and present-day terrestrial plants. Endoplasmic reticulum (ER), plasma membrane (PM), genes responsible for the biosynthesis of QC derivatives: chalcone synthase (CHS), chalcone isomerase (CHI), flavanone 3-hydroxylase (F3H), flavonol synthase (FLS) and flavonoid 3'-hydroxylase (F3'H) (Pollastri and Tattini 2011).

The ability of plant extracts to reduce metal salts into the less toxic NPs has been well known since the last 30 years; nevertheless the knowledge about the role of the single molecule present in plant extracts remains still scarce. Flavonoids present various chemical structures to fulfill many specific physiological functions during plant's life, including antioxidant and detoxifying activities. Hence, with the aim to investigate the actual potential of QC in NPs formation and to characterize how flavonoids can contribute to the reduction properties shown by plant extracts, in the last topic of my PhD thesis I evaluated the optimal conditions for QC to form silver NPs (AgNPs). The goal was obtained by performing an environment-friendly assay without use of toxic compounds/conditions and of high-energy-demanding supply.

Using three different pH buffers (pH 7.5, 8.5, 9.2) and two different QC concentrations (0.1 and 0.01mM), I followed the AgNPs formation using different approaches such as spectrofotometric/ single particles ICP-MS / TEM and DLS analysis. The obtained data provided indication in terms of optimum pH ranges for incubation buffer, metal salt and flavonoid concentration and shape/dimensional characteristics.

The results evidenced, as already observed in literature (Amin et al. 2012), that the best conditions for obtaining high amount of small (diameter lesser than 20 nm) round-shaped, silver NPs were alkaline pH (9.2) and 0.1 mM QC.

The size and shape dimensions are very important parameters for the application of these nanostructures in further development of their medicinal or nutraceutical organic capping. The possibility to implement the protocol presented in my thesis will allow preparing different NPs for different targets. Subsequently, the acquired knowledge would be greatly useful in order to define a green technology protocol, as well as a cheap and environmentally sustainable method, for synthesis of stable NPs, with well-characterized specific shapes and dimensions.

Taken together all these findings provide hints for further scientific investigation on the role of flavonoids in various metabolic activities and their possible utilization in industrial processes. In particular, their complex chemical structure and their known reactivity may be exploited in innovative processes, such as those regarding the recycle of biomass in the context of the circular economy. Therefore, the high content of flavonoids present in many waste products of farming activities could find a highly lucrative application in industrial production lines such as nanomaterial technology. Moreover, the modulation or stimulation effect exerted by flavonoids on plant defense system could be exploited in biological pest management and control with low environmental impact on valuable crops.

BIBLIOGRAPHY

for Introduction and Discussion

Agati, G., and Tattini, M. (2010). Multiple functional roles of flavonoids in photoprotection. New Phytologist *186*, 786–793.

Agati, G., Azzarello, E., Pollastri, S., and Tattini, M. (2012). Flavonoids as antioxidants in plants: Location and functional significance. Plant Science *196*, 67–76.

Agati, G., Brunetti, C., Di Ferdinando, M., Ferrini, F., Pollastri, S., and Tattini, M. (2013). Functional roles of flavonoids in photoprotection: new evidence, lessons from the past. Plant Physiol. Biochem. *72*, 35–45.

Amin, M., Anwar, F., Janjua, M.R.S.A., Iqbal, M.A., and Rashid, U. (2012). Green synthesis of silver nanoparticles through reduction with *Solanum xanthocarpum* L. berry extract: characterization, antimicrobial and urease inhibitory activities against *Helicobacter pylori*. Int J Mol Sci *13*, 9923–9941.

An, Y., Feng, X., Liu, L., Xiong, L., and Wang, L. (2016). ALA-induced flavonols accumulation in guard cells is involved in scavenging H_2O_2 and inhibiting stomatal closure in Arabidopsis cotyledons. Front. Plant Sci. *7*.

Ananga, A., Georgiev, V., Ochieng, J., Phills, B., and Tsolova, V. (2013). Production of anthocyanins in grape cell cultures: a potential source of raw material for pharmaceutical, food, and cosmetic industries.

Andolfo, G., Ruocco, M., Di Donato, A., Frusciante, L., Lorito, M., Scala, F., and Ercolano, M.R. (2015). Genetic variability and evolutionary diversification of membrane ABC transporters in plants. BMC Plant Biology *15*, 51.

Au, K.K.C., Pérez-Gómez, J., Neto, H., Müller, C., Meyer, A.J., Fricker, M.D., and Moore, I. (2012). A perturbation in glutathione biosynthesis disrupts endoplasmic reticulum morphology and secretory membrane traffic in Arabidopsis thaliana. Plant J. *71*, 881–894.

Bais, H.P., Weir, T.L., Perry, L.G., Gilroy, S., and Vivanco, J.M. (2006). The role of root exudates in rhizosphere interactions with plants and other organisms. Annu Rev Plant Biol *57*, 233–266.

Bassham, D.C. (2015). Plant biology: Pigments on the move. Nature *526*, 644–645.

Bondonno, C.P., Croft, K.D., Ward, N., Considine, M.J., and Hodgson, J.M. (2015). Dietary flavonoids and nitrate: effects on nitric oxide and vascular function. Nutr. Rev. *73*, 216–235.

Brand, W., van der Wel, P.A.I., Rein, M.J., Barron, D., Williamson, G., van Bladeren, P.J., and Rietjens, I.M.C.M. (2008). Metabolism and transport of the citrus flavonoid hesperetin in Caco-2 cell monolayers. Drug Metab. Dispos. *36*, 1794–1802.

Buer, C.S., Muday, G.K., and Djordjevic, M.A. (2007). Flavonoids are differentially taken up and transported long distances in *Arabidopsis*. Plant Physiol *145*, 478–490.

Buer, C.S., Muday, G.K., and Djordjevic, M.A. (2008). Implications of long-distance flavonoid movement in Arabidopsis thaliana. Plant Signal Behav *3*, 415–417.

Buer, C.S., Imin, N., and Djordjevic, M.A. (2010). Flavonoids: new roles for old molecules. J Integr Plant Biol *52*, 98–111.

Çakır, B., and Kılıçkaya, O. (2013). Whole-genome survey of the putative ATP-Binding Cassette transporter family genes in *Vitis vinifera*. PLOS ONE *8*, e78860.

Chanoca, A., Kovinich, N., Burkel, B., Stecha, S., Bohorquez-Restrepo, A., Ueda, T., Eliceiri, K.W., Grotewold, E., and Otegui, M.S. (2015). Anthocyanin vacuolar inclusions form by a microautophagy mechanism. Plant Cell *27*, 2545–2559.

Chemler, J.A., Yan, Y., and Koffas, M.A. (2006). Biosynthesis of isoprenoids, polyunsaturated fatty acids and flavonoids in *Saccharomyces cerevisiae*. Microb Cell Fact *5*, 20.

Day, A.J., Gee, J.M., DuPont, M.S., Johnson, I.T., and Williamson, G. (2003). Absorption of quercetin-3-glucoside and quercetin-4′-glucoside in the rat small intestine: the role of lactase phlorizin hydrolase and the sodium-dependent glucose transporter. Biochemical Pharmacology *65*, 1199–1206.

Ditta, A., Arshad, M., and Ibrahim, M. (2015). Nanoparticles in sustainable agricultural crop production: applications and perspectives. Nanotechnology and plant sciences, M.H. Siddiqui, M.H. Al-Whaibi, and F. Mohammad, eds. (Springer International Publishing), pp. 55–75.

Dueñas, M., Surco-Laos, F., González-Manzano, S., González-Paramás, A.M., Gómez-Orte, E., Cabello, J., and Santos-Buelga, C. (2013). Deglycosylation is a key step in biotransformation and lifespan effects of quercetin-3-O-glucoside in *Caenorhabditis elegans*. Pharmacol. Res. *76*, 41–48.

Falcone Ferreyra, M.L., Rius, S.P., and Casati, P. (2012). Flavonoids: biosynthesis, biological functions, and biotechnological applications. Front Plant Sci *3*.

Filippi, A., Petrussa, E., Peresson, C., Bertolini, A., Vianello, A., and Braidot, E. (2015). In vivo assay to monitor flavonoid uptake across plant cell membranes. FEBS Open Bio *5*, 748–752.

Filippi, A., Petrussa, E., Rajcevic, U., Čurin Šerbec, V., Passamonti, S., Renzone, G., Scaloni, A., Zancani, M., Vianello, A., and Braidot, E. (2016). Flavonoid interaction with a chitinase from grape berry skin: protein identification and modulation of the enzymatic activity. Molecules *21*, 1300.

Francisco, R.M., Regalado, A., Ageorges, A., Burla, B.J., Bassin, B., Eisenach, C., Zarrouk, O., Vialet, S., Marlin, T., Chaves, M.M., et al. (2013). ABCC1, an ATP binding cassette protein from grape berry, transports anthocyanidin 3-O-Glucosides. Plant Cell *25*, 1840–1854.

Gallo, M., Vinci, G., Graziani, G., De Simone, C., and Ferranti, P. (2013). The interaction of cocoa polyphenols with milk proteins studied by proteomic techniques. Food Research International *54*, 406–415.

Ghasemzadeh, A., and Ghasemzadeh, N. (2011). Flavonoids and phenolic acids: role and biochemical activity in plants and human. JMPR *5*, 6697–6703.

Gholami, A., De Geyter, N., Pollier, J., Goormachtig, S., and Goossens, A. (2014). Natural product biosynthesis in Medicago species. Nat Prod Rep *31*, 356–380.

Goiris, K., Muylaert, K., Voorspoels, S., Noten, B., De Paepe, D., E Baart, G.J., and De Cooman, L. (2014). Detection of flavonoids in microalgae from different evolutionary lineages. J. Phycol. *50*, 483–492.

Gomez, C., Terrier, N., Torregrosa, L., Vialet, S., Fournier-Level, A., Verriès, C., Souquet, J.-M., Mazauric, J.-P., Klein, M., Cheynier, V., et al. (2009). Grapevine MATE-type proteins act as vacuolar H+-dependent acylated anthocyanin transporters. Plant Physiol. *150*, 402–415.

Gomez, C., Conejero, G., Torregrosa, L., Cheynier, V., Terrier, N., and Ageorges, A. (2011). In vivo grapevine anthocyanin transport involves vesicle-mediated trafficking and the contribution of anthoMATE transporters and GST. The Plant Journal *67*, 960–970.

Gonzales, G.B., Van Camp, J., Vissenaekens, H., Raes, K., Smagghe, G., and Grootaert, C. (2015). Review on the use of cell cultures to study metabolism, transport, and accumulation of flavonoids: from mono-cultures to co-culture systems. COMPREHENSIVE REVIEWS IN FOOD SCIENCE AND FOOD SAFETY *14*, 741–754.

Graziani, Y., and Chayoth, R. (1979). Regulation of cyclic amp level and synthesis of DNA, RNA and protein by quercetin in ehrlich ascites tumor cells. Biochemical Pharmacology *28*, 397–403.

Halbwirth, H. (2010). The creation and physiological relevance of divergent hydroxylation patterns in the flavonoid pathway. International Journal of Molecular Sciences *11*, 595–621.

Hassan, M.A., Fuertes, M.M., Sánchez, F.J.R., Vicente, O., and Boscaiu, M. (2015). Effects of salt and water stress on plant growth and on accumulation of osmolytes and antioxidant compounds in cherry tomato. Notulae Botanicae Horti Agrobotanici Cluj-Napoca *43*, 1–11.

He, F., Mu, L., Yan, G.-L., Liang, N.-N., Pan, Q.-H., Wang, J., Reeves, M.J., and Duan, C.-Q. (2010). Biosynthesis of anthocyanins and their regulation in colored grapes. Molecules *15*, 9057–9091.

Higgins, C.F. (2007). Multiple molecular mechanisms for multidrug resistance transporters. Nature *446*, 749–757.

Horikoshi, S., and Serpone, N. (2013). Introduction to nanoparticles. In microwaves in nanoparticle synthesis, S. Horikoshi, and N. Serpone, eds. (Wiley-VCH Verlag GmbH & Co. KGaA), pp. 1–24.

Huang, H., Xiao, X., Ghadouani, A., Wu, J., Nie, Z., Peng, C., Xu, X., and Shi, J. (2015). Effects of natural flavonoids on photosynthetic activity and cell integrity in *Microcystis aeruginosa*. Toxins (Basel) *7*, 66–80.

Izaguirre, M.M., Scopel, A.L., Baldwin, I.T., and Ballaré, C.L. (2003). Convergent responses to stress. Solar ultraviolet-B radiation and *Manduca sexta* herbivory elicit overlapping transcriptional responses in field-grown plants of *Nicotiana longiflora*. Plant Physiol. *132*, 1755–1767.

Jabeen, E., Janjua, N.K., Ahmed, S., Murtaza, I., Ali, T., and Hameed, S. (2017). Radical scavenging propensity of Cu(2+), Fe(3+) complexes of flavonoids and in-vivo radical scavenging by Fe(3+)-primuletin. Spectrochim Acta A Mol Biomol Spectrosc *171*, 432–438.

Jasinski, M., Ducos, E., Martinoia, E., and Boutry, M. (2003). The ATP-binding cassette transporters: structure, function, and gene family comparison between rice and Arabidopsis. Plant Physiol. *131*, 1169–1177.

Jin, C.W., You, G.Y., He, Y.F., Tang, C., Wu, P., and Zheng, S.J. (2007). Iron deficiency-induced secretion of phenolics facilitates the reutilization of root apoplastic iron in Red Clover. Plant Physiol *144*, 278–285.

Jung, B., Ludewig, F., Schulz, A., Meißner, G., Wöstefeld, N., Flügge, U.-I., Pommerrenig, B., Wirsching, P., Sauer, N., Koch, W., et al. (2015). Identification of the transporter responsible for sucrose accumulation in sugar beet taproots. Nature Plants *1*, 14001.

Jurasekova, Z., Domingo, C., Garcia-Ramos, J.V., and Sanchez-Cortes, S. (2014). Effect of pH on the chemical modification of quercetin and structurally related flavonoids characterized by optical (UV-visible and Raman) spectroscopy. Phys Chem Chem Phys *16*, 12802–12811.

Kang, J., Park, J., Choi, H., Burla, B., Kretzschmar, T., Lee, Y., and Martinoia, E. (2011). Plant ABC Transporters. Arabidopsis Book *9*.

Kesharwani, J., Yoon, K.Y., Hwang, J., and Rai, M. (2009). Phytofabrication of silver nanoparticles by leaf extract of *Datura metel*: hypothetical mechanism involved in synthesis. Journal of Bionanoscience *3*, 39–44.

Klein, M., and Roos, W. (2009). Handling dangerous molecules: transport and compartmentation of plant natural products. In Plant-Derived Natural Products, A.E. Osbourn, and V. Lanzotti, eds. (Springer US), pp. 229–267.

Kumar, S., and Pandey, A.K. (2013). Chemistry and biological activities of flavonoids:

an overview. The Scientific World Journal *2013*, e162750.

Kutchan, T.M. (2005). A role for intra- and intercellular translocation in natural product biosynthesis. Current Opinion in Plant Biology *8*, 292–300.

Landi, M., Tattini, M., and Gould, K.S. (2015). Multiple functional roles of anthocyanins in plant-environment interactions. Environmental and Experimental Botany *119*, 4–17.

Lin, J.-K., and Weng, M.-S. (2006). Flavonoids as nutraceuticals. In The Science of Flavonoids, E. Grotewold, ed. (Springer New York), pp. 213–238.

Mahajan, M., Ahuja, P.S., and Yadav, S.K. (2011). Post-transcriptional silencing of flavonol synthase mRNA in tobacco leads to fruits with arrested seed set. PLOS ONE *6*, e28315.

Marais, J.P.J., Deavours, B., Dixon, R.A., and Ferreira, D. (2006). The stereochemistry of flavonoids. In The Science of Flavonoids, E. Grotewold, ed. (Springer New York), pp. 1–46.

Martinez, L., and Falson, P. (2014). Multidrug resistance ATP-binding cassette membrane transporters as targets for improving oropharyngeal candidiasis treatment. Advances in Cellular and Molecular Otolaryngology *2*.

Mellway, R.D., Tran, L.T., Prouse, M.B., Campbell, M.M., and Constabel, C.P. (2009). The wound-, pathogen-, and ultraviolet B-responsive MYB134 gene encodes an R2R3 MYB transcription factor that regulates proanthocyanidin synthesis in poplar. Plant Physiol *150*, 924–941.

Metz, K.M., Sanders, S.E., Miller, A.K., and French, K.R. (2014). Uptake and impact of silver nanoparticles on *Brassica rapa*: an environmental nanoscience laboratory sequence for a nonmajors course. J. Chem. Educ. *91*, 264–268.

Michalak, A. (2006). Phenolic compounds and their antioxidant activity in plants growing under heavy metal stress. Polish Journal of Environmental Studies *15*.

Mithöfer, A. (2002). Suppression of plant defence in rhizobia–legume symbiosis. Trends in Plant Science *7*, 440–444.

Mittal, A.K., Chisti, Y., and Banerjee, U.C. (2013). Synthesis of metallic nanoparticles using plant extracts. Biotechnology Advances *31*, 346–356.

Møller, I.M. (2001). Plant mitochondria and oxidative stress: Electron transport, NADPH turnover, and metabolism of reactive oxygen species. Annu. Rev. Plant Physiol. Plant Mol. Biol. 52, 561–591.

Mouradov, A., and Spangenberg, G. (2014). Flavonoids: a metabolic network mediating plants adaptation to their real estate. Front Plant Sci *5*, 620.

Nakabayashi, R., Mori, T., and Saito, K. (2014). Alternation of flavonoid accumulation under drought stress in *Arabidopsis thaliana*. Plant Signal Behav *9*, e29518.

Ng, J.L.P., Hassan, S., Truong, T.T., Hocart, C.H., Laffont, C., Frugier, F., and Mathesius, U. (2015). Flavonoids and auxin transport inhibitors rescue symbiotic nodulation in the *Medicago truncatula* cytokinin perception Mutant cre1. Plant Cell *27*, 2210–2226.

de Pascual-Teresa, S., Moreno, D.A., and García-Viguera, C. (2010). Flavanols and anthocyanins in cardiovascular health: a review of current evidence. Int J Mol Sci *11*, 1679–1703.

Pawlikowska-Pawlęga, B., Ignacy Gruszecki, W., Misiak, L., Paduch, R., Piersiak, T., Zarzyka, B., Pawelec, J., and Gawron, A. (2007). Modification of membranes by quercetin, a naturally occurring flavonoid, via its incorporation in the polar head group. Biochimica et Biophysica Acta (BBA) - Biomembranes *1768*, 2195–2204.

Peer, W.A., Brown, D.E., Tague, B.W., Muday, G.K., Taiz, L., and Murphy, A.S. (2001). Flavonoid accumulation patterns of transparent testa mutants of arabidopsis. Plant Physiol. *126*, 536–548.

Petrussa, E., Braidot, E., Zancani, M., Peresson, C., Bertolini, A., Patui, S., and Vianello, A. (2013). Plant flavonoids—biosynthesis, transport and involvement in stress responses. International Journal of Molecular Sciences *14*, 14950–14973.

Pinheiro, P.F., and Justino, G.C. (2012). Structural analysis of flavonoids and related compounds - A Review of Spectroscopic Applications.

Pollastri, S., and Tattini, M. (2011). Flavonols: old compounds for old roles. Ann. Bot. *108*, 1225–1233.

Poór, M., Zrínyi, Z., and Kőszegi, T. (2016). Structure related effects of flavonoid aglycones on cell cycle progression of HepG2 cells: Metabolic activation of fisetin and quercetin by catechol-O-methyltransferase (COMT). Biomed. Pharmacother. *83*, 998–1005.

Ramos, S., Goya, L., and Martín, M.A. Antioxidative stress actions of Cocoa in colonic cancer-Chapter 20. MyScienceWork.

Rausher, M.D. (2006). The evolution of flavonoids and their genes. In The Science of Flavonoids, E. Grotewold, ed. (Springer New York), pp. 175–211.

Razavi, M., Salahinejad, E., Fahmy, M., Yazdimamaghani, M., Vashaee, D., and Tayebi, L. (2015). Green chemical and biological synthesis of nanoparticles and their biomedical applications. In Green Processes for Nanotechnology, V.A. Basiuk, and E.V. Basiuk, eds. (Springer International Publishing), pp. 207–235.

Rea, P.A. (2007). Plant ATP-binding cassette transporters. Annu Rev Plant Biol *58*, 347–

375.

Remy, E., and Duque, P. (2014). Beyond cellular detoxification: a plethora of physiological roles for MDR transporter homologs in plants. Front Physiol *5*, 201.

Roytrakul, S., and Verpoorte, R. (2007). Role of vacuolar transporter proteins in plant secondary metabolism: *Catharanthus roseus* cell culture. Phytochem Rev *6*, 383–396.

Samanta, A., Das, G., and Das, S.K. (2011). Roles of flavonoids in plants. International Journal of Pharmaceutical Science and Technology *6*, 12–35.

Scalbert, A., Johnson, I.T., and Saltmarsh, M. (2005). Polyphenols: antioxidants and beyond. Am J Clin Nutr *81*, 215S–217S.

Selvaraj, S., Krishnaswamy, S., Devashya, V., Sethuraman, S., and Krishnan, U.M. (2014). Flavonoid-metal ion complexes: a novel class of therapeutic agents. Med Res Rev *34*, 677–702.

Singh, M., Kaur, M., and Silakari, O. (2014). Flavones: An important scaffold for medicinal chemistry. European Journal of Medicinal Chemistry *84*, 206–239.

Singh, O., Kaur, R., and Mahajan, R.K. (2016). Flavonoid-surfactant interactions: A detailed physicochemical study. Spectrochim Acta A Mol Biomol Spectrosc *170*, 77–88.

Spencer, J.P.E. (2009). Flavonoids and brain health: multiple effects underpinned by common mechanisms. Genes Nutr *4*, 243–250.

Srinivas, K., King, J.W., Howard, L.R., and Monrad, J.K. (2010). Solubility and solution thermodynamic properties of quercetin and quercetin dihydrate in subcritical water. Journal of Food Engineering *100*, 208–218.

Szakiel, A., and Janiszowska, W. (2002). The mechanism of oleanolic acid monoglycosides transport into vacuoles isolated from *Calendula officinalis* leaf protoplasts. Plant Physiology and Biochemistry *40*, 203–209.

Tarahovsky, Y.S., Kim, Y.A., Yagolnik, E.A., and Muzafarov, E.N. (2014). Flavonoid–membrane interactions: involvement of flavonoid–metal complexes in raft signaling. Biochimica et Biophysica Acta (BBA) - Biomembranes *1838*, 1235–1246.

Thul, S.T., and Sarangi, B.K. (2015). Implications of nanotechnology on plant productivity and its rhizospheric environment. In Nanotechnology and Plant Sciences, M.H. Siddiqui, M.H. Al-Whaibi, and F. Mohammad, eds. (Springer International Publishing), pp. 37–53.

Tian, X.-J., Yang, X.-W., Yang, X., and Wang, K. (2009). Studies of intestinal permeability of 36 flavonoids using Caco-2 cell monolayer model. Int J Pharm *367*, 58–64.

Tiwari, M., Sharma, D., Singh, M., Tripathi, R.D., and Trivedi, P.K. (2014). Expression of OsMATE1 and OsMATE2 alters development, stress responses and pathogen susceptibility in Arabidopsis. Scientific Reports *4*, 3964.

Trantas, E.A., Koffas, M.A.G., Xu, P., and Ververidis, F. (2015). When plants produce not enough or at all: metabolic engineering of flavonoids in microbial hosts. Front. Plant Sci. *6*.

Tsimogiannis, D.I., and Oreopoulou, V. (2006). The contribution of flavonoid C-ring on the DPPH free radical scavenging efficiency. A kinetic approach for the 3′,4′-hydroxy substituted members. Innovative Food Science & Emerging Technologies *7*, 140–146.

Vachali, P.P., Li, B., Besch, B.M., and Bernstein, P.S. (2016). Protein-flavonoid interaction studies by a Taylor dispersion Surface Plasmon Resonance (SPR) technique: A Novel Method to Assess Biomolecular Interactions. Biosensors (Basel) *6*.

Valle, D., C, J., Buide, M.L., Casimiro-Soriguer, I., Whittall, J.B., and Narbona, E. (2015). On flavonoid accumulation in different plant parts: variation patterns among individuals and populations in the shore campion (Silene littorea). Front. Plant Sci. *6*.

Watkins, J.M., Hechler, P.J., and Muday, G.K. (2014). Ethylene-induced flavonol accumulation in guard cells suppresses reactive oxygen species and moderates stomatal aperture. Plant Physiol. *164*, 1707–1717.

Willenbrink, J., and Doll, S. (1979). Characteristics of the sucrose uptake system of vacuoles isolated from red beet tissue. Kinetics and specifity of the sucrose uptake system. Planta *147*, 159–162.

Yamane, H. (2013). Biosynthesis of phytoalexins and regulatory mechanisms of it in rice. Biosci. Biotechnol. Biochem. *77*, 1141–1148.

Yazaki, K., Sugiyama, A., Morita, M., and Shitan, N. (2008). Secondary transport as an efficient membrane transport mechanism for plant secondary metabolites. Phytochem Rev *7*, 513–524.

Yuan, Y., Liu, Y., Wu, C., Chen, S., Wang, Z., Yang, Z., Qin, S., and Huang, L. (2012). Water deficit affected flavonoid accumulation by regulating hormone metabolism in *Scutellaria baicalensis* georgi roots. PLOS ONE *7*, e42946.

Zhao, J. (2015). Flavonoid transport mechanisms: how to go, and with whom. Trends in Plant Science *20*, 576–585.

Zhao, J., and Dixon, R.A. (2010). The “ins” and “outs” of flavonoid transport. Trends Plant Sci. *15*, 72–80.

POSTER PRESENTATIONS

JOINT CONGRESS SIBV - SIGA
8-11 SEPTEMBER 2015
MILANO
University of Milano

Flavonoid uptake across plant membranes: cheap and fast *in vivo* assay

Antonio Filippi, Elisa Petrussa, Carlo Peresson, Alberto Bertolini, Angelo Vianello and Enrico Braidot

ABSTRACT

Flavonoids have attracted a growing and motivated interest, due to their strong ability to face the oxidative stresses in plants and humans. Unfortunately, their subcellular transport and accumulation within cells and tissues still remain unclear. Here we suggest an assay able to **follow *in vivo* the transport of the flavonoid quercetin**, using diphenylboric acid 2-aminoethyl ester (DPBA), as fluorescent probe in not-pigmented *Vitis vinifera* cell cultures and *Pisum sativum* stem microsomes.

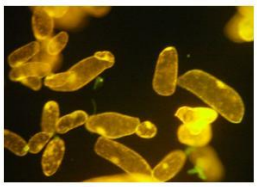

Fig.1 Grapevine cell image under fluorescent light

INTRODUCTION

Flavonoids are plant polyphenolic secondary metabolites with a common three ring structure, playing a large number of essential physiological functions. Such diversified flavonoid roles rely on a finely-regulated transport and subcellular accumulation systems, involving several pathways. Due to the complexity of the phenomenon, a comprehensive view has not yet proposed. Up to date only time-consuming chromatographic or expensive radioactive methodologies has been used. Quercetin (QC) has been used as model molecule for flavonoid transport. Like most of the flavonoids, QC is poorly fluorescent in aqueous solutions, but exhibits an increased fluorescence if bound to specific probes such as DPBA, an esterified moiety commonly used in microscopic analysis.

RESULTS AND DISCUSSION

V. vinifera suspension cells (NPC) and *P. sativum* stem microsomes were loaded with 0.05% and 0.0001% DPBA (w/v), respectively, and then different QC concentrations were added. After a washing step, used to discard the excess of probe, cells showed a rising rate of fluorescence, due to the increasing ($\Delta F \bullet s^{-1}$) of the given QC concentrations (Fig. 1). The fluorescence inside protoplasts was measured by spectrofluorimetric analysis (Fig. 2).

To verify if the complex DPBA/QC was unspecifically bound to outer cell components and could be released by cells, NPC incubated with DPBA and QC, was then treated with 0.3% SDS (Fig. 3). Blue trace shows that the addition of QC determined an increase of fluorescence, which was reversed by the subsequent addition of SDS.

In agreement, the uptake was prevented if the vesicles were pre-treated with SDS (green trace).

The presence of QC within the cells was assessed quantifying it by DPBA in cell methanolic extracts (Fig. 4). Different typologies of QC transport across membranes were characterized in *P. sativum* microsomes, by using a concentration of 100 nM QC (Fig. 5), where the difference between blue vs red and red vs green columns defines secondary and primary transport, respectively. Green column is representative of passive uptake.

AIM, OBJECTIVE AND INNOVATION

Up to date, spectrophotometric and fluorimetric methodologies dealing with flavonoid transport *in vivo* face difficulties: time-consuming HPLC analysis, flavonoid instability at different pH, high costs and problems of management of the radioactive labelling.

For this reason, this method, based on flavonoid detection by means of DPBA-binding, may be a new tool useful to follow *in vivo* flavonoid accumulation into plant cells.

The fluorimetric method here proposed allows to follow and **characterize biochemical parameters of flavonoid transport into plant cells**, mediated by membrane carriers. This **protocol** appears to be **reliable, stable** during long-lasting experiments, allowing an **easy-to-use**, **cheap** and **fast** and moreover **direct** evaluation of flavonoid accumulation process.

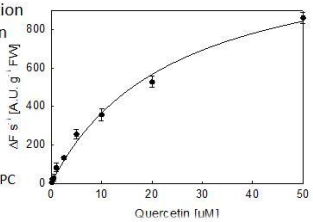

Fig.2 *In vivo* QC uptake in NPC

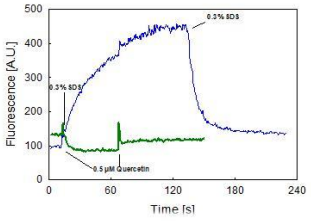

Fig.3 Spectrofluorimetric analysis of DPBA/QC movement in NPC

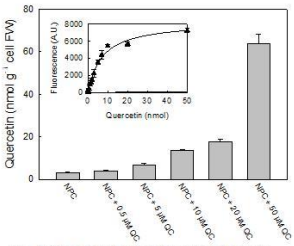

Fig.4 QC determination in cell methanolic extracts of NPC

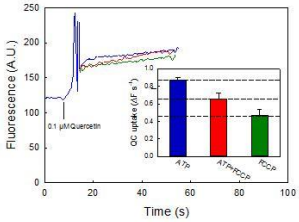

Fig. 5. Transport characterization of 100 nM of QC in *P. sativum* stem microsomes.

dott. Antonio Filippi antoniofilippi@yahoo.it
Info:
Tel. +39 0432 558767

References

J. H. Lee, Y. Kim, M. H. Hoang, H. Jun, S. Lee. Rapid quantification of cellular flavonoid levels using quercetin and a fluorescent diphenylboric acid 2-amino ethyl ester probe. *Food Science and Biotechnology*, Volume 23, Issue 1, pp 75-79, 2014.

UNIVERSITÀ DEGLI STUDI DI UDINE
DEPARTMENT OF AGRICULTURAL AND ENVIRONMENTAL SCIENCES
PhD school «Agricultural Science and Biotechnology»

Flavonoid interaction with grape chitinase: natural and innovative plant defense inductors

Antonio Filippi[1], Elisa Petrussa[1], Sabina Passamonti[2], Andrea Scaloni[3], Vladka Čurin Šerbec[4], Uroš Rajčević[4] and Enrico Braidot[1]

[1] Dipartimento di Scienze Agro-Alimentarie, Ambientali e Animali, Università di Udine, Via delle Scienze 91, 33100 Udine, Italy. [2] Dipartimento di Scienze della Vita, Università di Trieste, via L. Giorgieri 1, 34127 Trieste, Italy. [3] Istituto per il sistema produzione animale in ambiente Mediterraneo, CNR, Via Argine, 1085 - 80147 Napoli, Italy. [4]Blood Transfusion Centre of Slovenia, Zavod RS za transfuzijsko medicino, Šlajmerjeva 6, 1000 Ljubljana, Slovenia

INTRODUCTION

Due to their extensive cultivation, **grapevine** (*Vitis vinifera* L.) varieties are **sensitive to a great number of pathogens**. These infections provoke heavy damages and yield losses, finally affecting wine quality. The spread of diseases is generally controlled by applications of **chemical pesticides**. This controversial use/abuse of pesticides has recently been questioned, particularly in the framework of a more sustainable management of the agricultural practice, that takes in account of the evident climate changes. Then particular attention has been payed on the pesticide use reduction, in favour of the **plant defence system induction**, using natural moieties.

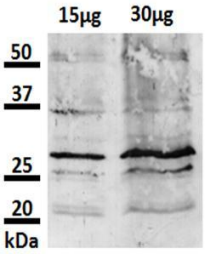

Figure 1. Western blotting of proteins from microsomial skin proteins (MSP) revealing candidates for anti-peptide Ab interaction. Western blotting was performed on Merlot MSP using mouse anti-BTL sequence Ab at the concentration of 5 µg ml^{-1}. Anti-mouse IgM (dilution 1:15,000) was used as secondary antibody. The JACK antibody reviled the presence of at least 5 bands. The most visible ▸bands were localized around 25 kDa.

Figure 2. Immunochemical analysis of grape MSP with a molecular mass in the25-27 kDa range. MP with an apparent mass 25-27 kDa (Fig. 1) was extracted from SDS-PAGE and subjected to 2-D electrophoresis. The "trains" of spots showing immunoreactive signals with anti-BTL Ab were matched to counterparts in the silver-stained gel. Spots of interest were subjected to MS analysis that revealed the presence of:
class IV chitinase : A
glucan endo-1,3-beta-glucosidase : B
triosephosphate isomerase and vicilin-like antimicrobial peptides 2-3 : C

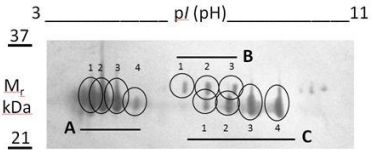

RESULTS

In the present study, an anti-bilitranslocase antibody (anti-BTL Ab), previously used to recognize proteins interacting with flavonoid, cross-reacted with MSP, obtained from red grape berry skin. 2-DE electrophoresis and mass-spectrometry analysis of the most abundant band at 25-27 kDa (Fig.1) unequivocally identified 3 **pathogenesis-related (PR) proteins** (A, B and C in Fig.2). The activity of one of these enzymes, **IV class chitinase**, was assessed. Interestingly, the *in vitro* chitinolytic activity, measured by both spectrophotometric and fluorimetric assays, was **modulated by** two different flavonoids: **quercetin** (QC: flavonol) and **catechin** (CA: flavanol) (Fig.3), in both commercial pure chitinase (from *S. griseus*) and grape microsomal extract. The antibody itself was able to inhibit the chitinolytic activity in a close experiment (Fig.4).

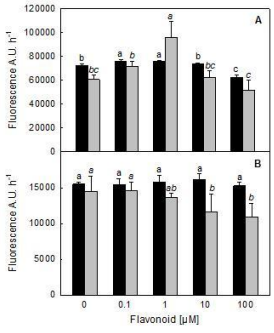

Figure 3. QC and CA modulation of the chitinase activity of *S. griseus* and grape MSP enzyme. Chitinolytic activity was measured with spectrophotometric assay on pure chitinase (panel A) and MSP extract (panel B). Different concentrations of CA (black bars) and QC (grey bars) were tested.
In both cases, a sort of hormetic curve was observed thus indicating that flavonoids may actually act as modulators, rather than mere inhibitors.

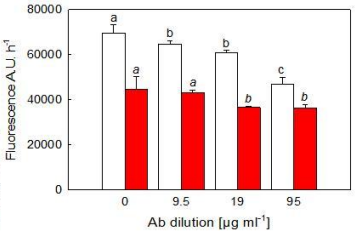

Figure 4. Inhibition of the chitinase activity of *S. griseus* and RGSM chitinase by anti-peptide Ab. Chitinolytic activity was measured by a spectrophotometric assay. 0.2 µg µl^{-1} of *S. griseus* chitinase (white bars) and 30 µg of grape MP (red bars) were assayed in the presence of increasing concentrations of anti-BTL Ab.

CONCLUSION / INNOVATIVES

These results highlighted the role of flavonoids not only as antioxidants or direct anti-microbial effectors, but also as modulators of plant growth and plant response to biotic stress. Further fallouts of the present work also lie in the possibility to reduce pesticide distribution by modulating PR protein-mediated resistance of grapevine by controlling flavonoid concentration in the fruit. So the present work leads in a better **environment protection**, by means of a reduction of pesticide distribution, and a consequent **reduction of pollution**.

dott. Antonio Filippi antoniofilippi@yahoo.it
Info: Tel. +39 0432 558767

References

Robinson, SP, AK Jacobs, IB Dry 1997. *A class iv chitinase is highly expressed in grape berries during ripening*. Plant Physiology 114: 771-778.
Kumar, S, AK Pandey 2013 Chemistry and biological activities of flavonoids: An overview Scientific World Journal.

UNIVERSITÀ DEGLI STUDI DI UDINE
DEPARTMENT OF AGRICULTURAL AND ENVIRONMENTAL SCIENCES
PhD school «Agricultural Science and Biotechnology»

Flavonoid (quercetin) facilitated/passive transport:

characterization by a DPBA-dependent uptake in microsomes

Antonio Filippi[1], Elisa Petrussa[1], Marco Zancani[1], Valentino Casolo[1], Valentina De Col[1], Francesco Boscutti[1] and Enrico Braidot[1]

[1] Dipartimento di Scienze Agrarolimentari, Ambientali ed Ambientali, Università di Udine, Via delle Scienze 91, 33100 Udine, Italy.

INTRODUCTION

Flavonoids consist of a large group of hydroxylated phenolic substances, ubiquitously present in plants, synthesized on the cytosolic side of endoplasmic reticulum. To fulfil their biological roles, flavonoid biosynthesis and storage in different compartments require an efficient membrane transport. In addition to the well-known mechanisms of primary and secondary transporters (e.g. ABCC1 and MATE) and vesicle-mediated traffic, a new hypothesis has been recently raised to explain the flavonoid accumulation pathways. The proposed process involves the facilitated/passive transport, which has not been hitherto deeply investigated from a physiological point of view.

MATERIALS AND METHODS

Pisum sativum stem microsomal vesicles (PSMV) were used as starting material for the characterization of membrane protein-mediated transport. The resuspension and assay buffer was 20 mM MES/KOH, 5 mM DTE, 0.25 M sucrose pH 5.5. The kinetics were performed by fluorimetric analysis using reading setup at 461 nm (EX) and 520 nm (EM). The methanolic extraction was performed in methanol at 66% in assay buffer. Samples were analyzed at Victor multilabel plate reader (EX filter at 485 nm; EM filter at 535 nm).

RESULTS

Transport into PSMV was analysed using different quercetin (QC) concentrations, by the fluorescence increase due to the 2-aminoethoxydiphenyl borate (DPBA)/QC complex formation (Fig. 1). The contribution of passive QC uptake was obtained and the passive transport was further characterized in the presence of different modulators (Tab. 1) and then confirmed by spectrofluorimetric determination of amounts of transported QC recovered in methanolic extracts (Fig. 2).

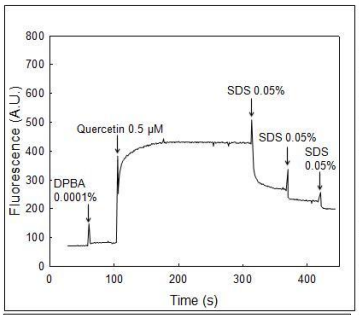

Fig. 1 Scheme of a fluorimetric kinetic of QC transport within *P. sativum* PSMV.

Treatment	Initial speed rate (Fluorescence A.U. mg*s^{-1})	Modulation (%)
CTRL	54,95 ± 14,28	100
DTE 5 mM	91,90 ± 11,41	167
pCMPS		
25 µM	53,34 ± 9,92	97
100 µM	25,81 ± 5,80	47
250 µM	4,06 ± 4,94	7
Phloretin		
8 µM	20,12 ± 3,58	37
32 µM	8,71 ± 7,00	16
80µM	2,70 ± 1,58	5
NEM		
0.1 µM	54,48 ± 12,26	99
1 µM	60,01 ± 11,72	109
10 µM	69,52 ± 13,31	126
40 µM	65,78 ± 10,24	119
DIAMIDE	NO SIGNIFICANT EFFECT	
DIDS	NO SIGNIFICANT EFFECT	

Tab. 1 Effect of passive transport and thiol-interacting modulators on initial speed rate of QC transport inside vesicles.

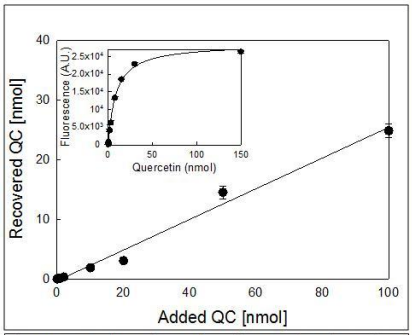

Fig. 2 Recovered QC after methanolic extraction of *P. sativum* PSMV.

CONCLUSION / INNOVATIVES

With the present work, we tried to characterize the involvement of the facilitated/passive transport of QC across microsomal membranes of *P. sativum*, using a new approach based on DPBA fluorescence. The data show that it is possible to follow the passive loading of QC inside the PSMV, as fluorescence increase of the complex DPBA/QC. The QC amount retrievable after extraction is proportional to the added flavonoid during the fluorimetric kinetic assay. Such a transport seems to be dependent on the redox poise of the environment, since the addition of the reducing agent (DTE) to the buffer enhanced transport speed rate, while the sulphidryl modifying agent (pCMPS) exerted an opposite effect.

The presented protocol is a cheap and easy-to-use method and is applicable to flavonoid passive transport studies, where its reliability is validated.

These results are promising in the framework of direct measurements of flavonoid transport, but further investigation is needed for assessing the method in the case of different experimental conditions.

dott. Antonio Filippi antoniofilippi@yahoo.it
Info: Tel. +39 0432 558767

References

Filippi, A., Petrussa, E., Peresson, C., Bertolini, A., Vianello, A., Braidot, E., In vivo assay to monitor flavonoid uptake across plant cell membranes, FEBS Open Bio (2015). doi:http://dx.doi.org/10.1016/j.fob.2015.08.009

UNIVERSITÀ DEGLI STUDI DI UDINE

DEPARTMENT OF AGRICULTURAL, FOOD, ENVIRONMENTAL AND ANIMAL SCIENCES

PhD school «Agricultural Science and Biotechnology»

Green synthesis of Ag nanoparticles using plant metabolites

Nano Innovation 2016 Rome, 20-23 September Conference & Exhibition

FILIPPI A., MATTIELLO A., MUSETTI R., MARCHIOL L., BRAIDOT E.
DI4A - Department of Agriculture, Food, Environment and Animal Sciences, UNIVERSITY OF UDINE

Rationale

Nanotechnology is an emerging and rapidly growing field whose dynamics and prospects pose many great challenges to scientists and engineers. In alternative to the dangerous chemical synthesis, recently scientists contributed to the development of a relatively new and largely unexplored area of research based on the green biosynthesis of nanomaterials and nanoparticles (NPs) (Mittal et al., 2013). The control over NPs size, shape, and morphology, combined with mild conditions of processing parameters (mainly in terms of temperature and pressure), is important for sustainable and cost-effective production of functional NPs (Peralta-Videa et al., 2016). Hundreds of different plant extracts have been tested to carry on this green synthesis of NPs but it is still not well known what could be the role of different single plant moieties. It has been demonstrated that various water-soluble plant metabolites (e.g., alkaloids, phenolic compounds, quinones, organic acids, and terpenoids), and co-enzymes could promote the reduction of metal ions and some studies indicated that these molecules play a role in NPs capping too (Mohammadinejad et al., 2016). At the University of Udine DI4A department, studies are underway with the aim to synthesize silver nanoparticles (AgNPs) using single secondary metabolites (e.g. quercetin and tannins).

Quercetin (QC) (Fig. 1) is a widely distributed natural flavonoid, found in many fruits, leaves and grains. It plays lots of physiological and chemical functions in plants like antioxidant agent, UV scavenger and metal chelator. Tannin (TA) (Fig. 1) is an astringent, polyphenolic molecule widely distributed in many species of plants. Thanks to their chemical structure, they play a role in protection from predation and in plant growth regulation. In addition, their strong antioxidant properties make these molecules the best candidates for metal reduction.

Experimental Design

Here are displayed the preliminary data obtained by using quercetin (QC) or tannin (TA) like reducing agents at the final concentration 1 mM and by changing the pH of the buffer (10 mM MOPS/KOH or Borax). After the addition of the silver nitrate ($AgNO_3$) at the final concentration of 25 µM the solutions were analyzed by spectrophotometer in order to check the appearance of the peak of absorbance caused by plasmon resonance, indicating AgNPs formation, and subsequently by ICP-MS to evaluate their size distribution (Fig.1).

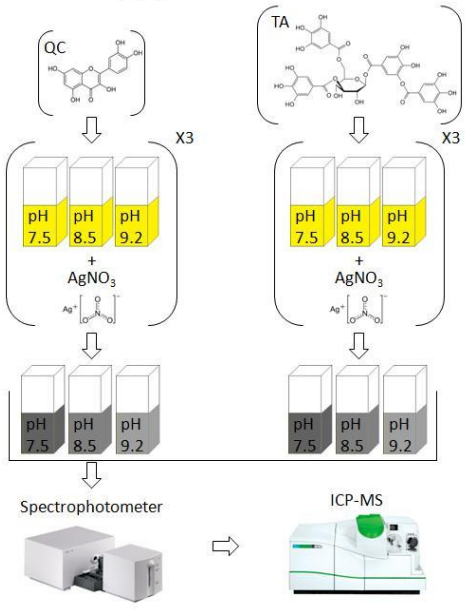

Figure 1 - Representative scheme of the methodology used to synthesize AgNPs.

Results and conclusion

The results obtained by the spectrophotometer of both the reducing agents at different pH are not displayed but all the curves obtained have an absorbance peak near to 420 nm which is typical for the AgNPs. The ICP analysis shows (Fig. 2):

1. NPs with smaller diameter at pH 9.2 using both TA and QC;
2. The amount of NPs is inversely proportional to the increasing pH values;
3. QC seems to be a better reducing agent with respect to TA.

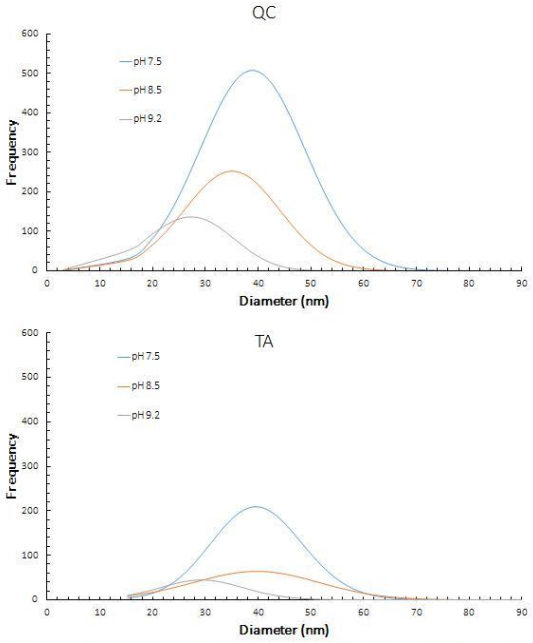

Figure 2 – Average size distribution (n=3) obtained from ICP-MS analysis of the samples at different pH (7.5, 8.5 and 9.2) and with different reducing agents (TA and QC)

References

- Mittal AK, et al, 2013. Biotechnol Adv, 31, 346-56.
- Mohammadinejad R., et al. 2016. Green Chem, 18, 20-52.
- Peralta-Videa JR et al. 2016. Nanotechnol Environ Eng, 1, 4

Corresponding Author

Prof. Luca Marchiol
0432.558611; marchiol@uniud.it
orcid.org/0000-0001-7426-1201
Scopus Author ID 6603644490

APPENDIX 1

Involvement of mammalian bilitranslocase-like protein(s) in chlorophyll catabolism of *Pisum sativum* L. tissues

J Bioenerg Biomembr (2014) 46:109–117
DOI 10.1007/s10863-014-9539-y

Involvement of mammalian bilitranslocase-like protein(s) in chlorophyll catabolism of *Pisum sativum* L. tissues

Carlo Peresson · Elisa Petrussa · Antonio Filippi · Federica Tramer · Sabina Passamonti · Uros Rajcevic · Sendi Montanič · Michela Terdoslavich · Vladka Čurin Šerbec · Angelo Vianello · Enrico Braidot

Received: 7 November 2013 / Accepted: 16 January 2014 / Published online: 9 February 2014

Abstract Putative pea bilin and cyclic tetrapyrrole transporter proteins were identified by means of an antibody raised against a bilirubin-interacting aminoacidic sequence of mammalian bilitranslocase (TC No. 2.A.65.1.1). The immunochemical approach showed the presence of several proteins mostly in leaf microsomal, chloroplast and tonoplast vesicles. In these membrane fractions, electrogenic bromosulfalein transport activity was also monitored, being specifically inhibited by anti-bilitranslocase sequence antibody. Moreover, the inhibition of transport activity in pea leaf chloroplast vesicles, by both the synthetic cyclic tetrapyrrole chlorophyllin and the heme catabolite biliverdin, supports the involvement of some of these proteins in the transport of linear/cyclic tetrapyrroles during chlorophyll metabolism. Immunochemical localization in chloroplast sub-compartments revealed that these putative bilitranslocase-like transporters are restricted to the thylakoids only, suggesting their preferential implication in the uptake of cyclic tetrapyrrolic intermediates from the stroma during chlorophyll biosynthesis. Finally, the presence of a conserved bilin-binding sequence in different proteins (enzymes and transporters) from divergent species is discussed in an evolutionary context.

Keywords Chlorophyll metabolism · Bilitranslocase · Leaf · *Pisum sativum* · Bilin transport · Stem

Abbreviations

Ab	Antibody
ABC	ATP-binding cassette
BSP	Bromosulfalein
BTL	Bilitranslocase
Chl	Chlorophyll
MRP	Multidrug resistance-associated protein
MV	Microsomal vesicles
PM	Plasma membrane

Introduction

Land plants possess three major cyclic tetrapyrroles (chlorophyll, heme and siroheme), representing co-factors for essential proteins (photosystem complexes, cytochromes, hemoglobins, nitrite and sulfite reductase, nitrogenase), as well as a linear tetrapyrrole (phytochromobilin in phytochrome) (Vavilin and Vermaas 2002; Mochizuki et al. 2010). Their synthesis takes place almost exclusively in chloroplasts, starting from 5-aminolevulinic acid via a common branched pathway (Vavilin and Vermaas 2002; Mochizuki et al. 2010).

Among these pyrroles, chlorophyll (Chl) is an essential metabolite for light energy capturing in the main photosynthetic organisms (cyanobacteria, algae and land plants). Chl

Electronic supplementary material The online version of this article (doi:10.1007/s10863-014-9539-y) contains supplementary material, which is available to authorized users.

C. Peresson · E. Petrussa · A. Filippi · A. Vianello · E. Braidot (✉)
Department of Agricultural and Environmental Sciences, Section of Plant Biology, University of Udine, Via delle Scienze 91, 33100 Udine, Italy
e-mail: enrico.braidot@uniud.it

F. Tramer · S. Passamonti
Department of Life Sciences, University of Trieste, via Giorgeri 1, 34127 Trieste, Italy

U. Rajcevic · S. Montanič · M. Terdoslavich · V. Čurin Šerbec
Blood Transfusion Centre of Slovenia, Šlajmerjeva 6, 1000 Ljubljana, Slovenia

biosynthesis, similarly to those of siroheme and heme, initially occurs in the stroma. Only Chl biosynthesis pathway, branching off the formation of protoporphyrinogen IX, continues in both envelope and thylakoids, while the last step of phytol esterification is confined to the thylakoid (Mochizuki et al. 2010; Joyard et al. 2009). The pathway of Chl breakdown, similarly to heme degradation in plants and animals, involves the oxidative cleavage of porphinoid macrocyclic ring (Mochizuki et al. 2010; Kräutler and Hörtensteiner 2006). In land plants this pathway leads to the formation of red pigment (linear fluorescent bilin) intermediates and then to accumulation of the final products of Chl breakdown, identified as colourless linear tetrapyrroles, called "non-fluorescent" chlorophyll catabolites (Kräutler and Hörtensteiner 2006). Differently from land plants, in green algae only linear red pigments, as Chl degradation end-metabolites, are produced (Kräutler and Hörtensteiner 2006; Engel et al. 1991). Chl degradation becomes an essential mechanism for recycling of nitrogen resources and for some developmental processes (e.g. fruit ripening and senescence), since it allows protection against potentially phototoxic Chl intermediates and catabolites (Hörtensteiner and Kräutler 2011). Significantly, the expression of many Chl catabolism-related genes is induced in response to several biotic and abiotic stresses, or during cell death events (Hörtensteiner and Kräutler 2011).

Chl catabolism implicates that its degradation products are exported from the chloroplast and imported into the vacuole of mesophyll cells, as in other detoxification processes (Hörtensteiner and Kräutler 2011; Matile et al. 1996, 1999). Catabolite transport through these membranes has been demonstrated to occur by so far unidentified active membrane transporters (Hörtensteiner and Kräutler 2011). Tonoplast transporters so far identified belong to the ATP-binding cassette (ABC) subfamily (Hinder et al. 1996; Lu et al. 1998; Tommasini et al. 1998). An example is represented by a multidrug resistance-associated transporter (AtMRP2) (Frelet-Barrand et al. 2008).

Cyclic tetrapyrroles also need to be transported through plastid membrane for their export to other subcellular compartments (Mochizuki et al. 2010). At present, scarce information is available regarding transport mechanism(s) of tetrapyrroles in plants (Mochizuki et al. 2010), except for the candidate of heme transporter, named *Arabidopsis* tryptophan-rich sensory protein (TSPO), a homologue of the protoporphyrin-binding mammalian benzodiazepine receptor (Lindemann et al. 2004; Vanhee et al. 2011). In addition, ABC subfamily transporters could also accomplish heme and porphyrin transport across chloroplast membrane, similarly to what reported for Chl catabolite (Mochizuki et al. 2010).

In mammalian systems, one of the major candidates for the hepatic uptake of heme catabolites (tetrapyrrolic biliverdin and bilirubin) from the blood is a plasma membrane anion carrier, named bilitranslocase (BTL, TC No. 2.A.65.1.1) (Passamonti et al. 2005a). This transporter is also expressed in the vascular endothelium, as well as in gastrointestinal (absorptive), hepatic and renal (excretory) epithelia (Maestro et al. 2010; Ziberna et al. 2012; Passamonti et al. 2009). Other BTL substrates are flavonoids (i.e. anthocyanins (Karawajczyk et al. 2007)) and nucleotides (Zuperl et al. 2011). Thus, mammalian BTL may function as a dietary flavonoid transporter in vascular endothelium cells (Maestro et al. 2010). In addition, BTL-like proteins have been identified by immunological and enzymatic studies in different membrane vesicles of plant organs (e.g., carnation petals, grape berries (Passamonti et al. 2005b, 2009; Braidot et al. 2008; Bertolini et al. 2009)), where they are hypothesized to be involved in intracellular membrane transport of flavonoids.

This study aimed at investigating the occurrence of BTL-like proteins in pea (*Pisum sativum*) seedlings, a particular developmental stage where chlorophyll synthesis and turnover could be rapidly induced after illumination. For this reason, pea seedlings represent a useful model to study heterotrophic tissues (dark grown) in comparison to autotrophic tissues (light grown). Immunological approach using a monoclonal antibody raised against a segment of rat liver BTL polypeptide was performed. The main result showed the presence of these transporters in pea photosynthesizing organs. In detail, BTL-like proteins were found both in chloroplast and tonoplast membranes of pea leaf, suggesting their putative involvement in Chl metabolism, as carriers of some cyclic tetrapyrrole intermediates or bilin catabolites, respectively.

Materials and methods

Plant material and chemicals

Etiolated pea (*Pisum sativum* L. cv. Alaska, Pioneer) stems (70 g fresh weight) were obtained by growing seedlings on sand for 7 days, in the dark, at 25 °C and 60 % relative humidity. Green pea stems (70 g fresh weight) were obtained by growing pea seedlings for 7 days, in the light (8 h continuous cycles), at 25 °C and 60 % relative humidity. Pea leaves (30 g fresh weight) were obtained by growing pea seedlings for 14 days, in the light (8 h continuous cycles).

Unless otherwise specified, reagents were purchased from Sigma-Aldrich.

Isolation of microsomal vesicles from pea stem and leaf

Microsomal vesicles (MV) from pea stem and leaf were isolated by homogenization in 190 ml of 0.25 M sucrose, 20 mM HEPES-Tris pH (7.6), 5 mM Na-EDTA, 1 mM DTE, 1 mM PMSF, 0.6 % PVPP and 0.3 % BSA at 4 °C with

a mortar and pestle and filtered through 100 μm nylon gauze. The homogenate was centrifuged at 2 800×*g* for 5 min in a Sorvall RC-5B centrifuge (SS-34 rotor) and the supernatant was subsequently centrifuged at 18 000×*g* for 12 min. The supernatant was collected and ultracentrifuged at 120 000×*g* for 36 min in Beckman L7-55 ultracentrifuge (Ty 70ti rotor, Fullerton, CA, USA). The pellet was further washed in 100 ml of 0.25 M sucrose, 20 mM HEPES-Tris (pH 7.0) and finally resuspended in 0.5 ml of the above buffer at a final protein concentration of 3–5 mg ml^{-1} and stored at −20 °C. Protein concentration was determined by the method of Bradford (Bradford 1976), using bovine serum albumin as the standard.

Isolation of chloroplast vesicles from pea leaf

Chloroplasts from pea leaf were isolated by centrifuging the homogenate at 200×*g* for 5 min in a Sorvall RC-5B centrifuge (SS-34 rotor) and subsequently the supernatant at 1 800×*g* for 5 min. The pellet, containing chloroplasts, was resuspended in 50 ml of 0.25 M sucrose, 20 mM HEPES-Tris (pH 7.0) and sonically irradiated (100 W, 30 s) in an ice bath by a Braun Labsonic 1510 Ultrasound generator (Melsungen AG, Germany). The suspension was finally ultracentrifuged at 120 000×*g* for 1 h in a Beckman L7-55 ultracentrifuge (Ty 70ti rotor, Fullerton, CA, USA). The pellet (chloroplast vesicles) was finally resuspended in 0.5 ml of the above buffer at a final protein concentration of 2–3 mg ml^{-1} and stored at −20 °C.

Purification of plasma membrane and tonoplast vesicles from pea leaf

Plasma membrane (PM) and tonoplast vesicles were isolated as described in Passamonti et al. (2005b), except that the 13 g two-phase system contained 6.7 % (w/w) Dextran T500 and 6.4 % (w/w) PEG3350.

Purification of pea leaf thylakoid and envelope membranes

Thylakoids and envelope membranes from chloroplast were isolated from pea leaf as described in (Gualberto et al. 1995) with minor modifications: grinding buffer used was 50 mM Hepes-KOH (pH 7.3), 0.33 M Sucrose and 2 mM EDTA.

Marker assays of different membrane fractions

ATPase activities (vanadate-sensitive, marker of PM enzyme; bafilomycin A_1-sensitive, marker of tonoplast enzyme; oligomycin-sensitive, marker of mitochondrial enzyme) were assayed as described in (Passamonti et al. 2005b). Chl (marker for chloroplast membrane) was extracted in acetone and detected by a diode spectrophotometer 8453 (Agilent, Santa Clara, CA, USA) at 663 and 646 nm, respectively. The total Chl content was determined according to the equations:

$$\mathrm{Chl}\,a\,(\mathrm{mg\,ml^{-1}}) = [12.21(A_{663})–2.81(A_{646})]$$
$$\mathrm{Chl}\,b\,(\mathrm{mg\,ml^{-1}}) = [20.13(A_{646})–5.03(A_{663})]$$

and converted to μg Chl mg^{-1} protein (Wellburn 1994).

Western blotting

Membrane proteins (30 μg) were separated by SDS-PAGE in 12 % polyacrylamide gel under reducing conditions as described in Passamonti et al. (2005b), with minor modifications: the samples were denatured at 80 °C. Immunoblotting was also performed, as described in Passamonti et al. (2005b), using the monoclonal purified antibody (Ab) at a concentration of 0.32 μg IgM ml^{-1}. Primary Ab MAP 2A8 was prepared by fusion of spleen lymphocytes with mouse myeloma NS1 cells using hybridoma technology. Mice were immunized with a multi-antigen peptide corresponding to segment 65–75 (EDSQGQHLSSF) of predicted primary structure of the bilitranslocase protein (Battiston et al. 1998). In a sequence of cell fusion, subcloning, immune- and functional tests, a specific monoclonal Ab MAP 2A8 was obtained. The immune reaction was detected by the activity of the alkaline phosphatase, conjugated to anti-mouse IgG Ab (1:30,000) developed in rabbit and able to also recognize IgM, as certified by the manufacturer SIGMA. Equivalent amounts of purified monoclonal Ab of the same isotype against blood group antigen B were used as negative controls.

Electrogenic bromosulfalein transport assay

Bromosulfalein (BSP) electrogenic transport assay was performed in pea subcellular fractions (20 μg of total protein) as previously described (Bertolini et al. 2009; Passamonti et al. 2010). Inhibition of the electrogenic BSP uptake by the anti-BTL Ab was examined after preincubation of pea leaf MV and chloroplast vesicles with increasing concentrations of the Ab (0.5–3 μg) at 25 °C for 5 min. Inhibition of the electrogenic BSP uptake was also examined in chloroplast vesicles by adding 50 μM of the porphyrin chlorophyllin and the bilin biliverdin to the assay medium.

Statistics

Data on electrogenic BSP transport are provided as mean ± S.D. of at least three independent plant extracts. Immunoblotting results are representative of at least three independent plant extracts.

Results

In order to identify BTL-like proteins in various pea organs and cell organelles, different membrane fractions were obtained from pea stems and leaves.

Expression of the BTL-like protein(s) in dark- and light-grown pea stem and leaf microsomal vesicles

The expression pattern of the BTL-like protein(s) in pea organs was obtained by immunoblot analysis of MV isolated from etiolated stem, green stem (light-grown) and leaf, after the separation of the proteins by SDS-PAGE (Fig. 1, panel a). The western blot shows that the anti-BTL Ab weakly reacted with a protein with an apparent molecular mass of approx. 70 kDa in etiolated (lane 1) and green (lane 2) stem MV. Instead, in leaf MV (lane 3) this Ab strongly reacted with a protein of approx. 70 kDa, but also with other two proteins with an apparent molecular mass of approx. 30 and 23 kDa, respectively. No reaction was detected when negative control was used (data not shown). A Western Blot assay was performed using anti V-ATPase as endogenous control to verify that similar protein concentration was present in the different membrane fractions (see Fig. 1S in the Supplementary Material).

Electrogenic BSP uptake in pea stem and leaf microsomal vesicles

Figure 1 (panel b) shows the valinomycin-dependent BSP uptake, at increasing concentrations, in MV isolated from different (etiolated and green stem, leaf) pea organs. The obtained three hyperbolic curves allowed to calculate the following Michaelis-Menten parameters: in MV obtained from etiolated stems (circles) V_{max}=0.40±0.02 μmol BSP min^{-1} mg^{-1} protein and K_M=1.22±0.30 μM BSP; in MV obtained from green stems (squares) V_{max}=0.77±0.05 μmol BSP min^{-1} mg^{-1} protein and K_M=4.91±1.18 μM BSP; in MV obtained from leaves (triangles) V_{max}=1.24±0.09 μmol BSP min^{-1} mg^{-1} protein and K_M=3.40±1.04 μM BSP.

Marker assays in different membrane fractions

In pea leaf, MV derive from the plasmalemma and different organelle membranes. The sub-fractionation analysis described in Fig. 2 (panel a) shows that the MV fractions mainly consisted of both plasma membrane and tonoplast, since the ATPase activity was partially inhibited by both vanadate (PM ATPase inhibitor) and bafilomycin A_1 (tonoplast ATPase inhibitor); by contrast, mitochondrial contamination was not relevant, since oligomycin (mitochondrial ATPase inhibitor) did not affect significantly the ATPase activity (Fig. 2, panel a). The extent of the inhibition of ATPase activity by vanadate and bafilomycin A_1 increased drastically in the fraction of PM (approx. 75 %) and

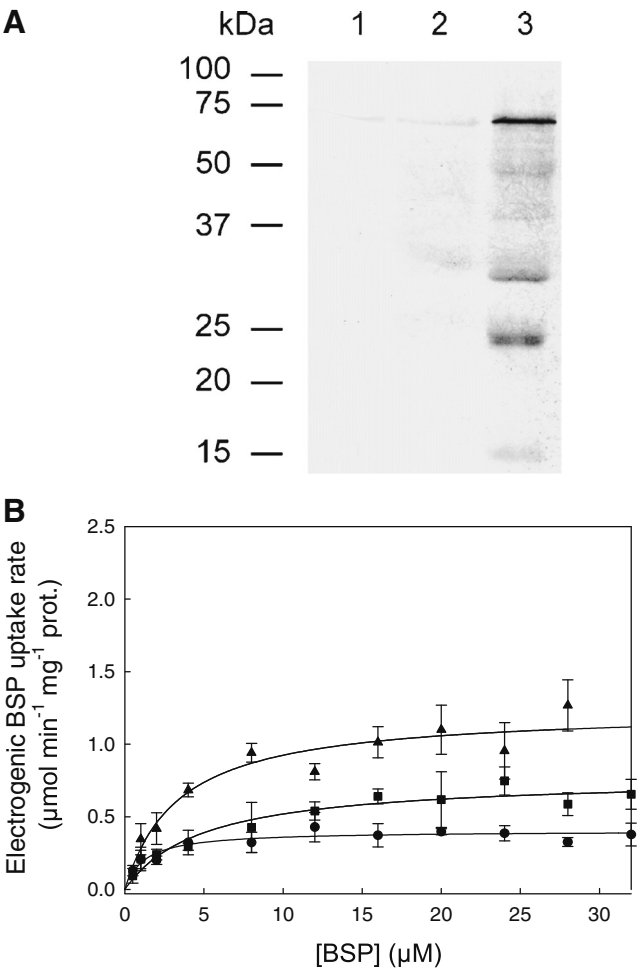

Fig. 1 Expression of the BTL-like proteins and evaluation of transport activities in MV isolated from differently illuminated pea organs. Panel **a** original western blot of protein expression in pea MV proteins (approx. 30 μg protein) obtained from etiolated stem (*lane 1*), green stem (*lane 2*) and leaf (*lane 3*). The values on the *left* represent the apparent molecular mass of molecular standards. Panel **b** characterization of electrogenic BSP transport into MV isolated from etiolated stem (*black circle*), green stem (*black square*) and leaf (*black triangle*). The dependence of the initial rate of electrogenic BSP uptake on BSP concentration was fitted to the equation $V = V_{max}[BSP]/(K_M + [BSP])$

tonoplast (approx. 72 %) vesicles, respectively, due to the purification procedure. In addition, the Chl measurement showed that the contamination of chloroplast in PM and tonoplast vesicles was, respectively, strongly reduced at approx. 48 % and 37 %, when compared to that of the microsomal fraction.

Finally, Chl contamination in the microsomal fraction isolated from pea leaf was lower than in chloroplast membrane (approx. 46 % of Chl content in chloroplast, Fig. 2, panel b).

Expression of the BTL-like protein(s) in pea leaf tonoplast, plasma membrane and chloroplast vesicles

The expression pattern of the BTL-like protein(s) was further evaluated in pea leaf membrane vesicles by using the same

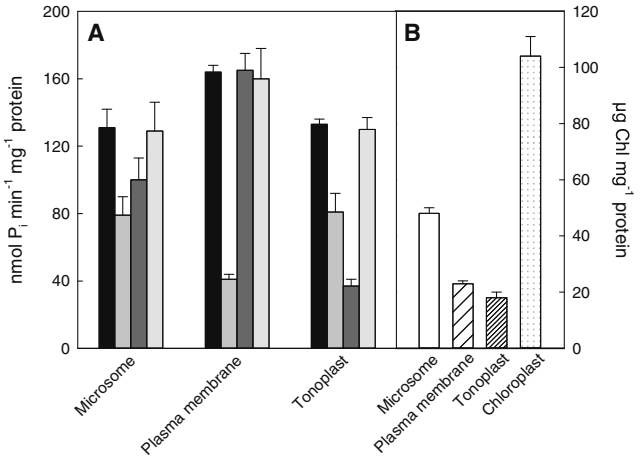

Fig. 2 Marker enzyme activities and Chl content in different isolated membrane fractions obtained from pea leaf. All enzyme activities were performed in the presence of 0.01 % (w/v) Triton X 100, for taking into account of the latent activity. Panel **a** shows ATPase activities: *black bars*, 1 mM ATP (control); *grey bars*, 1 mM ATP + 400 µM Vanadate; *dark grey bars*, 1 mM ATP + 100 nM Bafilomycin A_1; *light grey bars*, 1 mM ATP + 1 µg/ml Oligomycin. Panel **b** shows chlorophyll content

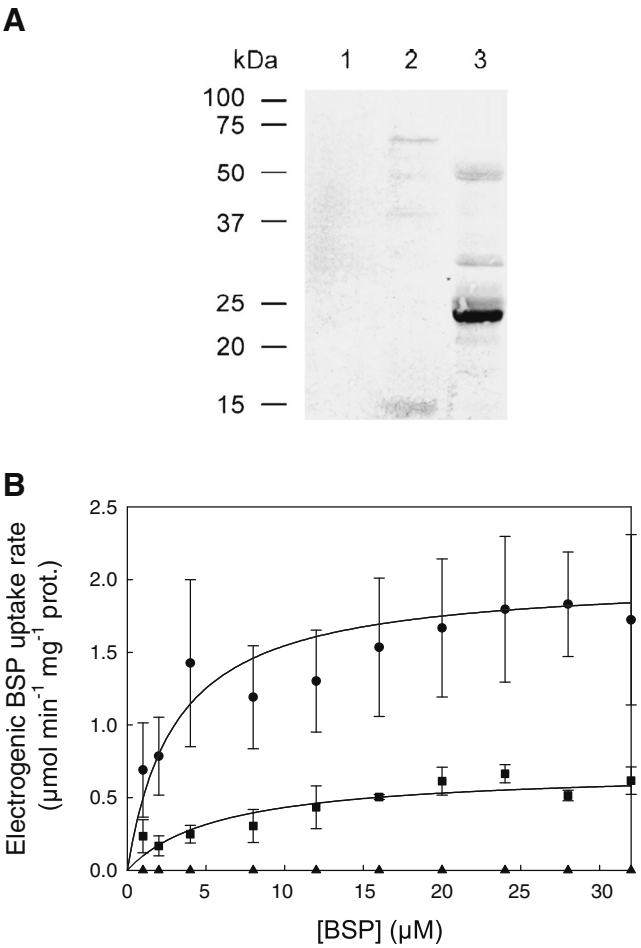

Fig. 3 Expression of the BTL-like proteins and evaluation of transport activities in different subcellular membranes of pea leaves. Panel **a** original western blot of protein expression in enriched vesicle fractions obtained from pea plasma membrane (*lane 1*), tonoplast (*lane 2*) and chloroplast (*lane 3*) (approx. 30 µg protein). The values on the *left* represent the apparent molecular mass of molecular standards. Panel **b** characterization of electrogenic BSP transport into chloroplast (*black circle*), tonoplast (*black square*) and PM (*black triangle*) vesicles isolated from pea leaves. The dependence of the initial rate of electrogenic BSP uptake on BSP concentration was fitted to the equation $V = V_{max}[BSP]/(K_M + [BSP])$

anti-BTL Ab (Fig. 3, panel a). In this case, two proteins at approx. 12 and 70 kDa were present with a weak signal only in tonoplast vesicles (lane 2), whereas the Ab strongly reacted with the protein at approx. 23 kDa and weakly with other two proteins at approx. 30 kDa and approx. 50 kDa, present in chloroplast vesicles (lane 3). No reaction was shown in PM vesicles (lane 1), as well as in all these samples when negative control was used (data not shown).

Electrogenic BSP uptake in pea leaf tonoplast, plasma membrane and chloroplast vesicles

The dependence of BSP uptake rate on the substrate concentration in the pea leaf membrane vesicles is shown in Fig. 3, panel b. In agreement with the above described result, chloroplast vesicles (circles) showed a higher BSP uptake with respect to tonoplast vesicles (squares). In plasma membrane vesicles (triangles) no BSP uptake was detectable. Even in this case, the data fitted the Michaelis-Menten equation and the derived parameters are $V_{max}=2.02\pm0.13$ µmol BSP min^{-1} mg^{-1} protein and $K_M=3.05\pm1.03$ µM BSP in chloroplast vesicles and $V_{max}=0.69\pm0.08$ µmol BSP min^{-1} mg^{-1} protein and $K_M=5.94\pm2.49$ µM BSP in tonoplast vesicles.

Inhibition of electrogenic BSP uptake in pea leaf microsomal and chloroplast vesicles

Vesicles obtained from both leaf microsomes and chloroplasts were preincubated with different amounts of anti-BTL Ab with the aim of confirming whether a BTL-related protein catalyzed electrogenic BSP uptake. Figure 4 shows that in leaf MV the anti-BTL Ab inhibited BSP uptake in an Ab concentration-dependent manner, in both leaf MV and chloroplast vesicles. Inhibition data were fitted to either a sigmoid equation, $y = y0 + a/\{1 + e-[(x-x0)/b]\}$, or a hyperbolic decay equation, $y = y_0 + (a*b)/(b + x)$, respectively. It could be calculated that maximal transport inhibition by the Ab (parameter a) was approx. 46 % and 69 %, in MV and chloroplast vesicles, respectively. In addition, both kinds of vesicles exhibited uninhibited transport activity when pre-immune sera were used, instead of the anti-BTL Ab (data not shown).

Finally, in chloroplast vesicles the transport activity was inhibited (approx. 40 %) by the chlorophyllin, a semisynthetic porphyrin derivative of Chl degradation (Fig. 5) and, at the same rate, by biliverdin, a linear tetrapyrrolic bile pigment, which is a product of heme catabolism.

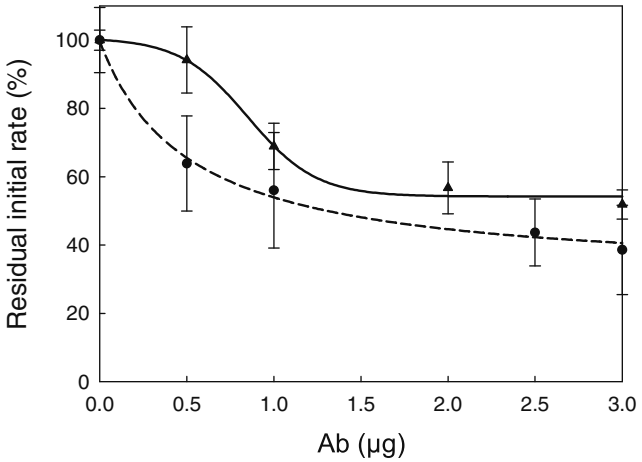

Fig. 4 Inhibition induced by increasing concentrations of anti-BTL Ab on electrogenic BSP transport in pea leaf MV (*black triangle*) and chloroplast vesicles (*black circle*). The initial rate was expressed as a percentage ± S.D. with respect to the control (without anti-BTL Ab). Data obtained from pea leaf MV were fitted (r^2=0.994) to the sigmoid y = y0 + a/{1 + e−[(x−x0)/b]}, where the parameters found were: y_0=54±2.4; a=46±4.8; x_0=0.85±0.08 μg; b=−0.20±0.07 μg. Data obtained from chloroplast vesicles were fitted (r^2=0.994) to an hyperbolic decay function y = y_0 + (a*b)/(b + x), where the parameters found were: y_0=31±3.9; a=69±4.4; b=0.51±0.12 μg

Expression of the BTL-like protein(s) in pea leaf chloroplast subcompartments

To further study the sub-organellar localization of BTL-like protein(s) in chloroplasts obtained from pea leaf, an immunoblot was performed after the separation of envelopes and thylakoids (Fig. 6). As it can be seen, a positive cross-reaction was observed at the level of the lower band at 23 kDa in both chloroplast (lane 1) and thylakoid vesicles (lane 2). In the latter membranes, an increase in the intensity of signal was observed, indicative of an enrichment of these proteins during fractionation and purification of chloroplast sub-compartments. There was no significant signal in the chloroplast (outer plus inner) envelope fractions (lane 3), and such evidence was also confirmed in fractions from spinach leaf (data not shown).

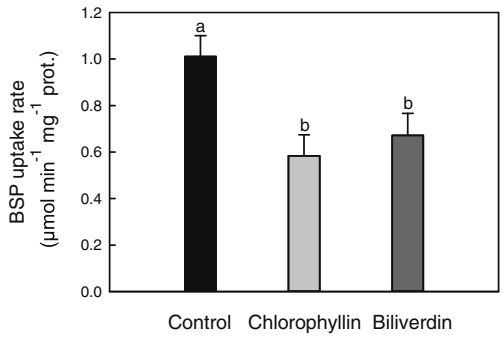

Fig. 5 Inhibition induced by 50 μM of tetrapyrrole chlorophyllin and bilin biliverdin on electrogenic BSP transport in chloroplast vesicles isolated from pea leaves. Uptake rate of the control was normalized as to 1 μmol BSP·mg^{-1} protein·min^{-1}. Means were compared by LSD (Least Significant Difference) according to Fisher's statistical test, and different letters assigned to means designate a statistical difference at $P \leq 0.05$

Discussion

In this work, the presence of protein(s), related to mammalian BTL, was identified in pea tissues, by using an Ab raised against the bilirubin-binding domain of rat liver BTL (Battiston et al. 1998). At least one of these proteins exhibited transport activity, as assessed by monitoring BSP uptake in different types of vesicles. These results are in agreement with those previously obtained in carnation petals (Passamonti et al. 2005b), where bilirubin interacted as a high-affinity ligand of both BTL and BTL-like proteins of liver and carnation microsomes, respectively. The inhibition of electrogenic BSP transport in chloroplast vesicles by chlorophyllin, biliverdin and the anti-BTL Ab (Figs. 4 and 5) is consistent with the hypothesis that these proteins might also be able to mediate a transport of both linear and cyclic tetrapyrroles. The expression pattern of BTL-like protein(s) and transport activity were correlated with the presence of a higher level of Chl and, presumably, of photosynthetic activity in pea green tissues (leaf > green stem > etiolated stem) (Fig. 1, panels a and b). In addition, a similar correlation with the photosynthetic metabolism could be found at sub-cellular level, because chloroplast membranes exhibited the highest level of BTL-like protein(s) and transport activity, when compared to plasma membrane and tonoplast (Fig. 3, panels a and b). The kinetic parameters, in particular V_{max}, of the transport activity measured in leaf MV and chloroplast vesicles are also similar and support this correlation. Moreover, the titration of the transporter protein(s) with the anti-BTL Ab (Fig. 4) confirms that chloroplast vesicles were richer than leaf MV in BTL-like transporter. Its localization in pea chloroplast thylakoids was specifically assessed by immunochemical assay (Fig. 6) and confirmed in spinach chloroplasts (data not shown). In addition, the sigmoidal pattern, exhibited by anti-BTL Ab inhibition in leaf MV, supports the hypothesis that the whole phenomenon may be due to the activity of more than one transporter given the membrane heterogeneity of these vesicles. On the contrary, in the case of chloroplast vesicles the hyperbolic curve, describing Ab inhibition, suggests the involvement of a unique protein in the transport activity.

Taken together, all the immunochemical results show that the protein bands, reacting with anti-BTL Ab in chloroplast and tonoplast membranes, possess different apparent molecular masses. Assuming that no proteolysis occurred, these data might suggest that the transporter could be composed by different monomeric components building up a multimeric protein. Current work on predicting the 3D structure of bilitranslocase from its primary sequence by multiple

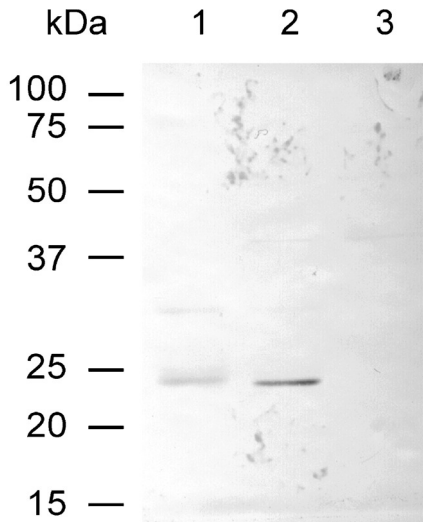

Fig. 6 Expression of the BTL-like proteins in different subcellular compartments of pea leaf chloroplasts. Original western blots of protein expression in enriched vesicle fractions obtained from pea chloroplasts (*lane 1*), thylakoids (*lane 2*) and outer and inner envelopes (*lane 3*) (approx. 30 μg protein). The values on the *left* represent the apparent molecular mass of molecular standards

computational approaches suggests that the transporter has four trans-membrane domains (Marjana Novič, National Institute of Chemistry, Slovenia, personal communication). Two trans-membrane domains have been accurately characterised . Though four trans-membrane domains could form the minimal aqueous pore, the native protein could also consist of a dimer. Furthermore, other proteins could strongly associate with the monomer and co-migrate under the prevailing electrophoretic conditions. More convincingly, distinct transport proteins/enzymes with different molecular masses, but related, respectively, to chlorophyll catabolism or synthesis, might also be inferred. This feature suggests the presence of conserved domains in tetrapyrrole-binding proteins (Perdih et al. 2012; Choudhury et al. 2013).

The double localization of this transporter(s) in both tonoplast vesicles and chloroplast membranes, but not in PM vesicles (Fig. 3, panels a and b), could indirectly indicate its (their) possible involvement in linear and cyclic tetrapyrrole transport into corresponding organelles. Regarding the BTL-like protein(s) present on the tonoplast membrane, they could be necessary for compartmentation of dangerous chlorophyll catabolites, as alternative carriers working in parallel with the already known ABC proteins and MRP (Hinder et al. 1996; Lu et al. 1998; Tommasini et al. 1998; Frelet-Barrand et al. 2008). The co-existence of several mechanisms for catabolite transport could be rationalized by two assumptions: i) plant metabolism is characterized by a biochemical redundancy; ii) and during steady-state turnover of Chl, huge amounts of these catabolites are accumulated in photosynthesizing cells (Hörtensteiner 2012). Therefore, these catabolites should be rapidly transported from one intracellular compartment to another, exploiting more than one mechanism of active transport.

The presence of BTL-like transporter(s) in chloroplasts suggests that these proteins could be involved in Chl biosynthetic and/or degradation pathways. The lack of cross-reactivity of anti-BTL Ab with protein in chloroplast envelopes implies that the export of chlorophyll degradation products and/or bilins does not involve BTL-like proteins, but rather other transporters, like ABC transporters (Hinder et al. 1996; Lu et al. 1998; Tommasini et al. 1998). On the other hand, the thylakoid localization of BTL-like protein(s) in pea chloroplasts (Fig. 6) and their different apparent molecular mass in comparison to those of tonoplast could support the hypothesis that cyclic tetrapyrroles are their preferential substrates rather than bilins, whose synthesis occurs instead in the stroma (Mochizuki et al. 2010; Joyard et al. 2009; Ferro et al. 2002, 2010). Indeed, since protoporphyrin IX is formed inside the thylakoid lumen, the uptake of its precursor protoporphyrinogen IX from the stroma, where the previous biosynthetic steps are localized, is necessary (Mochizuki et al. 2010). The accumulation of this intermediate and in particular its Mg-bound form is essential also for the chloroplast to nucleus signalling and affects tetrapyrrole biosynthesis

Table 1 Expression pattern of bilin-recognizing proteins in different species

Apparent molecular mass (≈ kDa)	Flowering plants		Fish	Mammals
	Pisum sativum	*Dianthus caryophyllus*	*Dicentrarchus labrax*	*Rattus norvegicus*
12	Vacuole	–	–	–
23	Chloroplast	–	–	–
30	Chloroplast	–	–	–
38	Vacuole	Vacuole[a]	Microsomes[b]	Plasma membrane[b]
50	Chloroplast Vacuole	Plasma membrane[a] Vacuole[a] Plasma membrane[a]	Microsome[b]	Plasma membrane[b] Microsome[b]
70	Vacuole	–	Microsome[b]	Microsome[b]

Apparent molecular masses are related to the specific localization of membrane proteins

[a] Ref. (Passamonti et al. 2005b)

[b] Ref. (Delneri et al. 2011)

(Surpin et al. 2002). Nevertheless, it has to be stressed that inhibitory activity of biliverdin on BSP uptake (Fig. 5) suggests that also linear tetrapyrroles interact with this BTL-like thylakoidal protein, similarly to what observed for phycobiliprotein in thylakoids of red algae and *Criptophyta* (Glazer and Wedemayer 1995; Ludwig and Gibbs 1989; Su et al. 2010).

The presence of chloroplast proteins, reacting with anti-BTL Ab raised against the bilirubin-binding domain, could be understood also in an evolutionary scenario. As previously described (Battiston et al. 1998), the amino acid sequence (residues 62–80) of the putative polypeptide chain of BTL, referred to as catalytic site, shows a high similarity (11 out of 19 residues) with a number of phycobilin-binding phycocyanins from several species of cyanobacteria, but also with a phycoerythrin of prochlorophyte species, a marine prokaryote (Hess et al. 1996). It is already known that the chromophore of phycobiliproteins is an open tetrapyrrole structure similar to bilirubin, whose building block (pyrrole) is involved in numerous functional molecules (i.e. cytochromes, chlorophyll, etc.). Therefore, it is not surprising that the sequence of this catalytic site recurs in different enzymes/transporters involved in bilin-based processes, the most ancestral of which is found in cyanobacteria. In the latter prokaryotes, a protein (approx. 20 kDa) has been shown in *Calothrix* (Hess et al. 1996; Santiago-Santos et al. 2004), corresponding to a component of phycobilisome, the light-harvesting antenna of cyanobacteria, known to contain phycobilins.

This apparatus necessarily evolved early in cyanobacteria, because linear and cyclic tetrapyrroles were essential for energy capture (chlorophylls and phycobilins) and as components of electron transport proteins (cytochromes). When cyanobacteria were then engulfed by a protist (primary endosymbiosis) to become plastids, this machinery was transferred to the arising eukaryotic cell (red algae, green algae, *Glaucophyta* and plants). This event was followed by secondary, tertiary and (perhaps) quaternary endosymbiosis, so that the enzymes/transporters related to processing heme-containing molecules could widespread in other algal organisms (Keeling 2010). In photosynthetic eukaryotic cells the heme-synthesizing genes soon formed a mosaic pathway, because some of the cyanobacterial genes were transferred to the nucleus (Obornik and Green 2005). This picture can help to explain why our Ab recognized more than one protein, with different molecular masses, particularly in green organs and chloroplasts, but also why BTL-like proteins are present in evolutionary divergent organisms, such as flowering plants, fish and mammals (Table 1) (Passamonti et al. 2005b; Delneri et al. 2011). Further work is needed to chemically characterise these various proteins, none of which seems to be encoded by annotated genes. The nucleotide sequence of rat liver bilitranslocase displays 96 % homology to the antisense strand of a segment of the ceruloplasmin cDNA. Thus it seems that a sense-antisense pair encode for either the ceruloplasmin or bilitranslocase (Passamonti et al. 2009).

The results here discussed could help to shed light on the metabolism and accumulation of bilins in plants. Actually, it appears crucial to further investigate in detail the final steps in the synthesis of photosynthetic pigments, as well as their final targeting into thylakoidal membranes. The presence of a BTL-like protein also in the tonoplast, suggests a possible involvement of these transporters during chlorophyll degradation, since the vacuole represents a compartment where catabolic metabolites are accumulated.

Aiming at fulfilling these questions, it would be necessary to purify the protein, for improving our knowledge about BTL-like primary structure and its similarities and/or homologies with other well-known transporters. In this frame, it will be essential the detailed comparison with the mammalian counterpart.

Acknowledgments This work was supported by European Regional Development Fund, Cross-Border Cooperation Italy-Slovenia Programme 2007–2013 (TRANS2CARE and AGROTUR projects).

Conflict of interest The authors declare that they have no conflict of interest.

References

Battiston L, Passamonti S, Macagno A, Sottocasa GL (1998) The bilirubin-binding motif of bilitranslocase and its relation to conserved motifs in ancient biliproteins. Biochem Biophys Res Commun 247(3):687–692. doi:10.1006/bbrc.1998.8868

Bertolini A, Peresson C, Petrussa E, Braidot E, Passamonti S, Macri F et al (2009) Identification and localization of the bilitranslocase homologue in white grape berries (*Vitis vinifera* L.) during ripening. J Exp Bot 60(13):3861–3871. doi:10.1093/Jxb/Erp225

Bradford M (1976) A rapid and sensitive method for the quantitation of microgram quantities of protein utilizing the principle of protein-dye binding. Anal Biochem 72:248–254

Braidot E, Petrussa E, Bertolini A, Peresson C, Ermacora P, Loi N et al (2008) Evidence for a putative flavonoid translocator similar to mammalian bilitranslocase in grape berries (*Vitis vinifera* L.) during ripening. Planta 228(1):203–213. doi:10.1007/s00425-008-0730-4

Choudhury AR, Perdih A, Zuperl S, Sikorska E, Solmajer T, Jurga S et al (2013) Structural elucidation of transmembrane transporter protein bilitranslocase: conformational analysis of the second transmembrane region TM2 by molecular dynamics and NMR spectroscopy. Biochim Biophys Acta Biomembr 1828(11):2609–2619. doi:10.1016/j.bbamem.2013.06.006

Delneri A, Franca R, Terdoslavich M, Montanic S, Serbec VC, Tramer F et al (2011) Identification and functional characterization of bilitranslocase in sea-bass (*Dicentrarchus labrax*) hepatopancreas. Anal Lett 44(18):2887–2900. doi:10.1080/00032719.2011.582548

Engel N, Jenny TA, Mooser V, Gossauer A (1991) Chlorophyll catabolism in *Chlorella protothecoides*—isolation and structure elucidation of a red bilin derivative. FEBS Lett 293(1–2):131–133. doi:10.1016/0014-5793(91)81168-8

Ferro M, Salvi D, Riviere-Rolland H, Vermat T, Seigneurin-Berny D, Grunwald D et al (2002) Integral membrane proteins of the

chloroplast envelope: identification and subcellular localization of new transporters. Proc Natl Acad Sci U S A 99(17):11487–11492. doi:10.1073/pnas.172390399

Ferro M, Brugiere S, Salvi D, Seigneurin-Berny D, Court M, Moyet L et al (2010) AT_CHLORO, a comprehensive chloroplast proteome database with subplastidial localization and curated information on envelope proteins. Mol Cell Proteomics 9(6):1063–1084. doi:10.1074/mcp.M900325-MCP200

Frelet-Barrand A, Kolukisaoglu HU, Plaza S, Ruffer M, Azevedo L, Hörtensteiner S et al (2008) Comparative mutant analysis of *Arabidopsis* ABCC-type ABC transporters: AtMRP2 contributes to detoxification, vacuolar organic anion transport and chlorophyll degradation. Plant Cell Physiol 49(4):557–569. doi:10.1093/Pcp/Pcn034

Glazer AN, Wedemayer GJ (1995) Cryptomonad biliproteins—an evolutionary perspective. Photosynth Res 46(1–2):93–105. doi:10.1007/Bf00020420

Gualberto JM, Handa H, Grienenberger JM (1995) Isolation and fractionation of plant mitochondria and chloroplasts: specific examples. Methods Cell Biol 50(50):161–175. doi:10.1016/S0091-679x(08)61029-8

Hess WR, Partensky F, vander Staay GWM, Garcia Fernandez JM, Borner T, Vaulot D (1996) Coexistence of phycoerythrin and a chlorophyll a/b antenna in a marine prokaryote. Proc Natl Acad Sci U S A 93(20):11126–11130. doi:10.1073/pnas.93.20.11126

Hinder B, Schellenberg M, Rodon S, Ginsburg S, Vogt E, Martinoia E et al (1996) How plants dispose of chlorophyll catabolites—directly energized uptake of tetrapyrrolic breakdown products into isolated vacuoles. J Biol Chem 271(44):27233–27236

Hörtensteiner S (2012) Update on the biochemistry of chlorophyll breakdown. Plant Mol Biol. doi:10.1007/s11103-012-9940-z

Hörtensteiner S, Kräutler B (2011) Chlorophyll breakdown in higher plants. Biochim Biophys Acta 1807(8):977–988

Joyard J, Ferro M, Masselon C, Seigneurin-Berny D, Salvi D, Garin J et al (2009) Chloroplast proteomics and the compartmentation of plastidial isoprenoid biosynthetic pathways. Mol Plant 2(6):1154–1180. doi:10.1093/Mp/Ssp088

Karawajczyk A, Dran V, Medic N, Oboh G, Passamonti S, Novic M (2007) Properties of flavonoids influencing the binding to bilitranslocase investigated by neural network modelling. Biochem Pharmacol 73(2):308–320. doi:10.1016/j.bcp.2006.09.024

Keeling PJ (2010) The endosymbiotic origin, diversification and fate of plastids. Philos Trans R Soc B Biol Sci 365(1541):729–748. doi:10.1098/rstb.2009.0103

Kräutler B, Hörtensteiner S (2006) Chlorophyll catabolites and the biochemistry of chlorophyll breakdown. In: Chlorophylls and bacteriochlorophylls: biochemistry, biophysics, functions and applications. Springer, The Netherlands

Lindemann P, Koch A, Degenhardt B, Hause G, Grimm B, Papadopoulos V (2004) A novel *Arabidopsis thaliana* protein is a functional peripheral-type benzodiazepine receptor. Plant Cell Physiol 45(6):723–733. doi:10.1093/Pcp/Pch088

Lu YP, Li ZS, Drozdowicz YM, Hörtensteiner S, Martinoia E, Rea PA (1998) AtMRP2, an *Arabidopsis* ATP binding cassette transporter able to transport glutathione S-conjugates and chlorophyll catabolites: functional comparisons with AtMRP1. Plant Cell 10(2):267–282. doi:10.1105/Tpc.10.2.267

Ludwig M, Gibbs SP (1989) Localization of phycoerythrin at the lumenal surface of the thylakoid membrane in *Rhodomonas lens*. J Cell Biol 108(3):875–884. doi:10.1083/jcb.108.3.875

Maestro A, Terdoslavich M, Vanzo A, Kuku A, Tramer F, Nicolin V et al (2010) Expression of bilitranslocase in the vascular endothelium and its function as a flavonoid transporter. Cardiovasc Res 85(1):175–183. doi:10.1093/Cvr/Cvp290

Matile P, Hörtensteiner S, Thomas H, Kräutler B (1996) Chlorophyll breakdown in senescent leaves. Plant Physiol 112(4):1403–1409

Matile P, Hörtensteiner S, Thomas H (1999) Chlorophyll degradation. Annu Rev Plant Physiol Plant Mol Biol 50:67–95. doi:10.1146/annurev.arplant.50.1.67

Mochizuki N, Tanaka R, Grimm B, Masuda T, Moulin M, Smith AG et al (2010) The cell biology of tetrapyrroles: a life and death struggle. Trends Plant Sci 15(9):488–498. doi:10.1016/j.tplants.2010.05.012

Obornik M, Green BR (2005) Mosaic origin of the heme biosynthesis pathway in photosynthetic eukaryotes. Mol Biol Evol 22(12):2343–2353. doi:10.1093/molbev/msi230

Passamonti S, Terdoslavich M, Margon A, Cocolo A, Medic N, Micali F et al (2005a) Uptake of bilirubin into HepG2 cells assayed by thermal lens spectroscopy—bilitranslocase. FEBS J 272(21):5522–5535. doi:10.1111/j.1742-4658.2005.04949.x

Passamonti S, Cocolo A, Braidot E, Petrussa E, Peresson C, Medic N et al (2005b) Characterization of electrogenic bromosulfophthalein transport in carnation petal microsomes and its inhibition by antibodies against bilitranslocase. FEBS J 272(13):3282–3296. doi:10.1111/j.1742-4658.2005.04751.x

Passamonti S, Terdoslavich M, Franca R, Vanzo A, Tramer F, Braidot E et al (2009) Bioavailability of flavonoids: a review of their membrane transport and the function of bilitranslocase in animal and plant organisms. Curr Drug Metab 10(4):369–394

Passamonti S, Tramer F, Petrussa E, Braidot E, Vianello A (2010) Electrogenic bromosulfalein transport in isolated membrane vesicles: implementation in both animal and plant preparations for the study of flavonoid transporters. Methods Mol Biol 643:307–335

Perdih A, Choudhury AR, Zuperl S, Sikorska E, Zhukov I, Solmajer T et al (2012) Structural analysis of a peptide fragment of transmembrane transporter protein bilitranslocase. PLoS ONE 7(6):e38967. doi:10.1371/journal.pone.0038967

Santiago-Santos MC, Ponce-Noyola T, Olvera-Ramirez R, Ortega-Lopez J, Canizares-Villanueva RO (2004) Extraction and purification of phycocyanin from *Calothrix* sp. Process Biochem 39(12):2047–2052. doi:10.1016/j.procbio.2003.10.007

Su HN, Xie BB, Zhang XY, Zhou BC, Zhang YZ (2010) The supramolecular architecture, function, and regulation of thylakoid membranes in red algae: an overview. Photosynth Res 106(1–2):73–87. doi:10.1007/s11120-010-9560-x

Surpin M, Larkin RM, Chory J (2002) Signal transduction between the chloroplast and the nucleus. Plant Cell 14:S327–S338. doi:10.1105/Tpc.010446

Tommasini R, Vogt E, Fromenteau M, Hörtensteiner S, Matile P, Amrhein N et al (1998) An ABC-transporter of *Arabidopsis thaliana* has both glutathione-conjugate and chlorophyll catabolite transport activity. Plant J 13(6):773–780. doi:10.1046/j.1365-313X.1998.00076.x

Vanhee C, Zapotoczny G, Masquelier D, Ghislain M, Batoko H (2011) The *Arabidopsis* multistress regulator TSPO is a heme binding membrane protein and a potential scavenger of porphyrins via an autophagy-dependent degradation mechanism. Plant Cell 23(2):785–805. doi:10.1105/tpc.110.081570

Vavilin DV, Vermaas WFJ (2002) Regulation of the tetrapyrrole biosynthetic pathway leading to heme and chlorophyll in plants and cyanobacteria. Physiol Plant 115(1):9–24. doi:10.1034/j.1399-3054.2002.1150102.x

Wellburn AR (1994) The spectral determination of chlorophyll a and chlorophyll b, as well as total carotenoids, using various solvents with spectrophotometers of different resolution. J Plant Physiol 144(3):307–313

Ziberna L, Tramer F, Moze S, Vrhovsek U, Mattivi F, Passamonti S (2012) Transport and bioactivity of cyanidin 3-glucoside into the vascular endothelium. Free Radic Biol Med 52(9):1750–1759. doi:10.1016/j.freeradbiomed.2012.02.027

Zuperl S, Fornasaro S, Novic M, Passamonti S (2011) Experimental determination and prediction of bilitranslocase transport activity. Anal Chim Acta 705(1–2):322–333. doi:10.1016/j.aca.2011.07.004

Appendix 2

Evidence of phytotoxicity and genotoxicity *in Hordeum vulgare* L. exposed to CeO_2 and TiO_2 nanoparticles

frontiers in Plant Science

ORIGINAL RESEARCH
published: 25 November 2015
doi: 10.3389/fpls.2015.01043

Evidence of Phytotoxicity and Genotoxicity *in Hordeum vulgare* L. Exposed to CeO_2 and TiO_2 Nanoparticles

*Alessandro Mattiello[1], Antonio Filippi[1], Filip Pošćić[1], Rita Musetti[1], Maria C. Salvatici[2], Cristiana Giordano[2,3], Massimo Vischi[1], Alberto Bertolini[1] and Luca Marchiol[1]**

[1] Department of Agriculture and Environmental Sciences, University of Udine, Udine, Italy, [2] Centro di Microscopie Elettroniche "Laura Bonzi", Istituto di Chimica dei Composti OrganoMetallici, Consiglio Nazionale delle Ricerche, Firenze, Italy, [3] Tree and Timber Institute, Istituto Per La Valorizzazione del Legno e delle Specie Arboree-CNR, Firenze, Italy

Engineered nanoscale materials (ENMs) are considered emerging contaminants since they are perceived as a potential threat to the environment and the human health. The reactions of living organisms when exposed to metal nanoparticles (NPs) or NPs of different size are not well known. Very few studies on NPs–plant interactions have been published, so far. For this reason there is also great concern regarding the potential NPs impact to food safety. Early genotoxic and phytotoxic effects of cerium oxide NPs ($n$$CeO_2$) and titanium dioxide NPs ($n$$TiO_2$) were investigated in seedlings of *Hordeum vulgare* L. Caryopses were exposed to an aqueous dispersion of $n$$CeO_2$ and $n$$TiO_2$ at, respectively 0, 500, 1000, and 2000 mg l^{-1} for 7 days. Genotoxicity was studied by Randomly Amplified Polymorphism DNA (RAPDs) and mitotic index on root tip cells. Differences between treated and control plants were observed in RAPD banding patterns as well as at the chromosomal level with a reduction of cell divisions. At cellular level we monitored the oxidative stress of treated plants in terms of reactive oxygen species (ROS) generation and ATP content. Again $n$$CeO_2$ influenced clearly these two physiological parameters, while $n$$TiO_2$ were ineffective. In particular, the dose 500 mg l^{-1} showed the highest increase regarding both ROS generation and ATP content; the phenomenon were detectable, at different extent, both at root and shoot level. Total Ce and Ti concentration in seedlings was detected by ICP-OES. TEM EDSX microanalysis demonstrated the presence of aggregates of $n$$CeO_2$ and $n$$TiO_2$ within root cells of barley. $n$$CeO_2$ induced modifications in the chromatin aggregation mode in the nuclei of both root and shoot cells.

Keywords: barley, cerium oxide nanoparticles, titanium oxide nanoparticles, genotoxicity, oxidative stress

OPEN ACCESS

Edited by:
Nelson Marmiroli, University of Parma, Italy

Reviewed by:
Margarita Sánchez-Domínguez, Centro de Investigación en Materiales Avanzados, S.C., Mexico
Jozsef Dudas, Medical University of Innsbruck, Austria

****Correspondence:***
Luca Marchiol
marchiol@uniud.it

Specialty section:
This article was submitted to Functional Plant Ecology, a section of the journal Frontiers in Plant Science

Received: *12 September 2015*
Accepted: *09 November 2015*
Published: *25 November 2015*

Citation:
Mattiello A, Filippi A, Pošćić F, Musetti R, Salvatici MC, Giordano C, Vischi M, Bertolini A and Marchiol L (2015) Evidence of Phytotoxicity and Genotoxicity in Hordeum vulgare L. Exposed to CeO_2 and TiO_2 Nanoparticles. Front. Plant Sci. 6:1043. doi: 10.3389/fpls.2015.01043

INTRODUCTION

It is estimated that by 2020 about six million people will be employed worldwide in industries that use nanotechnologies, which will have the potential to produce goods for a market of more than 3,000 billion dollars (Roco, 2011). There is therefore a tumultuous development of new materials justified by a rapid growth of technological and commercial applications. Model simulations demonstrated that flows of engineered nanomaterials (ENMs) are able to reach several natural

ecosystems (Colman et al., 2013). Cerium oxide nanoparticles (NPs; nCeO$_2$) and titanium oxide NPs (nTiO$_2$) are among the top ten most produced ENMs by mass (Keller et al., 2013) and used in cosmetics industries, in solar cells, paints, cements, coatings, in agriculture and the food industry (Gogos et al., 2012; Piccinno et al., 2012; Parisi et al., 2015). nCeO$_2$ and nTiO$_2$ were included in the list of ENMs of priority for immediate testing by the Organization for Economic Cooperation and Development (OECD, 2010). From point sources (e.g., discharges of wastewaters from industries or landfills), such materials will tend to accumulate in sediments and soils, exposing the organisms inhabiting these environments to potential risks (Liu and Cohen, 2014).

Plants are able to assimilate metal nanoparticles (MeNPs) largely depending on the type of plant and the size of MeNPs (Rico et al., 2011). In addition, the primary particle size of MeNPs is relevant for their bioavailability and therefore their toxicity (Van Hoecke et al., 2009), also raising questions on the potential for MeNPs exposure of crops and food safety (Hong et al., 2013). Experimental evidences were reported by Zhang et al. (2011) which studied the nCeO$_2$ uptake and translocation in cucumber, reporting an higher Ce assimilation in plants treated with 7 nm Ce than 25 nm ones. Clément et al. (2013) reported similar results for nTiO$_2$ on rapeseed plantlets treated with 14–25 nm particles. Another functional property that influences the MeNPs plant assimilation is the agglomeration/aggregation status that in turn is influenced directly by the zeta-potential (Navarro et al., 2008). Song et al. (2013a) demonstrated a negative correlation between nTiO$_2$ agglomeration/aggregation and assimilation in tomato. A similar behavior could be hypothesized also for nCeO$_2$.

Although there are potential positive applications of ENMs in agriculture (Parisi et al., 2015), studies on the toxicity of MeNPs have shown early negative consequences on crops due to genotoxic and phytotoxic effects (Miralles et al., 2012; Gardea-Torresdey et al., 2014). From an ecological point of view, this raises questions about potential risks due to the input of MeNPs in the food chain. Early plant MeNPs toxicity can be measured observing seed germination, root elongation, DNA mutations (López-Moreno et al., 2010a; Atha et al., 2012) or changes in biochemical parameters (Rico et al., 2013; Schwabe et al., 2013).

The aims of this study were to determine the early phytotoxic and genotoxic effects of nCeO$_2$ and nTiO$_2$ on barley (*Hordeum vulgare* L.) plants. The FAO ranks barley fourth in the top five cereals in the world ordered based on production tonnage (FAOSTAT, 2014) and the cereal is one of the major crops grown worldwide for human and animal consumption. Suspensions of nCeO$_2$ and nTiO$_2$ were prepared at 0, 500, 1000, and 2000 mg l^{-1}. Phytotoxicity of NPs was determined through percentage of germination and root elongation, ATP and ROS generation in root and leaf cells. Genotoxicity was investigated by the mitotic index and RAPDs. Ce and Ti uptake and translocation within seedling tissues were determined by inductively coupled plasma-optical emission spectroscopy (ICP-OES), while nCeO$_2$ and nTiO$_2$ within plant cells were detected by transmission electronic microscope and energy dispersive x-ray spectrometer (TEM–EDX).

MATERIALS AND METHODS

Nanoparticles Characterization

The cerium$^{(IV)}$ oxide (nCeO$_2$) and titanium$^{(IV)}$ oxide anatase (nTiO$_2$) powders with a nominal average particle size <25 nm were purchased from Sigma–Aldrich (Milwaukee, WI, USA). The specific surface area of the nCeO$_2$ and nTiO$_2$ was measured by the Brunauer–Emmett–Teller (BET) method by using the Surface Area and Pore Size Analyzer SA 3100 plus (Beckman Coulter, USA).

The nCeO$_2$ and nTiO$_2$ powders were suspended in deionized water at a concentration of 1000 mg l^{-1} and sonicated at 60°C for 30 min. The suspensions were characterized for Z-average size, measured as hydrodynamic diameter, zeta potential, via electrophoretic mobility, and polydispersity index (PDI), calculated from the signal intensity, by the dynamic light scattering (DLS) method using the Nano ZS90 (Malvern Instruments, UK). The nCeO$_2$ and nTiO$_2$ powder suspensions at three different concentrations (500, 1000, and 2000 mg l^{-1}) were prepared in MilliQ® water by sonication for 30 min at room temperature and then stirred for 15 min. The range of concentrations (0, 500, 1000, and 2000 mg L^{-1}) was chosen according to Yang and Watts (2005), Lin and Xing (2007), and López-Moreno et al. (2010a).

Seed Germination and Root Elongation

Caryopses of *H. vulgare* L. var. Tunika were provided by S.I.S. Società Italiana Sementi (San Lazzaro di Savena, Bologna, Italy). The caryopses were sterilized by orbital agitation with 70% ethanol for 2 min and then with 5% sodium hypochlorite plus some drops of Tween 80 for 30 min. They were rinsed six times with sterilized MilliQ® water. All caryopses were transferred in sterile conditions into 15 mm Petri dishes containing filter paper (Ø 90 mm Whatman No. 1) soaked with 8 ml of MilliQ® water (control treatment) or 8 ml of nCeO$_2$ or nTiO$_2$ suspensions at different concentrations. The Petri dishes were taped and placed in the dark at 21°C for 3 days. The germination percentage was calculated as the ratio of germinated seeds out the total seeds of each Petri dish. A second set of caryopses were treated for 7 days in the same conditions to evaluate root elongation and Ce and Ti uptake. The seedlings were photographed and Image J software (Schneider et al., 2012) was used to measure roots length. Root elongation was calculated as the average or the sum of all roots emerged from each seed. The experiments were performed in triplicate.

Mitotic Index

The germinated seedlings with actively growing roots (2.5 cm in length) were placed in the nCeO$_2$ and nTiO$_2$ suspensions (0, 500, 1000, 2000 mg l^{-1}) for 24 h. After treatment the root tips were fixed in 3:1 alcohol : acetic acid and then, kept in 70% ethanol at 4°C. The root tips were rinsed in deionized water for 5 min, hydrolyzed in 1N HCl for 8 min at 60°C, rinsed in deionized water for 5 min, stained in leuco-basic-fuchsine for 45 min and washed in tap water for 5 min. The root tips were then transferred to 45% acetic acid for 1 to 5 min, root caps were removed, and

the roots were dissected to release the meristematic cells. Ten tips per treatment were evaluated and each treatment was replicated three times, for a total of about 10,000 cell observations. The mitotic index was evaluated in Feulgen stained preparations as the percentage of dividing cells out of the total number of cells scored.

Random Amplified Polymorphic DNA (RAPD) Analysis

The genotoxicity of nCeO$_2$ and nTiO$_2$ was investigated by observing the band profile after a random amplified polymorphic DNA (RAPD) assay on six replicates per treatment obtained from seedlings exposed as for mitotic index experiment. Plant genomic DNA was extracted from root tips using the DNeasy Plant Mini Kit (QIAGEN®) according to manufacturer's protocol. PCR reactions were performed with 30 ng of genomic DNA as a template using six primer pairs: OPA04 (AATCGGGCTG), OPA10 (GTGATCGCAG), OPB01 (GTTTCGCTCC), OPB03 (CATCCCCCTG), OPB12 (CCTTGACGCA), and OPB20 (GGACCCTTAC). The PCR conditions consisted of an initial Taq polymerase activation at 95°C for 5 min, followed by 45 cycles of denaturation (95°C, 1 min), annealing (35°C, 1 min), and extension (72°C, 1 min) with a final extension for 10 min at 72°C. The PCR products were subjected to electrophoresis on 1.6% agarose in TBE 0.5%, for 2 h at 60 V/cm stained with GelRed® and photographed for band scoring.

Evaluation of ATP Content

ATP content was determined by means of the luciferin–luciferase luminometric assay (Lundin, 1984). Root and shoot of each seedling were separated, frozen with liquid nitrogen and ground to a fine powder. Tissue powder (100 ± 20 mg FW) was suspended in 1 ml of 50 mM Tris-HCl (pH 7.5), 0.05% (w/v) Triton X-100 and immediately kept at 95°C for 3 min to inactivate any possible hydrolytic activity. After cooling, samples were centrifuged to obtain the cellular soluble fraction in the supernatant. The sample assays were performed in a 96-well plate with ATPlite Luminescence ATP Detection Assay System, (PerkinElmer) according to manufacturer's protocol. Aliquots (20 μl) of soluble fraction were mixed with 20 μl of ATPlite buffer in 130 μl of 50 mM Tris-HCl (pH 7.5) and 5 mM $MgCl_2$. Signals were detected by a Multilabel Counter (WALLAC, model 1420, PerkinElmer, Waltham, MA, USA). Actual ATP concentration of each experiment (expressed as nmol ATP g^{-1} f. w.) was calculated by a calibration curve obtained with commercially purchased ATP (Sigma, USA) in a 8–100 nM range.

Reactive Oxygen Species (ROS) Determination

The generation of ROS was monitored by the method of Wang and Joseph (1999), using 2′,7′-dichlorodihydrofluorescein diacetate (H_2DCFDA) as a probe. Tissue powder (0.5 g f. w.) obtained from both roots and shoots was extracted in 2.5 ml cold acetone and incubated for 4 h at 4°C. After centrifugation at 1000 g for 10 min, the pellet was homogenized in 1 ml of 50 mM Tris-HCl (pH 7.5), 0.4 M sucrose and 1 mM EDTA by Turrax device. The sample was again centrifuged for 15 min and the supernatant stored at −80°C until analysis. Aliquots of sample (20 μl) were incubated in 96-well microplate with 5 μM H_2DCFDA and 180 μl of 50 mM Tris-HCl (pH 7.5). Detection was performed by fluorimetric assay using Multilabel Counter (WALLAC, model 1420, PerkinElmer) with orbital shaking and reading for 1.75 h at 5 min intervals with excitation filter set at 485 ± 10 nm and the emission filter set at 530 ± 10 nm. Values of relative fluorescence (RFU) were expressed as RFU mg^{-1} protein. Protein concentration was estimated by the Bradford (1976) method.

Cerium and Titanium in Seedling Tissues

The seedlings were washed by agitation with 0.01 M HNO_3 for 30 min and rinsed three times by agitation with MilliQ® water for 15 min. The seedling roots and shoots were then oven-dried at 105°C for 24 h and 0.5 g material was digested using 10 ml of HNO_3 in a microwave oven (CEM, MARS Xpress) according to the USEPA 3052 method (USEPA, 1995). After mineralization, the plant extracts were filtered (0.2 μm PTFE), diluted and analyzed. Total content of Ce and Ti was determined by an ICP-OES (Varian Inc., Vista MPX). The accuracy of the analytical procedure adopted for ICP-OES analysis was checked by running standard solutions every 20 samples. Yttrium was used as the internal standard.

TEM Observations and X-ray Microanalysis

The morphology of NPs was assessed by direct observation of suspension of nCeO$_2$ or nTiO$_2$ NPs under the TEM. Drops of suspensions (prepared as described above) were placed on carbon–formvar coated nickel grids, dried at room temperature and observed under a Philips CM 10 (FEI, Eindhoven, The Netherlands) TEM, operating at 80 kV.

For microscopic analyses *in planta*, tissues from seedlings treated with nCO$_2$ or nTiO$_2$ at 1000 and 2000 mg l^{-1} were sampled as in the root elongation experiment were sampled. Roots and shoots were excised, cut into small portions (2 mm × 3 mm) and fixed for 2 h at 4°C in 0.1% (w/vol) buffered sodium phosphate and 3% (w/v) glutaraldehyde at pH 7.2. They were then post-fixed with 1% osmium tetroxide (w/v) in the same buffer for 2 h, dehydrated in an ethanol series, and embedded in Epon/Araldite epoxy resin (Electron Microscopy Sciences, Fort Washington, PA, USA). For conventional TEM observations, serial ultrathin sections from embedded leaf tissues were cut with a diamond knife, mounted on uncoated 200 mesh copper grids (Electron Microscopy Sciences, Fort Washington, PA, USA), stained in uranyl acetate and lead citrate, and then observed under TEM as reported above.

For X-ray microanalysis, unstained ultrathin sections were placed on formvar/carbon-coated 200 mesh nickel grids and dried at room temperature. The nature of NPs observed in plant tissues was determined by a TEM (PHILIPS CM 12, FEI, Eindhoven, The Netherlands) equipped with an EDS-X-ray microanalysis system (EDAX, AMETEK, Mahwah NJ, USA, software EDAX Genesis). The images were recorded by

a Megaview G2 CCD Camera (Olympus; software iTEM FEI, Analysis Image Processing).

Data Analysis

One-way analysis of variance (ANOVA) was conducted to test differences in the plants' behavior. Tukey's Multiple Comparison test at 0.05 p level were used to compare means. Statistical analyses were performed using the SPSS program (SPSS Inc., Chicago, IL, USA, ver. 17). Principal Coordinate Analysis (PCoA) was computed based on the binary genetic distance option in GenAlEx v. 6.501 software (Peakall and Smouse, 2012). Graphics were produced using CoPlot (CoHort ver. 6.204, Monterey, CA, USA).

RESULTS

Nanoparticles Characterization

The specific surface values obtained by BET measurements were 46.1 $m^2\ g^{-1}$ for nCeO$_2$ and 61.6 $m^2\ g^{-1}$ for nTiO$_2$. The Z-average sizes of the nCeO$_2$ and nTiO$_2$ suspended in deionized water were 174 ± 1.2 nm and 925 ± 105 nm, respectively, these values result remarkable higher respect the declared producer dimensions. The zeta potentials were 0.027 ± 0.064 mV for nCeO$_2$ and 19.9 ± 0.55 mV nTiO$_2$. These parameter values put in evidence their instability, in fact for both NP types are included in the range of the NP instability (–30 mV ÷ +30 mV) and justify the differences between the declared dimension and the measured ones. The PDI of nCeO$_2$ and nTiO$_2$ were 0.339 ± 0.011 and 0.841 ± 0.173, respectively. These values indicate a narrow dimensional distribution of nCeO$_2$ respect to nTiO$_2$.

Caryopses Germination and Root Elongation

Effects of nCeO$_2$ and nTiO$_2$ on caryopses germination and root growth are shown in **Table 1**. Since there was not a statistically significant effect of concentrations for nCeO$_2$ and nTiO$_2$, our results demonstrate that, even at the highest level of concentration, caryopses germination is not affected by nCeO$_2$ or nTiO$_2$ (**Table 1**). At the end of our experiment the barley seedlings had reached coleoptile emergence. At this stage typically has between six and seven seminal roots (Knipfer and Fricke, 2011). In our experiment the number of seminal roots was not affected by nCeO$_2$ and nTiO$_2$ (**Table 1**). On the contrary, in both cases the development of root tissues was influenced in a similar manner by the treatments. In fact, there was a significant effect of both nCeO$_2$ ($p < 0.05$) and nTiO$_2$ ($p < 0.05$) on the average length of the seminal roots. *Post hoc* comparison tests indicated that root elongation in seedlings treated with 500 mg l^{-1} nCeO$_2$ and nTiO$_2$ was significantly lower than controls (–24.5 and –14.8%, respectively). At higher nCeO$_2$ and nTiO$_2$ concentrations we would have expected to see a further reduction in the development of seminal roots. However, this did not occur since the average length of seminal roots was similar to controls (**Table 1**).

Cerium and Titanium in Plant Tissues

Although without visible symptoms of phytotoxicity, the concentration of total Ce and Ti in the tissues of barley seedlings showed (i) a dose-response and (ii) a different magnitude of accumulation between Ce and Ti. **Table 2** shows the concentration of Ce and Ti in the fractions of barley seedlings. As expected Ce and Ti accumulated much more within root tissues than in the shoot ($p < 0.05$). Ce concentration in the roots increased significantly ($p < 0.05$) as the concentration of nCeO$_2$ in the growth medium increased (**Table 2**). A statistically significant effect of treatments in Ce accumulation in the shoots ($p < 0.001$) was verified. Mean comparisons showed differences among the treatments. Ce concentration in shoots did not significantly differ between the 500 and 1000 mg l^{-1} Ce treatment (38.3 and 98.1 mg Ce kg^{-1} DW, respectively), whereas at 2000 mg nCeO$_2$ L^{-1} a Ce concentration of 622 mg Ce kg^{-1} DW was observed in the shoots, which is significantly different from other values (**Table 2**).

Titanium concentrations in barley roots and shoots were one–two orders of magnitude lower compared to Ce. However, also in this case a statistically significant dose dependent increase was also observed. With the lowest nTiO$_2$ treatment (500 mg l^{-1}) Ti concentration in roots was negligible and no Ti was detected in shoots (**Table 2**). At the intermediate nTiO$_2$ treatment (1000 mg l^{-1}) the root tissues had 37.2 mg Ti kg^{-1} DW which is significantly lower ($p = 0.0001$) than 413 mg Ti kg^{-1} DW found at highest nTiO$_2$ treatment (**Table 2**). Finally, we verified that also Ti concentration in the shoots also responded positively to the treatments ($p < 0.001$). The mean Ti concentration detected in barley shoots were 7.83 mg kg^{-1} DW and 26.2 mg kg^{-1} DW for 1000 and 2000 mg nTiO$_2$ l^{-1}, respectively (**Table 2**).

TABLE 1 | Germination percentage of seeds, number of seminal roots and root length in barley seedlings treated with 0, 500, 100, and 2000 mg l^{-1} of nCeO$_2$ and nTiO$_2$.

Treatment	nCeO$_2$			nTiO$_2$		
	Germination (%)	Seminal roots (n)	Root length (mm)	Germination (%)	Seminal roots (n)	Root length (mm)
Ctrl	87 ± 1.76 a	5.2 ± 0.18 a	52.7 ± 4.13 a	88 ± 1.20 a	6.6 ± 0.34 a	53.3 ± 3.03 a
500 mg l^{-1}	83 ± 2.03 a	5.5 ± 0.22 a	39.8 ± 2.24 b	87 ± 1.76 a	6.1 ± 0.27 a	45.4 ± 2.85 b
1000 mg l^{-1}	80 ± 2.08 a	5.2 ± 0.26 a	45.8 ± 17.8 ab	85 ± 1.45 a	6.5 ± 0.22 a	53.9 ± 3.13 a
2000 mg l^{-1}	79 ± 1.86 a	4.9 ± 0.25 a	43.8 ± 1.72 ab	87 ± 1.76 a	6.4 ± 0.13 a	58.5 ± 2.97 a

Values are mean ± SE (n = 3). Different letters indicate statistical difference between treatments at Tuckey's test (p < 0.05).

TABLE 2 | Concentration of total Ce and Ti in roots and shoots of barley seedlings treated with 0, 500, 100, and 2000 mg l^{-1} of $nCeO_2$ and $nTiO_2$.

Treatment	Ce roots (mg kg^{-1} DW)	Ce coleoptile (mg kg^{-1} DW)	Ti roots (mg kg^{-1} DW)	Ti coleoptile (mg kg^{-1} DW)
Ctrl	<d.l.	<d.l.	<d.l.	<d.l.
500 mg l^{-1}	579 ± 168 b	38.3 ± 5.77 b	<d.l.	<d.l.
1000 mg l^{-1}	5262 ± 1751 b	98.1 ± 40.2 b	35.2 ± 17.3 b	7.83 ± 3.3 b
2000 mg l^{-1}	20,714 ± 5722 a	622 ± 95.1 a	412 ± 127 a	26.2 ± 8.71 a

Values are mean ± SE (n = 3). Different letters indicate statistical difference between treatments at Tuckey's test ($p < 0.05$).

Ce and Ti Nano-aggregates in Plant Tissues

The morphology of $nCeO_2$ and $nTiO_2$ NPs is visible in **Figures 1A,B**, respectively. Transmission electron microscopy analysis demonstrated that CeO_2 particles exhibited an approximate equi-axes shape with sharp edges (**Figure 1A**), while particle sharp edges are less evident in TiO_2. To assess the possible uptake of $nCeO_2$ or $nTiO_2$ from the culture medium to the root tissues and the translocation to the different parts of the plantlets, we performed ultrastructural analyses on roots and shoot tissues. Several clusters of NPs were found in cortical parenchymal tissues of roots, both in the case of $nCeO_2$ (**Figure 2A**) and $nTiO_2$ treatment, at all concentrations. Clusters were also observed in the xylem, even if in to lesser extent (**Figure 2B**). EDS-X ray microanalysis allowed the identification of the clusters as aggregates of Ce and Ti nanoparticles.

No NPs were detected in the shoots of $nCeO_2$ or $nTiO_2$ treated plantlets. The ultrastructure of all observed tissues appeared preserved. No necrosis or damage to membranes, nor cell modifications were detected. In general, the cell compartments were not significantly affected by treatments, except for the nuclei of parenchymal cells of root and shoot of seedlings treated with $nCeO_2$ (1000 and 2000 mg l^{-1}), which showed compact chromatin (**Figures 3A–D**).

ATP and ROS

The evaluation of ATP concentration aimed to evidence the energetic status in different fractions of barley seedlings exposed to $nCeO_2$ and $nTiO_2$. The different concentrations of $nCeO_2$ induced a statistically significant effect (**Figure 4**), with a trend of values peaking at 500 and 1000 mg l^{-1}, in root and lowering at 2000 mg l^{-1} in shoot samples. The highest $nCeO_2$ (2000 mg l^{-1}) reached a low concentration of ATP in roots, statistically comparable to control samples. On the contrary, $nTiO_2$ induce no significant changes of ATP concentration, since different $nTiO_2$ doses were similar to the controls in both roots and shoots (**Figure 4**).

The measurement of ROS was performed as marker for oxidative stress. Similarly to ATP content, $nCeO_2$ were able to induce an increase of a ROS formation at all the concentrations assayed (**Figure 5**), in comparison with the control, although no statistically significant differences were observed. Also for this parameter, a trend with a peak at 500 mg l^{-1} was present in both roots and shoots. In the case of $nTiO_2$ (**Figure 5**), the treatments did not show any difference, if compared with the control in roots, whereas a decrease of ROS level was observed at the higher dose (2000 mg l^{-1}) in shoots.

Mitotic Index and RAPDs

The mitotic index was significantly reduced by $nCeO_2$ 2000 mg l^{-1} (from 4 ± 1.2% in the control to 2.4 ± 1.2%). Instead, the $nCeO_2$ 500 and 1000 mg l^{-1} treatments with mean values of 4 ± 1.3% were very similar to the control (**Figure 6A**). The treatments with $nTiO_2$ with values of 6.2 ± 3.2%, 4.6 ± 3.2%, 4.9 ± 2.5% for the concentration at 500, 1000, and 2000 mg l^{-1}, respectively, were not significantly different from the control (4.9 ± 2.8%; **Figure 6A**).

The six primers used for the RAPD analysis amplified for a total of 40 representative bands in controls with a variable number of 3 to 9 (9, 5, 6, 3, 9, 8, bands, respectively, for OPA04, OPB01, OPA10, OPB20, OPB12, and OPB03). Amplification was highly reproducible since the same RAPD profile was observed within control replicates. A concentration effect was observed for the $nCeO_2$ treatments on the RAPD profiles. The same banding pattern as controls was obtained for the $nCeO_2$ 500 mg l^{-1} treatment, whereas new profiles at 1000 mg l^{-1} were observed and three additional bands appeared and eight disappeared. Even greater variability was observed at $nCeO_2$ 2000 mg l^{-1} with a total of 20 differences (appearing and disappearing bands) in treated plants (**Figures 6B,C**). The results were summarized by Principal Coordinates Analysis (PCoA), with almost 94% of the total variability explained by the two axes (**Figure 6D**). The overlap of the control and 500 mg l^{-1} treatments is notable, while the treatments at 1000 and 2000 mg l^{-1} are well separated in different quadrants. The band polymorphism in the different replicates at the higher concentration (2000 mg l^{-1}) can be noticed by the point cloud (**Figure 6D**). In a similar way to what was observed fro the mitotic index, the $nTiO_2$ treatments at each concentration have no effect on the RAPD profiles (**Figure 6D**).

DISCUSSION

Since plant nanotoxicology is a new field of investigation, specific ecotoxicological methods for the estimation of toxicity of ENPs have not yet been developed (Jośko and Oleszczuk, 2014). According to OECD guidelines, the acute effects of MeNPs on plant physiology are currently investigated by adapting the methods already used for traditional contaminants (Kühnel and Nickel, 2014). Evidence of MeNPs plant uptake and toxicity are still scarce and contradictory (Etheridge et al., 2013). This is likely because, compared to their bulk counterparts, MeNPs show particular properties, which are subjected to transformations (e.g., redox reactions, aggregation or agglomeration, and dissolution) according to different environmental factors. These

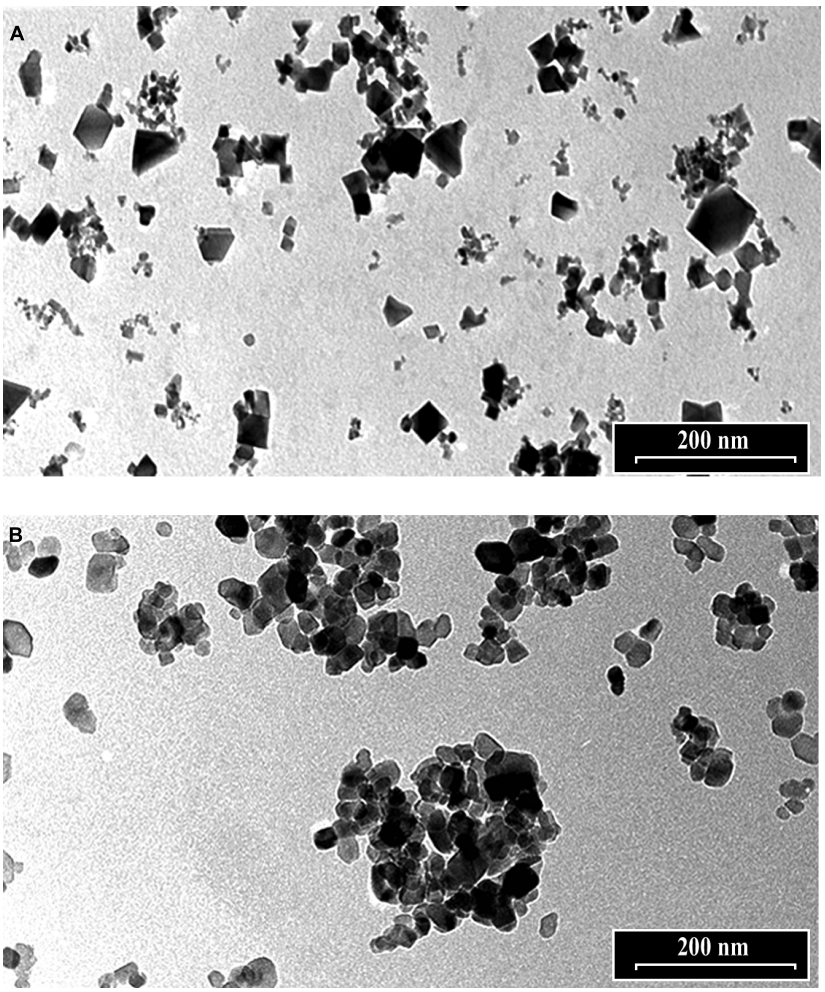

FIGURE 1 | Transmission electron microscope images of 1000 mg l^{-1} suspensions of (A) *n*CeO_2 and (B) *n*TiO_2.

changes might modify the ecotoxicological properties of MeNPs and thus, their interactions with the biota (Nowack et al., 2012; Maurer-Jones et al., 2013). However, despite these limitations, the experimental results obtained so far offer early indications on MeNPs phytotoxicity (Li et al., 2015; Rico et al., 2015a). Our data suggests that also in very simple experimental conditions, *n*TiO_2, as expected taking into account their intrinsic properties, forms bigger agglomerates with a wider dimensional distribution than *n*CeO_2.

nCeO_2 and *n*TiO_2 Affects Seed Germination and Seedling Development

Previous studies carried out in controlled conditions reported that the toxicity of MeNPs in the early stages of plant growth is likely due to the following factors: (i) chemical and physical properties which influence the release of ions or the aggregation of particles in more stable forms and (ii) the size and shape of the particles, which determine the specific surface area of MeNPs (Yang and Watts, 2005; Lin and Xing, 2007).

In agreement with Rico et al. (2015b), we found that germination of barley was unaffected by 500–2000 mg l^{-1} *n*CeO_2. This is in contrast with the results provided by López-Moreno et al. (2010a) who reported that suspensions of 2000 mg l^{-1} *n*CeO_2 significantly reduced seed germination in maize, cucumber, tomato, and soybean. Possible explanations could be the greater Ce tolerance of barley to the treatment if compared to other species and/or to the very small size of Ce NPs they used (7 nm). Another explanation could be related to the chemical and physical properties of *n*CeO_2, in particular his zeta potential value. This parameter is the cause of the agglomeration behavior of the *n*CeO_2 that brings to a low bioavailability and the absence of phytotoxic effects on the treated seeds regards the germination percentage.

Another important issue that plays a role on seed/NP interaction, is the methodology adopted for seed treatment. In fact, following Lin and Xing (2007), we prepared the barley seeds for germination trials by soaking them in distilled water before starting treatments, whereas López-Moreno et al. (2010a)

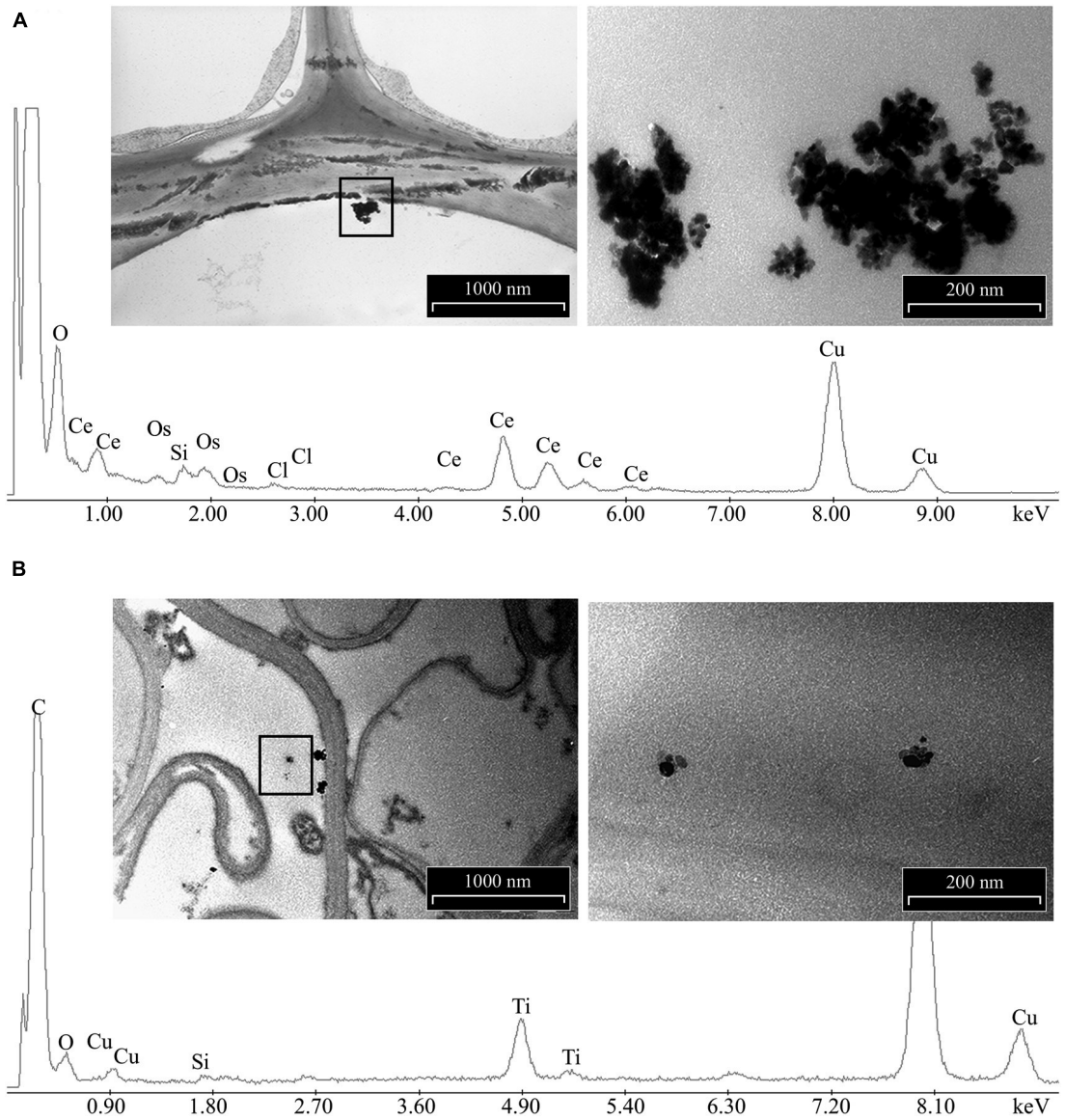

FIGURE 2 | Representative images of electron dense precipitates recovered in root tissues of *Hordeum vulgare* exposed to 1000 mg l^{-1} of (A) $nCeO_2$ and (B) $nTiO_2$ and X-ray spectra of elements recovered in. Insets represent enlarged regions where X-ray microanalyses have been performed. Presence of C, Os were due to sample preparation, Cu to the grids used as section support.

soaked the seeds directly in the $nCeO_2$ suspensions. This different experimental approach could result in a different exposure of germinating seeds to $nCeO_2$.

As regards Ti, there is a substantial agreement in literature on the fact that suspensions of $nTiO_2$ do not affect seed germination, with few exceptions, as reported by Zheng et al. (2005) and Feizi et al. (2012). Our results are in accordance with those reported by other authors on rice, lettuce, radish, cucumber, tomato, and pea (Boonyanitipong et al., 2011; Wu et al., 2012; Song et al., 2013a; Fan et al., 2014).

Besides the germination percentage, we observed a negative influence of the treatments with $nCeO_2$ and $nTiO_2$ on root elongation in barley seedlings. However, this did not occur in seedlings treated with $nCeO_2$ at the highest concentration, in which the root length was very similar to controls. In addition, in this case the literature reports contradictory evidence. López-Moreno et al. (2010a) reported that the root growth in maize and cucumber seedlings was significantly promoted by $nCeO_2$ (up to 4000 mg l^{-1}) whereas the same treatments resulted in a negative effect on root development in alfalfa and tomato. An inhibitory effect of $nTiO_2$ on root elongation in cucumber was reported by Mushtaq (2011). A decrease in the number of secondary lateral roots in pea seedlings was verified by Fan et al. (2014), whereas Boonyanitipong et al. (2011) did not record any effect on root length in rice seedlings exposed to $nTiO_2$. In our case, the different effect of the $nCeO_2$ and $nTiO_2$ on the root

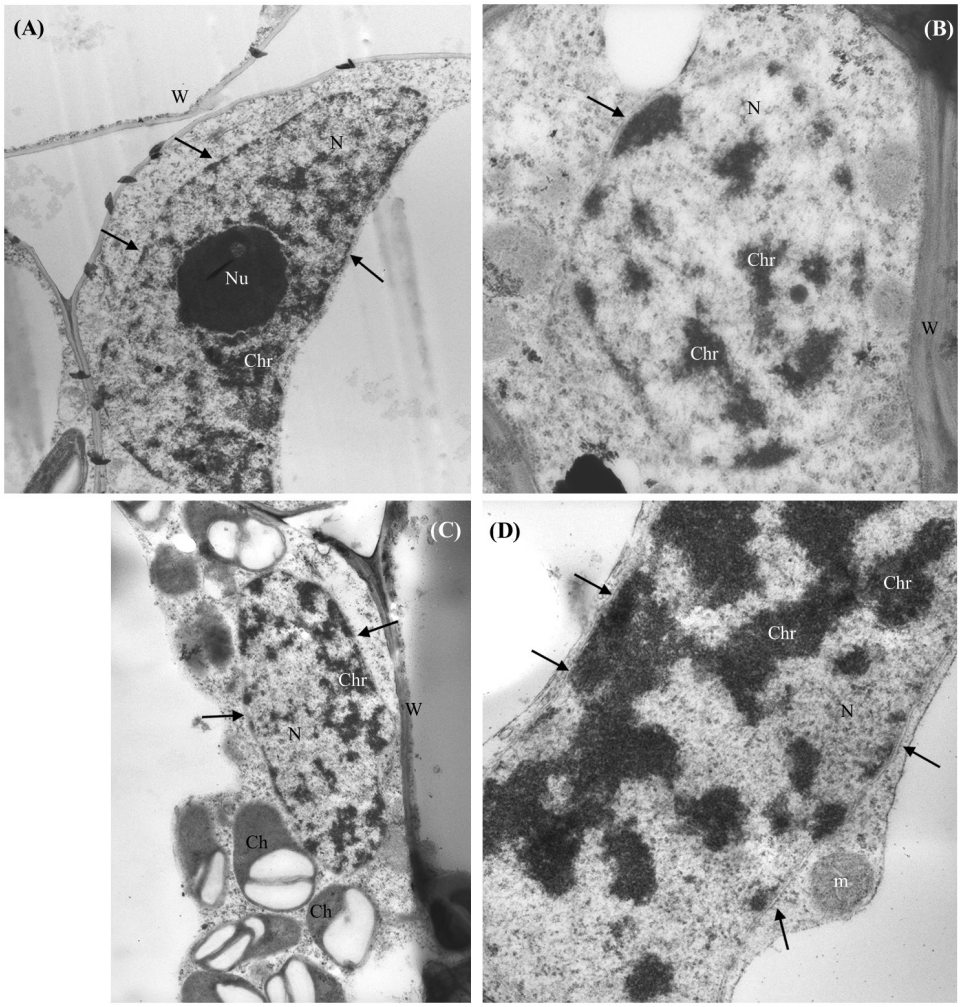

FIGURE 3 | Representative micrographs of nuclei (N) from shoot (A–C) and root (D) parenchymal cells of *Hordeum vulgare*. (A) Control untreated shoot: nucleus presents regular shape, nuclear membranes are intact (arrows), nucleolus (Nu) and chromatin (Chr) appear normally dispersed. **(B,C)** 1000 mg nCeO$_2$ l^{-1}-treated shoot and **(D)**, 1000 mg nCeO$_2$ l^{-1}- treated root: nuclei still present normal shape and apparently undamaged membranes, while chromatin shows condensation. Ch, chloroplasts; m, mitochondrion.

elongation is likely due to their different grade of agglomeration demonstrated by the z-average size and PDI values of nTiO$_2$ that results significantly higher than nCeO$_2$.

It might happen that the quantification analysis of trace metals in plant roots is disturbed by external contamination. In this case, the concentration of the element in the plant tissues could be significantly overestimated due to a fraction of metal, which is not taken up but simply adsorbed onto the external root surface. In our experiment, a concentration of Ce about 60 times greater than Ti, was found in barley root tissues. This substantial difference indicates that the procedures for preparation of the samples were conducted properly; otherwise, we would also have very high concentrations also for Ti.

Our results showed that the exposure of *H. vulgare* to nCeO$_2$, which are smaller and less aggregated than nTiO$_2$, resulted in a greater total Ce concentration in roots compared to Ti. In can therefore be assumed that, for some still unknown reasons, the model of root uptake of the two elements could differ, depending in part on the intrinsic properties of solubility and agglomeration properties of nCeO$_2$ and nTiO$_2$. On the other hand, this is in agreement with the findings by Zhang et al. (2011), who verified that cucumber roots absorbed higher amounts of 7 nm nCeO$_2$ than 25 nm ones. On the other, some studies pointed out the possibility of interactions between the root metabolism and MeNPs. Lin and Xing (2007) demonstrated that root exudates such as proteins, phenolic acids, and aminoacids have a role in the adsorption of ZnO NPs to the root surface of perennial ryegrass. More recently, Schwabe et al. (2015) observed that root uptake of dissolved Ce$^{(III)}$ was promoted by the dissolution of nCeO$_2$ at the medium-root interface in hydroponically growth sunflower and maize. A further confirmation about the role of root exudates on the adsorption of MeNPs was provided by Lv et al. (2015) and Ma et al. (2015), respectively, for nCeO$_2$ and nZnO, respectively. However, Lv et al. (2015) reported that a

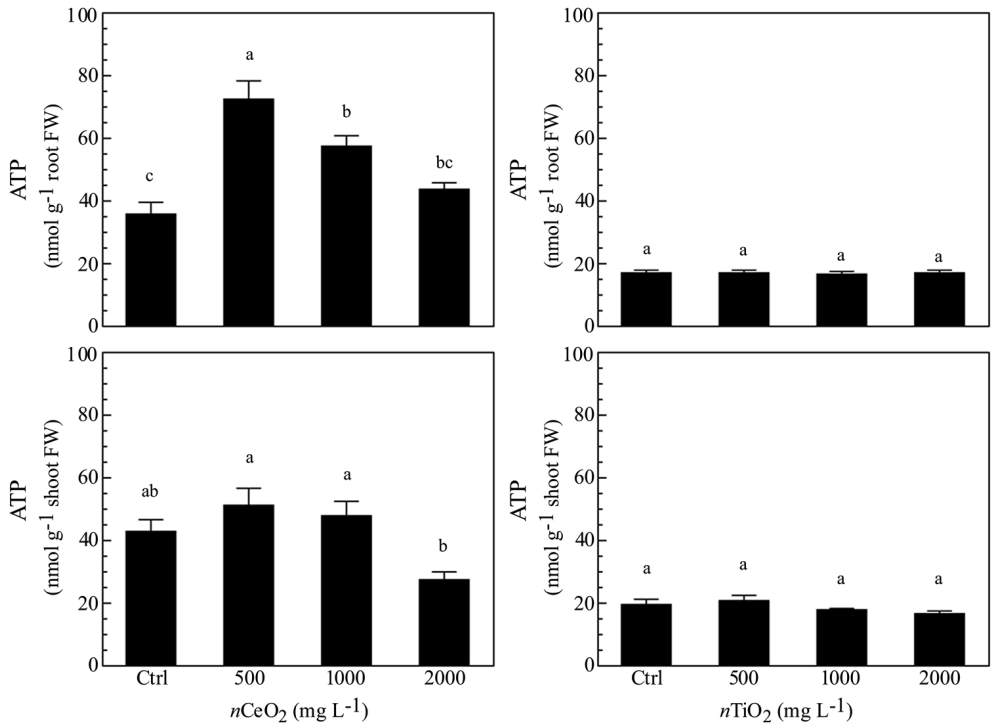

FIGURE 4 | Determination of ATP concentration in extracts obtained from plantlets of barley roots and shoots, grown on wet paper filters, in the presence of different concentrations of $nCeO_2$ and $nTiO_2$.

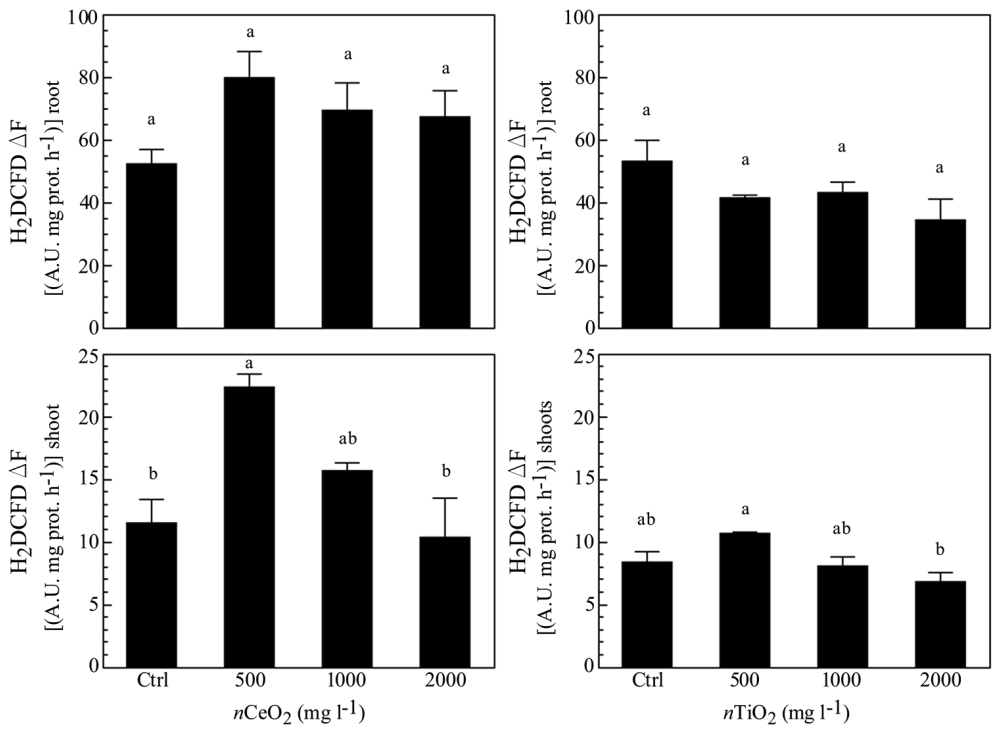

FIGURE 5 | Evaluation of reactive oxygen species (ROS) evolution in extracts obtained from plantlets of barley roots and shoots, grown on wet paper filters, in the presence of different concentrations of $nCeO_2$ and $nTiO_2$. The analysis was performed by means of a fluorimetric probe.

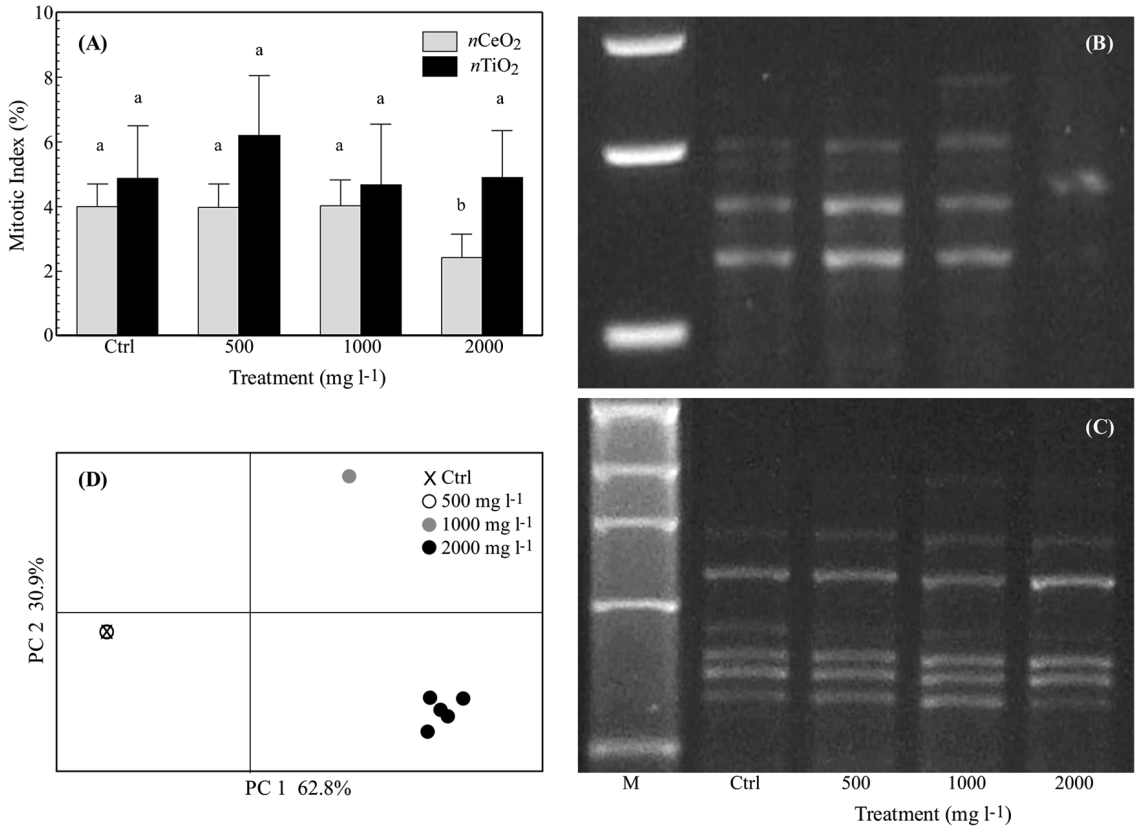

FIGURE 6 | (A) Mitotic index (%; mean ± SE) observed in root tips of seedlings of barley treated with 0–2000 mg l^{-1} of nCeO$_2$ and nTiO$_2$. Different letters indicate statistical difference between treatments at Tuckey's test ($p < 0.05$). **(B,C)** Representative RAPD profiles from the roots of barley seedlings treated with nCeO$_2$ **(B)** or nTiO$_2$ **(C)** at control, 500-2000 mg l^{-1}. The shown RAPD profiles were generated using primer OPA04 for nCeO$_2$ (it is shown an enlargement around polymorphic zone) and OPB12 for nTiO$_2$. The first line is a 1 kb DNA marker (M). **(D)** Principal coordinate analysis (PCoA) based on RAPD profiles from the barley roots with nCeO$_2$. Values on axes indicate the variance explained.

possible access of nZnO to the root tissues could be through the root apex or the meristematic zone to the lateral root system where the Casparian strip is not yet developed.

Root-to-shoot translocation of nCeO$_2$ has been previously described in soybean (Priester et al., 2012), tomato (Wang et al., 2012), cucumber (Zhao et al., 2013), and cotton (Van Nhan et al., 2015) after treatments with nCeO$_2$ suspensions. Different observations have been made on nCeO$_2$ root-to-shoot translocation in graminaceous crops. Schwabe et al. (2013) reported that wheat does not translocate nCeO$_2$ into the aerial tissues, whereas Rico et al. (2013, 2015a) reported the translocation of nCeO$_2$ from roots to rice grains and maize kernels, respectively. According to Rico et al. (2015b), we report evidence of Ce translocation from roots to the aerial part of barley. As regards Ti uptake and translocation, fewer data are available in the literature compared. However, our data are consistent with the findings reported by Song et al. (2013b) on tomato seedlings exposed to Ti at concentrations ranging from 50 to 5000 mg l^{-1}.

Finally, we reported that root length in barley seedlings treated with 500 mg nCeO$_2$ l^{-1} was significantly shorter than controls. This apparent dose-effect was not confirmed at higher nCeO$_2$ concentrations, since the root length was similar to that of controls. Similar evidence was reported by López-Moreno et al. (2010a). According to Nascarella and Calabrese (2012) and Bell et al. (2014), such unexpected results might be interpreted as a hormetic effect of nCeO$_2$ on root elongation in barley seedlings.

Plant Stress Induced by Nanoparticle Treatments

Within the plants, NPs may interact with the host cells, causing different effects, ranging from cell death (if the host is sensitive) to not relevant cell modifications (in the case of host tolerance), depending on their type, shape, and concentration (Rico et al., 2011; Gardea-Torresdey et al., 2014). The microscopic observations on barley seedlings indicated that both nCeO$_2$ and nTiO$_2$, at the used concentrations used, were able to enter the root tissues, being detected in the parenchymal cells and xylem vessels. Even though we did not observe Ce and Ti crystalline aggregates in the shoots, ICP analyses suggested a root-to-shoot mobilization of Ce and Ti ions. At histological level the accumulation of such elements induced limited injuries. On the contrary, important differences in the effects of treatments were obtained at nuclear level, where

only the nCeO$_2$ treatments induced visible modifications in the chromatin aggregation in the nuclei of root and shoot parenchymal cells.

Condensed chromatin and fragmented nuclei are described as part of the programmed cell death (PCD), occurring in response to different environmental stimuli and stresses, induced by pathogens (Lam et al., 2001) and by diverse abiotic factors (White, 1996; Kratsch and Wise, 2000) including the exposition to nanomaterials (Shen et al., 2010). PCD plays an important role in mediating plant adaptation to the environment. In cells that undergo programmed death, chromatin condenses into masses with sharp margins, and DNA is hydrolyzed into a series of fragments (Gladish et al., 2006). Dynamic compaction of chromatin is an important step in the DNA-damage response, because it activates DNA-damage-repair signaling (Burgess et al., 2014) in response to injuries.

The hypothesis of Ce-induced DNA damage in treated seedlings finds further support in the results obtained with the RAPD test. RAPD can potentially detect a broad range of DNA damage and mutations, so it is suitable for studying MeNPs genotoxicity (Atienzar and Jha, 2006). The RAPD modified patterns at high concentrations of nCeO$_2$ (1000–2000 mg l^{-1}) indicated a genotoxic effect, which could directly influence the cell cycle. This is further confirmed by the reduced mitotic index recorded in the samples treated with nCeO$_2$ 2000 mg l^{-1}, which clearly demonstrated the negative effect of high nCeO$_2$ concentrations on the cell cycle. Our results are in agreement with López-Moreno et al. (2010b), who demonstrated nCeO$_2$ genotoxicity on soybean plants subjected to treatments similar to those reported in our work.

It is still far too early to conclude if the observed effects were direct or indirect consequences of the treatments, since nCeO$_2$ were not found in the nucleus. As it is known that increasing oxidative stress leads to DNA damage, the higher presence of ROS in treated samples could cause modification in RAPD patterns. However, as our analysis on ROS indicated a peak at 500 mg nCeO$_2$ l^{-1}, it can be rationalized that lower concentrations triggered an initial oxidative signal, while only higher nCeO$_2$ doses were able to induce damage at nuclear level. The oxidative stress peak at 500 mg l^{-1} dose and could be rationalized by the well-known SOD mimetic activity attributable to nCeO$_2$, which could cause a dismutation of superoxide anions into H_2O_2. Since a similar pattern is also found for ATP measured in nCeO$_2$ treated tissues, it is suggested that the oxidative burst induced by the more effective dose of nCeO$_2$ could be associated to a stimulation of cellular respiration and a consequent increase in ATP production. This could be due to a defense response signal or an increased requirement for energy (Vranová et al., 2002).

On the contrary, the nTiO$_2$ treatments did not influence either the mitotic index or RAPD pattern. This is in contrast to Moreno-Olivas et al. (2014) who observed nTiO$_2$-induced genotoxicity in hydroponically cultivated zucchini. As the size of nTiO$_2$ they reported is comparable to that used in our work, the different results obtained can be explained by (i) the different cultivation systems (Petri dishes vs. full nutrient solution in hydroponics) and (ii) the nTiO$_2$ concentration used by Moreno-Olivas et al. (2014; 10-fold smaller). The latter potentially prevents the formation of big NP agglomerates, making them more bioavailable.

CONCLUSION

Although investigations into the effects of NPs in plants continue to increase, there are still many unresolved issues and challenges, in particular at the biota-nanomaterial interface (Nowack et al., 2015). In this multidisciplinary work, we studied the phytotoxic and genotoxic impact of nCeO$_2$ and nTiO$_2$ cerium and titanium oxide NP suspensions on the early growth of barley. Seed germination was not affected by the nCeO$_2$ and nTiO$_2$ suspensions, indicating that nCeO$_2$ and nTiO$_2$ are not allowed to enter the seed coatings. However, we verified that the concentration of Ce and Ti in the seedling fractions, as well as the root-to-shoot translocation, were dose-dependent. Then, we found signals of genotoxicity (RAPD banding patterns and mitotic index) and phytotoxicity in root cells (oxidative stress and chromatin modifications) resulting in a shortage of root elongation.

The different magnitude of bioaccumulation of Ce and Ti suggests a different uptake mechanism, likely due to the different behavior of nCeO$_2$ and nTiO$_2$. Recent studies have shown that plant toxic effects of nanomaterials are not merely due to the particle size and concentration of a suspension. Phytotoxicity of metal oxide NPs is related both to the direct adsorption of particles onto the root structures and to the aptitude of the metal ion to dissolve, possibly mediated by binding molecules produced by plants in the medium-root interface.

Our study had not the objective to investigate the details of the mechanisms by which the NPs entering within the roots. However, we verified the presence of both nCeO$_2$ and nTiO$_2$ into the root cells where an increase in oxidative stress occurred. More research needs to be conducted to verify whether germination can be affected by smaller nCeO$_2$ and nTiO$_2$. In addition, we need to understand if modification of the physical–chemical properties of NPs at the root interface can foster the plant uptake of Ce and Ti forms.

AUTHOR CONTRIBUTIONS

AM conducted the experiments. AF and AB provided the biochemical parameters. FP performed out the ICP and RAPD analysis. RM made TEM observation and observed MeNPs distribution *in planta*. CG and MS carried out TEM–EDAX observations. MV contributed to the mitotic index. LM designed, coordinated the study, performed statistical analysis, and prepared the figures. All authors were involved in manuscript writing. All authors contributed to the revision of the manuscript.

ACKNOWLEDGMENTS

This work was in part supported by a project funded by DISA – Department of Agriculture and Environmental Sciences, University of Udine, through Grant n.64 dd. 08-09.2014 (RANDOLPH – Relazioni tra nanoparticelle metalliche e piante superiori). The authors acknowledge technical assistance in the use of BET by Anastasios Papadiamantis and access to the lab facilities of the Environmental Nanoscience research group at Birmingham University (UK). The authors also thank Francesco Bertolini and Nicola Zorzin for their relevant contribution to the work.

REFERENCES

Atha, D. H., Wang, H., Petersen, E. J., Cleveland, D., Holbrook, D., Jaruga, P., et al. (2012). Copper oxide nanoparticle mediated DNA damage in terrestrial plant models. *Environ. Sci. Technol.* 46, 1819–1827. doi: 10.1021/es202660k

Atienzar, F. A., and Jha, A. N. (2006). The random amplified polymorphic DNA (RAPD) assay and related techniques applied to genotoxicity and carcinogenesis studies: a critical review. *Mutat. Res.* 613, 76–102. doi: 10.1016/j.mrrev.2006.06.001

Bell, I. R., Ives, J. A., and Jonas, W. B. (2014). Nonlinear effects of nanoparticles: biological Variability from Hormetic Doses, small particle sizes, and dynamic adaptive interactions. *Dose Response* 12, 202–232. doi: 10.2203/dose-response.13-025.Bell

Boonyanitipong, B., Kositsup, B., Kumar, P., Baruah, S., and Dutta, J. (2011). Toxicity of ZnO and TiO_2 nanoparticles on germinating rice seed *Oryza sativa* L. *Int. J. Biosci. Biochem. Bioinform.* 1, 282–285. doi: 10.7763/IJBBB.2011.V1.53

Bradford, M. (1976). A rapid and sensitive method for the quantitation of microgram quantities of protein utilizing the principle of protein-dye binding. *Anal. Biochem.* 72, 248–254. doi: 10.1016/0003-2697(76)90527-90523

Burgess, R. C., Burman, B., Kruhlak, M. J., and Misteli, T. (2014). Activation of DNA damage response signaling by condensed chromatin. *Cell Rep.* 9, 1703–1717. doi: 10.1016/j.celrep.2014.10.060

Clément, L., Hurel, C., and Marmier, N. (2013). Toxicity of TiO_2 nanoparticles to cladocerans, algae, rotifers and plants – Effects of size and crystalline structure. *Chemosphere* 90, 1083–1090. doi: 10.1016/j.chemosphere.2012.09.013

Colman, B. P., Arnaout, C. L., Anciaux, S., Gunsch, G. K., Hochella, M. F. Jr., Kim, B., et al. (2013). Low concentrations of silver nanoparticles in biosolids cause adverse ecosystem responses under realistic field scenario. *PLoS ONE* 8:e57189. doi: 10.1371/journal.pone.0057189

Etheridge, M. L., Campbell, S. A., Erdman, A. G., Haynes, C. L., Wolf, S. M., and McCullough, J. (2013). The big picture on nanomedicine: the state of investigational and approved nanomedicine products. *Nanomed. Nanotechnol. Biol. Med.* 9, 1–14. doi: 10.1016/j.nano.2012.05.013

Fan, R., Huang, Y. C., Grusak, M. A., Huang, C. P., and Sherrier, D. J. (2014). Effects of nano-TiO(2) on the agronomically-relevant Rhizobium-legume symbiosis. *Sci. Total Environ.* 466–467, 503–512. doi: 10.1016/j.scitotenv.2013.07.032

FAOSTAT (2014). *Food and Agricultural Commodities Production: Commodities by Regions*. Available at: http://faostat3.fao.org/faostat-gateway/go/to/browse/ranking/commodities_by_regions/E [accessed Sept 4, 2015]

Feizi, H., Moghaddam, P. R., Shahtahmassebi, N., and Fotovat, A. (2012). Impact of bulk and nanosized titanium dioxide (TiO_2) on wheat seed germination and seedling growth. *Biol. Trace Elem. Res.* 146, 101–106. doi: 10.1007/s12011-011-9222-7

Gardea-Torresdey, J. L., Rico, C. M., and White, J. C. (2014). Trophic transfer, transformation and impact of engineered nanomaterials in terrestrial environments. *Environ. Sci. Technol.* 48, 2526–2540. doi: 10.1021/es4050665

Gladish, D. K., Xu, J., and Niki, T. (2006). Apoptosis-like programmed cell death occurs in procambium and ground meristem of Pea (*Pisum sativum*) root tips exposed to sudden flooding. *Ann. Bot.* 97, 895–902. doi: 10.1093/aob/mcl040

Gogos, A., Knauer, K., and Bucheli, T. D. (2012). Nanomaterials in plant protection and fertilization: current state, foreseen applications, and research priorities. *J. Agric. Food Chem.* 60, 9781–9792. doi: 10.1021/jf302154y

Hong, J., Peralta-Videa, J. R., and Gardea-Torresdey, J. L. (2013). "Nanomaterials in agricultural production: benefits and possible threats?" in *Sustainable Nanotechnology and the Environment: Advances and Achievements,* eds N. Shamim and V. K. Sharma, *ACS Symposium Series* (Washington, DC: American Chemical Society).

Jośko, I., and Oleszczuk, P. (2014). Phytotoxicity of nanoparticles—problems with bioassay choosing and sample preparation. *Environ. Sci. Pollut. Res.* 21, 10215–10224. doi: 10.1007/s11356-014-2865-0

Keller, A., McFerran, S., Lazareva, A., and Suh, S. (2013). Global life cycle releases of engineered nanomaterials. *J. Nanopart. Res.* 15, 1692. doi: 10.1007/s11051-013-1692-4

Knipfer, T., and Fricke, W. (2011). Water uptake by seminal and adventitious roots in relation to whole-plant water flow in barley (*Hordeum vulgare* L.). *J. Exp. Bot.* 62, 717–733. doi: 10.1093/jxb/erq312

Kratsch, H. A., and Wise, R. R. (2000). The ultrastructure of chilling stress. *Plant Cell Environ.* 23, 337–350. doi: 10.1046/j.1365-3040.2000.00560.x

Kühnel, D., and Nickel, C. (2014). The OECD expert meeting on ecotoxicology and environmental fate — Towards the development of improved OECD guidelines for the testing of nanomaterials. *Sci. Tot. Environ.* 472, 347–353. doi: 10.1016/j.scitotenv.2013.11.055

Lam, E., Kato, N., and Lawton, M. (2001). Programmed cell death, mitochondria and the plant hypersensitive response. *Nature* 411, 848–853. doi: 10.1038/35081184

Li, K.-E., Chang, Z.-Y., Shen, C.-X., and Yao, N. (2015). "Toxicity of nanomaterials to plants," in *Nanotechnology and Plant Sciences*, eds M. H. Siddiqui, M. H. Al-Whaibi, and F. Mohammad (Cham: Springer International Publishing), 101–124.

Lin, D., and Xing, B. (2007). Phytotoxicity of nanoparticles: inhibition of seed germination and root growth. *Environ. Pollut.* 150, 243–250. doi: 10.1016/j.envpol.2007.01.016

Liu, H. H., and Cohen, Y. (2014). Multimedia environmental distribution of engineered nanomaterials. *Environ. Sci. Technol.* 48, 3281–3292. doi: 10.1021/es405132z

López-Moreno, M. L., de La Rosa, G., Hernández-Viezcas, J. A., Peralta-Videa, J. R., and Gardea-Torresdey, J. L. (2010a). X-ray Absorption Spectroscopy (XAS) corroboration of the uptake and storage of CeO_2 nanoparticles and assessment of their differential toxicity in four edible plant species. *J. Agric. Food Chem.* 58, 3689–3693. doi: 10.1021/jf904472e

López-Moreno, M. L., de la Rosa, G., Hernandez-Viezcas, J. A., Castillo-Michel, H., Botez, C. E., Peralta-Videa, J. R., et al. (2010b). Evidence of the differential biotransformation and genotoxicity of ZnO and CeO_2 nanoparticles on soybean (*Glycine max*) plants. *Environ. Sci. Technol.* 44, 7315–7320. doi: 10.1021/es903891g

Lundin, A. (1984). *Extraction and Automatic Luminometric Assay of ATP, ADP and AMP*. New York: Academic Press.

Lv, J., Zhang, S., Luo, L., Zhang, J., Yang, K., and Christie, P. (2015). Accumulation, speciation and uptake pathway of ZnO nanoparticles in maize. *Environ. Sci. Nano* 2, 68–77. doi: 10.1039/c4en00064a

Ma, Y., Zhang, P., Zhang, Z., He, X., Zhang, J., Ding, Y., et al. (2015). Where does the transformation of precipitated ceria nanoparticles in hydroponic plants take place? *Environ. Sci. Technol.* 49, 10667–10674. doi: 10.1021/acs.est.5b02761

Maurer-Jones, M. A., Gunsolus, I. L., Murphy, C. J., and Haynes, C. L. (2013). Toxicity of engineered nanoparticles in the environment. *Anal. Chem.* 85, 3036–3049. doi: 10.1021/ac303636s

Miralles, P., Church, T. L., and Harris, A. T. (2012). Toxicity, Uptake, and Translocation of engineered nanomaterials in vascular plants. *Environ. Sci. Technol.* 46, 9224–9239. doi: 10.1021/es202995d

Moreno-Olivas, F., Gant, V. U. Jr., Johnson, K. L., Peralta-Videa, J. R., and Gardea-Torresdey, J. L. (2014). Random amplified polymorphic DNA reveals that TiO2 nanoparticles are genotoxic to *Cucurbita pepo*. *J. Zhejiang Univ. Sci. A* 15, 618–623. doi: 10.1631/jzus.A1400159

Mushtaq, Y. K. (2011). Effect of nanoscale $Fe3O_4$, TiO_2 and carbon particles on cucumber seed germination. *J. Environ. Sci. Health A* 46, 1732–1735. doi: 10.1080/10934529.2011.633403

Nascarella, M. A., and Calabrese, E. J. (2012). A method to evaluate hormesis in nanoparticle dose-response. *Dose Response* 10, 344–354. doi: 10.2203/dose-response.10-025

Navarro, E., Baun, A., Behra, R., Hartmann, N. B., Filser, J., Miao, A.-J., et al. (2008). Environmental behavior and ecotoxicity of engineered nanoparticles to algae, plants, and fungi. *Ecotoxicology* 17, 372–386. doi: 10.1007/s10646-008-0214-0

Nowack, B., Baalousha, M., Bornhöft, N., Chaudhry, O., Cornelis, G., Cotterill, J., et al. (2015). Progress towards the validation of modelled environmental concentrations of engineered nanomaterials by analytical measurements. *Environ. Sci. Nano* 2, 421–428. doi: 10.1039/c5en00100e

Nowack, B., Ranville, J. F., Diamond, S., Gallego-Urea, J. A., Metcalfe, C., Rose, J., et al. (2012). Potential scenarios for nanomaterial release and subsequent alternation in the environment. *Environ. Toxicol. Chem.* 31, 50–59. doi: 10.1002/etc.726

OECD (2010). *List of Manufactured Nanomaterials and List of Endpoints for Phase One of the Sponsorship Programme for the Testing of Manufactured Nanomaterials: Revision*. Paris: OECD Environment, Health and Safety Publications Series on the Safety of Manufactured Nanomaterials.

Parisi, C., Vigani, M., and Rodríguez-Cerezo, E. (2015). Agricultural nanotechnologies: what are the current possibilities? *Nano Today* 10, 124–127. doi: 10.1016/j.nantod.2014.09.009

Peakall, R., and Smouse, P. E. (2012). GenAlEx 6.5: genetic analysis in Excel. Population genetic software for teaching and research – an update. *Bioinformatics* 28, 2537–2539. doi: 10.1093/bioinformatics/bts460

Piccinno, F., Gottschalk, F., Seeger, S., and Nowack, B. (2012). Industrial production quantities and uses of ten engineered nanomaterials in Europe and the world. *J. Nanopart. Res.* 14, 1109. doi: 10.1007/s11051-012-1109-9

Priester, J. H., Ge, Y., Mielke, R. E., Horst, A. M., Moritz, S. C., Espinosa, K., et al. (2012). Soybean susceptibility to manufactured nanomaterials with evidence for food quality and soil fertility interruption. *Proc. Natl. Acad. Sci. U.S.A.* 109, E2451. doi: 10.1073/pnas.1205431109

Rico, C., Morales, M., Barrios, A., McCreary, R., Hong, J., Lee, W., et al. (2013). Effect of cerium oxide nanoparticles on the quality of rice (*Oryza sativa* L.) grains. *J. Agric. Food Chem.* 61, 11278–11285. doi: 10.1021/jf404046v

Rico, C. M., Majumdar, S., Duarte-Gardea, M., Peralta-Videa, J. R., and Gardea-Torresdey, J. L. (2011). Interaction of nanoparticles with edible plants and their possible implications in the food chain. *J. Agric. Food Chem.* 59, 3485–3498. doi: 10.1021/jf104517j

Rico, C. M., Peralta-Videa, J. R., and Gardea-Torresdey, J. L. (2015a). "Chemistry, biochemistry of nanoparticles, and their role in antioxidant defense system in plants," in *Nanotechnology and Plant Sciences*, eds M. H. Siddiqui, M. H. Al-Whaibi, and F. Mohammad (Cham: Springer International Publishing), 1–18.

Rico, C. M., Peralta-Videa, J. R., and Gardea-Torresdey, J. L. (2015b). Differential effects of cerium oxide nanoparticles on rice, wheat, and barley roots: a Fourier Transform Infrared (FT-IR) microspectroscopy study. *Appl. Spectrosc.* 69, 287–295. doi: 10.1366/14-07495

Roco, M. M. (2011). The long view of nanotechnology development: the National Nanotechnology Initiative at 10 years. *J. Nanopart. Res.* 13, 427–445. doi: 10.1007/s11051-010-0192-z

Schneider, C. A., Rasband, W. S., and Eliceiri, K. W. (2012). NIH Image to ImageJ: 25 years of image analysis. *Nat. Methods* 9, 671–675. doi: 10.1038/nmeth.2089

Schwabe, F., Schulin, R., Limbach, L. K., Stark, W., and Burge, D. (2013). Influence of two types of organic matter on interaction of CeO_2 nanoparticles with plants in hydroponic culture. *Chemosphere* 91, 512–520. doi: 10.1016/j.chemosphere.2012.12.025

Schwabe, F., Tanner, S., Schulin, R., Rotzetter, A. C., Stark, W. J., Von Quadt, A., et al. (2015). Dissolved cerium contributes to uptake of Ce in presence of differently sized CeO_2-nanoparticles by three crop plants. *Metallomics* 7, 466–477. doi: 10.1039/c4mt00343h

Shen, C. S., Zhang, Q.-F., Li, J., Bi, F.-C., and Yan, N. (2010). Induction of programmed celle death in *Arabidopsis* and rice by single-wall carbon nanotubes. *Am. J. Bot.* 97, 1602–1609. doi: 10.3732/ajb.1000073

Song, U., Jun, H., Waldman, B., Roh, J., Kim, Y., Yi, J., et al. (2013a). Functional analysis of nanoparticle toxicity: a comparative study of the effects of TiO2 and Ag on tomatoes (Lycopersicon esculentum). *Ecotoxicol. Environ. Safe.* 93, 60–67. doi: 10.1016/j.ecoenv.2013.03.033

Song, U., Shin, M., Lee, G., Roh, J., Kim, Y., and Lee, E. J. (2013b). Functional Analysis of TiO2 Nanoparticle toxicity in three plant species. *Biol. Trace Elem. Res.* 155, 93–103. doi: 10.1007/s12011-013-9765-x

USEPA (1995). *EPA Method 3052: Microwave Assisted Acid Digestion of Siliceous and Organically Based Matrices*, 3rd Edn. Washington, DC: Test Methods for Evaluating Solid Waste.

Van Hoecke, K., Quik, J. T., Mankiewicz-Boczek, J., De Schamphelaere, K. A., Elsaesser, A., Van der Meeren, P., et al. (2009). Fate and effects of CeO_2 nanoparticles in aquatic ecotoxicity tests. *Environ. Sci. Technol.* 15, 4537–4546. doi: 10.1021/es9002444

Van Nhan, L., Ma, C., Rui, Y., Liu, S., Li, X., Xing, B., et al. (2015). Phytotoxic mechanism of nanoparticles: destruction of chloroplasts and vascular bundles and alteration of nutrient absorption. *Sci. Rep.* 5, 11618. doi: 10.1038/srep 11618

Vranová, E., Inzé, D., and Van Breusegem, F. (2002). Signal transduction during oxidative stress. *J. Exp. Bot.* 53, 1227–1236. doi: 10.1093/jexbot/53.372.1227

Wang, H., and Joseph, J. A. (1999). Quantifying cellular oxidative stress by dichlorofluorescein assay using microplate reader. *Free Radic. Biol. Med.* 27, 612–616. doi: 10.1016/S0891-5849(99)00107-0

Wang, Q., Ma, X., Zhang, W., Pei, H., and Chen, Y. (2012). The impact of cerium oxide nanoparticles on tomato (*Solanum lycopersicum* L.) and its implications for food safety. *Metallomics* 4, 1105–1112. doi: 10.1039/C2MT20149F

White, E. (1996). Life, death, and the pursuit of apoptosis. *Genes Dev.* 10, 1–15. doi: 10.1101/gad.10.1.1

Wu, S. G., Huang, L., Head, J., Chen, D. R., Kong, I. C., and Tang, Y. J. (2012). Phytotoxicity of metal oxide nanoparticles is related to both dissolved metals ions and adsorption of particles on seed surfaces. *J. Pet. Environ. Biotechnol.* 3, 126. doi: 10.4172/2157-7463.1000126

Yang, L., and Watts, D. J. (2005). Particle surface characteristics may play an important role in phytotoxicity of alumina nanoparticles. *Toxicol. Lett.* 158, 122–132. doi: 10.1016/j.toxlet.2005.03.003

Zhang, Z., He, X., Zhang, H., Ma, Y., Zhang, P., Ding, Y., et al. (2011). Uptake and distribution of ceria nanoparticles in cucumber plants. *Metallomics* 3, 816–822. doi: 10.1039/c1mt00049g

Zhao, L., Youping, S., Hernandez-Viezcas, J. A., Servin, A., Hong, J., Genhua, N., et al. (2013). Influence of CeO2 and ZnO nanoparticles on cucumber physiological markers and bioaccumulation of Ce and Zn: a life cycle study. *J. Agric. Food Chem.* 61, 11945–11951. doi: 10.1021/jf404328e

Zheng, L. F., Lu, S., and Liu, C. (2005). Effect of nano-TiO_2 on strength of naturally aged seeds and growth of spinach. *Biol. Trace Elem. Res.* 104, 83–91. doi: 10.1385/BTER:104:1:083

Conflict of Interest Statement: The authors declare that the research was conducted in the absence of any commercial or financial relationships that could be construed as a potential conflict of interest.